Université du Québec
INRS-Institut Armand-Frappier

Étude du rôle de la Synaptotagmine V au cours de la phagocytose et de la maturation du phagosome

Par
Adrien F. Vinet

Thèse présentée pour l'obtention du grade de Philosophiae doctor (PhD)
en Immunologie-Virologie

Jury d'évaluation

Président du jury et examinateur interne	Mathieu Cellier, PhD, INRS-Institut Armand Frappier
Examinateur externe	Michel Desjardins, PhD, Université de Montréal
Examinateur externe	Martin Olivier, PhD, Université McGill
Directeur de recherche	Albert Descoteaux, PhD, INRS-Institut armand Frappier

Résumé

De par leur rôle central au sein de l'immunité innée et leur participation à l'immunité acquise, l'étude des fonctions du macrophage est cruciale afin de pouvoir comprendre et contrôler l'invasion de l'organisme par de nombreux microorganismes pathogènes. Parmi les effecteurs de l'activité microbicide mis en jeu par les macrophages pour éliminer les microorganismes, la phagocytose tient un rôle prépondérant en éliminant les microbes et en permettant le développement de l'immunité adaptative via la présentation antigénique.

L'identification et la régulation des molécules impliquées dans ce processus d'internalisation ne sont que partiellement connues. Les résultats obtenus au cours de ces travaux nous ont conduit à l'identification d'un nouvel acteur de la phagocytose, la Synaptotagmine V (Syt V), qui contrôle le processus phagocytique à deux niveaux : lors de la formation du phagosome puis lors de sa maturation. Ainsi, ces travaux ont permis de proposer un rôle de la Syt V dans l'apport membranaire nécessaire à la formation du phagosome, ainsi qu'un mécanisme de régulation du recrutement de la pompe à proton V-ATPase et de la protéase cathepsine D au phagosome dépendant de la Syt V.

Dans une seconde partie, nous avons mis en relation le caractère régulateur de la Syt V pour la biogénèse du phagolysosome, avec l'altération de cette biogénèse par le promastigote du parasite *Leishmania donovani*. Nous avons alors pu observer que le LPG de *Leishmania donovani* empêchait l'acidification du phagosome et cela en inhibant le recrutement de la Syt V à la membrane du phagosome. Enfin nos résultats proposent une explication à l'observation de plusieurs études, démontrant que les promastigotes WT de *L. donovani* sont moins phagocytés que les mutants déficients pour le LPG. Nos résultats suggèrent que l'effet inhibiteur du LPG sur le recrutement de la Syt V est très précoce et qu'il pourrait ainsi empêcher l'apport membranaire dépendant de la Syt V lors de la phagocytose de particule de grandes tailles.

Table des Matières

Liste des figures

Revue de Littérature

Première publication

Deuxième publication

Troisième publication

Quatrième publication

Résultats supplémentaires

Discussion

Annexe 1

Liste des tableaux

Liste des abréviations

ADN	Acide désoxyribonucléique
ADNc	ADN complémentaire
ADP	Adénosine diphosphate
AP-2	Protéine adaptatrice-2
Arf	ADP Ribosylation Factor
ARN	Acide ribonucléique
ARNm	Acide ribonucléique messager
Arp	Actin related protein
Asp	Acylation stimulating protein
ATP	Adénosine triphosphate
BMM	Bone marrow-derived macrophages
BoNT	Toxine botulique
C3	Complément C3
CaMKII	Ca^{2+}/calmodulin-dependent protein kinase II
Cath	Cathepsine
CCL	CC chemokine ligand
Cdc42	Cell division cycle 42
CHO	Chinese hamster ovary
CMH	Complexe majeur d'histocompatibilité
COPI	Coat protein I
CR1/CR3	Récepteurs du complément
DAG	Diacylglycérol
DN	Dominant négatif
EEA1	Early Endosomal Antigen 1
ER	Réticulum endoplasmique
ERK	Extracellular signal-related kinase
ESCRT	Endosomal sorting complex required for transport-I
FcR	Recpteur à la portion constante (Fc) des IgG
fMLP	N-formyl-methionyl-leucyl-phenylalanine

FMN	Flavin Mononucleotide
FRN	Forme réactice nitrogéné
FRO	Forme réactive oxygénée
GAP	GTPase activating protein
GDI	GDP Dissociation Inhibitor
GDP	Guanosine diphosphate
GEF	Guanine nucleotide Exchange Factor
GFP	Green fluorescent protein
GP63	Glycoprotéine de surface de 63 kDa
GPI	Glycosylphosphatidyl-inositol
GTP	Guanosine triphosphate
HOPS	HOmotypic Protein Sorting
HNO	Nitroxyl
ICAM	Intercellular adhesion molecule
IgG	Immunoglobuline G
IL	Interleukine
IFN-γ	Interféron de type gamma
ITAM	Ig Tyrosine-based Activation Motif
JAK	Janus kinase
JNK	C-Jun NH2-terminal kinase
LAM	Lipoarrabinomannan
LAMP	Protéine membranaire associée aux lysosomes
LBPA	Lysobisphosphatidic Acid
LPG	Lipophosphoglycan
LPS	Lipopolysaccharide
MβCD	Méthyl-β-cyclodextrine
MAPK	Mitogen-activated protein kinase
MARCKS	Myritoylated Alanin-Rich C Kinase Substrate
MARCO	Macrophage receptor with collagenous structure
MBL	Lectine liant le mannose
MVB	Corps multi-vésiculaire

N_2O_3	Trioxyde dinitrogène
NADPH	Nicotinamide adenine dinucleotide phosphate oxidase
NF-κB	Nuclear factor kappa B
NO	Monoxyde d'azote
$NO_2^{\cdot}$	Dioxyde nitrogène
NOS	Nitric oxide synthase
NRAMP-1	Natural resistance-associated macrophage protein-1
NSF	N-ethyl-maleimide sensitive factor
OMS	Organisation mondial de la santé
$ONOO^-$	Péroxynitrite
PAMP	Pathogen-Associated Molecular Pattern
PCR	Réaction de polymérisation en chaîne
PDCD6IP	Programmed cell death-6-interacting protein
PFA	Paraformaldéhyde
pH	Potentiel d'hydrogène
PH	Pleckstrin homology domain
Phox	Phagocyte oxidase
PI	Phosphoinositide
PI(3)K	Phosphoinositide 3 kinase
PI(3)P	Phosphoinositide phosphate
PI(3,4,5)P3	Phosphoinositide triphosphate
PI(4,5)P2	Phosphoinositide biphosphate
PKC	Protéine kinase C
PRR	Pattern Recognition Receptors
PX	Phox Homology
RILP	Rab-Interacting Lysosomal Protein
RNAi	Interférence d'ARN
RT-PCR	Réaction de polymérisation en chaîne avec transcription inverse
Ser	Sérine

SH2	Src Homology domain 2
SHP	Src homology 2 domain phosphatase
si	Small interfering (RNA)
SIGN-R1	Specific intercellular adhesion molecule-grabbing nonintegrin receptor 1
SNAP	Synaptosome-associated protein
SNARE	Soluble N-ethylmaleimide-sensitive factor attachment protein receptor
SOCS	Suppressor of cytokine signalling
SR	Récepteurs scavengers
STAT	signal transducer and activator of transcription
Syk	Splenic tyrosine kinase
Syt	Synaptotagmine
TCR	Récepteur des cellules T
TeNT	Toxine tétanique
TfR	Récepteur de la transferrine
TGF-β	Transforming growth factor beta
Thl / Th2	Cellules T- helper
Thr	Théonine
TI-VAMP	Tetanus neurotoxin-insensitive vesicle-associated membrane protein
TLR	Toll-like receptor
TNFα	Tumor necrosis factor alpha
V-ATPase	Pompe à proton vacuolaire ATPase
VAMP	Vesicle associated membrane protein
VFT	Vps fifty three
VIH	Virus d'immunodéficience humaine
Vps	Vacuolar protein sorting
WASP	Wiskott-Aldrich Syndrome Protein
WT	Wild type (sauvage)

Préface

Les travaux présentés dans cette thèse sont regroupés sous forme de 4 publications. L'implication de l'auteur de cette thèse est ici définie pour chacun des articles.

Article I : Vinet A.F., Fukuda M. and Descoteaux A. (2008). The exocytosis regulator Synaptotagmin V controls phagocytosis. *The Journal of Immunology*, 181(8):5289-95.

Les expériences ont été conçues par A.F.V et A.D. et réalisées par A.F.V., l'article a été rédigé par A.F.V. et A. D.
M. F. a fournit le plasmide Syt V-GFP, l'anticorps anti-Syt V et a commenté le manuscrit.

Article II : Winberg M.E., Holm A., Eva Särndahla E., Vinet A.F., Descoteaux A., Magnusson K.E., Rasmusson B., Lerm M. (2009) *Leishmania donovani* lipophosphoglycan inhibits phagosomal maturation via action on membrane rafts. *Microbes and infection*, 11(2):215-22.

A.F.V. a conçu et réalisé la figure 2 dans son ensemble.

Article III : Vinet A.F., Fukuda M., Turco S.J., and Descoteaux A. The *Leishmania donovani* lipophosphoglycan excludes the vesicular proton-ATPase from phagosomes by impairing the recruitment of Synaptotagmin V. *PLoS Pathogens* 5(10): e1000628. doi:10.1371/journal.ppat.1000628.

Les expériences ont été conçues par A.F.V et A.D. et réalisées par A.F.V., l'article a été rédigé par A.F.V. et A. D.
M. F. a fournit le plasmide Syt V-GFP, l'anticorps anti-Syt V et a commenté le manuscrit. S.J.T. a fournit le LPG purifié et a commenté le manuscrit.

Article IV : Vinet A.F., Fukuda M., Turco S.J. and Descoteaux A. The *Leishmania donovani* lipophosphoglycan reduces phagocytosis rate by a Synaptotagmin V-dependent process.

Les expériences ont été conçues par A.F.V et A.D. et réalisées par A.F.V., l'article a été rédigé par A.F.V. et A. D.
M. F. a fournit le plasmide Syt V-GFP et l'anticorps anti-Syt V. S.J.T. a fournit le LPG purifié.

Annexe 1 : Vinet A.F.and Descoteaux A. (2009) Large scale phagosome preparations in macrophages. *Methods in Molecular Biology* (NE Reiner, Ed), Humana Press. 531:329-46.

Ce chapitre de livre a été rédigé par A.F.V. et A. D.

INTRODUCTION

Lors d'une infection, les phagocytes professionnels constituent la première ligne de défense de l'organisme et jouent donc un rôle clé dans l'organisation l'immunité innée (Aderem et Underhill, 1999). La phagocytose est initiée lors de la reconnaissance de composés de surface de la particule par des récepteurs membranaires phagocytiques qui permettent une polymérisation d'actine au site de contact et la formation du phagosome. Durant la naissance de ce phagosome, un apport membranaire issu de vésicules internes telles que les endosomes de recyclage ou les endosomes tardifs se produit au niveau de la coupe phagocytique (Bajno et al., 2000; Braun et al., 2004). Ce processus, appelé exocytose focale, intervient principalement lors d'une forte demande en membrane, c'est-à-dire lors de l'internalisation de particules de grande taille. Afin d'acquérir l'habilité à tuer et à dégrader les microorganismes, le phagosome nouvellement formé s'engage ensuite dans un processus hautement régulé de maturation, impliquant de nombreuses interactions avec les endosomes précoces, tardifs et les lysosomes (Desjardins et al., 1994; Jahraus et al., 1994; Mayorga, Bertini, et Stahl, 1991). Ces interactions sont de nature transitoires et sont caractérisées par la formation de pores de fusion entre deux organelles, autorisant l'échange de membrane et de contenu luminal (Desjardins et al., 1994). Ces évènements séquentiels de fusion et fission permettent ainsi l'acidification du phagosome et l'acquisition de diverses hydrolases participant à la biogénèse d'un phagolysosome microbicide.

Les interactions entre le phagosome et le compartiment endosomal sont finement régulées, notamment via les petites GTPases telles que Rab-5 et Rab-7 (Vieira, Botelho, et Grinstein, 2002). D'autres molécules de signalisation, incluant les membres de la famille des Proteine Kinase C (PKC) s'associent au phagosome selon diverses cinétiques durant la maturation du phagosome (Allen et Allgood, 2002; Breton et Descoteaux, 2000; Brumell et al., 1999; Larsen et al., 2000; Larsen et al., 2002; Zheleznyak et Brown, 1992). La PKC-α, par exemple, est importante pour l'acquisition de divers marqueurs des endosomes tardifs et des lysosomes tels que Rab-7, la Cathepsine-D (Cath-D), la Flotilline-1 ou LAMP-1 (Ng Yan Hing, Desjardins, et Descoteaux, 2004). Cependant les mécanismes permettant à la PKC-α de réguler la biogénèse du phagolysosome restent totalement inconnus.

Dans le but d'étudier ces mécanismes, nous avons adopté une stratégie visant à identifier les molécules formant un complexe avec la PKC-α durant la maturation du phagosome. Les étapes de cette approche protéomique sont les suivantes: l'isolation de phagosomes de cellules RAW 264.7 contenant des billes de latex, une séparation sur gel acrylamide dénaturant à deux dimensions des molécules obtenues par co-immunoprécipitation par l'anticorps anti PKC-α, et enfin une identification par spectrométrie de masse des partenaires potentiels de la PKC-α. Parmi les partenaires identifiés, la Synaptotagmine V (Syt V), qui est un régulateur de fusion membranaire dépendent du calcium, nous est apparu un candidat prometteur. En effet, les phénomènes de fusion membranaire sont omniprésents dans les macrophages, non seulement au cours de la phagocytose (c'est-à-dire dés la formation de la coupe phagocytique et tout au long de la maturation phagosomale) mais également lors du relargage de médiateurs pro-inflammatoires. Ainsi, malgré leur potentiel impact sur l'ensemble des phénomènes de fusion membranaire, les régulateurs de fusions tels que les membres de la famille des Syts ne sont quasiment pas étudiés chez les phagocytes.

L'objectif global de ces travaux était donc de caractériser la dynamique d'association et le/les rôle(s) de la Syt V au cours de la phagocytose, et lors d'un contexte d'infection par un microorganisme pathogène altérant le processus normal de phagocytose tel que le parasite *Leishmania donovani*. Pour ce faire, ce projet reposait sur quatre objectifs spécifiques :

1) Élucider les rôles de la Syt V lors de la formation du phagosome et de sa maturation
2) Déterminer un potentiel effet du parasite *L. donovani* sur l'acquisition de la Syt V au phagosome, notamment via son lipophosphoglycan (LPG)
3) Étudier les conséquences d'un tel impact sur les fonctions de la phagocytose lors d'une infection par *L. donovani*
4) Approfondir une potentielle régulation de la Syt V par PKC-α

Les résultats obtenus au cours de ce doctorat sont présentés sous forme de quatre articles. Le premier, traitant du rôle de la Syt V lors de la formation du phagosome, a été publié en 2008 dans *Journal of Immunology*. Le second, publié en 2009 dans *Microbes and Infections* et pour lequel l'auteur de cette thèse a collaboré, démontre l'importance des microdomaines lipidiques pour l'effet du LPG sur la maturation du phagosome et permet d'introduire l'article suivant. En effet, pour le troisième article, outre l'identification du rôle de la Syt V durant la maturation du phagosome, les résultats démontrent aussi l'impact du LPG sur le recrutement de la Syt V au niveau des microdomaines lipidiques et les conséquences de ce phénomène sur la maturation phagosomale. Ce troisième article a été publié par le journal *PLoS Pathogens*. Un quatrième article, sous forme de manuscrit, met en relation les conclusions du premier et du troisième article en présentant les effets du LPG de *L. donovani* durant la formation du phagosome et apporte des éléments de réponse au quatrième objectif concernant la relation entre Syt V et PKC-α. Un chapitre de livre pour la série *Methods in Molecular Biology* traitant de la technique d'isolation de phagosome et de ses applications est également présenté en annexe (Annexe 1).

Pour débuter cette thèse, une revue de littérature permet tout d'abord d'exposer les connaissances actuelles sur les principaux domaines de ces travaux : les macrophages et la phagocytose, les synaptotagmines et la fusion membranaire, ainsi que le *Leishmania* et son interaction avec le macrophage.

Revue de littérature

1 Rôle du macrophage dans l'immunité innée

1.1 Généralités sur le macrophage

Les macrophages sont des cellules phagocytiques professionnelles mononuclées. Leur origine provient de la moelle osseuse sous la forme de progéniteurs communs pour les monocytes et les neutrophiles se nommant CFU-GM (Colony-forming unit-granulocyte macrophage) (Metcalf, 1971). Durant leur maturation, les macrophages passent par les stades monoblastes, promonocytes dans la moelle osseuse, puis monocytes au niveau du système périphérique sanguin et enfin macrophages dans les tissus (Gordon et Taylor, 2005; van Furth et Cohn, 1968; van Furth et al., 1972). Cette maturation du macrophage s'accompagne d'un développement des activités phagocytiques et de l'expression des différents récepteurs tels que les récepteurs aux IgG ou aux C3. Ces macrophages montrent une grande diversité structurale et fonctionelle selon leur tissu de résidence. Par exemple, ils sont présents dans le poumon (macrophages alvéolaires), les tissus conjonctifs (histiocytes), les reins (cellules mésengliales), le foie (cellules de Küpffer), le cerveau (microglies) ou les os (ostéoclastes).

Les macrophages font partie des phagocytes, et à ce titre, ils possèdent une fonction de phagocytose des agents pathogènes et des débris cellulaires issus de cellules apoptotiques. Ces fonctions d'élimination sont absolument nécessaires pour la défense de l'hôte et le maintien de l'homéostasie tissulaire. En plus d'un rôle central dans l'immunité innée, les macrophages contribuent aussi à l'établissement de l'immunité adaptative par la production de cytokines pro-inflammatoires et la présentation antigénique aux cellules T (Emil, 2002). De par leur fonction de sentinelle pour détecter les microorganismes pathogènes (e.g. bactéries, parasites, virus ou champignons), les macrophages sont des composants clés du processus d'inflammation (Gomez, Boehmer, et Kovacs, 2005; Phillip, Christina, et Lesley, 2005). Une fois activés, les macrophages sécrètent différents médiateurs tels que des cytokines et chémokines qui sont cruciaux pour une réponse de l'immunité innée efficace (Figure 1).

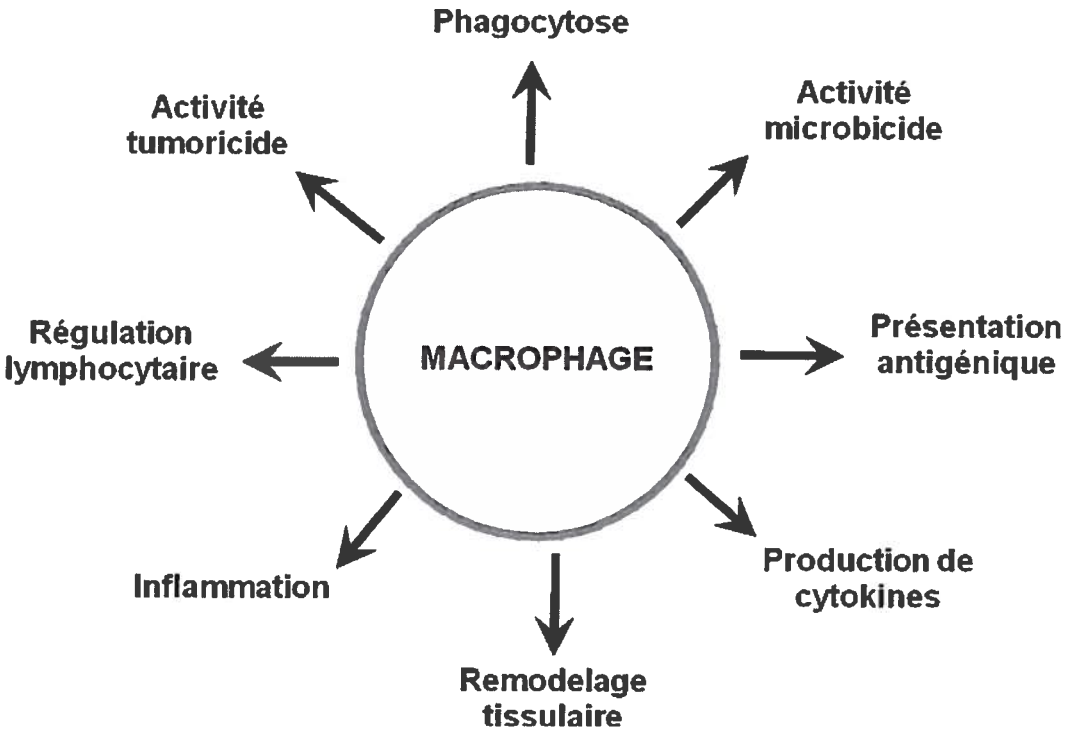

Adapté de (Woods, Lu, et Lowder, 2000)

Figure 1: Principales fonctions du macrophage.

1.2 Rôles de la phagocytose

Ce sont les observations de Metchnikoff, biologiste du développement, qui l'ont amené à formuler sa théorie sur le rôle protecteur de la phagocytose dans des organismes pluricellulaires à partir de 1882. Suite à une expérience sur des larves d'étoiles de mer, pendant laquelle il observe l'agrégation de cellules autour d'une épine introduite dans ces larves, il met en évidence le phénomène de la phagocytose et propose l'hypothèse que la fonction du phagocyte passe de "manger pour se nourrir à manger pour protéger l'organisme" (Tauber, 2003).

En fait, le phagocyte est considéré par Metchnikoff comme une cellule libre de toute attache, dont la fonction est restée inchangée au cours de l'évolution avec pour rôle de maintenir l'intégrité de l'organisme, que ce soit en le nourrissant, en éliminant les parties inutiles ou en le protégeant des invasions extérieures (Figure 2). En 1908, Metchnikoff recevra le Prix Nobel de physiologie et de médecine pour ses travaux sur l'immunité et la phagocytose.

Au niveau de l'organisme pluricellulaire, la phagocytose représente le processus par lequel les leucocytes internalisent des particules dont la taille est supérieure à 0,5/1 µm. Cette fonction constitue un mécanisme vital à la mise en place des tissus lors du développement, à l'homéostasie de l'organisme en cas de morts cellulaires, à l'élimination de synapses non fonctionnelles dans le système nerveux et bien sûr au bon fonctionnement du système immunitaire inné et de son dialogue avec l'immunité adaptative. Ce processus conservé phylogénétiquement, est donc un processus clé pour l'immunité innée. En effet, par l'ingestion de microorganismes pathogènes, les leucocytes phagocytiques accomplissent deux fonctions essentielles à l'immunité. Tout d'abord, ils initient la voie de destruction du microbe pathogène, en partie par une maturation du phagosome en phagolysosome, lequel est enrichi en enzymes hydrolytiques et autres composés oxygénés/nitrogénés. Ensuite, les phagocytes et plus particulièrement les cellules dendritiques, utilisent la phagocytose pour dégrader le microorganisme et diriger les antigènes vers les compartiments du CMH de classe I et II

(Larsson, Fonteneau, et Bhardwaj, 2001). La phagocytose possède donc un double rôle : un rôle d'effecteur de l'immunité innée ainsi qu'un rôle de passerelle entre les réponses immunitaires innées et acquises. La reconnaissance, notamment de la phosphatidylsérine, et la phagocytose des corps apoptotiques par les macrophages facilite aussi l'élimination et l'achèvement de la signalisation conduisant à l'apoptose (Hoeppner, Hengartner, et Schnabel, 2001; Reddien, Cameron, et Horvitz, 2001).

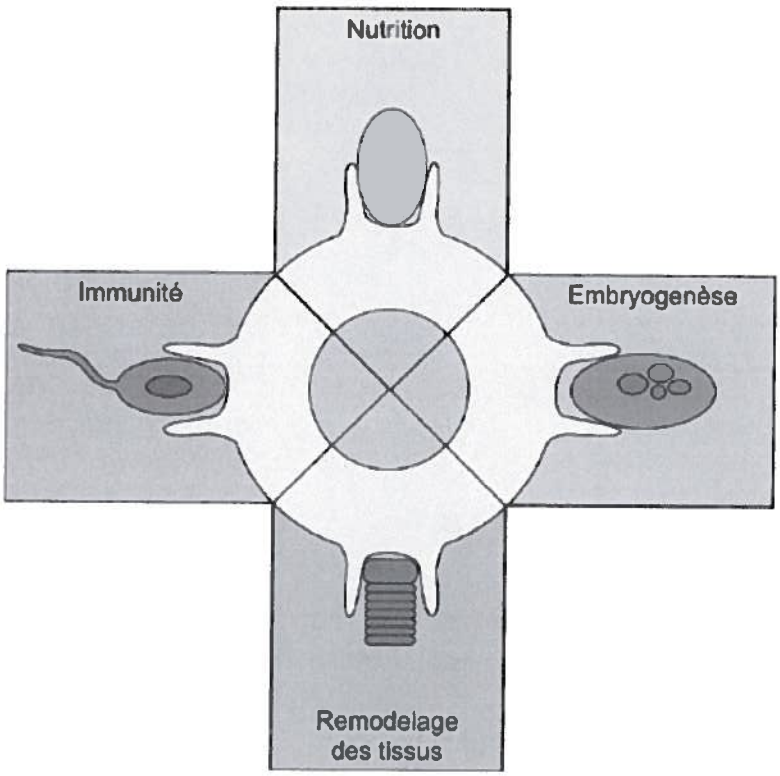

D'après (Desjardins, Houde, et Gagnon, 2005)

Figure 2: Les différentes fonctions de la phagocytose.

2 *Le phagosome*

La phagocytose aboutit à la formation d'une vacuole spécialisée, le phagosome. Suite à sa formation, il va subir de nombreuses modifications par échange de composants membranaires et luminaux fournis par d'autres organites. Cette maturation a pour but de produire un environnement microbicide. Celui-ci est obtenu par acidification progressive, production de dérivés réactifs oxygénés/nitrogénés, suivies de la libération et de l'activation de protéases et de peptides cationiques antimicrobiens. Ces conditions vont permettre l'élimination du microorganisme internalisé, mais permettent aussi de promouvoir la dégradation des molécules étrangères en fragments peptidiques antigéniques qui seront chargés sur des molécules de CMH II et I (Jutras et Desjardins, 2005).

Conceptuellement, la phagocytose peut être séparée en deux parties : la formation de la vacuole contenant la particule à ingérer (formation du phagosome), puis son évolution en un compartiment microbicide (maturation du phagosome).

2.1 La formation du phagosome

2.1.1 Les différents récepteurs phagocytiques

Les macrophages expriment une grande variété de récepteurs phagocytiques qui leur octroient la capacité d'internaliser la plupart des particules (Figure 3). Ces récepteurs peuvent reconnaitre des motifs particuliers aux microorganismes, alors que d'autres types de récepteurs phagocytiques sont ceux reconnaissant spécifiquement des opsonines liées à la surface de la particule (les récepteurs du complément et les récepteurs Fc) (Swanson et Hoppe, 2004). Ainsi, bien que la reconnaissance directe d'un agent pathogène soit un aspect fondamental de l'immunité innée, l'opsonisation permet une diversification du répertoire de reconnaissance du phagocyte (Stuart et Ezekowitz, 2005). Le processus de reconnaissance et de phagocytose implique de multiples interactions ligand-récepteur, et

il est maintenant clair que diverses opsonines incluant les immunoglobulines, les collectines et les composants du complément, guident les activités cellulaires nécessaires à l'internalisation du microorganisme pathogène (Aderem et Underhill, 1999; Underhill et Ozinsky, 2002). Un bon exemple est la réaction croisée entre les récepteurs Fc et les récepteurs du complément pour la phagocytose efficace des complexes immuns (Caron et Hall, 1998; Skoberne et al., 2006). Donc, bien qu'empruntant des voies de signalisation différentes, la liaison à l'ensemble de ces récepteurs phagocytiques initie la formation du phagosome et le phénomène de phagocytose (Figure 3), caractérisé par une maturation menant à la biogénèse du phagolysosome hautement microbicide.

2.1.1.1 Récepteurs Fc

Les récepteurs FcR reconnaissent la partie Fc des immunoglobulines. Bien qu'il existe différents types de ces récepteurs tels que les FcεR (pour les IgE), les FcαR (pour les IgA), et les trois types de récepteurs aux IgG, FcγRI, FcγRII et FcγRIII, seul le FcγRI lie les IgG monomériques avec une grande affinité, et représente le récepteur le plus étudié lors de la phagocytose. Les évènements détaillés qui mènent à l'extension de pseudopodes membranaires et l'internalisation de la particule durant une phagocytose initiée par les récepteurs Fcγ ont été en partie décryptés (Cox et al., 2000). L'évènement intracellulaire initial est la phosphorylation des récepteurs Fc eux-mêmes, c'est-à-dire de la partie cytoplasmique d'ITAM (Immunoreceptor Tyrosine-based Activation Motif) par des membres de la famille des Src (Fitzer-Attas et al., 2000; Gresham et al., 2000). Les sous-unités ITAMs servent ensuite de site d'arrimage et d'activation de Syk, qui à son tour phosphoryle divers substrats (Ghazizadeh, Bolen, et Fleit, 1994). Cette tyrosine kinase est absolument nécessaire pour l'internalisation de particules opsonisées aux IgG, mais pas pour des particules captées par d'autres récepteurs (Crowley et al., 1997; Kiefer et al., 1998), suggérant que d'autres kinases doivent être impliquées dans ces derniers cas. Les évènements qui suivent l'activation de Syk durant l'ingestion de la particule ne sont pas clairement compris, quoiqu'il en soit, le remodelage du cytosquelette d'actine est sans équivoque, car indispensable pour le phénomène d'extension des pseudopodes. Dans le cas des FcγR, la polymérisation d'actine est par exemple régulée par l'activation des

PI(3) kinases et des petites GTPases de la famille Rho telles que Rac1 et/ou Rac2, ainsi que Cdc42 (Caron et Hall, 1998). Les particules recouvertes d'IgG sont donc internalisées par un mécanisme de « fermeture à glissière » par lequel les pseudopodes semblent se former autour de la particule, la liant et l'internalisant à l'intérieur d'un phagosome resserré (Tjelle, Lovdal, et Berg, 2000).

2.1.1.2 Récepteurs du complément

Le système du complément est composé de diverses protéines qui réagissent entre elles afin d'opsoniser les agents pathogènes et afin d'induire une série de réponses inflammatoires renforçant la défense de l'hôte. Le système du complément prévient l'infection en trois étapes : (1) l'opsonisation des microorganismes pathogènes permettant leur internalisation par les phagocytes via les récepteurs du complément (C3b, C3bi), (2) le recrutement de cellules inflammatoires (C3a, C5a), (3) la destruction directe des microorganismes par la création de pores dans la membrane (C5b, C6, C7, C8, C9). Il existe plusieurs mécanismes régulateurs afin de prévenir une activation du complément défavorable à la surface de la cellule hôte. Par conséquent, le système du complément est un mécanisme majeur de reconnaissance d'agents pathogènes qui mène à une défense de l'hôte envers l'infection initiale. La phagocytose initiée par les récepteurs du complément s'exécute lors de la reconnaissance spécifique des composants du complément lié à la surface du microorganisme par les récepteurs correspondants du phagocyte.

Il existe trois voies distinctes au travers desquelles les composants du complément sont activés à la surface des microorganismes: la voie classique, la voie des lectines liant le mannose et la voie alternative. Chacune de ces voies suit une séquence de réactions générant une protéase clé appelée C3 convertase, laquelle produit le C3b. La voie classique est activée par des anticorps liés à la surface du microorganisme, lesquels lient le C1q qui est le premier composant de la voie classique. Cette configuration déclenche une cascade de protéases sur sérine qui clivent C3 en sa forme active, C3b. La voie des lectines est activée après reconnaissance du motif moléculaire de type lectine et à ce jour, trois membres ont été identifiés: les lectines liant le mannose (MBL), les ficolines et les

lectines de type C (SIGN-R1). Suite à la reconnaissance du motif, ces lectines s'associent avec des protéases sur sérine, lesquelles agissent comme le C1 de la voie classique en activant le composant C4 et en menant au stade central C3. En plus de la reconnaissance des structures de la surface bactérienne, SIGN-R1 peut aussi activer la voie du complément en se liant au C1q (Kang et al., 2006). Enfin, la voie alternative se différencie des deux autres voies par le fait qu'elle est activée par une réaction directe du C3 interne avec la surface du microorganisme. La liaison initiale du C3 à une surface activatrice mène à une amplification rapide du dépôt de C3b à travers l'action des protéases Facteurs B et Facteurs D de la voie alternative. Il est important de noter que le C3b déposé par les voies classiques ou des lectines peut également amener par la suite à une amplification du clivage protéolytique via l'action des Facteurs B et D.

Le produit final, C3bi, se lie à trois autres récepteurs du complément, CR1, CR3 (CD11b/CD18, intégrine aMb2) et CR4 (CD11c/CD18, intégrine aXb2). La liaison du C3bi aux CR3 induit plus fortement la phagocytose après l'activation du phagocyte. Le CR3 nécessite un signal d'activation additionnel afin d'opérer une liaison et une phagocytose efficace. Ces signaux d'activation peuvent être générés par de nombreux stimuli tels que les esters phorbol, les lipopolysaccharides (LPS), les cytokines, les facteurs de croissance, les chémokines... Ces signaux activent la PKC et induisent une transformation tertiaire des récepteurs de type intégrine qui se regroupent permettant une augmentation de l'affinité du récepteur (Griffin et Mullinax, 1985; Hughes et Pfaff, 1998; Ross et Vetvicka, 1993; Schmidt, Caron, et Hall, 2001; van Kooyk et Figdor, 2000; Williams et Solomkin, 1999; Wright et Griffin, 1985; Wright et Silverstein, 1982). La liaison et le regroupement de Mac-1 par les particules opsonisées au complément induisent une phosphorylation sur sérine du récepteur, qui active RhoA. Ce dernier permet aux kinases sur sérine/thréonine de mobiliser Arp2/3 et la machinerie basée sur l'actomyosine afin de provoquer un enfoncement lent de la particule dans la cellule (Caron et Hall, 1998; Olazabal et al., 2002).

2.1.1.3 Récepteurs non dépendants des opsonines

Parmi les récepteurs qui ne dépendent pas des opsonines, les PRR (Pattern Recognition Receptors) ont la capacité de reconnaître les particules en se liant à des composés spécifiquement présents à leur surface appelés PAMP (Pathogen-Associated Molecular Patterns) qui sont des structures moléculaires hautement conservées et présentes chez la plupart des microorganismes pathogènes (Figure 3). Ces PAMPs sont, par exemple, les peptidoglycans, le lipopolysaccharide, la flagelline, l'ADN bactérien ou l'ARN viral (Bianchi, 2007). La famille des PRR comprend les récepteurs mannose (MR), CD14, les récepteurs Toll-like (TLR), les dectines et les récepteurs scavengers (SR) (Gough et Gordon, 2000).

Ainsi, par exemple, le MR reconnaît les résidus mannose et fucose présents à la surface de nombreux agents pathogènes. Les SR furent à l'origine définis selon leur habilité à lier les lipoprotéines de faible densité (Goldstein et al., 1979), et de nos jours, ils sont divisés en 8 classes. Ils peuvent lier le LPS, l'acide lipoteichoique, l'ADN CpG bactérien, le β-glucan (Areschoug et Gordon, 2008; Mukhopadhyay et Gordon, 2004), et, de manière plus occasionelle les corps apoptotiques qui expriment la phosphatidylsérine (PS) à leur surface (Fadok et al., 2000; Pluddemann, Neyen, et Gordon, 2007) ou la PS des *Leishmania* (Platt et al., 1996; Savill et al., 1993; Tripathi et Gupta, 2003; Wanderley et al., 2005). Par exemple, MARCO (macrophage receptor with collagenous structure) fait partie de la classe A des SR et agit en tant que récepteur phagocytique pour des bactéries pathogènes telles que *S. pneumoniae* (Arredouani et al., 2004) et *N. meningitidis* (Mukhopadhyay et al., 2006). Un autre exemple concerne le CD36 (appartenant à la classe B), qui a un rôle de senseur pour l'acide lipoteichoique et les lipopeptides diacylés (Hoebe et al., 2005), et qui peut aussi agir comme co-récepteur pour TLR2. Suite à une stimulation avec des diacylglycérides, l'association du CD36 avec l'hétérodimère TLR2/6 au niveau des microdomaines lipidiques de la surface cellulaire est cruciale pour initier la signalisation en aval (Triantafilou et al., 2006). De nombreux autres SR de mammifères reconnaissent les PAMP et les études démontrent de plus en plus l'importante part que jouent les SR lors de l'immunité innée. On peut également noter

que plusieurs SR peuvent reconnaitrent un même microorganisme, et il est alors difficile de discriminer la contribution de chacun. Enfin, il existe plusieurs exemples dans la littérature de microorganismes pathogènes qui exploitent les SR afin de pénétrer dans la cellule hôte (Dubuisson, Helle, et Cocquerel, 2008; Rodrigues et al., 2008; Yalaoui et al., 2008).

Ainsi, la reconnaissance de ces PAMPs par les récepteurs non dépendants des opsonines du macrophage provoque l'internalisation des microorganismes reconnus ainsi que l'activation des voies de signalisation intracellulaire menant éventuellement à la production de cytokines pro-inflammatoires telles que le TNF (pour Tumor Necrosis Factor), l'IL-1 (Interleukine-1), l'IL-6 et/ou des chémokines (CCL2, CCL3 et CCL5) qui participent au recrutement d'autres cellules immunitaires au site d'infection et aident à coordonner la réaction inflammatoire (Doyle et O'Neill, 2006; Saito et Gale, 2007). Via la stimulation de certains de ces récepteurs, les macrophages relarguent également des réactifs oxygénés et nitrogénés responsables de l'élimination des microorganismes (Eze et al., 2000; Marcinkiewicz, Grabowska, et Chain, 1995). Beaucoup d'études se concentrent sur des récepteurs particuliers isolés, mais il ne faut pas perdre de vue que les mécanismes d'internalisation chez les phagocytes sont le résultat d'une contribution collective de plusieurs récepteurs impliqués dans la reconnaissance spécifique d'un agent pathogène. Les membres de la famille des TLR sont connus pour fortement contribuer à l'activation des phagocytes et au relargage de cytokines pro-inflammatoires (Gerold, Zychlinsky, et de Diego, 2007; Miyake, 2007). Cependant, le rôle des TLR dans la phagocytose est un domaine qui est débattu avec ferveur dans la littérature. D'un côté, certains auteurs soutiennent que la signalisation initiée par les TLR de surface, qui sont recrutés au phagosome lors de l'internalisation de microbes, est critique pour la maturation du phagosome (Blander, 2007; Blander et Medzhitov, 2004); (Blander et Medzhitov, 2006a; Blander et Medzhitov, 2006b). D'un autre côté, certains auteurs soutiennent que la maturation du phagosome se produit de manière indépendante de la signalisation des TLR (Russell et Yates, 2007a; Russell et Yates, 2007b; Yates, Hermetter, et Russell, 2005; Yates et Russell, 2005). Cela rend difficile la tâche

d'assigner un rôle de la signalisation des TLR durant la maturation phagosomale, d'autres études seront nécessaires afin de clarifier l'ambigüité actuelle.

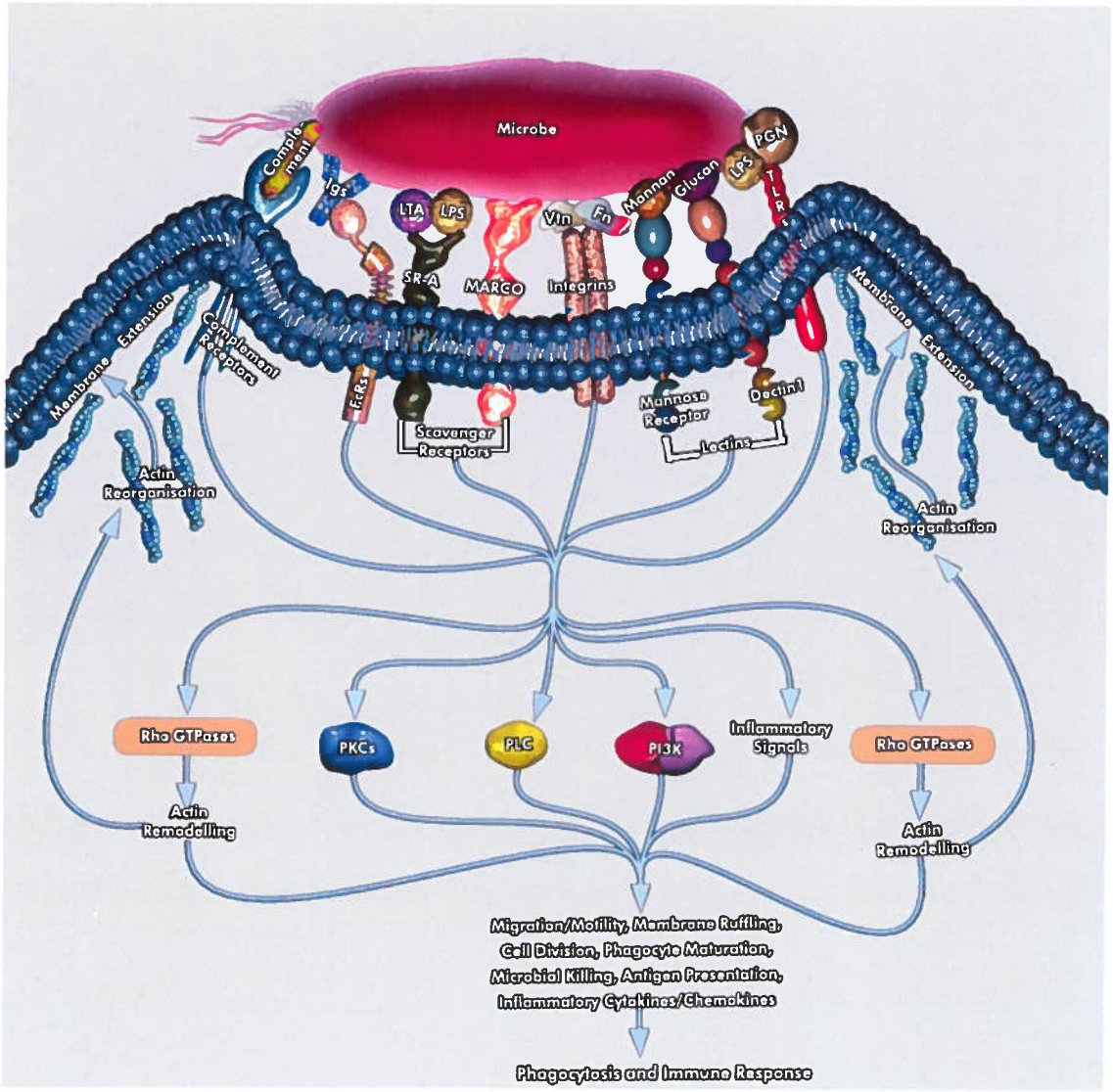

Figure 3: Interaction avec les récepteurs phagocytiques et signalisation induite lors de la phagocytose de microbes. De multiples récepteurs reconnaissent simultanément les microbes par une interaction directe ou par une interaction avec des opsonines liées à la surface des microorganismes. La stimulation des récepteurs phagocytiques induit diverses voies de signalisation afin de remodeler le cytosquelette d'actine et d'initier la formation du phagosome.

2.1.2 Formation du phagosome et apport membranaire

2.1.2.1 Réorganisation du cytosquelette d'actine

L'actine existe sous deux formes, une forme monomérique d'actine-G et une forme polymérique d'actine-F (Schmidt et Hall, 1998; Southwick et Stossel, 1983). Une fois que la particule est liée à des récepteurs de surface, une polymérisation transitoire et localisée (Greenberg, 1995; Swanson et Baer, 1995) est nécessaire à l'internalisation, comme cela fut démontré par l'utilisation des cytochalasines. Ces inhibiteurs pharmacologiques affectent l'assemblage des filaments d'actine et bloquent l'internalisation des particules chez les phagocytes et les organismes modèles tels que *Dictyostelium discoideum* (Axline et Reaven, 1974; Maniak et al., 1995; Zigmond et Hirsch, 1972). Les phagosomes précoces sont entourés par une couche distincte d'actine-F, qui disparait lorsque s'amorce la maturation du phagosome (Aderem et Underhill, 1999; Greenberg et al., 1991).

Le recrutement de l'actine-F à la coupe phagocytique n'est pas spécifique à un type de récepteur. En effet, bien que le phagosome naissant initié via les récepteurs Fcγ, mannoses et scavengers entraine des protusions et des extensions riches en actine-F, celle-ci est aussi enrichie au niveau d'un phagosome naissant lors d'une phagocytose initiée par les récepteurs du complément (phagocytose de type II en « enfoncement »). La polymérisation de l'actine-F lors de la phagocytose est régulée par divers facteurs. Par exemple, les PI(3,4,5)P et PI(4,5)P sont impliqués (Vieira, Botelho, et Grinstein, 2002), tout comme les petites GTPases telle que la famille des Rho, qui régulent aussi la morphologie de la cellule et la réorganisation du cytosquelette d'actine en plus de la phagocytose (Chimini et Chavrier, 2000; Qualmann et Mellor, 2003). Ainsi, deux membres de cette famille, Rac1 et Cdc42, sont essentiels à l'internalisation régulée par les récepteurs Fcγ, alors que RhoA est essentiel à la phagocytose via les récepteurs du complément (Caron et Hall, 1998). Ces petites GTPases de la famille des Rho sont activées par les facteurs échangeurs de guanine (GEF), cependant, aucun GEF n'a pour le

moment été démontré clairement comme lié à la phagocytose. Une autre petite GTPase importante pour la phagocytose via les récepteurs Fcγ est Arf-6 (ADP-ribosylation factor-6), qui est nécessaire à l'extension membranaire lors de la phagocytose, possiblement en interagissant avec la voie Rac1 (Zhang et al., 1998). La signalisation en aval des petites GTPases provoque par la suite l'activation et le recrutement de nombreux autres facteurs durant le processus d'internalisation.

2.1.2.2 Le phénomène d'exocytose focale

Durant la phagocytose de particules de taille importante et/ou d'un grand nombre de particules, une quantité de membrane considérable est internalisée, et la cellule doit compenser sa perte de surface membranaire plasmique. Un phénomène d'exocytose focale d'endomembrane issue de vésicules internes a alors lieu au niveau du site de phagocytose (Figure 4). En effet, les endosomes tardifs (Braun et al., 2004) et de recyclage (Bajno et al., 2000) semblent être les principaux contributeurs, même si les lysosomes ont également été démontrés comme impliqués dans ce processus lorsque la demande en membrane est extrêmement importante (Czibener et al., 2006; Huynh et al., 2007). Une fusion directe du réticulum endoplasmique (ER) avec le phagosome naissant fut observé par Desjardins et collègues (Gagnon et al., 2002) au niveau de macrophages J774 ayant internalisé des billes de latex, des particules opsonisées, des bactéries ou des parasites, suggérant que le ER pourrait être une source majeure de membrane interne durant la phagocytose (Desjardins, 2003). De plus, une autre étude a montré que le ER était important pour la phagocytose de billes de grande taille, mais pas de petite taille (Becker, Volchuk, et Rothman, 2005). Cependant d'autres études sont contradictoires, faisant du rôle du ER dans la phagocytose un débat qui n'est pas clos. En effet, l'importance du ER durant le processus phagocytique pourrait être différent selon la nature de la cellule phagocytique ou de la particule phagocytée (Gagnon et al., 2002; Henry et al., 2004; Rogers et Foster, 2007; Touret et al., 2005). D'autre part, il n'y a aucune contribution de la part de l'appareil de Golgi (Zhang et al., 1998). Un aspect important qui n'est que peu pris en considération jusqu'à maintenant est que ces phénomènes de fusions très précoces représentent non seulement un apport membranaire,

mais permettent aussi le relargage de composés tels que les cytokines pro-inflammatoires (Kay et al., 2006; Murray et al., 2005) et de protéines membranaires spécifiques qui constitue le phagosome précoce et initie sa maturation (Braun et Niedergang, 2006).

Ainsi, la formation d'un phagosome initiée par la reconnaissance d'une particule de grande taille serait dépendante de l'exocytose d'endosomes positifs pour les SNARE (soluble NSF-attachment protein receptor proteins) cellubrévine VAMP-3 et TI-VAMP/VAMP-7 (Bajno et al., 2000; Braun et al., 2004), impliquant fort probablement des syntaxines telles que les Syn 2, 3 ou 4, qui sont connues pour être associées à la membrane plasmique du macrophage (Hackam et al., 1996). Les Syn 13 (présentes sur les endosomes de recyclages) et Syn 7 (associées aux endosomes tardifs) pourraient être relarguées au niveau du phagosome lors de sa formation et pourraient ensuite réguler les fusions avec le compartiment endocytique puisque leur inhibition n'affecte pas l'internalisation mais seulement la maturation des phagosomes (Collins et al., 2002). Enfin, les petites GTPases Rab-11 et Arf-6 (ADP-ribosylation factor-6) seraient importantes pour diriger et lier les organelles positifs pour VAMP-3 comme sources d'endomembrane au phagosome naissant (Cox et al., 2000; Niedergang et al., 2003).

2.2 Maturation du phagosome et biogénèse du phagolysosome

Une maturation du phagosome est nécessaire parce que le phagosome nouvellement formé n'a pas encore de propriétés microbicides. Son contenu est principalement issu du milieu extracellulaire et sa membrane est en partie composée de membrane plasmique. Par conséquent la membrane phagosomale et son contenu doivent subir un remodelage considérable afin de transformer l'environnement inoffensif du phagosome en environnement hautement microbicide. La maturation du phagosome implique une séquence complexe d'évènements de fusion et de fission avec le compartiment endosomal, appelé « Kiss and Run » (Desjardins et al., 1994). Ainsi le phagosome acquiert successivement les marqueurs spécifiques des endosomes précoces

(tels que EEA1 ou Rab-5), tardifs (Rab-7), puis des lysosomes (LAMP-1) (Desjardins et al., 1994) (Figure 4). Cependant, le processus de maturation que le phagosome va subir dépend aussi de la nature inerte ou virulente de la particule qu'il contient. En effet, lorsque la particule internalisée est inerte (débris cellulaire, corps apoptotique, microorganisme non virulent), ce compartiment précoce devient mature, aboutissant à la formation d'un phagolysosome fonctionnel dont le contenu est dégradé. Cependant, lorsque la particule est un microorganisme intracellulaire, celui-ci utilise des stratégies variées afin d'éviter la maturation de la vacuole et le compartiment membranaire précoce est alors le siège d'une compétition entre l'hôte et le microorganisme. Ainsi, ces microorganismes intracellulaires altèrent la formation d'un phagolysosome délétère pour eux et favorisent l'élaboration d'une niche de survie et/ou de réplication. Par exemple, certaines bactéries mettent en place des systèmes de sécrétion leur permettant d'injecter, dans le cytoplasme de la cellule hôte, des complexes ADN-protéines ou des protéines modifiant le métabolisme cellulaire.

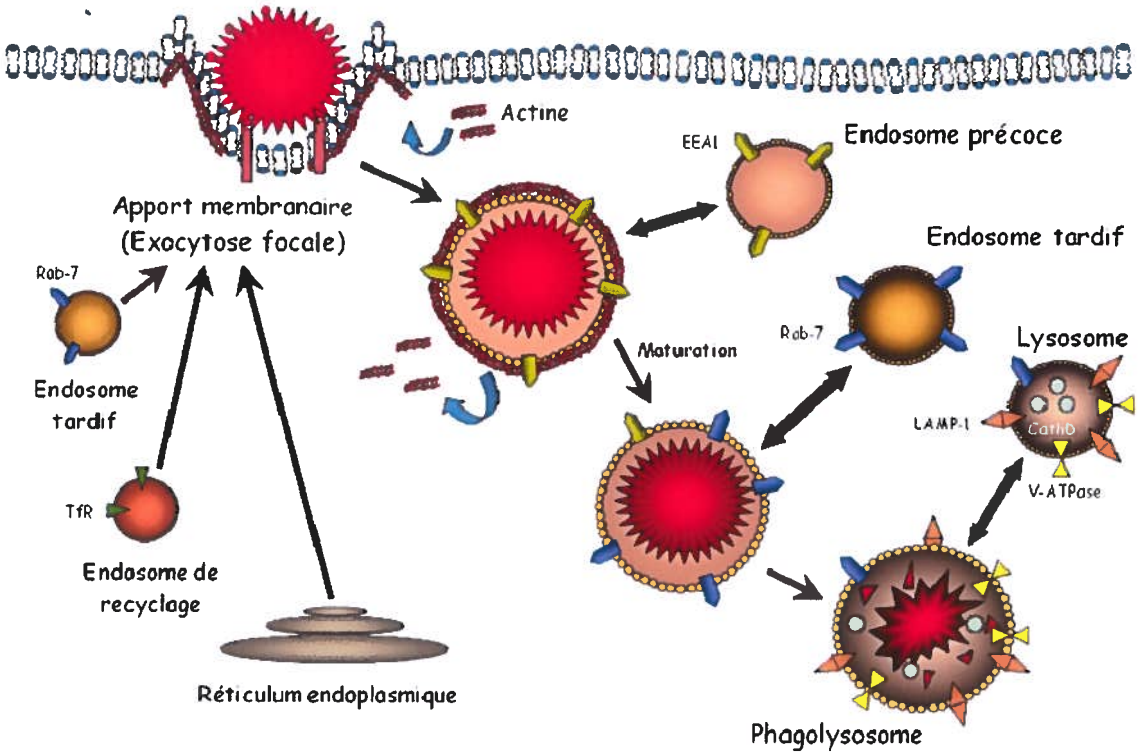

Figure 4: Modèle de phagocytose chez le macrophage. Le microorganisme est reconnu par les récepteurs phagocytiques, qui initient la formation du phagosome notamment via la réorganisation du cytosquelette d'actine. Lors de l'internalisation de particules de grande taille, une exocytose focale de vésicules internes apporte un supplément de membrane, nécessaire à la formation du phagosome précoce. Immédiatement après sa formation, le phagosome subit une dépolimérisation de l'actine l'entourant et amorce sa maturation notamment par des interactions avec le compartiment endosomal. Le processus de phagocytose aboutit finalement à la formation d'un phagolysosome hautement microbicide caractérisé, par exemple, par la présence d'hydrolases telles que la Cath D et par un contenu acide via l'acquisition de pompe à proton vacuolaire-ATPase (V-ATPase).

2.2.1 Le phagosome précoce

Les phagosomes nouvellement formés acquièrent rapidement les propriétés des endosomes précoces. Ainsi, ils ont la capacité de fusionner avec les endosomes précoces et les endosomes de recyclages mais sont inaptes à fusionner avec les lysosomes (Desjardins et al., 1997; Mayorga, Bertini, et Stahl, 1991). Leur lumen est légèrement acide et pauvre en activité hydrolytique (Mukherjee, Ghosh, et Maxfield, 1997). La petite GTPase Rab-5A est très importante pour le phagosome précoce puisqu'elle intègre un rôle de régulation pour le ciblage, la liaison et la fusion des endosomes précoces (Bucci et al., 1992). Rab-5A agit via divers effecteurs, incluant le complexe p150-hVPS34, EEA1 et des protéines SNARE. La kinase sur Ser et Thr p150 permet le recrutement de hVPS34, une PI3K de classe 3 qui génère à son tour PI(3)P sur la membrane du phagosome précoce (Vieira et al., 2001). PI(3)P permet l'ancrage des protéines effectrices telles que EEA1, sur la face cytosolique du phagosome via les domaines FYVE et PX (Gaullier et al., 1998; Kanai et al., 2001). EEA1, qui interagit également directement avec Rab-5 (Lawe et al., 2000), serait un pont qui lierait les endosomes précoces aux vésicules endocytiques entrantes (Callaghan et al., 1999), et aurait probablement un rôle équivalent au niveau des phagosomes. De plus, EEA1 interagit avec la Syntaxine 13 (McBride et al., 1999), une protéine SNARE requise pour la fusion membranaire, et des NSF essentielles au désassemblage et recyclage des complexes SNARE (Mills, Urbe, et Clague, 2001).

Des évènements de fissions membranaires régulent probablement la membrane du phagosome afin que celle-ci conserve une taille constante malgré les étapes répétées de fusion avec les vésicules endosomales. De manière similaire aux endosomes précoces, les auteurs pensent que les phagosomes seraient capables de recycler les molécules vers la membrane plasmique par un processus faisant intervenir COPI (Coat Protein I), les protéines Arf et des Rab GTPases (Botelho et al., 2000). Par exemple, Rab-11A, qui est connu pour réguler le recyclage des endosomes à la membrane plasmique, participe aussi à la récupération des constituants du phagosome au plasmalemme (Leiva et al., 2006). De

même que pour les endosomes, les protéines de la membrane phagosomale destinées à la dégradation subissent une ubiquitination et sont associées au complexe ESCRT requis pour le transport (Lee et al., 2005). Enfin, en plus du bourgeonnement à des fins de recyclage externe, les phagosomes détournent le contenu destiné à la dégradation vers des vésicules intraluminales. De telles vésicules seraient issues d'un bourgeonnement interne de la membrane du phagosome d'une manière similaire à la génération de corps multivésiculaires (MVB). Ce phénomène se produit initialement à un stade intermédiaire puisque ces vésicules possèdent des propriétés qui ne sont pas caractéristiques des phagosomes précoces, sans être typiques des phagosomes tardifs (Flannagan, Cosio, et Grinstein, 2009). Chez les MVBs, le composant final du complexe ESCRTIII force l'extrusion des vésicules à l'intérieur du lumen de l'organelle en conjonction avec l'ATPase VPS4A (Hanson et al., 2008; Muziol et al., 2006).

2.2.2 Le phagosome tardif

Une fois les protéines à recycler éliminées, le phagosome continue sa maturation vers un stade tardif, lequel est caractérisé par un pH luménal plus acide (5.5-6.0) via l'acquisition de pompes à proton V-ATPases (Desjardins et al., 1994). Le phagosome tardif est aussi enrichi en protéases et en LAMP. Il n'existe que peu de données sur le phagosome tardif (Desjardins et al., 1994). La petite GTPase Rab-7A, qui est un marqueur caractéristique de cet organelle, est connu pour son rôle de régulateur des échanges entre phagosomes et endosomes tardifs/lysosomes (Bucci et al., 2000; Harrison et al., 2003). Le complexe VpsC-HOPS (HOmotypic Protein Sorting), qui régule la transition des endosomes positifs pour Rab-5A vers des endosomes positifs pour Rab-7A (Rink et al., 2005), possède probablement une fonction similaire durant la maturation du phagosome. Cependant, alors que VpsC-HOPS régule les échanges vésiculaires et la fusion pendant la biogénèse du lysosome, ce complexe n'est pas nécessaire pour le recrutement de Rab-7A (Peterson et Emr, 2001; Poupon et al., 2003). Quoiqu'il en soit, Rab-7A permet le recrutement de plusieurs effecteurs à la membrane de la vacuole. Parmi ceux-ci, on retrouve RILP (Rab-Interacting Lysosomal Protein), qui permet le

mouvement centripète du phagosome tardif et des lysosomes en reliant la membrane au complexe moteur dynéine-dynactine (Harrison et al., 2003; Jordens et al., 2001). La fusion des endosomes et des lysosomes est favorisée lorsque ces organelles sont proches de la membrane de telle sorte que les protéines SNARE telles que VAMP7 et VAMP8 puissent compléter cette fusion (Antonin et al., 2000; Wade et al., 2001). La proximité physique pourrait également favoriser la fusion des phagosomes. Bien que nécessaires, Rab-7A et RILP ne sont pas les seuls régulateurs de la maturation du phagosome tardif. Il a été démontré par exemple qu'un antagoniste de la PI(3)K bloquait la maturation du phagosome malgré l'acquisition de Rab-7A et RILP (Vieira et al., 2003), ce qui implique qu'un mécanisme dépendant des inositides est aussi essentiel.

La récupération et l'élimination des composants de la membrane se produisent aussi durant ce stade. Tout comme les endosomes tardifs, les phagosomes tardifs contiennent des LBPA (Lysobisphosphatidic Acid), un lipide caractéristique que l'on retrouve au niveau du lumen des vésicules MVBs. PDCD6IP (Programmed cell death-6-interacting protein, aussi connu sous le nom d'ALIX), qui lie LBPA et peut lier ESCRTI et ESCRTIII (Odorizzi, 2006) dans les endosomes, participerait au processus de bourgeonnement interne.

2.2.3 Le phagolysosome

Le sommet culminant du processus de maturation représente le phagolysosme qui est alors l'organelle microbicide ultime. Les phagolysosomes sont dotés d'un armement complet et sophistiqué dans le but d'éliminer et de dégrader les microorganismes. Ils sont générés via la fusion des lysosomes par un processus dépendant de Rab-7A et sont fortement acides (pH luménal pouvant atteindre 4.5) via l'insertion de pompes V-ATPases supplémentaires nécessaires au maintient d'un tel pH. Les phagolysosomes peuvent être différentiés des phagosomes tardifs par leur pauvreté en LBPA ou en membrane enrichie en PI(3)P (Gillooly et al., 2000; Kobayashi et al., 1998), par leur contenu enrichi en cathepsines matures et par leur absence en récepteurs du mannose-6-

phosphate (Griffiths et al., 1988). Les phagolysosomes possèdent également des peptides cationiques ainsi qu'un système oxydant composé de la NADPH oxydase.

2.2.4 Acidification du phagosome

Durant sa maturation, le phagosome s'acidifie. Cette acidification semble être un pré-requis indispensable à la fonction microbicide du phagolysosome. Tout d'abord, la plupart des enzymes lysosomales digestives ont une activité optimale pour un pH acide. De plus, la production de peroxyde d'hydrogène et d'autres réactifs oxygénés nécessite de grandes quantités de protons (Vieira, Botelho, et Grinstein, 2002). Enfin, l'acidification est importante pour la maturation du phagosome elle-même.

L'acidification du phagosome se produit durant deux étapes. Tout d'abord une acidification précoce de faible ampleur a lieu, cependant les mécanismes mis en jeu sont mal connus (Hackam et al., 1997). Ensuite, les pompes à proton de type V-ATPase sont transférées à la membrane du phagosome durant les stades tardif de la maturation (Beyenbach et Wieczorek, 2006). Les pompes à proton V-ATPases qui acidifient le lumen du phagosome consistent en un complexe cytoplasmique V_1 qui hydrolyse l'ATP et transfère l'énergie à un complexe V_0 associé à la membrane qui transloque les ions H^+ au travers de la double couche lipidique (Beyenbach et Wieczorek, 2006). L'acidification du phagosome créée un environnement hostile qui entrave la croissance des microbes (Huynh et Grinstein, 2007): non seulement cela agit directement sur le métabolisme de certains microorganismes, mais cela favorise aussi l'activité de nombreuses enzymes du phagocyte dont l'activité optimale nécessite un certain pH acide. De plus, le gradient H^+ transmembranaire ainsi généré par la V-ATPase est utilisé pour expulser du lumen phagosomal les nutriments essentiels aux microorganismes. La V-ATPase facilite également la génération de superoxyde (O_2^-) en transportant les ions H^+ et compensant par conséquent les charges négatives transloquées par la NADPH oxydase. Les produits de l'oxydase peuvent aussi se combiner avec H^+ dans le lumen du phagosome pour générer des formes réactives oxygénées plus complexes (FRO).

L'acidification du phagosome n'est pas seulement une conséquence de la formation du phagolysosome, mais semble également un élément du processus de maturation puisqu'elle contrôle directement les échanges membranaires (Gordon, Hart, et Young, 1980). La dissipation du gradient de pH au travers de la membrane du phagosome par l'addition de bases faibles ou par interférence avec l'activité de l'ATPase arrête la maturation, empêchant la formation du phagolysosome. Ainsi, des études concernant la voie endocytique suggèrent que l'acidification est requise pour l'assemblage des complexes COPI (Aniento et al., 1996) et pour le recrutement d'Arf6 et de la cytohesine 2 (aussi connue sous le nom d'ARNO) (Hurtado-Lorenzo et al., 2006).

2.2.5 Réactifs oxygénés et espèces nitrogénées

La phagocytose est généralement accompagnée d'une génération d'ions superoxydes à partir des précurseurs des formes réactives de l'oxygène (FRO), par le complexe NADPH oxydase du phagocyte (Figure 5). Les NADPH oxydases de la famille Nox sont des protéines facilitant le transfert des électrons à travers les membranes biologiques. En général, l'accepteur d'électron est l'oxygène et le produit du transfert d'électron est l'anion superoxyde. L'enzyme NADPH oxydase est composée de multiples sous-unités qui sont désassemblées et inactives dans les cellules au repos. Elles s'assemblent au niveau de la membrane plasmique et phagosomale suite à l'activation du phagocyte. Ce complexe est composé du flavocytochrome b_{558} associé à la membrane (composé de deux sous-unités, $gp91^{phox}$ ou Nox-2 et $p22^{phox}$), de quatre composants cytosoliques, $p47^{phox}$, $p67^{phox}$, $p40^{phox}$ et la petite GTPase Rac (1 ou 2) (Nauseef, 2004). L'activation de la NADPH oxydase met en jeu différentes voies de signalisation aboutissant à la phosphorylation des sous-unités cytosoliques $p47^{phox}$ et $p67^{phox}$ et conduit à un regroupement des différents composants cytosoliques en un hétérotrimère $p47/p67/p40^{phox}$ à la membrane du phagosome, lequel interagit avec le flavocytochrome b_{558} (Bokoch et Diebold, 2002; Brown et al., 2003). La liaison de la sous-unité $p67^{phox}$ avec le cytochrome b_{558} induit la transition d'une conformation inactive en une forme active, ce qui permet le transfert d'électrons (Paclet et al., 2000). Le cytochrome b_{558} fixe

du NADPH et du FAD, et contient deux hèmes dont les potentiels d'oxydoréduction extrêmement bas lui permettent de réduire directement l'oxygène de l'air. L'importance des FRO pour l'élimination des microorganismes pathogènes a notamment été démontrée par des individus avec des mutations causant une inactivation partielle ou totale de l'oxydase (Babior, 2004). Ces patients souffrent de maladies granulomateuses chroniques caractéristiques d'infections récurrentes pouvant mener à la mort (Heyworth, Cross, et Curnutte, 2003).

Tout comme les FRO, l'oxyde nitrique (NO·) et les formes réactives nitrogénées (FRN) font partie des effecteurs antimicrobiens importants. Les FRN sont importants chez les macrophages chez lesquels ils ont été étudiés en détail. L'activité de la nitrique oxyde synthase induite (NOS2), l'isoforme le plus important pour les phagocytes, est régulée au niveau transcriptionnel. La production de FRN nécessite une synthèse *de novo* de la protéine en réponse à des agonistes proinflammatoires (Fang, 2004). La synthase fonctionne comme un dimère: une sous-unité transfère des électrons de la NADPH à la FAD, puis au FMN (Flavin Mononucleotide) et à l'hème du fer de la sous-unité adjacente, afin de produire le NO· et la citrulline, à partir de la L-arginine et de l'oxygène (Stuehr, 1999). Contrairement aux ions superoxides, NO· est synthétisé du côté cytoplasmique du phagosome, mais possède la capacité de diffuser au travers de la membrane pour atteindre les cibles intraphagosomales (Webb et al., 2001). Une fois au sein de l'environnement luminal où il rencontre les FRO, NO· peut procéder à une conversion spontanée ou catalytique aboutissant à la formation de divers FRN tels que le dioxyde nitrogène (NO2·), le péroxynitrite (ONOO-), le trioxyde dinitrogène (N2O3), les complexes de fer dinitrosyle, les nitrosothiols et le nitroxyl (HNO) (Fang, 2004). Les FRO et les FRN entrent en synergie pour exercer un effet fortement toxique envers les microorganismes intraphagosomaux. Ils interagissent avec de nombreuses cibles, telles que les thiols, les métaux, les résidus de protéines tyrosines, les acides nucléiques et les lipides. Ainsi les protéines sont inactivées et les lipides sont transformés par les dommages oxydatifs. De plus, l'ADN microbial peut être victime de dommages irréparables. Finalement, ces réactions affectent le métabolisme des microorganismes afin de prévenir leur réplication.

2.2.6 Les peptides et protéines antimicrobiennes

Une série de protéines contrecarrant la croissance des microorganismes complètent l'inventaire phagosomal des outils antimicrobiens (Figure 5). Elles peuvent être grossièrement subdivisées entre celles qui empêchent la croissance et celles qui compromettent l'intégrité du microorganisme.

2.2.6.1 NRAMP1

La prévention de la croissance peut être accomplie en limitant la disponibilité de nutriments essentiels à l'intérieur du phagosome. Les phagocytes secrètent ainsi des capteurs de fer dans le lumen ou insèrent des transporteurs dans la membrane phagosomale. Un tel capteur peut être la lactoferrine, une glycoprotéine contenu dans les granule du neutrophile et qui est relarguée dans le lumen phagosomal où il séquestre le fer nécessaire à certains microorganismes (Masson, Heremans, et Schonne, 1969). L'autre stratégie est illustrée par NRAMP1 (Natural Resistance-Associated Macrophage Protein 1, aussi appelée SLC11A1), qui est une protéine membranaire intégrale exprimée au niveau des endosomes tardifs et des lysosomes et qui est recrutée à la membrane du phagosome peu après l'internalisation du microorganisme. NRAMP1 exerce un effet bactériostatique en évacuant du lumen phagosomal des cations divalents tels que Fe^{2+}, Zn^{2+} et Mn^{2+} (Cellier, Courville, et Campion, 2007). Fe^{2+} et Zn^{2+} sont des cofacteurs d'enzymes microbiennes constitutives, et Mn^{2+} est nécessaire au fonctionnement de la superoxyde dismutase, une enzyme protectrice clé exprimée par certain microorganismes.

2.2.6.2 Défensines, cathélicidines, et lysozymes

Des mécanismes plus directs déployés par les phagosomes pour affecter l'intégrité des microorganismes pathogènes impliquent les défensines, les cathélicidines, les lysozymes, et un assortiment de lipases. Les défensines, lesquelles sont sous-divisées en groupes α et β, sont de petite taille, liées par des polypeptides disulphides d'environ 10

kDa, et emmagasinées chez les neutrophiles à l'intérieur des granules azurophiles ou primaires (Lehrer, Lichtenstein, et Ganz, 1993). Les défensines se lient aux molécules chargées négativement à la surface du microbe. Elles induisent alors une perméabilisation de la membrane des bactéries $Gram^+$ et $Gram^-$ en formant des canaux multimériques perméables aux ions (Lehrer, Lichtenstein, et Ganz, 1993). Les cathélicidines sont aussi de petites protéines d'environ 10 kDa, que les neutrophiles emmagasinent sous forme de précurseurs dans les granules secondaires (Zanetti, 2005). Ces précurseurs sont convertis en espèces actives par l'élastase, une protéine des granules primaires qu'elles rencontrent fort probablement dans le lumen phagosomal. Les cathélicidines agissent en perméabilisant la paroi cellulaire et la membrane interne des bactéries $Gram^+$, ainsi que les membranes internes et externes des bactéries $Gram^-$ (Lehrer, Lichtenstein, et Ganz, 1993).

2.2.6.3 Hydrolases

Les phagosomes sont aussi équipés d'un assortiment d'endopeptidases, d'exopeptidases et d'hydrolases qui dégradent divers composants microbiens. Les endopeptidases sont constituées de protéases sur cystéine et aspartate, alors que les exopeptidases sont constituées de protéases cystéine et sérine. Les endopeptidases et plus particulièrement la famille C1 des protéases cystéine sont particulièrement importantes, car elles génèrent de façon très efficace des substrats pour les exopeptidases (Pillay, Elliott, et Dennison, 2002). Dans les phagosomes, les cathepsines sont les hydrolases les plus abondantes et de nombreux membres de cette famille tels que les cathepsines B, D, H, L, S et Z composent le phagosome maturant (Claus et al., 1998; Garin et al., 2001; Lennon-Dumenil et al., 2002). L'acquisition et l'activation temporelle de ces hydrolases durant la maturation du phagosome sont essentielles au contrôle de son contenu protéolytique et conduit à une dégradation progressive des antigènes. Les antigènes ainsi générés possèdent la taille adéquate pour leur présentation à la surface des cellules par les molécules de classe II. De plus, il a été démontré que non seulement la cathepsine D participe à la dégradation de la particule en peptide, mais en plus possède un rôle essentiel dans l'activation de la protéine CMH II permettant l'apprêtement peptidique

(Bryant et al., 2002; Ramachandra, Boom, et Harding, 2008). Les cathepsines sont initialement synthétisées sous forme inactive avec un pro-peptide en N-terminal lié à leur site catalytique, empêchant une éventuelle activation au niveau du réticulum endoplasmique et de l'appareil de golgi. Lors de leur passage dans ce dernier, les cathepsines sont glycosylées et phosphorylées sur des résidus mannose, puis transportées vers les compartiments endosomaux via les récepteurs mannose-6-phosphate (Nakagawa et Rudensky, 1999). L'environnement acide des endosomes va favoriser le clivage du pro-peptide par auto-digestion ou par d'autres enzymes, afin de générer des hydrolases matures. Les hydrolases, et plus particulièrement les cathepsines qui résident au niveau des endosomes et des lysosomes, ont un pH optimal pour leur activité assez réduite, ce qui a l'avantage de confiner leur activité à des stades de maturation spécifiques du compartiment endosomal (Trombetta et Mellman, 2005). Par exemple, la Cath H possède une activité optimale pour un pH neutre alors que les Cath S, B, et L sont instables à un tel pH (Claus et al., 1998; Quraishi et al., 1999; Turk et al., 1999). La Cath D, quant à elle, possède une très bonne activité dans un milieu très acide (Horikoshi et al., 1998). Les cathepsines sont également régulées par certains inhibiteurs endogènes tels que la cystatine C (inhibe les Cath B, L et S) (Konduri et al., 2002; Pierre et Mellman, 1998; Vray, Hartmann, et Hoebeke, 2002) ou l'isoforme p41 de la chaine invariante Ii (inhibe les Cath L et H) (Bevec et al., 1996). La caractérisation du recrutement individuel des hydrolases a été documentée de manière biochimique, par immunofluorescence (Claus et al., 1998; Garin et al., 2001; Ullrich, Beatty, et Russell, 1999), et récemment, la mise au point d'outils quantitatifs a permis de définir plus précisément le statut hydrolytique du lumen phagosomal (Yates, Hermetter, et Russell, 2005; Yates, Hermetter, et Russell, 2009).

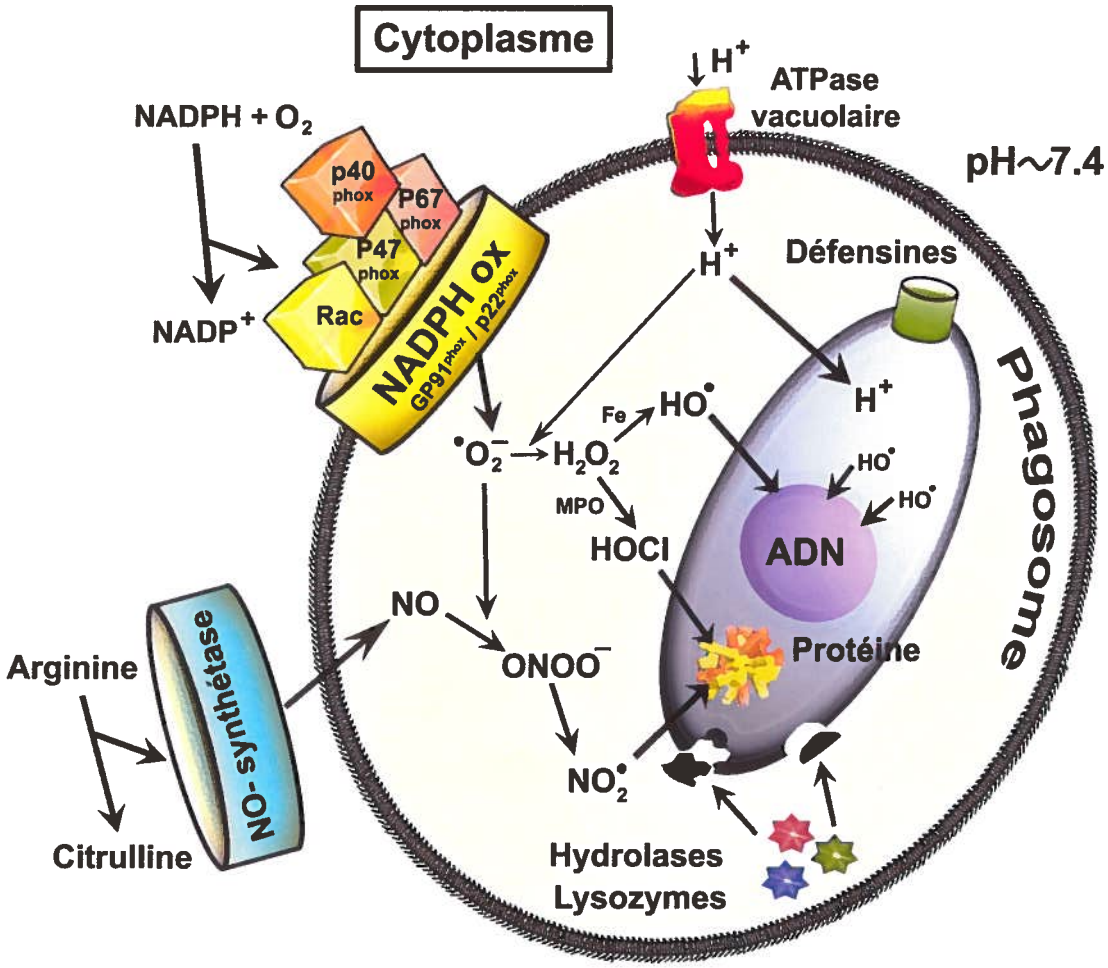

Figure 5: Activités microbicides du phagolysosome. Le phagolysosome possède diverses stratégies altérant l'intégrité de l'ADN, des lipides et/ou des protéines afin de tuer et dégrader les microorganismes phagocytés. Ces principales activités microbicides sont l'acidification du lumen phagosomal via le recrutement des pompes à proton V-ATPase à la membrane du phagosome, la production de réactifs oxygénés via la formation de la NADPH oxydase, la production de réactifs nitrogénés grâce à la NO synthétase, l'action de défensines, de lysozymes et de diverses hydrolases.

2.3 Rôle des microdomaines lipidiques de la membrane phagosomale

Les microdomaines lipidiques se composent principalement d'un assemblage de cholestérol et de sphingolipides au niveau du feuillet extracellulaire de la double bicouche lipidique, conférant une hétérogénéité intrinsèque à la membrane plasmique. Ainsi, selon leur affinité pour différents lipides, les protéines se distribuent de manière hétérogène au niveau de ces divers microdomaines. Par exemple, les molécules responsables de l'attachement des microorganismes peuvent s'associer à ces microdomaines membranaires provoquant une association des microorganismes avec ces domaines. Cela est le cas de bactéries telles que les *Mycobacteria* ou *Brucella*, pour lesquelles une accumulation de cholestérol a été démontrée au site d'entrée du macrophage, importante pour l'efficacité de son internalisation (Gatfield et Pieters, 2000; Naroeni et Porte, 2002). Il fut proposé également que le CR3 fonctionne en tant que récepteur pour *Mycobacterium kansanii* et nécessite une association avec les microdomaines lipidiques afin de réguler la phagocytose (Le Cabec, Cols, et Maridonneau-Parini, 2000). La phagocytose initiée via les récepteur Fc est dépendante des microdomaines lipidiques puisqu'il fut démontré que la phosphorylation sur tyrosine des récepteurs Fcγ par des Src résidant au niveau de microdomaines lipidiques intacts, était indispensable au réarrangement du cytosquelette d'actine nécessaire à la formation du phagosome (Strzelecka-Kiliszek, Kwiatkowska, et Sobota, 2002).

Les microdomaines lipidiques sont impliqués dans de très nombreux processus cellulaires importants et notamment diverses voies de signalisation (Kurzchalia et Parton, 1999). Des études ont démontré la nécessité de microdomaines intacts pour les mécanismes de fusion membranaire impliquant le recyclage des SNARE à la membrane plasmique par exemple (Lafont et al., 1999). Plusieurs études ont démontré la présence de ces microdomaines lipidiques au niveau de la membrane du phagosome (Dermine et al., 2001; Dermine et al., 2005; Winberg et al., 2009) et leur importance pour le bon fonctionnement de la phagocytose et de l'activité microbicide associée à celle-ci. Par exemple, les microdomaines sont importants pour la formation d'une NADPH oxydase

fonctionnelle et notamment pour le recrutement et l'orientation spatiale de protéines phox par rapport au cytochrome b_{558}. La désorganisation du cholestérol inhibe la production de FRO dû à une altération de la translocation des sous-unités cytosoliques phox à la membrane (Vilhardt et van Deurs, 2004). Un autre exemple plus indirect de l'importance de ces microdomaines lipidiques durant la phagocytose concerne la manipulation des fonctions du macrophage hôte par l'action du LPG, qui est le glycoconjugué le plus abondant de la surface du *Leishmania donovani* promastigote. En effet, celui-ci a pour effet une rétention d'actine suite à la formation du phagosome et une inhibition de la maturation du phagosome. Or, les résultats de plusieurs études suggèrent que le LPG s'insère au niveau des microdomaines et les désorganisent, ce qui expliquerait les effet du LPG sur la phagocytose de la cellule hôte (Dermine et al., 2001; Dermine et al., 2005; Winberg et al., 2009). Ces expériences démontrent notamment qu'une altération de l'intégrité de ces domaines via l'utilisation d'un composé chimique éliminant le cholestérol membranaire (méthyl-β-cyclodextrine) a pour conséquence de prévenir les effets du LPG, ce qui suggère fortement un rôle crucial des microdomaines intacts pour la dynamique du cytosquelette d'actine et la maturation du phagosome (Winberg et al., 2009). L'utilisation de la méthyl-β-cyclodextrine a également permis de mettre en évidence l'importance de ces microdomaines pour le bon fonctionnement de l'activité ATPase des pompes à proton. De plus, une analyse en spectrométrie de masse a démontré que la pompe à proton V-ATPase était un composant majeur des microdomaines. Ces résultats confirment ainsi un possible rôle de ces microdomaines qui pourrait être crucial dans le fonctionnement des facteurs microbicides du phagosome tardif (Yoshinaka et al., 2004).

3 *Les Synaptotagmines et la fusion membranaire*

3.1 La famille des Synaptotagmines

Les Synaptotagmines (Syts) sont une famille de protéines transmembranaires qui ont un rôle de «senseur calcique» (détecteur-effecteur) majeur dans l'exocytose synaptique mais également au niveau de cellules sécrétrices. Tous les membres de cette famille traversent la membrane une fois, possèdent un domaine luménal court en N-terminal et une importante région cytoplasmique en C-terminal contenant deux domaines C2 connectés par un court lien (Figure 6A). Les domaines C2 en tandem des synaptotagmines, identifiés avant tout sur l'isoforme Syt I au niveau des vésicules synaptiques (Perin et al., 1990), sont similaires à la région C2 régulatrice qui confère à certains isoformes des PKC une activité de liaison au Ca^{2+} et à la phosphatidylsérine (Nalefski et Falke, 1996; Sutton et Sprang, 1998). Les domaines C2A et C2B des Syts sont indépendamment constitués d'un repliement compact de type β en sandwich, formé par une double structure de quatre feuillets β. Les résidus acides (Asp) des boucles flexibles à l'intérieur des domaines C2 jouent un rôle crucial dans la coordination des ions Ca^{2+} (Figure 6B). Cependant des différences ont été découvertes dans la forme des poches de liaison du Ca^{2+}, dans le potentiel électrostatique de surface et la stoichiométrie des ions Ca^{2+} pour les deux domaines.

La Syt I, qui est l'isoforme le plus étudié jusqu'à maintenant, semble lier trois ions Ca^{2+} au niveau du domaine C2A, et deux au niveau du domaine C2B (Chapman, 2002; Fernandez et al., 2001; Sutton et al., 1995; Sutton, Ernst, et Brunger, 1999) via les poches constituées par les résidus Asp au bout des domaines C2 (Fernandez et al., 2001; Sutton et al., 1995). Ces liaisons provoquent alors un changement de charge de la région (négative vers positive) qui permet aux domaines C2 d'interagir et de s'insérer en partie au niveau des membranes chargées négativement (Herrick et al., 2006; Hui, Bai, et Chapman, 2006).

Plusieurs ligands des domaines C2 ont été rapportés pour la Syt I (et II) tels que des protéines, des cations divalents, des phospholipides ou des polyphosphates inositol solubles (Chapman, 2002; Sudhof, 2002)(Figure 7). Il a été proposé que leur liaison aux domaines C2 régulait l'exocytose et l'endocytose synaptiques. Par exemple, la liaison de la Syt I au complexe SNARE, dépendante du Ca^{2+}, permet la fusion vésiculaire synaptique dépendante du Ca^{2+} (Bai, Tucker, et Chapman, 2004; Tucker, Weber, et Chapman, 2004; Zhang et al., 2002). Cependant, une liaison indépendante du Ca^{2+} de la Syt I avec des t-SNARE hétérodimériques, impliquée dans l'exocytose de vésicules synaptiques, a également été décrite (Rickman et al., 2004a). De même, une liaison du domaine C2B indépendante du Ca^{2+} à la protéine AP-2 et/ou stonine-2 du complexe de la clathrine semble impliquée dans le contrôle de l'endocytose des vésicules synaptiques (Walther et al., 2004) (Figure 7). D'un point de vue structural, une séquence polybasique du feuillet β4 du domaine C2B est nécessaire pour la liaison de diverses molécules telles qu'AP-2 et les polyphosphates insitol (Fukuda et Mikoshiba, 1997), et pourrait réguler l'exocytose et l'endocytose des vésicules synaptiques. Un motif WHXL au niveau du feuillet β8 du domaine C2B semble aussi requis pour l'arrimage des vésicules synaptiques à la membrane plasmique (Fukuda et al., 2000). De plus, Il est nécessaire à la maintenance de la structure du domaine C2B. Ces liaisons, notamment au domaine C2B, ne sont pas totalement indépendantes et la liaison de ligands sur un site pourrait affecter la fonction des autres sites de liaison.

Les Syts I et II subissent plusieurs modifications post-traductionnelles (phosphorylation, N- et O-glycosylation sur le domaine extracellulaire (Fukuda, 2002), acylation au dessous du domaine transmembranaire (Fukuda et al., 2001)), et, par exemple, les glycosylations et palmitoylations de la Syt I seraient nécessaires au ciblage efficace de la Syt I vers les vésicules de sécrétion (Atiya-Nasagi et al., 2005; Han et al., 2004; Kang et al., 2004).

Des mutations au niveau des sites de liaison du Ca^{2+} sur les domaines C2 de Syts issues de neurones ont révélé des résultats surprenants. Par exemple, lorsque les sites de liaison du domaine C2A étaient neutralisés, une altération de la transmission synaptique n'a pas été observée (Stevens et Sullivan, 2003). De plus, la neutralisation d'un seul site

spécifique de liaison du Ca^{2+} a augmenté le relargage de manière comparable à une activation de ce site (Pang et al., 2006; Stevens et Sullivan, 2003). En ce qui concerne le domaine C2B, des substitutions au niveau des sites de liaison au Ca^{2+} ont démontré que le domaine C2B était absolument nécessaire aux fonctions des Syts (Mackler et al., 2002; Nishiki et Augustine, 2004). Toutefois, il est apparu que chaque site de liaison jouait des rôles différents.

La liaison du Ca^{2+} au domaine C2B joue donc un rôle plus critique que le domaine C2A lors de la transmission synaptique. Cette différence pourrait s'expliquer par le fait que le domaine C2B s'engage dans une liaison avec la PS et les protéines SNARE d'une manière distincte du domaine C2A, et participe spécifiquement à des interactions additionnelles indispensables à la fusion (liaison au PIP_2 et auto-association) (Fukuda et Mikoshiba, 2000; Schiavo et al., 1996).

Des différentes approches expérimentales utilisées pour définir la fonction des Syts durant l'exocytose provoquée par le Ca^{2+}, il apparaît que lorsque la liaison du Ca^{2+} est empêchée, la fusion est inhibée. Au contraire, lorsque le Ca^{2+} se lie de façon normale, les Syts permettent d'accélérer la fusion en effectuant un travail physique sur la double couche lipidique et les protéines SNARE. Par ces interactions (et sûrement d'autres), les Syts contrôlent la machine de fusion en fonction de la concentration intracellulaire en Ca^{2+}, ce qui inclut l'ouverture et la cinétique de dilatation des pores de fusion (Wang et al., 2006). Une surexpression de différents isoformes de Syts est associée à une modulation de la dilatation du pore de fusion (Wang et al., 2001). De plus, les différents domaines des Syts semblent contrôler le choix entre une fusion totale ou de type « kiss and run » (Wang et al., 2003).

Bien que des progrès significatifs aient été réalisés dans notre compréhension des mécanismes de l'exocytose provoquée par le Ca^{2+} et le rôle qu'y joue la Syt, de nombreuses questions restent sans réponses, notamment en ce qui concerne le mécanisme précis de régulation des Syts. Sans oublier que la complexité de la machine de fusion augmente au fur et à mesure que des protéines interagissant avec les SNARE sont mises en évidence.

L'ensemble des résultats fonctionnels et structuraux développés ci-dessus concernent la Syt I ou II, et, bien que les Syts partagent une structure similaire de leurs domaines et un haut degré d'homologie de leurs domaines C2, tous les membres de cette famille ne lient pas le Ca^{2+}. En effet, les Syts liant le calcium incluent les Syt I, II, III, V, VI, VII, IX et X. Les autres membres (Syt IV et XI à XVII) ne lient pas de Ca^{2+} dû au manque de résidus accepteurs ou d'une orientation spatiale des résidus acides spécifique. Des analyses détaillées n'ont pas encore été réalisées pour tous les isoformes, cependant de récentes études indiquent que les Syt I, II, III, V, VI, IX et X lient les membranes contenant de la phosphatidylsérine en fonction de la concentration en Ca^{2+} (Fukuda, 2003a; Fukuda, 2003b; Hui et al., 2005). En se basant sur leur affinité pour le calcium et la rapidité de l'exocytose qu'ils régulent, les isoformes de la famille des Syts ont été classifiés en trois groupes distincts (Hui et al., 2005). Il a été proposé que durant l'évolution, les Syts ont divergé afin de détecter différentes gammes de concentration en calcium. Cette diversification permet alors à ces isoformes de réguler la fusion de divers organelles avec la membrane plasmique selon la concentration en calcium (Sugita et al., 2002).

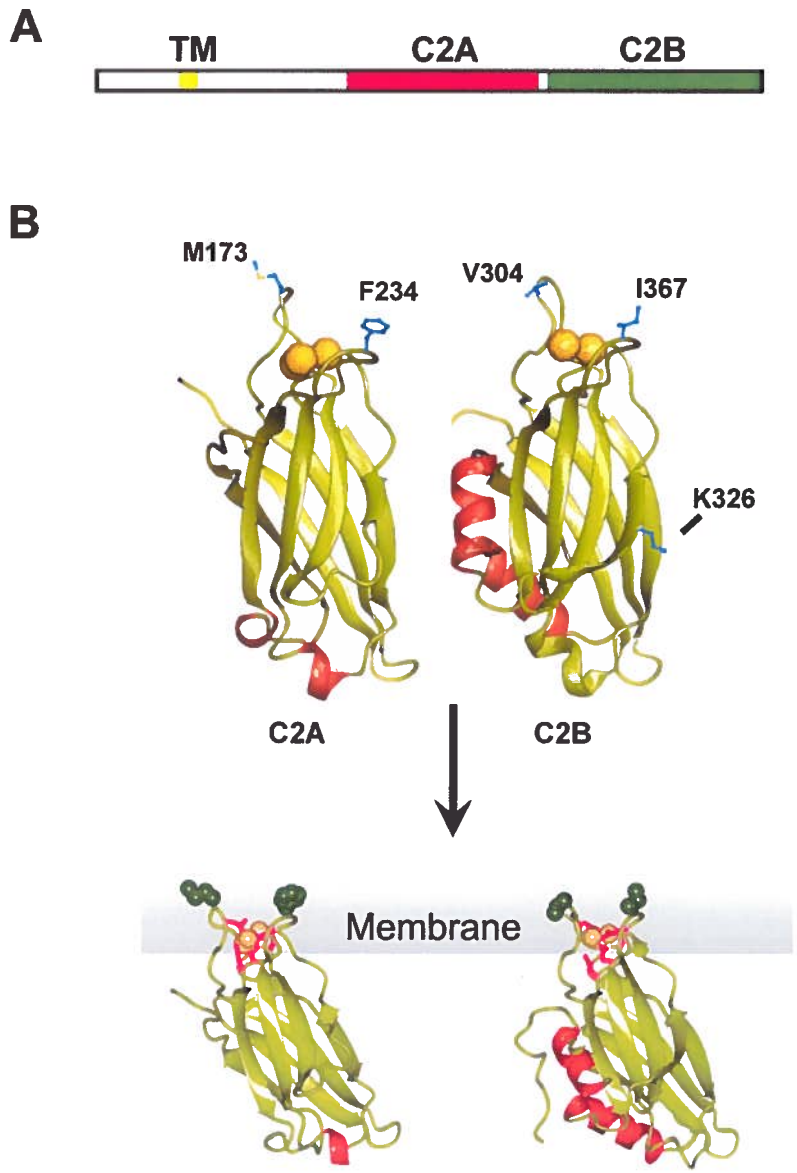

Adapté de (Fernandez et al., 2001; Sutton et al., 1995; Martens et McMahon, 2008)

Figure 6: Structure de la Syt I. A, représentation des différents domaines de la Syt I (TM, région transmembranaire). B, structure des domaines C2 de la Syt I. Les ions Ca^{2+} (sphères jaunes) se lient aux 5 résidus Asp (résidus rouge) sur les boucles au bout des domains C2A et C2B. Cette liaison neutralise le potentiel électrostatique négatif de surface de cette region et permet aux domaines C2 d'intéragir avec les lipides de la membrane.

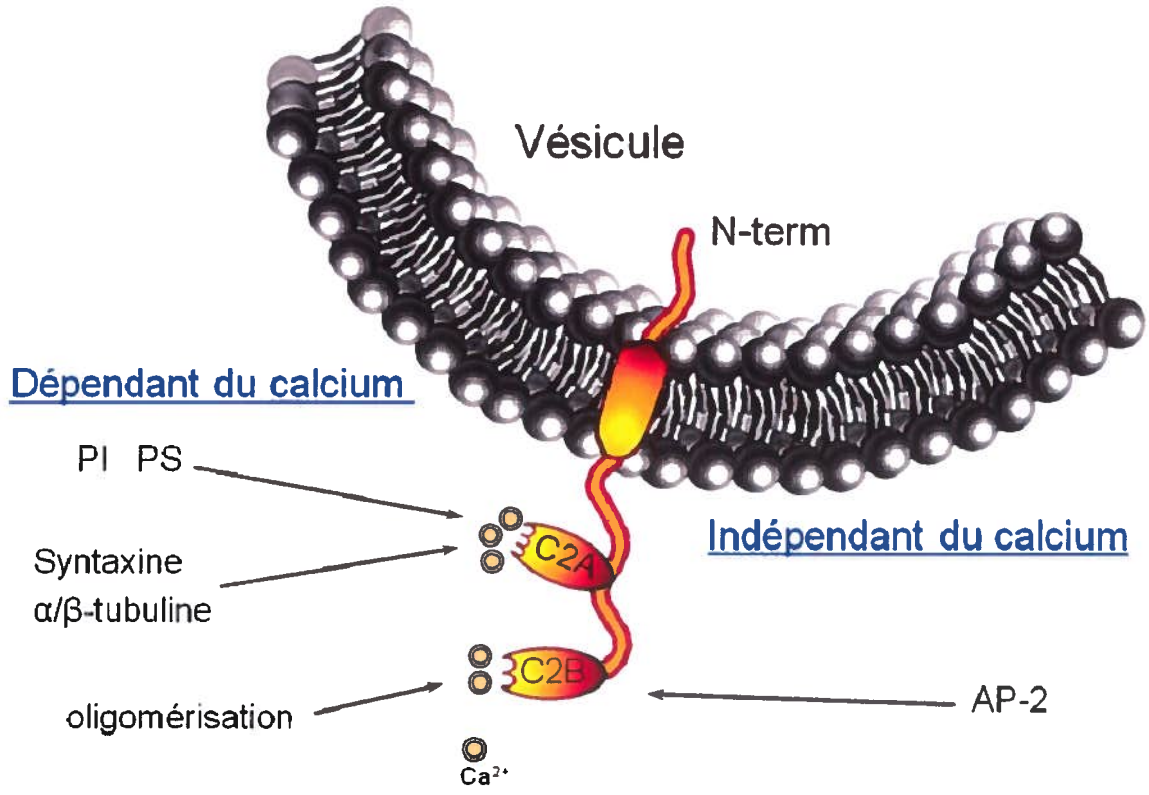

Figure 7: Exemples de partenaires des Syts. Les molécules se liant aux Syts d'une manière dépendante au calcium sont les plus étudiées, mais quelques liaisons indépendantes du calcium tel que le complexe AP-2 ont également été rapportées.

3.2 La fusion membranaire

Les cellules eucaryotes possèdent un réseau complexe de membranes intracellulaires et leurs différents compartiments (réticulum endoplasmique, appareil de Golgi, endosomes, lysosomes, membrane plasmique) communiquent entre eux grâce à des vésicules qui bourgeonnent d'un compartiment donneur et fusionnent avec un compartiment accepteur. Durant le trafic membranaire, trois étapes se succèdent: le bourgeonnement de vésicules à partir d'un compartiment donneur, le déplacement de ces vésicules vers un compartiment accepteur, et leur fusion avec ce dernier. Par le processus de fusion membranaire, les deux structures membranaires fusionnent en une seule et le contenu des compartiments se mélange de manière partielle ou totale. Par exemple, il en est ainsi au cours de l'exocytose lorsque la membrane de la vésicule de sécrétion fusionne avec la membrane plasmique et libère son contenu dans le milieu extracellulaire.

3.2.1 Les protéines impliquées durant la fusion membranaire

Au cours du trafic membranaire, les protéines SNARE ont un rôle clé. C'est James Rothman et ses collaborateurs, dans les années 1980, qui ont mis en évidence le rôle des protéines SNARE. En effet, leurs travaux sur le trafic membranaire leur ont permis d'observer que le transport de diverses molécules, au sein de l'appareil de Golgi reconstitué in vitro, était sensible au N-éthyl-maléimide qui est un puissant agent oxydant inhibiteur d'une classe d'ATPases. Ces travaux ont identifié la NSF (N-ethyl-maleimide sensitive factor) comme une protéine cytosolique ayant un rôle clé dans la fusion membranaire. L'attachement de NSF aux membranes dépend d'autres protéines cytosoliques: les SNAP (soluble NSF attachment proteins). Par la suite, la recherche des récepteurs membranaires du complexe NSF-SNAP a permis d'isoler des récepteurs aux SNAP ou SNARE.

Plusieurs membres de la famille des SNARE ont été identifiés. Les principaux sont la synaptobrévine ou VAMP (vesicle associated membrane protein) qui sont des SNARE vésiculaires (v-SNARE), ainsi que la syntaxine et SNAP-25 (synaptosomal associated protein of 25 kDa) qui sont, quand à elles, des SNARE cibles (t-SNARE) (Sollner et al., 1993). Les dernières expériences qui ont permis d'identifier les différentes protéines SNAREs furent effectuées à partir d'un extrait de cerveau. Les cellules neuronales sont en effet un modèle de choix car elles sont le siège de très nombreux processus mettant en jeu des fusions membranaires notamment au cours de la libération de neurotransmetteurs par les vésicules synaptiques.

3.2.2 Les étapes de fusion membranaire et leur régulation

3.2.2.1 L'arrimage

La fusion membranaire comprend plusieurs étapes (Figure 8). L'une des étapes précédant la fusion membranaire consiste en l'arrimage des vésicules avec leur membrane cible (Figure 8). Les SNARE ne jouent probablement pas un rôle important dans cette phase précoce. D'autres protéines, appelées facteurs d'arrimage (tethering factors) sont impliqués dans cette étape comme par exemple le complexe protéique appelé exocyste (Sec3p, Sec5p, Sec6p, Sec8p, Sec10, Sec15p, Exo70p, Exo84p) qui est impliqué dans l'arrimage des vésicules d'exocytose à la membrane plasmique chez la levure en marquant des domaines spécifiques de la membrane plasmique où se produit l'exocytose (Finger et Novick, 1998). Plusieurs sous-unités de l'exocyste interagissent avec des petites GTPases impliquées dans le trafic membranaire. Il existe également d'autres complexes protéiques du même type que l'exocyste tels que Vps52/53/54 appelé VFT (Vps fifty three), qui est impliqué dans le transport des endosomes vers l'appareil de Golgi, Sec34/35, qui joue un rôle dans le transport rétrograde au sein de l'appareil de Golgi (Whyte et Munro, 2001). La fusion homotypique d'endosomes précoces implique la petite GTPase Rab-5, son facteur d'échange rabex5, son effecteur la rabaptine-5, la protéine EEA1 et la syn 13, une t-SNARE des endosomes qui serait activée localement

par EEA1 (Christoforidis et al., 1999). L'ensemble de ces données suggère que l'arrimage met en jeu des complexes de protéines, recrutées séquentiellement sous la dépendance d'un signal contrôlé par des petites GTPases et pourraient définir les sites de fusion membranaire, probablement en activant localement la machinerie SNARE.

3.2.2.2 L'amorçage

La seconde étape représente l'amorçage, important dans la préparation de la fusion membranaire. Les mutations des gènes codant pour les protéines Sec1/Munc18 et Munc13 par exemple, induisent des phénotypes de défaut de sécrétion chez la levure, le nématode et la souris (Verhage et al., 2000). La protéine n-Sec1/Munc18 interagit avec l'extension N-terminale des syntaxines et les maintient dans une conformation fermée (Misura, Scheller, et Weis, 2000). En effet, le domaine N-terminal de la syntaxine se replie sur son motif SNARE, empêchant ainsi la formation des complexes avec les v-SNARE et inhibant la fusion membranaire. L'activation de la syntaxine se fait si n-Sec1/Munc18 est déplacée par Munc13, un autre partenaire du domaine N-terminal de la syntaxine. Munc13 a été particulièrement bien étudié dans les neurones dans lesquels cette protéine joue un rôle primordial dans l'amorçage de la libération de neurotransmetteurs en activant la syn 1 (Ashery et al., 2000). Alors que des homologues de n-Sec1/Munc-18 contrôlent les autres voies de trafic membranaire, les homologues de Munc13 sont très peu connus.

3.2.2.3 La régulation par les synaptotagmines

La fusion membranaire est finement contrôlée. Dans le cas de l'exocytose conduisant à la libération de neurotransmetteurs ou d'hormones par exemple, le phénomène de fusion est déclenché par une augmentation de la concentration intracellulaire de calcium. Les Syts, qui sont des protéines transmembranaires en majorité sensibles au calcium, sont présentes au niveau des vésicules et impliquées dans cette régulation. En effet, l'augmentation de calcium stimule l'interaction des Syts avec le

complexe SNARE et les phospholipides (Davis et al., 1999). Les Syts seraient alors responsables de la dépendance au calcium de la libération de neurotransmetteurs (Fernandez-Chacon et al., 2001). Il est possible que la Syt participe également à la génèse du pore de fusion (Wang et al., 2001) c'est à dire qu'avant l'entrée du calcium, elle bloquerait la fusion, le complexe SNARE étant partiellement assemblé, puis, après l'entrée de calcium, elle se lierait au complexe SNARE et permettrait ainsi la fusion membranaire (Figure 8).

3.2.2.4 Le recyclage des SNARE

La dissociation des complexes SNARE est une étape importante. En effet, chaque vacuole porte à la fois des v- et des t-SNARE qui sont dissociées par NSF et les SNAP, pour être libérées et de nouveau disponibles (Littleton et al., 2001; Mayer, Wickner, et Haas, 1996). Au cours de cet événement, la synaptobrévine et les autres protéines vésiculaires se retrouvent dans la membrane plasmique et la v-SNARE est renvoyée vers son compartiment donneur d'origine. Dans la synapse, la synaptobrévine est recyclée par endocytose d'une manière dépendante du calcium, dans de nouvelles vésicules synaptiques qui participeront aux prochaines vagues de libération de neurotransmetteurs (Sankaranarayanan et Ryan, 2001). L'homéostasie cellulaire est ainsi maintenue à chaque instant par un perpétuel recyclage des protéines SNARE.

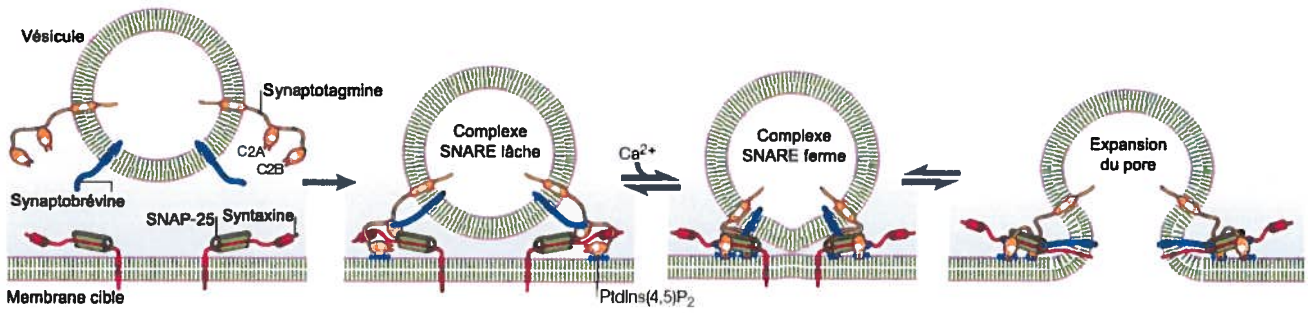

Adapté de (Chapman, 2002)

Figure 8: Rôle de la Syt au cœur de la machinerie de fusion membranaire. Les acteurs de cette machinerie, présentés ici, sont la Syt, les SNARE (synaptobrevine, syntaxine et SNAP-25) et le PI(4,5)P2. Il est clair que d'autres facteurs jouent un rôle dans le processus d'exocytose/endocytose mais ils ne sont pas considérés pour ce schéma. Durant l'étape d'arrimage, les complexes SNAREs puis la Syt s'assemblent partiellement, créant un état de fusion intermédiaire. Suite à l'afflux de calcium, la Syt lie à la fois les ions calcium et les phospholipides de la membrane, ce qui cause une perturbation mécanique responsable de la formation d'un pore de fusion. Les détails moléculaires concernant les interactions entre la Syt et le complexe SNARE, ainsi que les détails sur les changements de conformation provoqués par l'afflux calcique sont à déterminer.

3.3 Rôle des Synaptotagmines chez les phagocytes

3.3.1 La Synaptotagmine II

Chez les neutrophiles, les granules fusionnent avec la membrane plasmique ou avec la membrane du phagosome d'une manière dépendante du calcium et la fusion de chaque type de granule nécessite une concentration différente de Ca^{2+} (Borregaard et al., 1993; Lew et al., 1986; Nusse et al., 1998; Rosales et Ernst, 1997). Cette fusion est non seulement nécessaire à la sécrétion et à la régulation des récepteurs membranaires, mais elle est également nécessaire à la phagocytose et la formation des pseudopodes (Booth, Trimble, et Grinstein, 2001; Jaconi et al., 1990). La Syt II a été identifiée par western blot chez les neutrophiles humains et semblerait associée spécifiquement aux granules (Lindmark et al., 2002). Suite à une stimulation au fMLP, la Syt II est transloquée à la membrane plasmique. De plus, la Syt II est aussi transloquée au phagosome lors d'une phagocytose initiée via les récepteurs du complément en présence de Ca^{2+}, tout comme LAMP-1, bien que ces deux protéines semblent être présentes sur des compartiments différents (Lindmark et al., 2002). Même si les auteurs envisagent un potentiel rôle de la Syt II dans la régulation dépendante du Ca^{2+} de l'exocytose du neutrophile et durant les évènements de fusion du phagolysosome, aucune étude n'a pour le moment confirmé ces hypothèses.

3.3.2 La Synaptotagmine VII

Tout comme la Syt I, la Syt VII est un membre de la famille des Syts très conservé au cours de l'évolution, et se trouve associée aux lysosomes. Un des rôles de la Syt VII concerne la régulation de l'exocytose lysosomale (Martinez et al., 2000; Reddy, Caler, et Andrews, 2001; Roy et al., 2004) ce qui a amené les auteurs à définir un possible rôle de cet isoforme lors de la phagocytose. Leurs résultats indiquent que la Syt VII est impliquée dans le mécanisme d'apport membranaire issu de lysosomes vers le

phagosome naissant, et que ce mécanisme nécessite la présence de Ca^{2+} intracellulaire (Czibener et al., 2006). Ces données confirment également l'implication des vésicules lysosomales lors de l'exocytose focale. La Syt VII joue aussi un rôle lors de la fusion phagolysosomale et permet de limiter la croissance intracellulaire de bactéries pathogènes, telles que *Salmonella typhimurium* ou *Yersinia pseudotuberculosis*, par un mécanisme analogue à la régulation de l'exocytose lysosomale initiée par une altération de la membrane (Roy et al., 2004). Ainsi, la réponse de réparation membranaire pourrait protéger les cellules contre les agents pathogènes provoquant une perméabilisation de la membrane de la cellule hôte. En effet, les systèmes de sécrétion de type III bactériens, qui perméabilisent la membrane et causent un influx de Ca^{2+}, favorisent l'exocytose des lysosomes et inhibent la survie intracellulaire chez les cellules issues de souris WT mais pas pour des cellules issues de souris Syt VII $^{-/-}$ (Roy et al., 2004).

3.4 La Synaptotagmine V

Les deux isoformes Syt V et IX sont présentes au niveau des vésicules à cœur dense de certaines cellules endocrines et sont impliquées dans le contrôle de l'exocytose (Fukuda et al., 2002; Iezzi et al., 2004; Lynch et Martin, 2007; Saegusa, Fukuda, et Mikoshiba, 2002; Shin et al., 2004; Tucker et al., 2003; Zhang et al., 2002). Bien que les Syt V et IX appartiennent à des sous-familles différentes de Syts (Sudhof, 2002), elles sont souvent confondues dans la littérature car deux séquences différentes de la Syt V ont été rapportées en même temps par différents groupes, et chacune d'elles fut souvent référencées comme Syt IX (Craxton et Goedert, 1995; Hudson et Birnbaum, 1995; Li et al., 1995). À cause de cette confusion, il est très difficile de distinguer les deux isoformes Syt V (ou Syt IX) par leur nom. Dans le but de les distinguer, le tableau 1 (Fukuda et Sagi-Eisenberg, 2008) décrit en résumé les points importants à considérer. Ainsi, le nombre d'acides aminés (491 AA pour Syt V Vs 386 AA pour Syt IX), la similarité de séquence avec les autres isoformes (III/V/VI Vs I/II/IX) et les citations, (Li et al., 1995) vs (Craxton et Goedert, 1995), permettent de les distinguer. La Syt V de 386 AA identifiée par Craxton est en général appelée Syt IX et nous avons décidé d'adhérer à

cette nomenclature. Seule Molly Craxton a appelé la Syt V de 491 AA identifiée par Li et al. Syt IX dans ses publications suivantes.

Très peu d'études se sont intéressées à la Syt V. Il a été démontré que la Syt V était exprimée au niveau des cellules neuronales, des cellules α du pancréas et des cellules β issues de la lignée cellulaire INS-1E (Iezzi et al., 2004; Saegusa, Fukuda, et Mikoshiba, 2002). Le traitement des cellules par des siRNA Syt V cause une réduction dramatique de la sécrétion d'hormone par les cellules INS-1E (Iezzi et al., 2004), suggérant que la Syt V fonctionne aussi comme un « senseur calcique » lors de l'exocytose de vésicules à cœur dense.

	Syt V (491 AA/Li-Syt V)	Syt IX (386 AA/Craxton-Hudson-Syt V)
Taille (AA)	491	386
Chromosome	11p15.4 (humain), 7 F2 (souris), 1q33 (rat)	19q (humain), 7A1 (souris), 1q12 (rat)
Gène dans la base de données	Syt9	Syt5
Sous-famille de Syts	Syts I, II et IX	Syts III, V, VI et X
Distribution tissulaire	Cerveau	Cerveau
Localisation subcellulaire	Vésicules à cœur dense chez les neurones et les cellules-α du pancréas	Vésicules à cœur dense chez les cellules endocrines. Compartiment de recyclage perinucléaire chez les mastocytes RBL-2H3
Fonction proposée	« Senseur calcique » potentiel pour l'exocytose des vésicules à cœur dense	Potentiel senseur calcique pour l'exocytose des vésicules à cœur dense des cellules endocrines. Control du relargage protéique par les granules des mastocytes
Anticorps disponibles commercialement	Aucun	Anti-Syt V (BD Transduction/Santa Cruz)
Références (citées en tant que Syt V)	(Fukuda, Kanno, et Mikoshiba, 1999; Iezzi et al., 2004; Saegusa, Fukuda, et Mikoshiba, 2002)	(Craxton, 2001; Craxton, 2004; Craxton et Goedert, 1995; Craxton, Olsen, et Goedert, 1997; Hudson et Birnbaum, 1995)
Références (citées en tant que Syt IX)	(Craxton, 2001; Craxton, 2004)	(Fukuda, 2004; Fukuda, 2006; Fukuda et al., 2002; Grise et al., 2007; Haberman et al., 2003; Haberman et al., 2005; Haberman et al., 2007; Iezzi et al., 2005; Iezzi et al., 2004; Li et al., 1995; Lynch et Martin, 2007; Rickman et al., 2004b; Shin et al., 2004; Tucker et al., 2003; Zhang et al., 2002)

D'après (Fukuda et Sagi-Eisenberg, 2008)

Tableau 1: Éléments à considérer afin de distinguer les Syt V et IX dans la littérature et les bases de données.

4 *Généralités sur le parasite Leishmania et la leishmaniose*

4.1 Le parasite *Leishmania*

Les *Leishmania* spp. sont des parasites protozoaires qui causent diverses maladies chez l'homme, de l'infection cutanée limitée au soi jusqu'à la leishmaniose disséminante et diffuse de type cutanée, mucocutanée et viscérale. Le contrôle de cette maladie, qui affecte plus de 20 millions de personnes mondialement, est entravé par l'absence de vaccin.

4.2 Manifestation clinique

Les leishmanioses regroupent un large éventail de maladies parasitaires qui ont pour caractéristiques symptomatologiques communes : fièvre, abdomen volumineux, faiblesse généralisée, maux de tête et vertiges, perte de poids, transpiration abondante et diarrhée. On distingue principalement trois types de leishmanioses (Figure 9). Durant la leishmaniose viscérale, aussi appelée Kala-azar, *L. donovani* se dissémine et infecte les macrophages du foie, de la rate et de la moelle osseuse. Cette infection est chronique et mortelle si elle n'est pas traitée. La leishmaniose cutanée, une infection caractérisée par la présence de lésions ulcérantes de la peau, est causée par *L. major*, *L. tropica*, *L. mexicana* et diverses espèces et sous-espèces d'Amérique du sud. Dans la plupart des cas, les lésions guérissent, bien que certaines formes persistent et se disséminent. La leishmaniose mucocutanée, une variante de la forme cutanée, est causée par *L. braziliensis braziliensis*. Ce parasite possède un tropisme particulier pour les macrophages de la région oro-naso-pharyngienne. Le tropisme spécifique pour certains tissus des espèces de *Leishmania* reste un phénomène très peu connu. De nombreux facteurs pourraient être impliqués tels que la sensibilité du parasite à la température et au complément, ou bien la permissivité des diverses populations de macrophage.

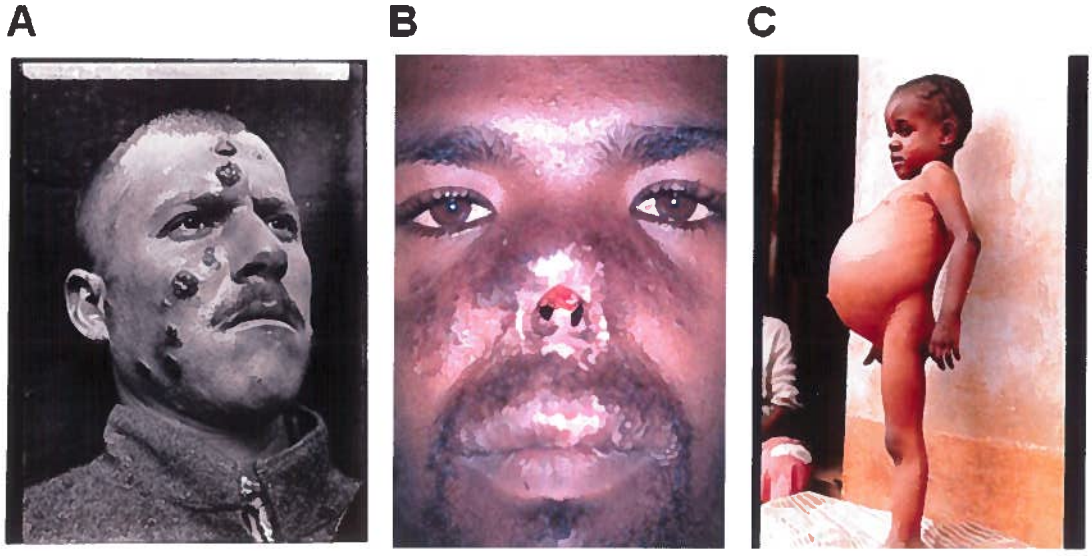

Figure 9: Les différents types de Leishmanioses. *A*, papules de la leishmaniose cutanée. *B*, destruction de la paroi nasale due à la leishmaniose muco-cutanée. *C*, hépatosplénomégalie causée par la leishmaniose viscérale.

4.3 Épidémiologie

Selon l'OMS, les leishmanioses sont endémiques dans 88 pays (dont 72 sont des pays en développement) et 4 continents : Afrique, Amérique du nord et du sud, Asie et Europe. Au total, 350 millions de personnes sont exposées au risque de la maladie. Le taux de létalité de la maladie est souvent très élevé en raison de l'absence de moyens diagnostiques et de médicaments. La leishmaniose viscérale non traitée a un taux de létalité de 100%, alors que sous traitement, ce taux est de 10%. Chaque année, on compte 2 millions de nouveaux cas des diverses formes de leishmanioses (dont 500 000 pour la forme viscérale) et le nombre de cas de leishmanioses dans le monde entier est estimé à 12 millions, 1/3 seulement des nouveaux cas étant officiellement déclarés.

4.4 Traitements

La thérapie contre la leishmaniose est principalement basée sur l'antimoine pentavalent qui fut développé durant la première moitié du siècle dernier, mais qui est toxique. Ces dernières décennies, des médicaments alternatifs sont devenus disponibles (Croft, Seifert, et Yardley, 2006), cependant, la plupart des thérapies contre la leishmaniose sont issues de re-formulation de médicaments déjà connus. Ceci est en grande partie dû au fait que, d'une part la biologie du parasite et d'autre part, la réponse immunitaire de l'hôte, ne sont pas bien connus (Croft et Yardley, 2002; Scott, 2003).

En réalité, l'ensemble du développement de nouveaux médicaments contre la leishmaniose est lent. Par exemple, la paramomycine fut décrite au milieu des années 1980 comme efficace contre les leishmanioses cutanées et viscérales, mais n'est entrée en phase clinique que récemment. De même, la sistamaquine fut identifiée au milieu des années 70 et depuis, seules les phases d'essais I / II ont été complétées avec divers degrés de succès (Croft, Seifert, et Yardley, 2006; Jha et al., 2005). Finalement, l'efficacité de la miltefosine est connue depuis le milieu des années 80, mais elle n'entra sur le marché comme un médicament de choix contre la leishmaniose viscérale qu'en 2002 en Inde, et

en 2005 contre la leishmaniose cutanée en Colombie (Croft, Seifert, et Yardley, 2006; Soto et al., 2004). Cependant, l'utilisation de la miltefosine est limitée dû aux effets secondaires tératogènes et à un potentiel développement d'une résistance (Perez-Victoria, Castanys, et Gamarro, 2003; Singh et Sivakumar, 2004).

Il est à noter que les antimoniaux pentavalents toxiques, qui constituent le principal traitement de la leishmaniose, ont presque été abandonnés en Inde en raison du manque de réponse de *Leishmania donovani* contre la glucantime et la N-méthyl glucamine, bien qu'elles soient encore efficaces dans le reste du monde (Croft, Seifert, et Yardley, 2006; Croft et Yardley, 2002). Une formulation liposomale d'amphotéricine B (AmBisome) est maintenant utilisée en Inde, même si l'amphotéricine B et la pendamidine sont fortement toxique et causent des effets secondaires déplaisants tels que la fièvre (Chia et McManus, 1990; McGuire et al., 2005).

Il ne faut pas oublier non plus que malheureusement, une mauvaise utilisation des composants antileishmanioses a provoqué une augmentation de la fréquence des résistances aux médicaments et à contribué à l'émergence de co-infections avec le virus d'immunodéficience humain (VIH) (Cohen, 1992; Desjeux, 2004; Singh et Sivakumar, 2004).

4.5 Cycle de vie de *Leishmania donovani* (Figure 10)

La transmission du parasite est orchestrée par la mouche des sables femelle du genre *Phlebotomus* (dans l'ancien monde) ou du genre *Lutzomyia* (dans le nouveau monde). Dans le tube digestif de l'insecte vecteur, les parasites existent sous la forme promastigote, celle-ci mesurant approximativement 10 à 20 µm de long et 2 µm de large avec un long flagelle antérieur. Ces promastigotes non infectieux qui se divisent (procyclique) sont attachés à l'épithélium du tube digestif et se transforment en une forme infectieuse qui ne se divise plus (métacyclique) (Sacks, 1989). Les promastigotes métacycliques se détachent ensuite des cellules de l'épithélium digestif et migrent vers la

zone antérieure du tractus digestif. L'injection des promastigotes infectieux dans le vertébré hôte se produit suite au repas sanguin de la mouche des sables infectée. Une fois à l'intérieur de l'hôte, les promastigotes résistent à l'action lytique du complément et sont phagocytés par les macrophages, directement ou après l'infection de neutrophiles initialement recrutés au site de piqûre du moustique (van Zandbergen et al., 2004). Une fois à l'intérieur du macrophage, les parasites se transforment en amastigotes qui ont une forme ovale ou ronde et une taille de 2 à 5 µm sans flagelle. Cette forme prolifère à l'intérieur d'un compartiment phagolysosomal acide riche en hydrolases (Alexander et Vickerman, 1975; Chang et Dwyer, 1976). La prolifération des parasites cause par la suite une rupture des macrophages et une libération des amastigotes qui peuvent infecter d'autres macrophages ainsi que d'autres cellules phagocytiques (telles que les cellules dendritiques) ou phagocytiques non professionnelles (telles que les fibroblastes) dans une moindre mesure. Lorsqu'elle se nourrit sur un mammifère infecté, la mouche des sables peut ingérer des cellules contenant des amastigotes et durant la digestion du repas sanguin, les amastigotes sont relargués. Ils se différentient en promastigotes pouvant s'attacher à l'épithélium du tube digestif pour éviter d'être excrétés.

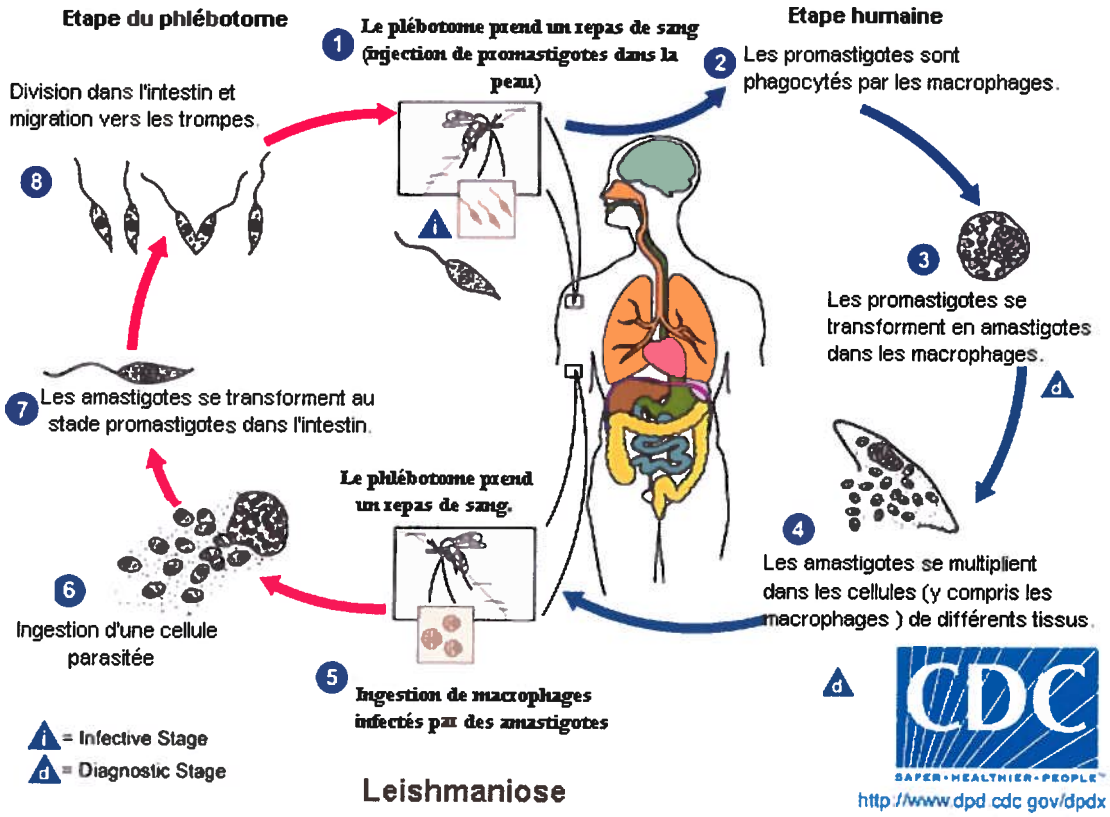

Figure 10: Cycle de vie de *Leishmania donovani*.

4.6 Le lipophosphoglycan (LPG)

Le LPG est le glycolipide de surface le plus abondant de la forme promastigote, avec approximativement 5 millions de copies par cellule. Les niveaux de LPG sont au contraire très fortement régulés à la baisse chez les amastigotes. La structure de cette molécule, qui comprend 4 domaines, est illustrée par la figure 11A (Turco et Descoteaux, 1992). Les 4 domaines du LPG de *L. donovani* sont : (i) une ancre 1-*O*-alkyl-2-*lyso*-phosphatidyl(*myo*)inositol, (ii) un core glycan, (iii) des unités répétées Galβ1,4Manα1-PO_4, et (iv) une coiffe d'oligosaccharide. Il existe un polymorphisme spécifique à l'espèce ou à la souche au niveau de la coiffe et de la structure des unités répétées, alors que l'ancre lipidique et le core glycan sont conservés (Turco et Descoteaux, 1992). De plus, durant la métacyclogénèse, le LPG subit une transformation menant à doubler ses unités répétées (Figure 11B). L'élongation du LPG est aussi accompagnée de changements dans la structure de la coiffe et de substitutions des unités répétées, ce qui permet la régulation de la liaison du parasite sur l'épithélium du tube digestif de la mouche des sables, ainsi que de son relargage lors d'un repas sanguin (Sacks et Kamhawi, 2001).

Afin d'étudier le rôle de ces phosphoglycans au niveau du vecteur et de l'hôte, plusieurs mutants au niveau de la synthèse de composants du LPG et du Galβ1,4Manα1-PO_4 ont été utilisés pour diverses espèces de *Leishmania* (Figure 11C). Ainsi, chez *Leishmania donovani*, le mutant *lpg1*-KO sécrète les unités répétées Galβ1,4Manα1-PO_4 de la même manière que la souche sauvage, mais ne possède pas l'habilité d'assembler un core glycan LPG fonctionnel (Huang et Turco, 1993), ce qui exclut l'expression d'un LPG de pleine taille à la surface du parasite. Le mutant *lpg2*-KO exprime un LPG tronqué Gal(α1,6)Gal(α1,3)Gal(β1,3)[Glc(α1-P)]Man(α1,3)Man(α1,4)GN(α1,6)-PI, et est incapable de synthétiser les unités répétées Galβ1,4Manα1-PO_4 (Descoteaux et al., 1995). Ces mutants ont mis en évidence que l'importance des phosphoglycans dans l'établissement de l'infection à l'intérieur du macrophage n'était pas universelle. En effet, le cas de *L. mexicana* montre que les glycoconjugués contenant le Galβ1,4Manα1-PO_4 ne

sont pas nécessaires à la virulence de la forme promastigote (Ilg, Demar, et Harbecke, 2001), alors que les mutants défectueux en LPG et Galβ1,4Manα1-PO_4 de *L. donovani* et *L. major* ne survivent pas lors de la phagocytose (Lodge et Descoteaux, 2005a; McNeely et Turco, 1990; Spath et al., 2000; Turco, Spath, et Beverley, 2001).

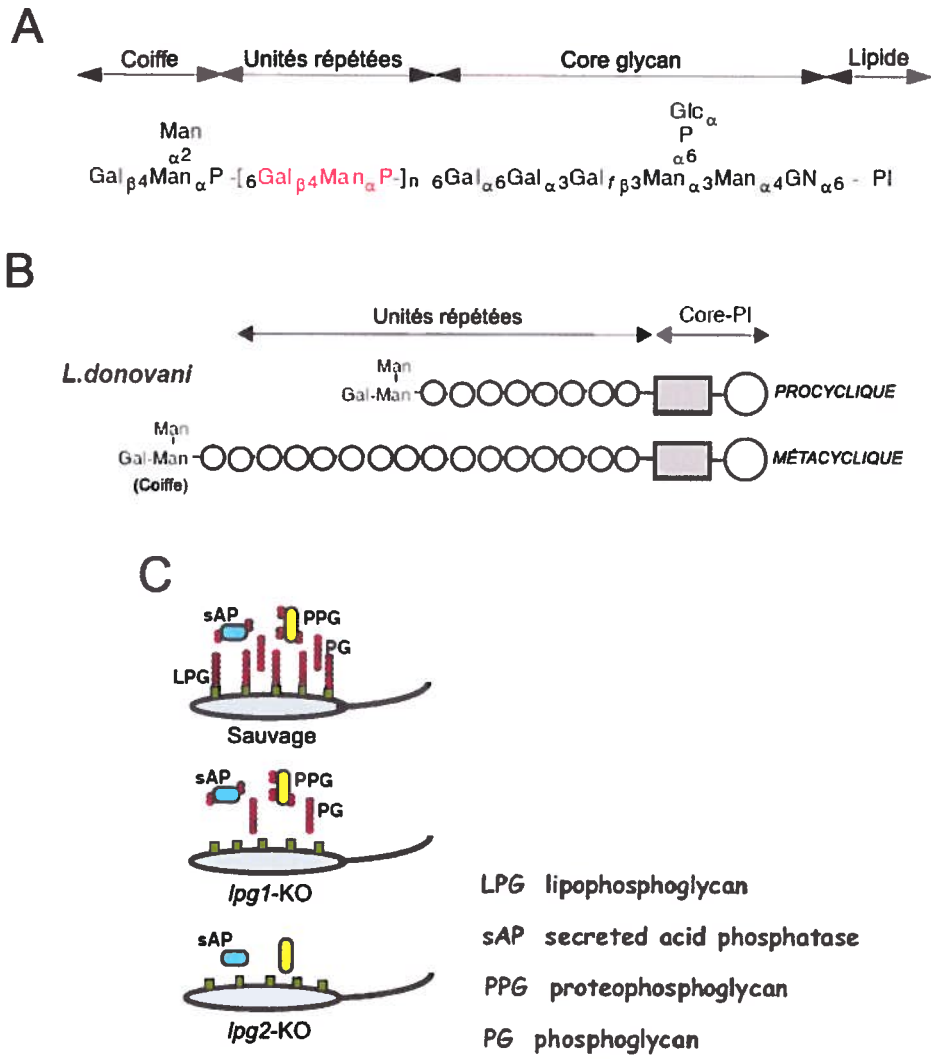

Figure 11: Le lipophosphoglycan de *L. donovani*. *A*, domaines et structure du LPG de *L. donovani*. *B*, représentation shématique du LPG au stade procyclique et métacyclique du promastigote. *C*, représentation schématisée des promastigotes de type WT, *lpg1*-KO et *lpg2*-KO.

5 *Interaction entre le Leishmania et le macrophage : rôle du lipophosphoglycan*

5.1 Attachement du parasite et phagocytose

L'internalisation des promastigotes de *Leishmania* passe par la voie classique de la phagocytose. Lorsque le promastigote métacyclique se retrouve dans le système sanguin de l'hôte, il est rapidement opsonisé par le complément, mais il n'est pas détruit par le complexe lytique de celui-ci grâce au fait que le LPG plus long du stade métacyclique protègerait le parasite par rapport au stade procyclique (Puentes et al., 1990). De plus, la métalloprotéase GP63 du parasite clive le C3b en C3bi qui est la forme inactive, ce qui empêche la formation du complexe d'attaque membranaire (Brittingham et al., 1995; Brittingham et Mosser, 1996). Plusieurs molécules issues du parasite et du macrophage sont alors impliquées dans l'attachement des promastigotes. À la surface des macrophages, les récepteurs du complément CR1 et CR3 (Mac-1), le récepteur mannose-fucose, et p150,95 participent à la liaison du promastigote, bien que leur importance et contribution respectives restent à établir clairement (Blackwell, 1985; Kane et Mosser, 2000). Les glycoconjugués de surface incluant le LPG et GP63 participent au processus d'attachement, directement ou indirectement, puisqu'ils représentent des molécules acceptrices de diverses opsonines telles que C3b et C3bi (Joshi et al., 2002; Kane et Mosser, 2000), la lectine liant le mannane (Green et al., 1994), ou les galectines (Pelletier et al., 2003; Pelletier et Sato, 2002). Cependant, le LPG n'est pas nécessaire à l'attachement en tant que tel puisque les *Leishmania* mutants pour l'expression du LPG sont phagocytés de la même façon ou même de façon plus importante que la souche sauvage (McNeely et Turco, 1990).

Suite à leur liaison aux récepteurs phagocytiques du macrophage, les promastigotes sont internalisés en faisant intervenir le cytosquelette d'actine car un traitement des macrophages avec un agent dépolymérisant de l'actine tel que la

Cytochalasine inhibe leur internalisation (Prive et Descoteaux, 2000). Il a également été démontré l'importance des petites GTPases de la famille Rho lors de ce processus. Comme nous l'avons vu, ces GTPases jouent un rôle clé lors de la phagocytose en régulant le réarrangement du cytosquelette d'actine (Chimini et Chavrier, 2000; Etienne-Manneville et Hall, 2002), et bien que la forme promastigote se lie à divers récepteurs, une opsonisation rapide par le complément favorise une internalisation via les récepteurs du complément impliquant RhoA. L'internalisation du promastigote non opsonisé fait quant à lui intervenir les GTPases Rac1 et Cdc42 (Lodge et Descoteaux, 2005a).

Les mécanismes impliqués dans l'internalisation de la forme amastigote sont encore moins bien compris. Il a été rapporté que la capture de l'amastigote de *L. amazoniensis* par le macrophage nécessite une polymérisation d'actine et une colocalisation de d'actine-F, de paxilline et de taline à la coupe phagocytique (Love, Mentink Kane, et Mosser, 1998). Tout comme les promastigotes de *L. donovani*, l'état d'opsonisation des amastigotes de *L. amazoniensis* détermine le mode d'entrée. En effet, l'internalisation de l'amastigote par les cellules CHO implique les GTPases Rho et Cdc42. Lorsque les amastigotes sont opsonisés avec des IgG et internalisés par des récepteurs Fc exprimés par les cellules CHO, Rac1 est activé et requis pour la capture du parasite (Morehead, Coppens, et Andrews, 2002). En résumé, ces diverses observations tendent à démontrer que l'internalisation des *Leishmania* promastigotes et amastigotes suit les voies classiques des divers récepteurs phagocytiques mis en jeu et nécessite de la même façon une réorganisation du cytosquelette d'actine pour laquelle le parasite joue peu ou pas de rôle actif.

5.2 Fonctions du macrophage altérées par le parasite

5.2.1 Accumulation d'actine-F et inhibition de la maturation phagosomale

Quelques minutes après l'internalisation d'une particule, l'actine-F associée au phagosome naissant se dissocie, et le phagosome nouvellement formé interagit avec le compartiment endosomal. Ces interactions pourraient être facilitées par un meilleur accès à la membrane du phagosome lorsque l'actine-F s'est dépolymérisée (Aderem et Underhill, 1999). A la différence des endosomes précoces, les interactions entre les endosomes tardifs/lysosomes et les phagosomes contenant les promastigotes de *L. donovani* ou *L. major* sont inhibées (Dermine et al., 2000; Desjardins et Descoteaux, 1997), et le recrutement de marqueurs tels que Rab-7 et LAMP-1 est fortement retardé (Scianimanico et al., 1999) (Figure 12). Ces observations pourraient s'expliquer par une accumulation anormale d'actine-F à la périphérie du phagosome contenant le promastigote de *L. donovani*. En effet, le remodelage du phagosome régulé par l'actine est caractérisé par une accumulation progressive d'actine-F périphagosomale qui pourrait interférer avec le recrutement de transmetteurs de signal et de vésicules au phagosome contenant la forme promastigote de *L. donovani* (Holm et al., 2001). L'analyse de l'impact du LPG sur le recrutement et la rétention des molécules de la cellule hôte impliquées dans le réarrangement du cytosquelette d'actine a permis d'approfondir le mécanisme sous-jacent (Lodge et Descoteaux, 2005a). Par exemple, Rac1 et RhoA sont présentes au niveau des phagosomes contenant la forme promastigote indépendamment de la présence de LPG. Cependant, Cdc42 n'est présent qu'au niveau des phagosomes contenant le promastigote WT et reste associé plus de deux heures après le début de la phagocytose, alors qu'il se dissocie rapidement des phagosomes contenant les promastigotes n'exprimant pas le LPG. D'autres effecteurs tels que Arp2/3, WASP, α-actinin, Myosin II et Nck s'accumulent selon une cinétique similaire à l'actine-F et Cdc42 sur les phagosomes contenant le promastigote WT, de manière dépendante du LPG. Ainsi, Cdc42, qui est recruté de manière très précoce à la membrane phagosomale (Hoppe et Swanson, 2004), représente une première cible pour attirer ensuite d'autres

molécules de l'actine-F sur le phagosome naissant. Cependant, les mécanismes permettant au LPG de conserver la petite GTPase au niveau de la membrane sont encore peu connus. Des hypothèses telles que l'inhibition de la forme GTP de Cdc42 par inactivation de RhoGAP, ou l'altération de l'intégrité des microdomaines lipidiques membranaires par le LPG menant à une inhibition de la fonction RhoGEF sont plausibles. D'autres facteurs que l'inactivation des GTPases de la famille Rho pourraient contribuer au désassemblage de l'actine-F durant la phagocytose (Scott et al., 2005). Il a été proposé par exemple, que la disparition des PI(4,5)P2 avait un rôle crucial dans l'arrêt de l'accumulation d'actine et de son désassemblage et pourraient potentiellement être la cible du LPG.

Ainsi, l'inhibition de la biogénèse du phagolysosome est strictement dépendante des unités répétées du LPG (Tolson, Turco, et Pearson, 1990) puisque les phagosomes contenant des promastigotes mutants pour la synthèse du LPG suivent une maturation rapide en un phagolysosome fonctionnel (Desjardins et Descoteaux, 1997; Scianimanico et al., 1999). L'insertion du LPG dans la double couche lipidique altère les propriétés fusogéniques du phagosome (Tolson, Turco, et Pearson, 1990), et pourrait être responsable de l'inefficacité des interactions entre les endosomes et le phagosome (Miao et al., 1995). De plus, il a été démontré que le LPG désorganise les microdomaines lipidiques (Dermine et al., 2001; Dermine et al., 2005; Winberg et al., 2009). Ces microdomaines spécialisés riches en cholestérol sont enrichis en flotilline-1, NADPH oxidase, sous-unité de la V-ATPase et même en certaines synaptotagmines (Galli, McPherson, et De Camilli, 1996; Gil et al., 2005; Vilhardt et van Deurs, 2004). Une autre protéine associée aux microdomaines lipidiques est PKC-α. Il a été démontré que l'expression d'un dominant négatif de cette enzyme ou alors la présence de LPG avait comme conséquence une accumulation d'actine-F et une inhibition du recrutement de LAMP-1 (Holm et al., 2003; Holm et al., 2001). Cela pourrait s'expliquer par le fait que PKC-α phosphoryle MARCKS (Myritoylated Alanin-Rich C Kinase Substrate) qui est une protéine interagissant avec l'actine-F (Allen et Aderem, 1995a; Allen et Aderem, 1995b).

Bien que les promastigotes de *L. donovani* et *L. major* inhibent la maturation du phagosome, ce n'est pas nécessairement le cas de toutes les espèces de *Leishmania*. Par exemple, *L. amazoniensis* est internalisé dans un phagosome qui acquiert toutes les caractéristiques lysosomales (Courret et al., 2002). De plus, les promastigotes de *L. mexicana* déficients en LPG se différentient en amastigotes et prolifèrent aussi efficacement que les sauvages dans des macrophages péritonéaux (Ilg, Demar, et Harbecke, 2001). On peut d'ailleurs noter que les amastigotes de *L. amazoniensis* et *L. mexicana* résident tout deux dans de grandes vacuoles parasitophores communales, contrairement aux phagosomes resserrés contenant un seul *L. donovani* ou *L. major* (Antoine et al., 1998).

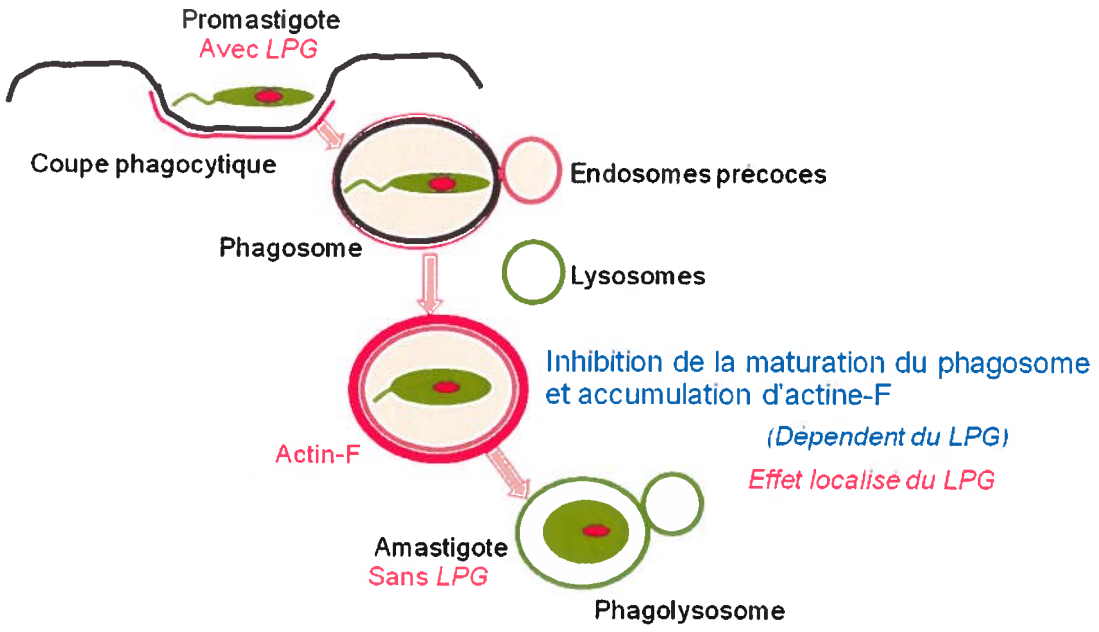

D'après (Lodge et Descoteaux, 2005b)

Figure 12: Le promastigote de *Leishmania donovani* altère la maturation phagosomale. Le LPG de *L. donovani* provoque une accumulation d'actine autour du phagosome le contenant, ce qui pourrait réduire les interactions de ce phagosome avec les endosomes tardifs et les lysosomes. La maturation est donc retardée, laissant le temps aux promastigotes de se différencier en amastigotes ne sécrétant pas / peu de LPG.

5.2.2 Action du LPG sur PKC-α

En s'insérant dans les radeaux lipidiques de la membrane du phagosome, le LPG permet aux promastigotes de *L. donovani* de désorganiser ces plateformes qui sont cruciales pour de nombreuses voies de signalisations et permet d'altérer les fonctions phagosomales (Dermine et al., 2001; Dermine et al., 2005). Plusieurs études ont également démontré que le LPG avait un effet d'inhibition sur l'activité de la PKC-α (Descoteaux, Matlashewski, et Turco, 1992; Giorgione, Turco, et Epand, 1996; McNeely et al., 1989), ainsi que sur son recrutement au phagosome (Holm et al., 2001). Étant donné l'importance de l'activité de cette enzyme pour le recrutement de différents marqueurs du phagolysosome tels que Rab-7, la Cath D, la Cath S, LAMP-1 et la Flotilline (Ng Yan Hing, Desjardins, et Descoteaux, 2004), l'inhibition de l'activité/recrutement de cette kinase au phagosome contenant le promastigote de *L. donovani* pourrait compléter les dispositifs que le parasite met en place pour retarder la maturation du phagosome et permettre sa survie.

5.2.3 Altération de la production de FRO et FRN

Un autre effet du LPG sur les mécanismes microbicides du macrophage concerne l'assemblage et la fonction du complexe de la NADPH oxydase. En effet, bien qu'une infection des macrophages par les *L. donovani* WT et déficients en LPG provoquent un relargage similaire d'ions superoxyde, la génération de ces superoxydes au niveau des phagosomes est différente. Le LPG exclue spécifiquement les composants cytosoliques $p47^{phox}$ et $p67^{phox}$ du phagosome, sans avoir d'impact sur la phosphorylation de $p47^{phox}$ et sa liaison à $p67^{phox}$. Tout comme le LPG n'empêche pas non plus l'acquisition de $gp91^{phox}$ ou Rac1 (Lodge, Diallo, et Descoteaux, 2006). Ainsi, en ciblant spécifiquement $p47^{phox}$ et $p67^{phox}$, les promastigotes de *L. donovani* préviennent l'assemblage de la NADPH oxidase.

La production de FRN est également un puissant leishmanicide comme le prouve les souris $NOS2^{-/-}$ qui sont incapables de contrôler une infection par *Leishmania* (Diefenbach et al., 1998) et il a été démontré que la sécrétion d'oxyde nitrique était inhibé lorsque les macrophages étaient stimulés par du LPG purifié (Proudfoot et al., 1996; Proudfoot, O'Donnell, et Liew, 1995).

5.2.4 Modulation de la sécrétion de cytokines

De par leur rôle de contrôle de la pathogénèse, la sécrétion de cytokines est une cible de choix pour le parasite afin de survivre et d'établir son infection. Par exemple, *Leishmania* inhibe la production de cytokines pro-inflammatoires telles que l'IL-1β, le TNF-α et l'IL-12 (Carrera et al., 1996; Descoteaux et Matlashewski, 1989; Hatzigeorgiou et al., 1996; Piedrafita et al., 1999; Reiner, 1987). De plus, *Leishmania* induit la production de cytokines anti-inflammatoires telles que l'IL-10, l'IL-4 et le TGF-β (Chatelain, Varkila, et Coffman, 1992; Kane et Mosser, 2001; Kopf et al., 1996; Rodrigues, Santana da Silva, et Campos-Neto, 1998) afin de favoriser son entrée dite « silencieuse » dans le macrophage.

5.2.5 Autres voies de signalisation altérées

Les voies de signalisation impliquées dans la sécrétion de cytokines sont altérées par le promastigote, comme par exemple les voies p38 MAPK, ERK1/2 et JNK qui ne sont pas activées suite à la phagocytose de *L. donovani* (dû au LPG dans le cas de ERK) (Prive et Descoteaux, 2000). De même, *Leishmania* agit sur les voies JAK/STAT, notamment via l'induction de régulateur négatifs de ces voies tels que les phosphotyrosine phosphatase SHP-1 (Blanchette et al., 1999; Forget et al., 2001), potentiellement des protéines SOCS (Bertholet et al., 2003; de Veer et al., 2003) ou en dégradant STAT-1α (Forget, Gregory, et Olivier, 2005).

Première publication

(Le régulateur d'exocytose Synaptotagmine V contrôle la phagocytose chez le macrophage)

Résumé de la première publication

Vinet A.F., Fukuda M. and Descoteaux A. (2008). The exocytosis regulator Synaptotagmin V controls phagocytosis. *The Journal of Immunology*, 181(8):5289-95.

Les Synaptotagmines jouent un role clé dans la regulation de l'exocytose dependante du calcium et dans la fusion membranaire, deux évènements cruciaux lors du processus phagocytique. Dans la cette étude, nous étudions le rôle de la Syt V dans la phagocytose. Chez le macrophage, la Syt V est localisée au niveau des endosomes de recyclage et au niveau de structures comparables aux filipodes, elle est de plus recrutée au phagosome naissant de manière indépendante du récepteur phagocytique stimulé. La technique d'interférence à ARN a révélé un rôle de cette protéine dans la régulation de la phagocytose, particulièrement sous conditions de haute demande en membrane. Cependant, l'inhibition de l'expression de Syt V n'a pas eu d'effet sur le recrutement du marqueur lysosomal LAMP-1 au phagosome. Ces résultats illustrent l'importance de la Syt V dans la régulation d'une importante fonction innée du macrophage. De plus, nos résultats sont cohérents avec le fait que l'exocytose focale d'organelles endocytiques est un évènement clé lors de la formation du phagosome et suggèrent que la Syt V régule en partie ce processus.

The exocytosis regulator Synaptotagmin V controls phagocytosis in macrophages

Adrien F. Vinet*, Mitsunori Fukuda†, and Albert Descoteaux*[2]

* INRS- Institut Armand-Frappier, Université du Québec, Laval, QC, Canada H7V 1B7

†Department of Developmental Biology and Neurosciences, Graduate School of Life Sciences, Tohoku University, Sendai, Miyagi 980-8578, Japan

Running title: The exocytosis regulator Synaptotagmin V in phagocytosis

Keywords: Monocytes/Macrophages; Phagocytosis; Signal transduction

This work was supported by Canadian Institutes of Health Research grant MT-29033. A.D. is a chercheur-boursier of the FRSQ and the holder of a Canada Research Chair. A.F.V. was partly supported by a doctoral fellowship from the Fondation Armand-Frappier.

Address correspondence and reprint requests to Dr Albert Descoteaux, INRS- Institut Armand-Frappier, 531 boul des Prairies, Laval, QC, Canada H7V 1B7. E-mail: albert.descoteaux@iaf.inrs.ca

Abbreviations used in this paper: SNARE, soluble N-ethylmaleimide-sensitive factor attachment protein receptor; Syt, synaptotagmin; IgG-SRBC, IgG-opsonized SRBC; PEM, peritoneal exudate macrophages; PKC, protein kinase C; siRNA, small interfering RNA; RNAi, RNA interference.

Summary

Synaptotagmins (Syts) play a key role in the regulation of Ca^{2+}-triggered exocytosis and membrane fusion events, two crucial events associated to the phagocytic process. In the present study, we investigated the role of Syt V, a regulator of focal exocytosis, in phagocytosis. In macrophages, Syt V is localized on recycling endosomes and on filopodia-like structures and is recruited to the nascent phagosomes independently of the phagocytic receptor engaged. Silencing of Syt V by RNA interference revealed a role for this protein for phagocytosis, particularly under conditions of high membrane demand. In contrast, silencing of Syt V had no effect on the recruitment of the lysosomal marker LAMP1 to phagosomes, indicating that phagosome maturation is not regulated by Syt V. Collectively, these results illustrate the importance of Syt V in the regulation of an important innate function of macrophages. Furthermore, our results are consistent with the concept that focal exocytosis of endocytic organelles is a key event in phagocytosis and suggest that Syt V regulates this process.

Introduction

Phagocytosis is an essential arm of the innate response against infections, as it represents the process by which professional phagocytes internalize and destroy invading microorganisms (1, 2). During internalization, target particles are surrounded by pseudopods and are engulfed in a vacuole, the phagosome, which rapidly matures into a microbicidal phagolysosome. Whereas the nascent phagosome is formed to a large extent by invagination of the plasma membrane (3), the membrane surface required to internalize multiple or large targets may represent an area equivalent to the entire cell surface (4). Such a requirement suggests that membrane from intracellular sources contributes to the phagocytic process. Indeed, phagosome formation is accompanied by the exocytosis of endomembranes into the plasmalemma (4). Two compartments contribute to focal exocytosis during phagocytosis: the VAMP3- and Rab-11-positive recycling endosomes (5, 6, 7) and the TI-VAMP/VAMP7-positive late endosomes/lysosomes (8). Evidence that soluble *N*-ethylmaleimide-sensitive factor attachment protein receptors (SNAREs)[3] associated to the endoplasmic reticulum are required for phagocytosis support a role for this organelle during phagocytosis (9, 10). However, this remains controversial (11). Nevertheless, the fact that both vesicle- and plasma-membrane associated SNAREs are essential for focal exocytosis and particle internalization (4, 5, 8, 10) illustrates the importance of membrane fusion regulators during phagocytosis.

Synaptotagmins (Syts) are a large family of transmembrane proteins characterized by the presence of tandem C2 domains which act as Ca^{2+} sensor, and regulate membrane fusion during exocytosis via interaction with SNAREs and membrane lipids (12, 13). Although several SNAREs modulate phagocytosis by controlling membrane fusion during focal exocytosis, little is known concerning the potential roles of Syts in phagocytosis. This is an important issue because for the SNARE complex to drive rapid membrane fusion in response to Ca^{2+} influx, additional factors, including a Ca^{2+} sensor(s), are required. In this regard, a recent study revealed that consistent with its role as a

regulator of lysosomal exocytosis (14, 15, 16), Syt VII plays a key role in the delivery of lysosomal membrane to the phagosome (17), possibly acting in concert with VAMP7 (8). In neutrophils, the presence of Syt II on phagosomes suggested a role for this Ca^{2+} sensor during phagocytosis and secretion (18).

Several signaling molecules, including members of the protein kinase C (PKC) family of protein serine/threonine kinases, are activated during phagocytosis and associate to the phagosome during the maturation process (19, 20, 21, 22, 23). We previously obtained evidence that PKC-α plays a role in phagolysosome biogenesis (24), and, while investigating the mechanisms by which PKC-α modulates phagocytosis, we identified Syt V (25) as a molecule potentially interacting with PKC-α in phagosomes preparations (A.F.V. and A.D., unpublished observations). Syt V is predominantly associated to dense-core vesicles in neuronal cells (26) and pancreatic β cells where it regulates vesicle exocytosis (27, 28). In this study, we provide evidence that, in macrophages, Syt V plays a role in the regulation of phagocytosis.

Materials and methods

Cell culture

Peritoneal exudate macrophages (PEM) were obtained from peritoneal lavages of 8- to 10-wk-old female C57BL/6 mice (Charles River Laboratories). PEM and the mouse macrophage cell lines J774 and RAW 264.7 were cultured in DMEM with L-glutamine (Life Technologies) supplemented with 10% heat-inactivated FBS (HyClone), 10 mM HEPES (pH 7.4), and antibiotics (complete medium) in a 37°C incubator with 5% CO_2. *Leishmania donovani* promastigotes (strain 1S) were grown as described (29).

Syt V-GFP expression vector and stable transfection in RAW 264.7 cells

The SytV-GFP cDNA (26) was inserted into the *Not*I site of the bicistronic expression vector pCIN-4 (30). The resulting construct was electroporated into RAW 264.7 cells as described (31). Transfectants were selected in complete medium containing 500 μg/ml G418 (Life Technologies) and individual clones were harvested, expanded, and examined for Syt V-GFP expression.

RT-PCR

Total RNA was extracted with RNAzol B (Tel-Test), treated with DNaseI (BD Biosciences), and reverse transcribed with AMV reverse transcriptase (USB). cDNA was used for PCR using the following forward (F) and reverse (R) primers for Syt V: F: 5'-CCCTTTTTGGTGTCTCTCTTTTCG-3' (AD-329) and R: 5'-AGTCCTTGGCAGGCAGATTGAC-3' (AD-330). For hypoxanthine phosphoribosyltransferase, the primers were F: 5'-GTTGGATACAGGCCAGACTTTGTTG-3' (AD-55) and R: 5'-GATTCAACTTGCGCTCATCTTAGGC-3' (AD-56).

Phagosome preparation and isolation

Adherent macrophages (5 x 10^7 per 150 x 20 mm tissue culture dishes) were incubated with latex beads (0.75 μm diameter, 10% suspension, blue dyed; Sigma-Aldrich) diluted 1/25 in 10 ml complete medium at 37°C for 30, 60, 90, or 120 min. Cells were then washed three times in cold PBS at 4°C and scrapped with a rubber policeman in cold PBS. Phagosomes were isolated by flotation on a sucrose gradient as described (24).

Western blots

Cells and purified phagosomes were lysed in ice-cold lysis buffer (20 mM Tris-HCl (pH 7.5) and 1% Nonidet P-40) containing protease and phosphatase inhibitors. Phagosomal proteins (30 μg) and total cell lysates (10 μg) were separated on 8% SDS-PAGE, transferred onto Hybond-ECL membranes (Amersham Biosciences), and immunodetection was achieved by chemiluminescence (Amersham Biosciences).

Antibodies

The rabbit anti-Syt V spacer Ab was raised against the cytoplasmic region between the transmembrane and the C2 domain (aa 71–216) and was affinity-purified.The rat anti-Lamp1 developed by J. T. August (1D4B) was obtained through the Developmental Studies Hybridoma Bank at the University of Iowa, and the National Institute of Child Health and Human Development. The monoclonal anti-EEA1 Ab was from Dr. Michel Desjardins (Université de Montreal, Montreal, Canada). Monoclonal rat anti-mouse transferrin receptor TfR Ab was from Cedarlane Laboratories.

RNA interference (RNAi)

For the silencing of Syt V by RNAi, we used a small interfering RNA (siRNA) corresponding to nucleotides 94–112 of Syt V cDNA (28), whereas an siRNA specific to GFP (32) was used as a negative control. Adherent RAW 264.7 cells were transfected with siRNA duplexes at a final concentration of 240 nM using OligoFectamine (Invitrogen) as described (32). A BLAST search against the mouse genome sequence

database was performed to ensure that the chosen siRNA sequences targeted only the mRNA of interest.

Phagocytosis assays

IgG-opsonized SRBC (IgG-SRBC) were prepared as described (19). Red fluorescent beads of different diameters (0.75 μm from Estapor microsphere and 3 μm from Polyscience) were opsonized with mouse IgG. Zymosan (Sigma-Aldrich), Zymosan-Alexa 488 and -Alexa 568 (Molecular Probes) and *L. donovani* promastigotes were opsonized with mouse serum (33). For synchronized phagocytosis assays, macrophages were incubated with particles at a particle-to-cell ratio of 15:1 (unless otherwise specified) for 20 min at 4°C. Excess particles were removed and phagocytosis was triggered by transferring the cells to 37°C for the indicated time points before processing for microscopy.

Microscopy and immunofluorescence

Macrophages were fixed, permeabilized using 0.1% Triton X-100, and nonspecific surface FcγR binding were blocked using 1% BSA, 2% goat serum, 6% milk, and 50% FBS. Particle internalization was quantified by immunofluorescence microscopy. Results are based on at least 100 cells chosen by blinded scoring in triplicate. For distribution and colocalization experiments, cells were labeled with the appropriate combinations of primary Abs (anti-Syt V, LAMP-1, transferrin receptor, EEA1, or PKC-α), and secondary Abs (anti-rabbit AlexaFluor 568 or AlexaFluor 488, anti-rat AlexaFluor 488, anti-mouse AlexaFluor 488, or anti-mouse AlexaFluor 568; Molecular Probes). All coverslips were mounted on slides with Fluoromount-G (Southern Biotechnology Associates). Detailed analysis of protein localization on the phagosome was performed essentially as described (29) using an oil immersion Nikon Plan Apo 100 (N.A. 1.4) objective mounted on a Nikon Eclipse E800 microscope equipped with a Bio-Rad Radiance 2000 confocal imaging system (Bio-Rad). Statistical analyses were performed using Student's two-tail two-sample unequal variance test.

Results

Syt V is expressed in macrophages

Using a proteomic approach, we sought to identify proteins in latex bead-phagosome lysates that coimmunoprecipitated with PKC-α (A.F.V. and A.D., unpublished observations), and we found several proteins including Syt V (NP_068689). Two Syt V sequences were reported at the same time, and the 491AA-Syt V identified by Li et al. (34) will be analyzed in this paper. Given the importance of Syts in the regulation of exocytosis and membrane fusion (13, 35), we further investigated the potential role of Syt V in phagocytosis. Syt V had not previously been shown to be expressed in macrophages and we confirmed by RT-PCR that it is expressed in the macrophage lines RAW 264.7 and J774 (Fig. 1*A*). The PC12 neuronal cell line was used as a positive control. Using an Ab against the Syt V spacer domain (26), we detected by Western blot the presence of Syt V in J774 and PC12 cell lysates as well as in 90 min-old latex bead-phagosome extracts (Fig. 1*B*). Confocal immunofluorescence microscopy revealed that Syt V is present on intracellular vesicles and on filopodia-like structures (Fig. 1*C*). After 30-min phagocytosis, we observed the recruitment of Syt V to phagosomes containing various particles (latex beads, zymozan, serum opsonized-zymozan, and IgG-SRBC) (Fig. 1*D*). Using RAW 264.7 cells stably expressing a Syt V-GFP fusion protein, we observed that similar to Syt V, Syt V-GFP was recruited to phagosomes containing either latex beads, zymozan, serum opsonized-zymozan, or IgG-SRBC (Fig. 1*D*). To assess the specificity of our anti-Syt V Ab, we performed immunofluorescence staining in the absence or the presence of the GST-Syt V spacer domain fusion protein used for immunization. As shown in Fig. 1*E*, presence of the GST-Syt V spacer domain strongly reduced Syt V staining on both intracellular vesicles and on zymozan-containing phagosomes in PEM. Taken together, these data indicate that Syt V is recruited to phagosomes, independently of the phagocytic receptors involved.

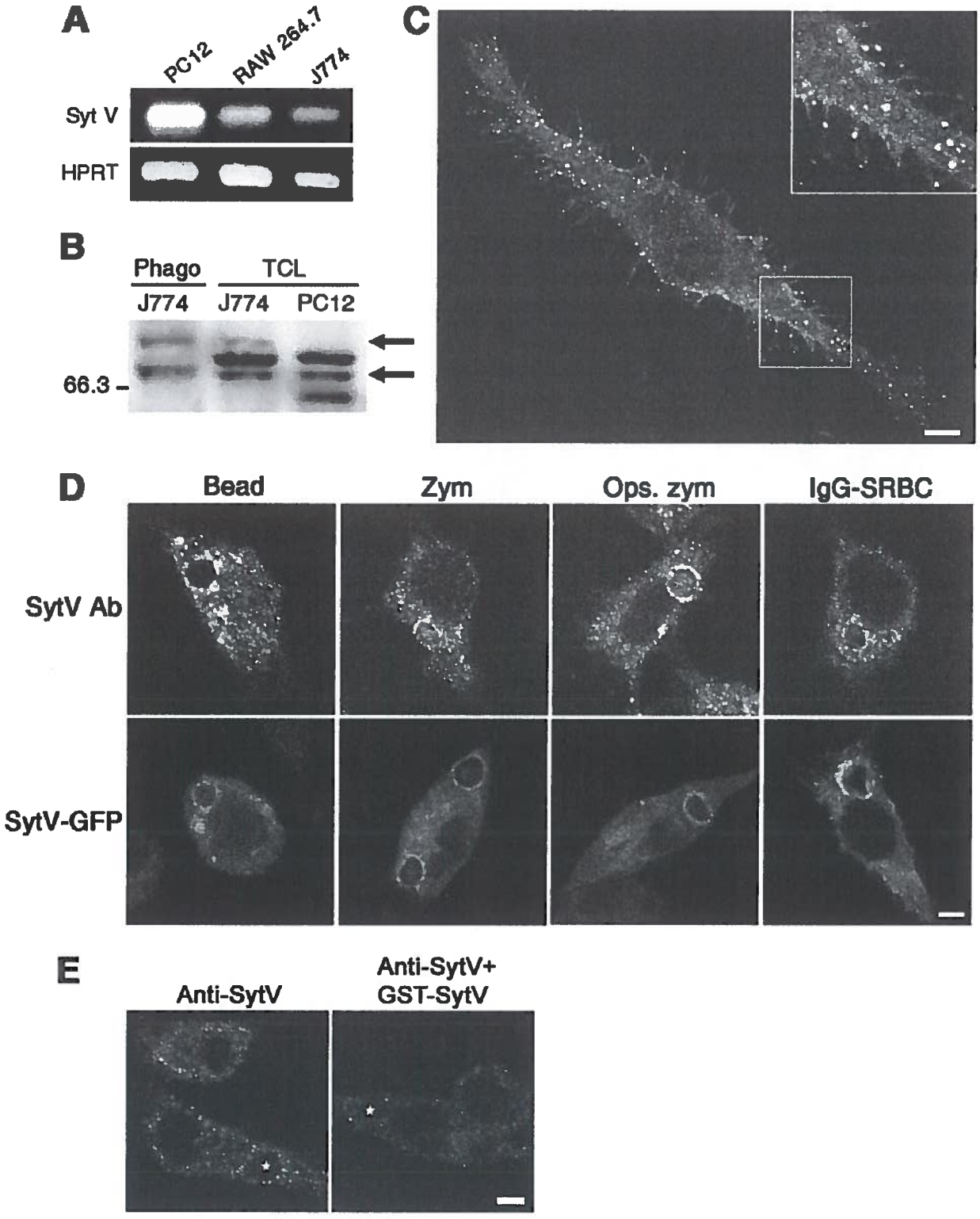
A
PC12
RAW 264.7
J774
Syt V
HPRT
B
Phago
TCL
J774
J774
PC12
66.3
C
D
Bead
Zym
Ops. zym
IgG-SRBC
SytV Ab
SytV-GFP
E
Anti-SytV
Anti-SytV+
GST-SytV

FIGURE 1. Syt V is expressed in macrophages and is recruited to phagosomes. *A*, Syt V is expressed in RAW 264.7 and J774 macrophages, as assessed by RT-PCR. PC12 cells were used as positive control. *B*, Syt V is present in total cell and phagosome lysates from J774 cells. Western blot analysis was performed on 30-μg 90-min-old phagosome lysates and 10 μg total cell lysates (TCL). PC12 cells were used as positive control. Arrows show the two Syt V forms present in macrophages. *C*, Syt V is localized on intracellular vesicles and on filopodia-like structures in RAW 264.7 cells, as determined by confocal microscopy. Bar, 5 μm. *D*, Syt V is recruited to phagosomes independently of the phagocytic receptor involved. RAW 264.7 cells or RAW 264.7 cells stably expressing the Syt V-GFP fusion protein were allowed to internalize either latex beads, zymozan, serum-opsonized zymozan, or IgG-SRBCs for 30 min. Syt V (*top panel*) and Syt V-GFP (*bottom panel*) were localized by confocal microscopy. Bar, 3 μm. *E*, Immunolocalization of Syt V in the presence of the GST-Syt V spacer domain fusion protein used to generate the anti-Syt V Ab eliminated most of the Syt V labeling both on intracellular vesicles and on zymozan-containing phagosomes (indicated by an *) in PEM. Bar, 3 μm. Results are representative of three independent experiments.

Syt V associates to phagosomes

To further characterize the recruitment of Syt V to phagosomes, we first determined its kinetics of phagosomal association during the phagocytosis of serum-opsonized zymozan. Confocal microscopy revealed that in both RAW 264.7 cells and PEM, Syt V was recruited early to phagosomes and remained throughout the maturation process (Fig. 2*A*). The recruitment of Syt V-GFP to phagosomes containing serum-opsonized zymozan followed a kinetics pattern similar to that of Syt V (Fig. 2*B*). Similarly, Western blot on J774 latex bead phagosomes lysates prepared at various time points after the start of phagocytosis showed that the relative abundance of the two phagosome-associated Syt V forms varies during the phagosome maturation process (Fig. 2*C*). These two forms of Syt V may represent different posttranslational modifications, such as phosphorylation, as previously observed with Syt IV and Syt IX (36, 37). We next compared the recruitment kinetics of Syt V and LAMP1 to phagosomes containing serum opsonized-zymozan by confocal microscopy. Consistent with its lysosomal localization, we detected LAMP1 on phagosomes at later time points (60 and 90 min), whereas Syt V was present from early time points (Fig. 3*A*). The observation that Syt V and LAMP1 were recruited to phagosomes with distinct kinetics is consistent with the lack of colocalization of both proteins (Fig. 3*A*) and indicated that Syt V is not associated with late endosomal or lysosomal compartments. Furthermore, Syt V showed occasional colocalization with the early endosome marker EEA1, whereas it frequently colocalized with the recycling and early endosome marker transferrin receptor (Fig. 3*B*). These results indicate that Syt V associates with the recycling endosomal compartment.

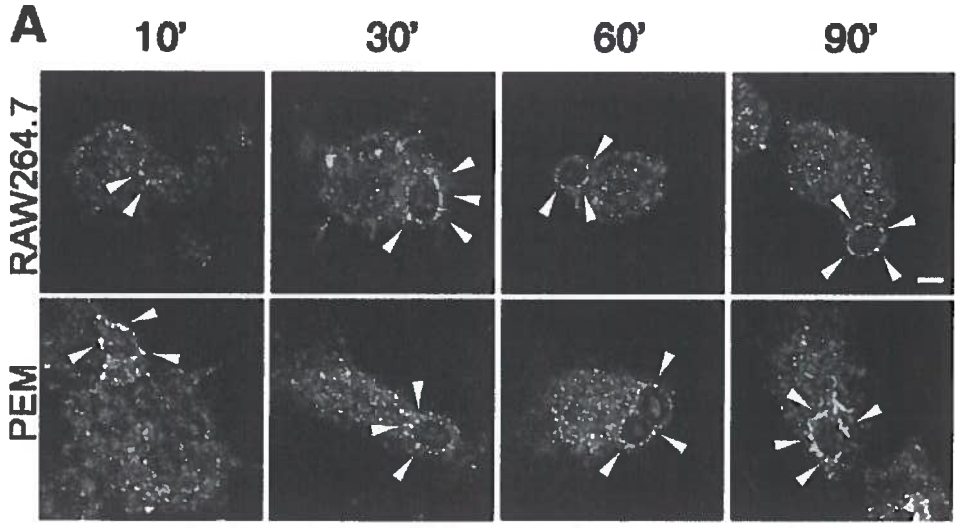
A
10'
30'
60'
90'
RAW264.7
PEM

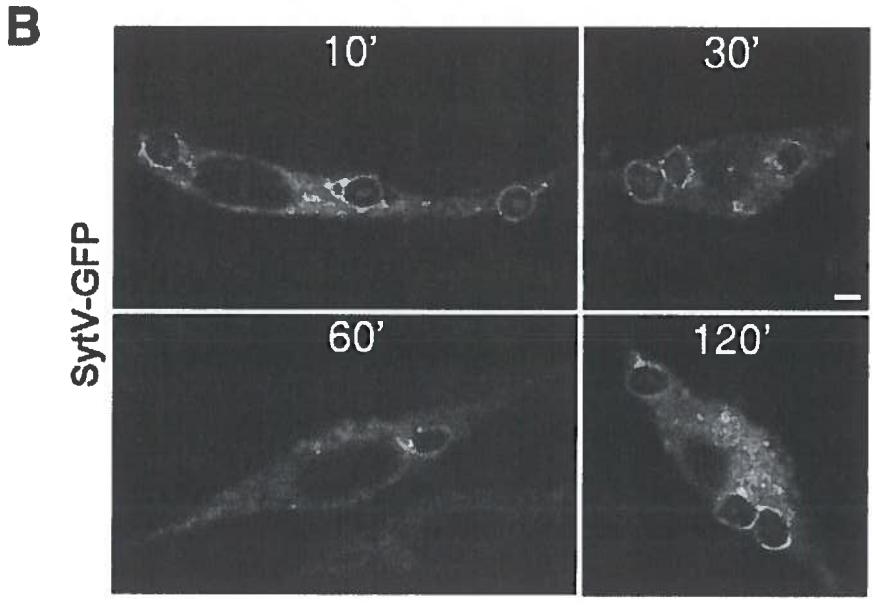
B
10'
30'
60'
120'
SytV-GFP

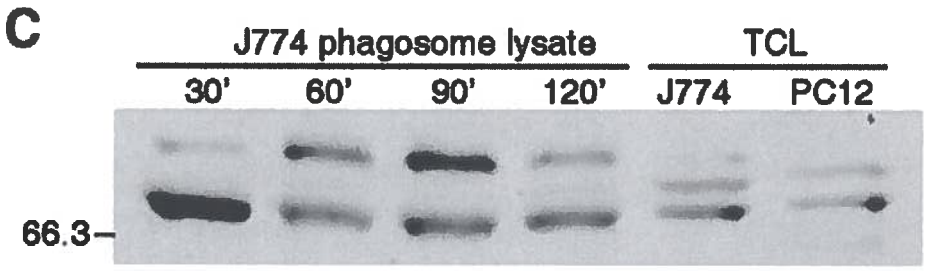
C
J774 phagosome lysate
TCL
30'
60'
90'
120'
J774
PC12
66.3

FIGURE 2. Syt V is recruited early to phagosomes and remains during the maturation process. *A*, Syt V was localized by confocal microscopy at various time points after the initiation of internalization of serum-opsonized zymozan by either RAW 264.7 cells (*upper row*) or PEM (*lower row*). Bar, 3 μm. *B*, Syt V-GFP was localized by confocal microscopy at various time points after the initiation of internalization of serum-opsonized zymozan by RAW 264.7 cells stably expressing Syt V-GFP. Bar, 3 μm. *C*, Two Syt V forms are present on latex bead-containing phagosomes isolated from J774 cells at various time points after the start of internalization. Western blot analysis was performed on 30-μg phagosomes lysates and 10 μg total cell lysates (TCL) from J774 and PC12 cells. Similar results were obtained in three independent experiments.

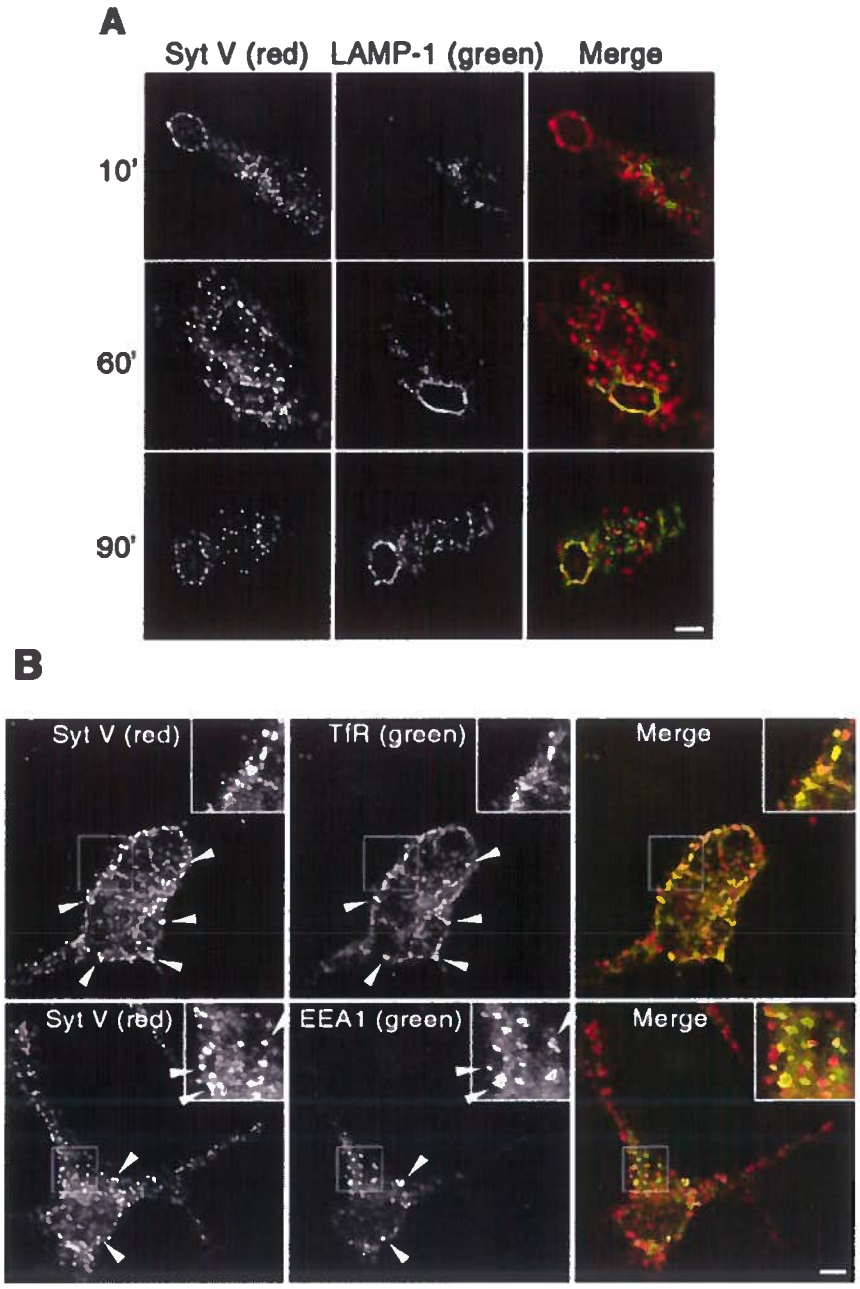

FIGURE 3. Intracellular localization of Syt V in PEM. *A*, Syt V and LAMP1 do not colocalize and associate to serum-opsonized zymozan-phagosomes with distinct kinetics. Bar, 3 μm. *B*, Syt V colocalizes with the recycling endosome marker transferin receptor (shown by arrowheads, *upper row*), whereas little colocalization was observed with the early endosome marker EEA1 (shown by arrowheads, *lower row*). Bar, 3 μm.

Syt V is required for phagocytosis but not phagosome maturation

To study the potential role of Syt V in phagocytosis, we used RNAi to inhibit its expression. Transfection of RAW 264.7 cells with a siRNA to Syt V (28), significantly decreased Syt V levels after 24 h (Fig. 4*A*). In contrast, intensity of the two Syt V forms was similar in RAW 264.7 macrophages transfected with a siRNA to GFP and in control mock-transfected RAW 264.7 cells. Confocal immunofluorescence analysis indicated that Syt V was efficiently silenced by the siRNA Syt V treatment with most cells showing reduced fluorescence intensity (Fig. 4*B*). We next determined the impact of Syt V silencing on the phagocytosis of serum opsonized-zymozan and IgG-SRBC. Both CR- and FcγR-mediated phagocytosis were inhibited by over 50% in the absence of Syt V, revealing its role in phagocytosis (Fig. 4*C*). Importantly, this inhibition was not the consequence of a defective particle binding, as Syt V depletion had no effect on the association of serum opsonized-zymozan and IgG-SRBC to macrophages (Fig. 4*C*). Given that Syt V remains associated to phagosomes after particle internalization, we investigated its possible role in phagosome maturation. Silencing of Syt V had no effect on the recruitment of the lysosomal marker LAMP1 to zymosan-containing phagosomes (Fig. 4*D*), suggesting that Syt V does not a play a significant role in regulating interactions between phagosomes and lysosomes.

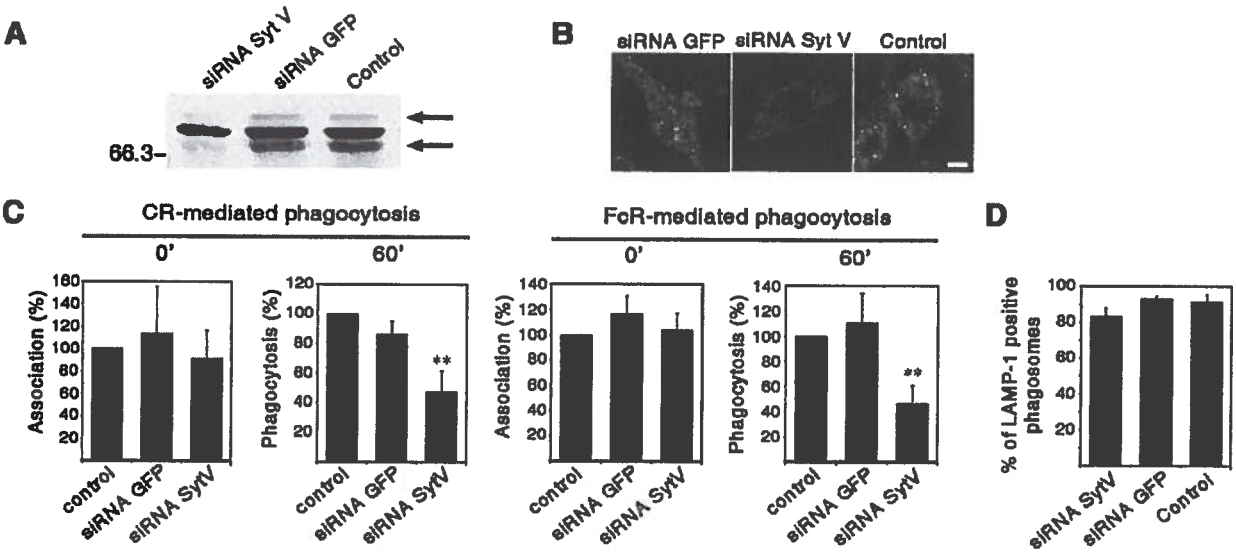

FIGURE 4. Silencing of Syt V impairs phagocytosis. RAW 264.7 cells were transfected with either a siRNA to Syt V or a siRNA to GFP, or only mock transfected (control), and incubated for 24 h. siRNA to Syt V efficiently reduced Syt V levels as shown by Western blot (*A*) and confocal immunofluorescence microscopy (*B*). Bar, 3 μm. In *A*, arrows show the two Syt V forms present in macrophages. The *middle band* is nonspecific. *C*, siRNA Syt V inhibited CR- and FcγR-mediated phagocytosis (60 min) but not particle binding (0 min). Particle association and phagocytosis were calculated on at least 100 cells, in triplicate. (**, $p \leq 0.0005$ vs siRNA GFP). *D*, LAMP1 is recruited to zymozan-phagosomes in siRNA Syt V-treated macrophages, as determined 90 min after the start of phagocytosis.

Phagocytosis of large particles and high particle loads is impaired in the absence of SytV

To address the possibility that Syt V regulates membrane delivery at the phagocytic cup, we determined its requirement for phagocytosis under conditions of high particle loads and for the internalization of large particles. RAW 264.7 cells treated with siRNA Syt V were exposed to serum opsonized-zymozan at various particle-to-cell ratios (Fig. 5*A*). At 10 min after the initiation of phagocytosis, we observed a 50% inhibition of internalization for the 10:1 ratio and over 70% inhibition of internalization for the 40:1 particle-to-cell ratio in siRNA Syt V-treated cells (Fig. 5*B*) with respect to control cells. After 60 min, the impact of higher particle-to-cell ratio was less important than at 10 min. Similar results were obtained for the phagocytosis of the promastigote form of *Leishmania donovani*, a protozoan parasite that replicates inside macrophages (Fig. 5*B*). We next compared the ability of siRNA Syt V-treated cells and control cells to internalize 0.75 μm and 3 μm IgG-opsonized latex beads at particle-to-cell ratios of 10:1 and 40:1. Silencing of Syt V strongly inhibited the internalization of 3 μm IgG-beads, whereas phagocytosis of 0.75 μm IgG-beads by siRNA Syt V-treated cells was similar to that observed in controls cells (Fig. 6). This suggests that Syt V is involved in the regulation of membrane supply under phagocytic conditions where important quantities of membrane are required.

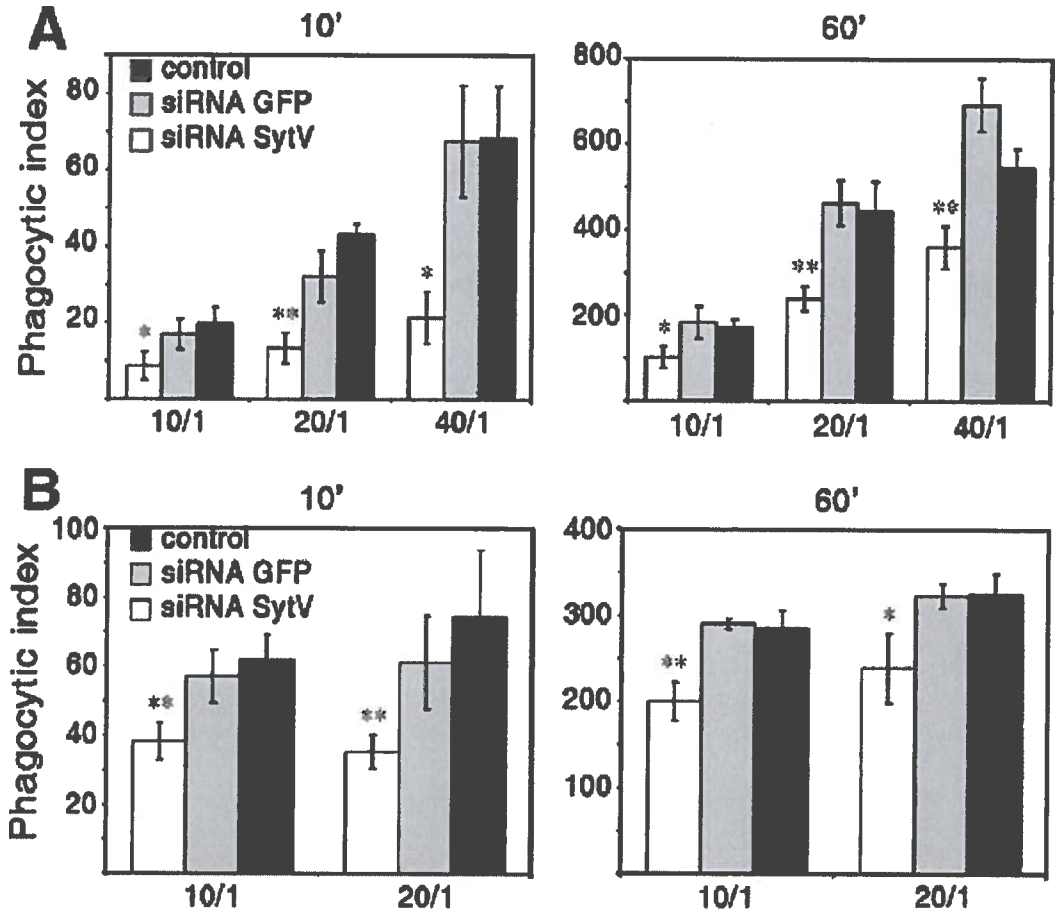

FIGURE 5. Inhibition of phagocytosis in siRNA Syt V-treated cells increases with particle load. The phagocytosis defect of cells treated with siRNA Syt V increases with particle load. Macrophages were incubated with increasing ratios of serum-opsonized zymozan (*A*) or *L. donovani* promastigotes (*B*) and particle internalization was determined after 10 min and 60 min. The phagocytic index was calculated on at least 100 cells in triplicate (*A* and *B*) (*, $p \leq 0.005$; **, $p \leq 0.0005$ vs RNAi GFP).

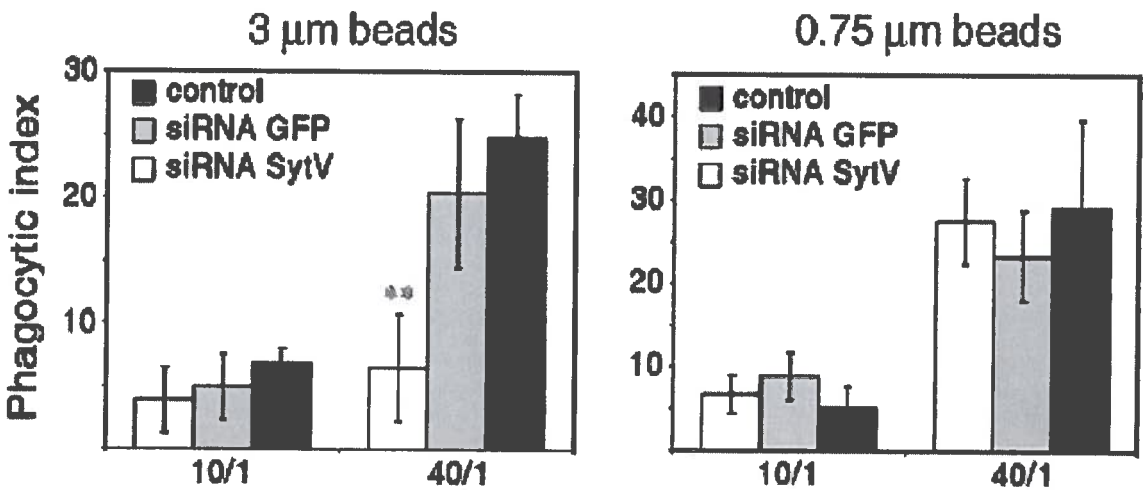

FIGURE 6. Inhibition of phagocytosis in siRNA Syt V-treated cells increases with particle size. The phagocytosis defect of cells treated with siRNA Syt V increases with particle size. Macrophages were fed with either 3- or 0.75-µm IgG-opsonised beads at ratios of 10:1 and 40:1 and particle internalization was determined after 10 min. The phagocytic index was calculated on at least 100 cells in triplicate (**, $p \leq 0.0005$ vs RNAi GFP).

Discussion

Syts play a key role in the regulation of Ca^{2+}-triggered exocytosis and membrane fusion, two important events associated to the phagocytic process. In this study, we identified the Ca^{2+}-dependent exocytosis regulator Syt V as a recycling endosome-associated protein that is recruited to the nascent phagosome in macrophages, independently of the phagocytic receptor involved. Silencing of Syt V by RNAi revealed a critical role for this protein in phagocytosis, particularly in the presence of large particles or a large particle load. Thus, given its role as a regulator of exocytosis (28), Syt V may control the mobilization of recycling endosomes as a source of endomembrane during phagocytosis.

Despite their role as regulators of membrane fusion events, few studies have addressed the potential involvement of Syts in the phagocytic process. The best-characterized Syt in phagocytosis is the ubiquitous Syt VII, which regulates Ca^{2+}-dependent exocytosis of lysosomes (14). In the absence of Syt VII, phagocytosis is impaired particularly under conditions of high membrane demand (17). In neutrophils, Syt II is present on granules and is recruited to the phagosome, but its role remains to be determined (18). Current knowledge on the distribution and function of Syt V is very limited. Previous studies showed that it is a dense-core vesicle-specific Syt that regulates Ca^{2+}-dependent exocytosis in brain and endocrine tissues. Hence, in neuronal PC12 cells and in the brain, Syt V is found on dense-core vesicles that undergo Ca^{2+}-dependent exocytosis and, in contrast to other Syts, is absent from synaptic-like microvesicles (26). Consistent with a direct role in Ca^{2+}-dependent stimulation of exocytosis, silencing of Syt V by RNAi strongly inhibited hormone exocytosis by pancreatic β cells (28). In macrophages, we found that Syt V is mainly associated to recycling endosomes and is also present on filopodia-like structures. Recycling endosomes are key players in phagocytosis as this subcompartment of the endocytic pathway is one of the prominent sources of endomembrane recruited to the phagocytic cup (11, 38). Hence, several recycling endosome-associated molecules involved in the regulation of membrane fusion

such as VAMP3, Rab11, and Arf6 are recruited to the nascent phagosomes and contribute to the internalization process (5, 6, 7, 39, 40). The recruitment of Syt V to the nascent phagosome is consistent with its localization on recycling endosomes and is functionally important, as phagocytosis of various types of particles was inhibited following its depletion by RNAi. This inhibition was particularly severe when macrophages depleted in Syt V were fed with large particles or with a large particle load. Given that Syt V is a regulator of exocytosis (26, 28), these observations are consistent with a role for Syt V in regulating focal exocytosis of recycling endosomes during phagocytosis. The possibility that Syt V acts in concert with known SNAREs and recycling endosome-associated regulators of phagosome formation (VAMP3, Rab11, and Arf6) remains to be determined. Recruitment of Syt V to the phagosome independently of the phagocytic receptor engaged and its requirement for CR- and FcγR-mediated phagocytosis indicate that Syt V is part of the general phagocytic machinery.

The association of Syt V with the phagosome throughout the maturation process raised the possibility that it regulates interactions with the endocytic system. However, acquisition of the lysosomal marker LAMP1 was normal in the absence of Syt V, indicating that Syt V is not involved in phagosome maturation. One possible role for phagosome-associated Syt V could be the regulation of phagosome maintenance and/or expansion (41, 42). Indeed, as intravacuolar microorganisms proliferate within their host cell, the area of phagosome membrane must increase to accommodate the replicating pathogens. This may involve interactions with host cell organelles and vesicular compartments, but the underlying mechanisms remain poorly understood.

Syt V was not only present on at the phagocytic cup and on phagosomes but also on plasma membrane, notably on filopodia-like structures. This finding is consistent with the possibility that Syt V-containing recycling endosomes fuse with the plasma membrane to release their content and suggests a more general role for Syt V. Delivery of membrane from recycling endosomes to the phagocytic cup allows rapid release of TNF-α and expands the membrane for phagocytosis (43). Upon macrophage activation, there is an increased vesicular and recycling endosomes trafficking to accommodate cytokine secretion and this is related to the up-regulation of the expression of relevant SNAREs

(43, 44, 45). Current studies are addressing the possible role of Syt V in proinflammatory cytokine secretion during phagosome formation.

Acknowledgments

We thank Marcel Desrosiers for assistance with confocal microscopy and Dr. Eric Prina for comments and suggestions.

Footnotes

The costs of publication of this article were defrayed in part by the payment of page charges. This article must therefore be hereby marked *advertisement* in accordance with 18 U.S.C. Section 1734 solely to indicate this fact.

Received for publication March 12, 2008. Accepted for publication August 15, 2008.

References

1. Aderem, A., D. M. Underhill. 1999. Mechanisms of phagocytosis in macrophages. *Annu. Rev. Immunol.* 17: 593-623.

2. Stuart, L. M., R. A. Ezekowitz. 2005. Phagocytosis: elegant complexity. *Immunity* 22: 539-550.

3. Silverstein, S. C.. 1977. Endocytic uptake of particles by mononuclear phagocytes and the penetration of obligate intracellular parasites. *Am. J. Trop. Med. Hyg.* 26: 161-169.

4. Hackam, D. J., O. D. Rotstein, C. Sjolin, A. D. Schreiber, W. S. Trimble, S. Grinstein. 1998. v-SNARE-dependent secretion is required for phagocytosis. *Proc. Natl. Acad. Sci. USA* 95: 11691-11696.

5. Bajno, L., X. R. Peng, A. D. Schreiber, H. P. Moore, W. S. Trimble, S. Grinstein. 2000. Focal exocytosis of VAMP3-containing vesicles at sites of phagosome formation. *J. Cell Biol.* 149: 697-706.

6. Cox, D., D. J. Lee, B. M. Dale, J. Calafat, S. Greenberg. 2000. A Rab11-containing rapidly recycling compartment in macrophages that promotes phagocytosis. *Proc. Natl. Acad. Sci. USA* 97: 680-685.

7. Niedergang, F., E. Colucci-Guyon, T. Dubois, G. Raposo, P. Chavrier. 2003. ADP ribosylation factor 6 is activated and controls membrane delivery during phagocytosis in macrophages. *J. Cell Biol.* 161: 1143-1150.

8. Braun, V., V. Fraisier, G. Raposo, I. Hurbain, J. B. Sibarita, P. Chavrier, T. Galli, F. Niedergang. 2004. TI-VAMP/VAMP7 is required for optimal phagocytosis of opsonised particles in macrophages. *EMBO J.* 23: 4166-4176.

9. Becker, T., A. Volchuk, J. E. Rothman. 2005. Differential use of endoplasmic reticulum membrane for phagocytosis in J774 macrophages. *Proc. Natl. Acad. Sci. USA* 102: 4022-4026.

10. Hatsuzawa, K., T. Tamura, H. Hashimoto, S. Yokoya, M. Miura, H. Nagaya, I. Wada. 2006. Involvement of syntaxin 18, an endoplasmic reticulum (ER)-localized SNARE protein, in ER-mediated phagocytosis. *Mol. Biol. Cell* 17: 3964-3977.

11. Huynh, K. K., J. G. Kay, J. L. Stow, S. Grinstein. 2007. Fusion, fission, and secretion during phagocytosis. *Physiology* 22: 366-372.

12. Jahn, R., T. Lang, T. C. Sudhof. 2003. Membrane fusion. *Cell* 112: 519-533.

13. Sudhof, T. C.. 2004. The synaptic vesicle cycle. *Annu. Rev. Neurosci.* 27: 509-547.

14. Martinez, I., S. Chakrabarti, T. Hellevik, J. Morehead, K. Fowler, N. W. Andrews. 2000. Synaptotagmin VII regulates $Ca^{(2+)}$-dependent exocytosis of lysosomes in fibroblasts. *J. Cell Biol.* 148: 1141-1149.

15. Reddy, A., E. V. Caler, N. W. Andrews. 2001. Plasma membrane repair is mediated by $Ca^{(2+)}$-regulated exocytosis of lysosomes. *Cell* 106: 157-169.

16. Roy, D., D. R. Liston, V. J. Idone, A. Di, D. J. Nelson, C. Pujol, J. B. Bliska, S. Chakrabarti, N. W. Andrews. 2004. A process for controlling intracellular bacterial infections induced by membrane injury. *Science* 304: 1515-1518.

17. Czibener, C., N. M. Sherer, S. M. Becker, M. Pypaert, E. Hui, E. R. Chapman, W. Mothes, N. W. Andrews. 2006. Ca^{2+} and synaptotagmin VII-dependent delivery of lysosomal membrane to nascent phagosomes. *J. Cell Biol.* 174: 997-1007.

18. Lindmark, I. M., A. Karlsson, L. Serrander, P. Francois, D. Lew, B. Rasmusson, O. Stendahl, O. Nusse. 2002. Synaptotagmin II could confer Ca^{2+} sensitivity to phagocytosis in human neutrophils. *Biochim. Biophys. Acta* 1590: 159-166.

19. Breton, A., A. Descoteaux. 2000. Protein kinase C-α participates in FcγR-mediated phagocytosis in macrophages. *Biochem. Biophys. Res. Commun.* 276: 472-476.

20. Brumell, J. H., J. C. Howard, K. Craig, S. Grinstein, A. D. Schreiber, M. Tyers. 1999. Expression of the protein kinase C substrate pleckstrin in macrophages: association with phagosomal membranes. *J. Immunol.* 163: 3388-3395.

21. Larsen, E. C., J. A. DiGennaro, N. Saito, S. Mehta, D. J. Loegering, J. E. Mazurkiewicz, M. R. Lennartz. 2000. Differential requirement for classic and novel PKC isoforms in respiratory burst and phagocytosis in RAW 264.7 cells. *J. Immunol.* 165: 2809-2817.

22. Zheng, L., T. P. Zomerdijk, C. Aarnoudse, R. van Furth, P. H. Nibbering. 1995. Role of protein kinase C isozymes in Fcγ receptor-mediated intracellular killing of *Staphylococcus aureus* by human monocytes. *J. Immunol.* 155: 776-784.

23. Zheleznyak, A., E. J. Brown. 1992. Immunoglobulin-mediated phagocytosis by human monocytes requires protein kinase C activation: evidence for protein kinase C translocation to phagosomes. *J. Biol. Chem.* 267: 12042-12048.

24. Ng Yan Hing, J. D., M. Desjardins, A. Descoteaux. 2004. Proteomic analysis reveals a role for protein kinase C-α in phagosome maturation. *Biochem. Biophys. Res. Commun.* 319: 810-816.

25. Fukuda, M., R. Sagi-Eisenberg. 2008. Confusion in the nomenclature of synaptotagmins V and IX: which is which?. *Calc. Bind. Prot.* 3: 1-3.

26. Saegusa, C., M. Fukuda, K. Mikoshiba. 2002. Synaptotagmin V is targeted to dense-core vesicles that undergo calcium-dependent exocytosis in PC12 Cells. *J. Biol. Chem.* 277: 24499-24505.

27. Gut, A., C. Kiraly, M. Fukuda, K. Mikoshiba, C. Wollheim, J. Lang. 2001. Expression and localisation of synaptotagmin isoforms in endocrine (β)-cells: their function in insulin exocytosis. *J. Cell Sci.* 114: 1709-1716.

28. Iezzi, M., G. Kouri, M. Fukuda, C. B. Wollheim. 2004. Synaptotagmin V and IX isoforms control Ca^{2+}-dependent insulin exocytosis. *J. Cell Sci.* 117: 3119-3127.

29. Lodge, R., A. Descoteaux. 2005. *Leishmania donovani* promastigotes induce periphagosomal F-actin accumulation through retention of the GTPase Cdc42. *Cell. Microbiol.* 7: 1647-1658.

30. Rees, S., J. Coote, J. Stables, S. Goodson, S. Harris, M. G. Lee. 1996. Bicistronic vector for the creation of stable mammalian cell lines that predisposes all antibiotic-resistant cells to express recombinant protein. *BioTechniques* 20: 102-104. *106, 108–110.*

31. Stacey, K. J., I. L. Ross, D. A. Hume. 1993. Electroporation and DNA-dependent cell death in murine macrophages. *Immunol. Cell Biol.* 71: 75-85.

32. Flandin, J. F., F. Chano, A. Descoteaux. 2006. RNA interference reveals a role for TLR2 and TLR3 in the recognition of *Leishmania donovani* promastigotes by interferon-γ-primed macrophages. *Eur. J. Immunol.* 36: 411-420.

33. Lodge, R., T. O. Diallo, A. Descoteaux. 2006. *Leishmania donovani* lipophosphoglycan blocks NADPH oxidase assembly at the phagosome membrane. *Cell. Microbiol.* 8: 1922-1931.

34. Li, C., B. Ullrich, J. Z. Zhang, R. G. W. Anderson, N. Brose, T. C. Sudhof. 1995. Ca^{2+}-dependent and -independent activities of neural and non-neural synaptotagmins. *Nature* 375: 594-599.

35. Bai, J., E. R. Chapman. 2004. The C2 domains of synaptotagmin: partners in exocytosis. *Trends Biochem. Sci.* 29: 143-151.

36. Mori, Y., M. Higuchi, Y. Hirabayashi, M. Fukuda, Y. Gotoh. 2008. JNK phosphorylates synaptotagmin-4 and enhances Ca^{2+}-evoked release. *EMBO J.* 27: 76-87.

37. Haberman, Y., I. Ziv, Y. Gorzalczany, M. Fukuda, R. Sagi-Eisenberg. 2005. Classical protein kinase C(s) regulates targeting of synaptotagmin IX to the endocytic recycling compartment. *J. Cell Sci.* 118: 1641-1649.

38. Braun, V., F. Niedergang. 2006. Linking exocytosis and endocytosis during phagocytosis. *Biol. Cell* 98: 195-201.

39. Zhang, Q., D. Cox, C.-C. Tseng, J. G. Donaldson, S. Greenberg. 1998. A requirement for ARF6 in Fcγ receptor-mediated phagocytosis in macrophages. *J. Biol. Chem.* 273: 19977-19981.

40. Allen, L. A., C. Yang, J. E. Pessin. 2002. Rate and extent of phagocytosis in macrophages lacking vamp3. *J. Leukocyte Biol.* 72: 217-221.

41. Xu, S., A. Cooper, S. Sturgill-Koszycki, T. van Heyningen, D. Chatterjee, I. Orme, P. Allen, D. Russell. 1994. Intracellular trafficking in *Mycobacterium tuberculosis* and *Mycobacterium avium*-infected macrophages. *J. Immunol.* 153: 2568-2578.

42. Ramsden, A. E., D. W. Holden, L. J. Mota. 2007. Membrane dynamics and spatial distribution of *Salmonella*-containing vacuoles. *Trends Microbiol.* 15: 516-524.

43. Murray, R. Z., J. G. Kay, D. G. Sangermani, J. L. Stow. 2005. A role for the phagosome in cytokine secretion. *Science* 310: 1492-1495.

44. Pagan, J. K., F. G. Wylie, S. Joseph, C. Widberg, N. J. Bryant, D. E. James, J. L. Stow. 2003. The t-SNARE syntaxin 4 is regulated during macrophage activation to function in membrane traffic and cytokine secretion. *Curr. Biol.* 13: 156-160.

45. Stow, J. L., A. P. Manderson, R. Z. Murray. 2006. SNAREing immunity: the role of SNAREs in the immune system. *Nat. Rev. Immunol.* 6: 919-929.

Deuxième publication

(Le lipophosphoglycan de *Leishmania donovani* inhibe la maturation du phagosome en agissant sur les radeaux membranaires)

Résumé de la deuxième publication

Winberg ME, Holm A, Sarndahl E, Vinet AF, Descoteaux A, et al. (2009). *Leishmania donovani* lipophosphoglycan inhibits phagosomal maturation via action on membrane rafts. *Microbes and Infections*, 11: 215-222.

Le lipophosphoglycan (LPG), qui est le principal glycoconjugué de surface de la forme promastigote de *Leishmania donovani*, est crucial pour l'établissement de l'infection dans les macrophages. Le LPG est constitué d'un polymère de Galβ1,4Manα-PO_4 répétés, attachés à une ancre membranaire lysophosphatidylinosotol. Le LPG est transferré du parasite à la membrane du macrophage de l'hôte durant la phagocytose et induit une accumulation d'actine-F, qui corrèle avec une inhibition de la maturation du phagosome. Les propriétés biophysiques du LPG suggèrent qu'il pourrait s'intercaller à l'intérieur des microdomaines membranaires de la cellule hôte. Le but de cette étude était d'analyser si l'effet du LPG sur la maturation du phagosome dépend de son action sur les microdomaines lipidiques membranaires. Nous montrons que le LPG s'accumule dans les microdomaines pendant la phagocytose de *Leishmania donovani* et que la désorganisation de ces microdomaines prévient les effets du LPG sur l'accumulation de l'actine-F périphagosomale et la maturation du phagosome. Ces résultats indiquent que des microdomaines lipidiques intacts sont nécessaires au LPG afin de manipuler les fonctions de la cellule hôte. En conclusion, le LPG s'associe aux microdomaines lipidiques de la cellule hôte et exerce son action sur l'actine et la maturation du phagosome via l'altération des fonctions de ces microdomaines.

Leishmania donovani lipophosphoglycan inhibits phagosomal maturation via action on membrane rafts

Martin E. Winberg[a,1], Asa Holm[a,1,2], Eva Sarndahl[a,3], Adrien F. Vinet[b], Albert Descoteaux[b], Karl-Eric Magnusson[a], Birgitta Rasmusson[a], Maria Lerm[a,*]

[a] Div. of Med. Microbiology, Dept. of Clinical and Experimental Medicine, Faculty of Health Sciences, Linkoping University, SE-581 85 Linkoping, Sweden

[b] INRS-Institut Armand-Frappier, Laval, QC, Canada

* Corresponding author. Tel.: +46 13 22 47 79; fax: +46 13 22 47 89. E-mail address: maria.lerm@liu.se (M. Lerm).

[1] These authors contributed equally.

[2] Present address: Department of Microbiology, Tumor and Cell Biology, Karolinska Institutet, Sweden.

[3] Present address: Department of Biomedicine, School of Health and Medical Sciences, Orebro University, Sweden.

Keywords: *Leishmania*; Lipophosphoglycan; Membrane rafts; Phagosomal maturation; Actin

Received 8 September 2008; accepted 17 November 2008

Abstract

Lipophosphoglycan (LPG), the *major* surface glycoconjugate on *Leishmania donovani* promastigotes, is crucial for the establishment of infection inside macrophages. LPG comprises a polymer of repeating Galβ1,4Manα-PO_4 attached to a lysophosphatidylinositol membrane anchor. LPG is transferred from the parasite to the host macrophage membrane during phagocytosis and induces periphagosomal F-actin accumulation correlating with an inhibition of phagosomal maturation. The biophysical properties of LPG suggest that it may be intercalated into membrane rafts of the host-cell membrane. The aim of this study was to investigate if the effects of LPG on phagosomal maturation are mediated via action on membrane rafts. We show that LPG accumulates in rafts during phagocytosis of *L. donovani* and that disruption of membrane rafts abolished the effects of LPG on periphagosomal F-actin and phagosomal maturation, indicating that LPG requires intact membrane rafts to manipulate host-cell functions. We conclude that LPG associates with membrane rafts in the host cell and exert its actions on host-cell actin and phagosomal maturation through subversion of raft function.

Introduction

The protozoan parasite *Leishmania donovani* causes visceral *Leishmania*sis (Kala Azar), and is transmitted to humans by infected *Phlebotomus* sand flies [1]. Its life cycle includes a flagellated, infective promastigote form primarily expressed in the gut of the sand fly, and an amastigote form, which is induced inside the macrophage phagosome in the mammalian host.

The ability of *L. donovani* to survive inside macrophages is crucial for establishment of infection [2], and depends on the action of several molecules including lipophosphoglycan (LPG) [3]. LPG is a polymer of the repeating Galβ1,4Manα-PO_4 unit linked to the membrane of the promastigote via a unique lipid anchor; 1-*O*-alkyl-2-*lyso*-phosphatidyl(*myo*)inositol with an unusually long saturated fatty acid chain of 24–26 C [4].

LPG has several effects on macrophage functions [5], including inhibition of phagosomal maturation [6], [7] and [8]. This is illustrated by the finding that wild type (WT) promastigotes block phago-lysosomal formation, whereas mutants lacking phosphoglycans, including LPG, are found in a phago-lysosomal compartment [6], [7] and [8]. LPG causes accumulation of F-actin around phagosomes carrying WT *L. donovani* [8]. The periphagosomal F-actin, which could act as a physical barrier to prevent phago-lysosomal fusion, is formed through impaired dissociation of the actin regulators Cdc42 and Rac1 from the phagosomal membrane [9], [10] and [11]. Upon parasite attachment, LPG is transferred from the promastigote surface to the host-cell plasma membrane [12]. The lipid anchor of LPG is characterized by an extended, saturated fatty acid residue [13], suggesting that it may be intercalated into host-cell detergent-resistant membranes, DRM. We have recently shown that lipoarabinomannan (LAM) from *Mycobacterium tuberculosis*, whose molecular structure is reminiscent of LPG, is inserted into the membrane rafts of the host cell [14]. From this platform, LAM is able to delay phagosomal maturation, thereby being beneficial for *M. tuberculosis* virulence. The aim of the present study was to investigate whether LPG from *L. donovani* acts in a similar manner.

Materials and methods

Cells

Human monocyte-derived macrophages were isolated from heparinised donor blood as previously described [14]. The cells were differentiated in Macrophage SFM supplemented with 100 U/ml penicillin, 100 mg/ml streptomycin, and 4 mM l-glutamine (Life Technologies). The cells were used after ten days of differentiation. Bone marrow-derived macrophages (BMM) were obtained by growing marrow cells from female BALB/c mice at 37 °C in 5% CO2 in complete medium [Dulbecco's Modified Eagle Medium with glutamine (Life Technologies Inc., ON, Canada), containing 10% heat-inactivated FBS (Hyclone, Logan, UT), 10 mM HEPES pH 7.4, and antibiotics] in the presence of 15% (v/v) L929 cell-conditioned medium for seven days. BMM were made quiescent by culturing them in the absence of CSF-1 for 18 h prior to being used.

Cholesterol depletion

To deplete cholesterol, the medium was exchanged for fresh Macrophage SFM containing 10 mM β-cyclodextrin (βCD, Sigma Chemical Co) followed by incubation at 37 °C for 60 min. After three washes in 37 °C KRG with 2% bovine serum albumin (BSA, Boehringer-Mannheim GmBH) (KB), fresh Macrophage SFM was added. Using Amplex Red Cholesterol Assay Kit (Molecular Probes) we found that βCD extracted 60% of the cholesterol in the cells (not shown). Incubation in βCD made the cells round up, but viability was not significantly affected (not shown). Incubating the cholesterol-depleted cells in 10% AB serum over-night restored morphology and function (not shown).

Phagocytic prey and phagocytosis

Wild type *L. donovani* 1S promastigotes (WT) and the isogenic Galβ1,4Manα-PO_4-defective mutant *lpg2*$^{-}$KO, both expressing green fluorescent protein (GFP), were prepared as previously described [8]. The promastigotes were cultured at 26 °C in modified M199 medium with 500 μg/ml G418 (all from Gibco BRL/Life Technologies) [3]. Expression of GFP was assessed by fluorescence microscopy. The promastigotes were spun down and resuspended in the same volume of fresh growth medium 12–14 h before the experiment. Before addition to the macrophages, the promastigotes were again spun down and resuspended in fresh Macrophage SFM at 37 °C. Promastigotes in stationary phase of growth were added to the cells at a parasite-to-cell ratio of 10:1. After 20 min at 37 °C and 5% CO_2 (pulse), excess and unbound parasites were removed by three washes. Preparations for analysis of the distribution of LPG in the plasma membrane were fixed for 15 min at 4 °C in 2.0 % (w/v) paraformaldehyde (PFA, Sigma Chemical Co.) in KRG, and washed in PBS. For analysis of phagocytic capacity, periphagosomal F-actin and phagosomal maturation, incubation was continued at 37 °C for 30 min (chase), followed by fixation, as described above.

Fluorescent labeling

GM-1: cells were pre-fixed in 0.1% PFA in PBS, stained with Alexa Fluor 488-conjugated cholera toxin subunit B (CtxB) (Molecular Probes, Inc.) in PBS, washed and post-fixed for 15 min. LAMP-1 or LPG: fixed cells were incubated with PBS pH 7.6 with 2% BSA, 10% normal goat serum (Dakopatts AB) and 0.1% saponin (Sigma Chemical Co.), followed by washing and incubation with rat monoclonal antibodies against LAMP-1 (kindly provided by Dr. Sven Carlsson, Umeå University) or mouse monoclonal antibodies against LPG (CA7AE, Cedarlane Laboratories), washed and incubated with Alexa594 Fluor-conjugated goat anti-rat or anti-mouse antibodies (Molecular Probes, Inc.). Controls for unspecific labelling were made by substituting the primary antibody with purified rat or mouse IgG (not shown). F-actin: fixed cells were treated with PBS pH 7.6 with 2% BSA and 100 μg/ml lysophosphatidylcholine (Sigma Chemical Co.) and incubated with Alexa Fluor 594-conjugated phallacidin (Molecular Probes, Inc.). All

cells were washed and mounted in an anti-fading medium with 20% Airvol 203 (Air Products and Chemicals, Utrecht, The Netherlands) and 4% Citifluor/Glycerol (Citifluor Ltd.) in 20 mM Tris buffer (pH 8.5) and left to set at 4 °C overnight.

Confocal microscopy

Confocal imaging was performed in a Sarastro 2000 microscope (Molecular Dynamics) equipped for dual activation and detection through a Nikon microscope with an ×60, NA 1.4 oil immersion objective. The 488 nm and 514 nm lines of the Argon laser were used for parallel excitation of FITC/GFP and Alexa594 Fluor. "535 nm" and "595 nm" beam splitters were employed for separation of the excitation and emission light, respectively. A 540DF30 band pass filter was employed for detection of the green signal (FITC/GFP) and an EFLP 600 long pass emission filter for the red signal (Alexa594 Fluor). This filter set-up ensured negligible red fluorescence in the green channel or vice versa.

Analysis of translocation of LAMP-1

Translocation of LAMP-1 to individual phagosomes was investigated in randomly selected confocal images of cholesterol-depleted or control cells after phagocytosis of WT *L. donovani* promastigotes for 20 + 30 min or 1 μg/ml purified LPG for 50 min instead of the parasites. The translocation of LAMP-1 to individual phagosomes containing GFP-expressing promastigotes was classified as either (+) or (–). Typically, 50–100 cells, from preparations done in duplicate on two or three independent occasions were analyzed under each condition.

Quantification of phagocytosis and periphagosomal F-actin

Phagocytic capacity was assessed after a 30-min chase to allow maximal internalization of the promastigotes. The number of GFP-expressing promastigotes per cell was counted in randomly scanned confocal images of samples labelled with Alexa594-phallacidin. All data were normalized against controls phagocytosing *lpg2*$^{-}$KO promastigotes. The results were compiled from results from three independent experiments.

Periphagosomal F-actin was measured in randomly scanned confocal images of Alexa594-phallacidin-labelled samples containing GFP-expressing promastigotes as described in Ref. [8]. In short, the F-actin rim around each phagosome, i.e. periphagosomal F-actin, was manually traced in the red channel of the confocal image, the fluorescence intensity profile along the trace recorded, and the median intensity of the profile calculated. To avoid potential overlaps with cortical F-actin, only the part of the phagosome facing the cytosol was studied. The results were compiled from data obtained from samples prepared on at least three independent occasions. To compensate for possible variations in instrument performance between experimental days, all results were normalized against data from phagosomes in control cells incubated for 20 + 30 min with WT promastigotes and measured in parallel. The cells were focused in white light to avoid destruction of the fluorophores by bleaching and biased selection of certain sections of the preparations. Image analysis was performed on a Silicon Graphics OS2 workstation equipped with ImageSpace v3.2 (Molecular Dynamics).

Fractionation of cell membranes and detection of membrane components

Detergent-resistant membranes were isolated as described in Refs. [14] and [15] with some modifications. Briefly, adherent cells were incubated in 4 °C lysis buffer, containing 1% Triton X-100 (Merck–Schuchard), 2 μg/ml Aprotinin, 2 μg/ml Pepstatin, 2 μg/ml Leupeptin and 1 mM Pefa-block (all from Roche Diagnostics Corporation) for 30 min. Nuclei and whole cells were spun down at 500 g for 10 min. The supernatant was mixed with an equal volume of 85% sucrose (w/v in lysis buffer) and transferred to an ultracentrifugation tube. A step gradient was constructed by overlaying the sucrose-sample mixture with 5 ml 30% sucrose followed by a layer of 3 ml 5% sucrose. The gradient was centrifuged for 17–19 h at 200 000 g in an ultracentrifuge with a Beckman SW 41 rotor. After centrifugation, 10 fractions of 1 ml each were collected from top to bottom of the tube. The fractions were labelled 10 (top) to 1 (bottom, containing Triton X-100 soluble material). The fractions were transferred to nitrocellulose membranes by dot-blot, and blocked in 5% non-fat milk in Tris-buffered saline (TBS) with 0.05% Tween overnight at 4 °C. GM-1 was detected using horse radish peroxidase (HRP)-

conjugated CtxB (1:2500, Sigma Chemical Co.). Mouse monoclonal antibodies (all diluted 1:1000) were used to detect the repeating Galβ1,4Manα-PO_4 units present on LPG (CA7AE, Cedarlane Laboratories), CD44 and CD45, followed by HRP-conjugated goat anti-mouse antibodies (1:5000) (all from DAKO). The blots were analyzed with a commercial enhanced chemiluminescence (ECL) detection kit (Amersham Bioscience). Labelling was quantified from digital images of the blots using ImageJ v1.32j.

Colocalization of LPG and lipid rafts

Late stationary phase L. *donovani* promastigotes were opsonized with mouse serum [10]. Zymosan particles (Sigma-Aldrich) were washed, and coated with purified LPG, kind gift from Dr. S. Turco, University of Kentucky, Lexington, KY, USA) as described [8]. For synchronized phagocytosis assays, macrophages were incubated at a particle-to-cell ratio of 10:1 for 15 min at 4 °C. Excess particles were removed and phagocytosis was triggered by transferring the cells at 37 °C for the indicated time points. Macrophages were next fixed, permeabilized, and blocked as previously described [16]. Cells were incubated with the anti-LPG mouse monoclonal antibody (CA7AE) and labelled with Alexa488 Fluor-conjugated goat anti-mouse antibody (Molecular Probes, Inc.) and Alexa Fluor 594-conjugated cholera toxin subunit B (Molecular Probes, Inc.). All coverslips were mounted on slides with Fluoromount-G (Southern Biotechnology Associates). Detailed analysis of protein localization on the phagosome was performed essentially as described [10] using an oil immersion Nikon Plan Apo 100 (N.A. 1.4) objective mounted on a Nikon Eclipse E800 microscope equipped with a Bio-Rad Radiance 2000 confocal imaging system (Bio-Rad).

Statistical analysis

Statistical analysis was performed using Student's t-test. Error bars are SEM.

Results

LPG localizes to membrane rafts in *L. donovani*-infected macrophages

The cholera toxin subunit B (CtxB) binds to glycosphingolipids with a strong affinity for GM-1 and a lower affinity for other gangliosides [17], and can therefore be used as a marker for membrane rafts [18]. Fluorescent labelling of MDM with CtxB revealed that a substantial part of the plasma membrane contained GM-1 (not shown). Membrane extraction with cold Triton X-100 followed by density centrifugation, fractionation and dot-blot [14] showed that GM-1 was present in fractions 7 and 8 (Fig. 1A), indicative of the membrane raft fraction [19]. Another raft marker, CD44 [20], was also enriched in fractions 7 and 8 (Fig. 1A), whereas CD45, a molecule which is excluded from rafts [21], was found only in fraction 1 corresponding to the Triton X-100 soluble fraction (Fig. 1A). Membrane rafts are enriched in cholesterol [22] and [23], and cholesterol depletion by agents such as β-cyclodextrin (βCD) disrupts their structure and function [24]. The cholesterol content of MDM was reduced by approximately 60% after incubation in 10 mM βCD for 60 min at 37 °C (not shown). Cholesterol-depleted macrophages remained adherent, but displayed a more rounded morphology compared to controls (not shown). Membrane fractionation showed a pronounced reduction of CD44 in rafts following incubation in βCD as well as a 50% loss of GM-1 reactivity (Fig. 1A). When MDM were infected with WT *L. donovani* promastigotes, dot-blot analysis of the membrane fractions revealed an enrichment of LPG in fractions 7 and 8 (corresponding to membrane rafts; Fig. 1B). However, the promastigote membrane itself also contains rafts rich in LPG [25], and the detergent-resistant membrane in fractions 7 and 8 could thus represent a mixture of macrophage and promastigote rafts. To assess whether the detected raft fractions originated from the macrophages and/or the parasites, we subjected the equal number of parasites as used for infections to Triton X-100 extraction followed by density gradient centrifugation and dot-blot. When comparing this sample with a preparation of macrophages plus promastigotes, we found that LPG originating from

promastigote rafts represented approximately 50% of the total amount of LPG detected in fractions 7 and 8 (not shown).

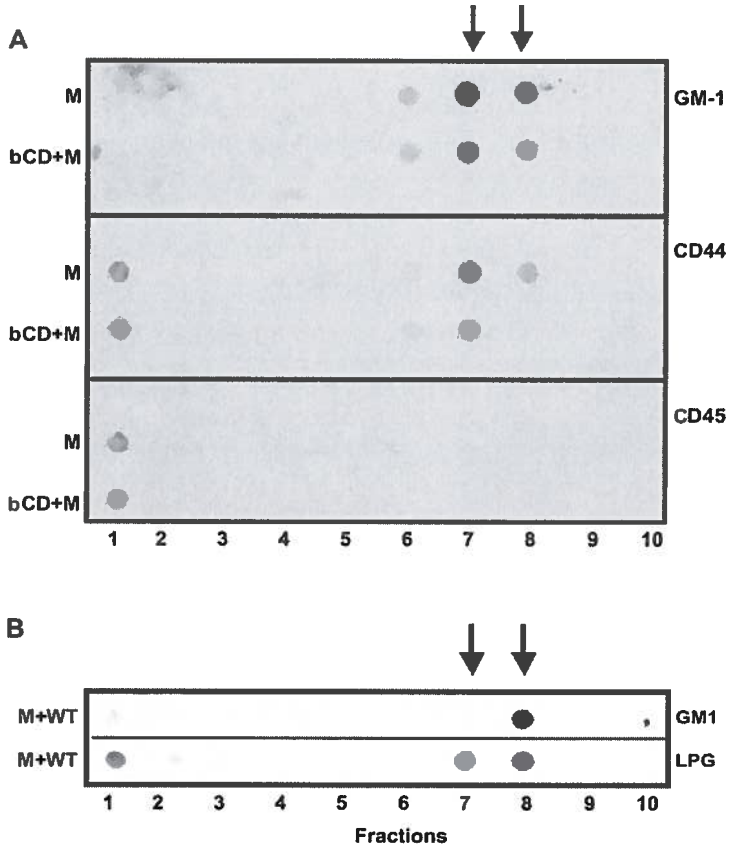

Figure 1. Dot-blot analysis of membrane fractions from human monocyte-derived macrophages (MDMs). Lysates of MDMs were applied on a sucrose gradient and fractionated by centrifugation. Ten fractions were collected and analyzed using dot-blot. To disrupt membrane rafts the MDMs were preincubated in β-cyclodextrin (βCD) before lysis. GM1 was detected with the β-subunit of cholera toxin, CD44 and CD45 were detected with mouse monoclonal antibodies. Blots from representative experiments are shown (n = 3–5) in **A**. Arrows indicate fractions containing membrane rafts (fraction 7 and 8), characterized by the presence of GM1 and CD44 and the absence of CD45. **B**: Analysis of GM1 and LPG after membrane fractionation of MDMs infected with WT *L. donovani* promastigotes.

To further demonstrate the localization of LPG in membrane rafts, we infected macrophages with either WT promastigotes or LPG-coated zymozan. As shown in Fig. 2A, at 10 min (left panel) and 30 min (right panel) after the initiation of phagocytosis, LPG was present in the phagosome membrane and colocalized with GM-1 (arrows). We also observed that at 30 min, the distribution of GM-1 labelling in the phagosomal membrane was more uniform than at 10 min, suggesting that LPG may influence raft integrity. Similar results were obtained following the internalization of LPG-coated zymozan, where colocalization of LPG and GM1 was observed at the phagosomal membrane (Fig. 2B).

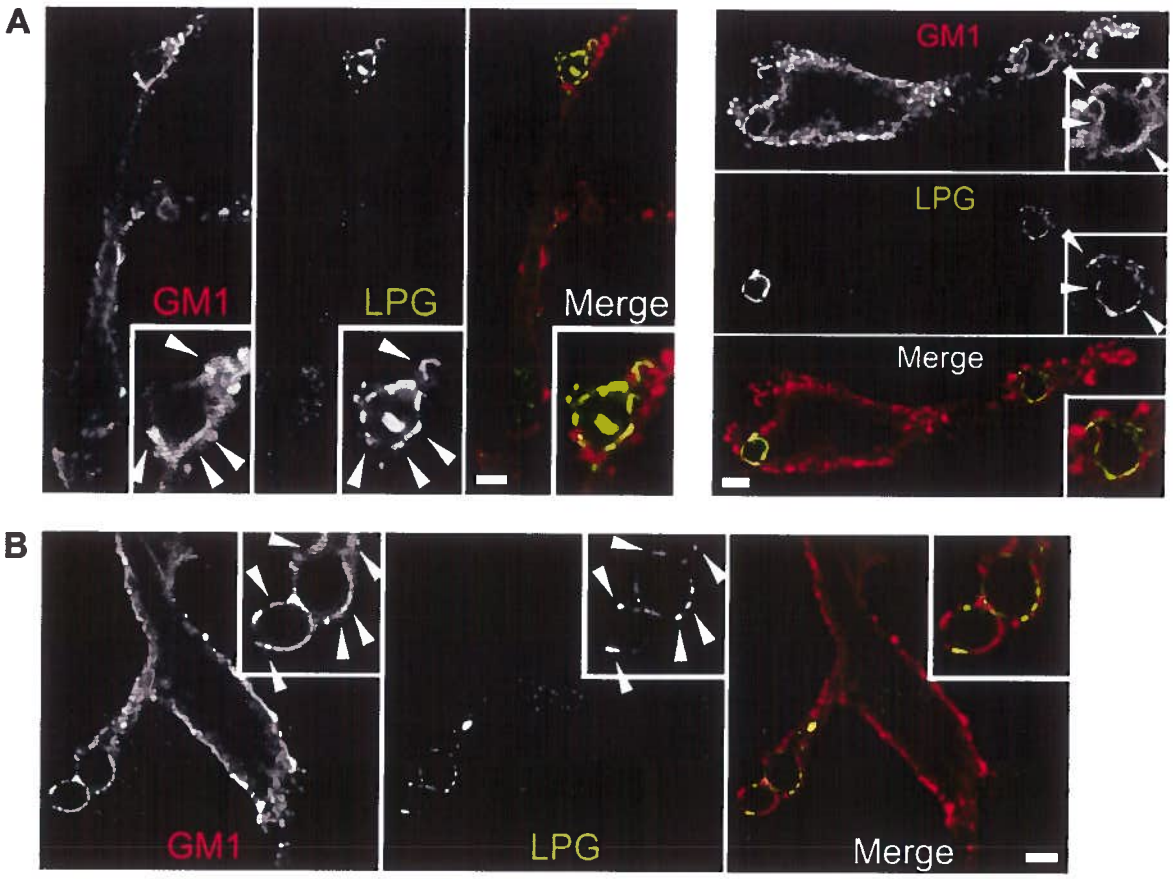

Figure 2. Insertion of LPG into GM1-positive lipid rafts on phagosomal membranes. **A**. BMM were infected with WT promastigotes for 10 min (left panel) or 30 min (right panel), fixed, and labelled for LPG (green) and GM1 (red). Colocalization analysis showed that LPG is delivered early to GM1-enriched domain on newly forming phagocytic cup (left panel). Insertion of LPG into lipid microdomains is accompanied by a loss of the punctuated distribution of GM1 in the phagosomal membrane (right panel). **B**. BMM were allowed to internalize LPG-coated zymozan for 10 min, fixed, and labelled for LPG (green) and GM1 (red). LPG colocalizes with GM1-enriched domain. Bar, 3 μm.

The effect of LPG on phagosomal maturation requires membrane rafts

To further investigate the importance of membrane rafts in *Leishmania* pathogenesis, we studied the effect of cholesterol extraction on phagocytosis, periphagosomal F-actin and phagosomal maturation in *L. donovani*-infected cells. Macrophages ingested *lpg2*$^{-}$KO promastigotes slightly more effectively than WT promastigotes (Fig. 3). Cholesterol depletion reduced the capacity of macrophages to ingest *L. donovani* by 29% for *lpg2*$^{-}$KO promastigotes and by 36% ($p < 0.01$) for WT promastigotes compared to non-treated cells (Fig. 3). Quantification of periphagosomal F-actin around promastigote-containing phagosomes showed that its accumulation around phagosomes carrying WT promastigotes was reduced in cholesterol-depleted cells (1.0 ± 0.08 vs. 0.62 ± 0.06, $p < 0.001$; Fig. 4A). Cholesterol depletion itself caused a slight increase in periphagosomal F-actin (0.59 ± 0.04 vs. 0.46 ± 0.03, $p < 0.01$) around phagosomes containing the *lpg2*$^{-}$KO mutant (Fig. 4A). The decreased levels of F-actin around WT promastigote-containing phagosomes in cholesterol-depleted cells correlated with increased translocation of the late endosomal marker LAMP-1 to these phagosomes (Fig. 4B–E). Thus 62.5 (±5.9, SEM) % of WT promastigote-containing phagosomes were LAMP-1 positive in cholesterol-depleted macrophages, compared to 27.0 (±3.1, SEM) % in control cells ($p < 0.01$). We found no evidence of reduced transfer of LPG to the plasma membrane of cholesterol-depleted macrophages compared to controls (not shown).

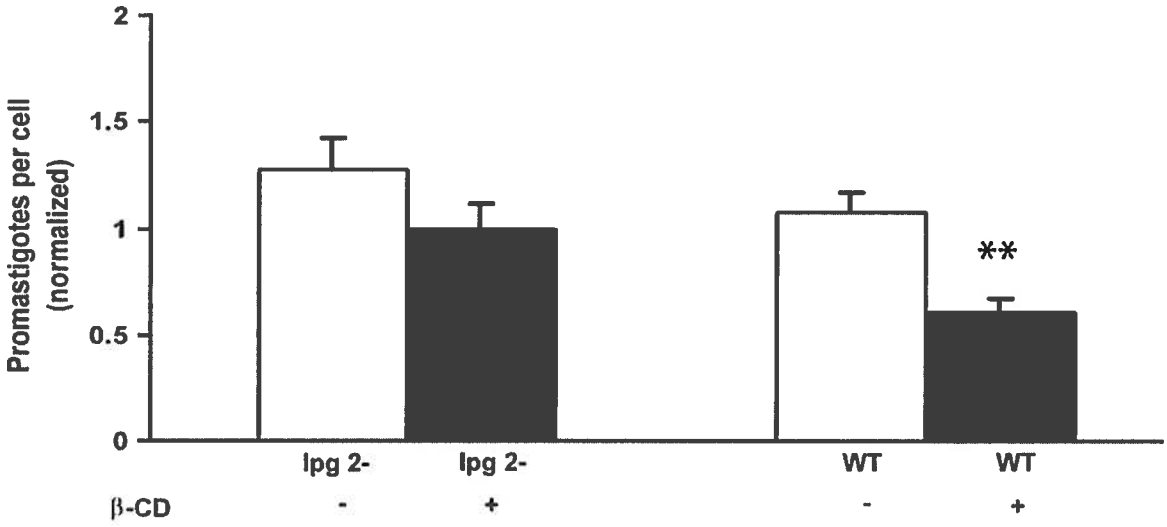

Figure 3. Phagocytic capacity of monocyte-derived macrophages (MDMs) interacting with *L. donovani* promastigotes. Cholesterol was extracted from the plasma membrane of MDMs using β-cyclodextrin (βCD). The cells were then infected with GFP-expressing WT or *lpg2*$^{-}$KO promastigotes followed by fixation. The preparations were labelled with phallacidin and the average number of promastigotes per cell, in random confocal images, was assessed. Each group contains data from 124 to 308 cells from at least three independent experiments. Error bars indicate standard error of the mean (SEM). ** represents statistically significant differences $p < 0.01$.

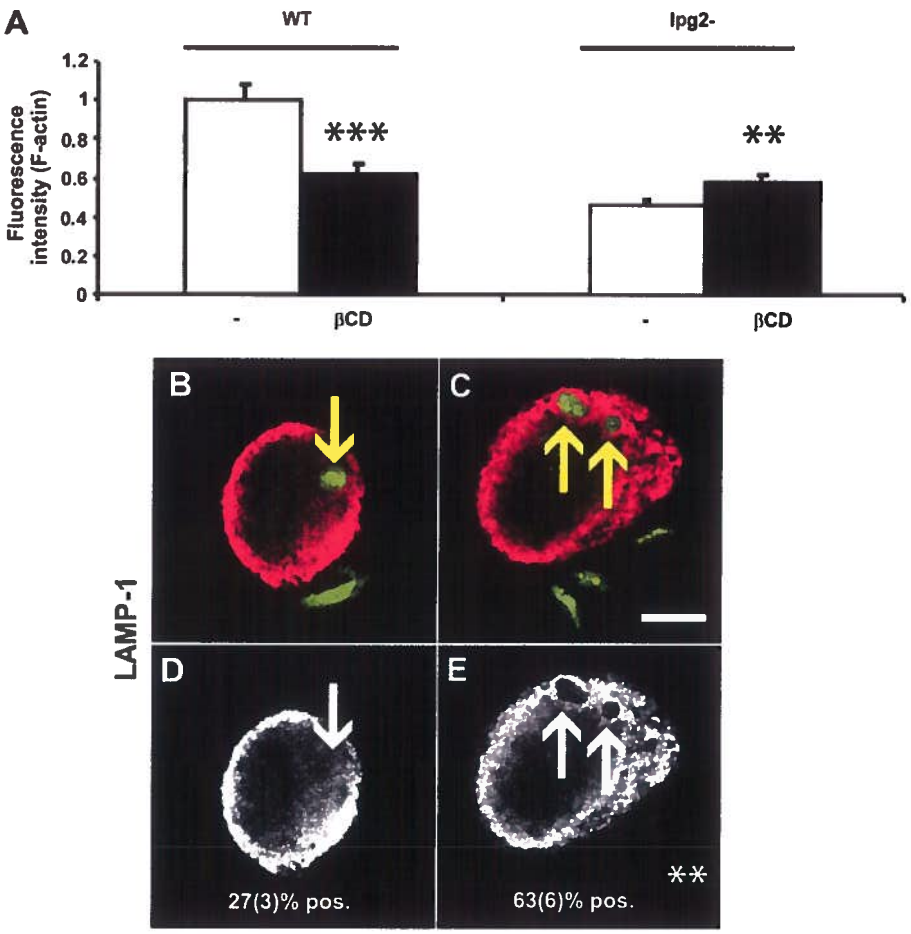
A
WT
Ipg2-
Fluorescence intensity (F-actin)
1.2
1
0.8
0.6
0.4
0.2
0
***
**
-
βCD
-
βCD
LAMP-1
B
C
D
E
27(3)% pos.
63(6)% pos.
**

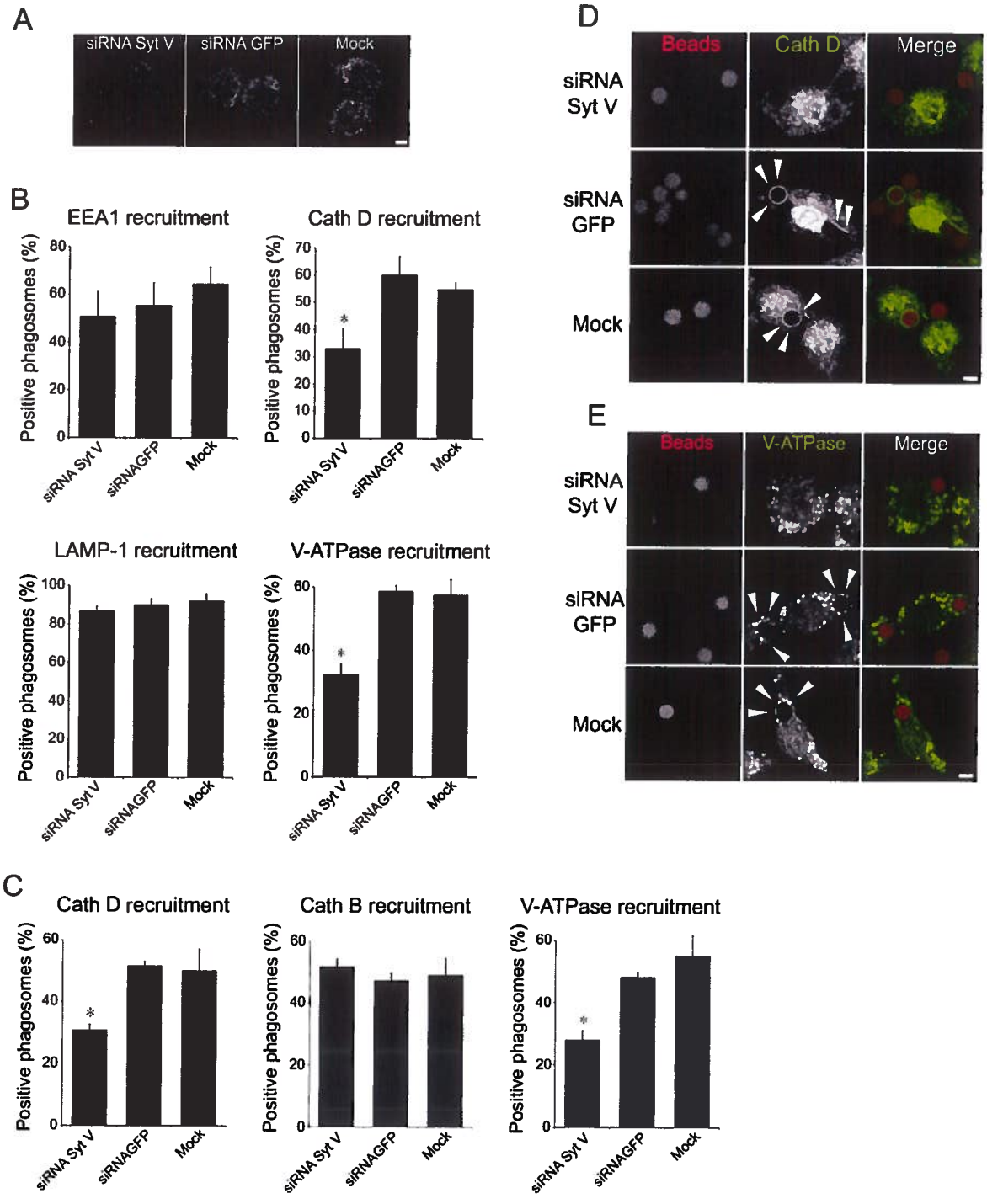
A
siRNA Syt V
siRNA GFP
Mock
B
EEA1 recruitment
Cath D recruitment
LAMP-1 recruitment
V-ATPase recruitment
Positive phagosomes (%)
siRNA Syt V
siRNAGFP
Mock
C
Cath D recruitment
Cath B recruitment
V-ATPase recruitment
D
Beads
Cath D
Merge
siRNA Syt V
siRNA GFP
Mock
E
Beads
V-ATPase
Merge
siRNA Syt V
siRNA GFP
Mock

Figure 1. Silencing of Syt V impairs the recruitment of cathepsin D and the V-ATPase to phagosomes. RAW 264.7 cells were transfected with either a siRNA to Syt V, a siRNA to GFP, or only mock transfected, and incubated for 24 h. Efficiency of Syt V silencing was verified by confocal immunofluorescence microscopy (*A*). *B* and *C*, RAW 264.7 cells were allowed to internalize Zym (*B*) or latex beads (*C*) after siRNA transfection. Phagosomal recruitments were determined at 15 min for EEA1 and at 2 h for cathepsin D, cathepsin B, and LAMP1 on at least 100 phagosomes for each condition. Data are shown as the percentage of phagosomes showing recruitment. Five independent experiments were performed and the bars show the standard deviations of one representative triplicate (*, $p \leq 0.05$). *D* and *E*, representative confocal images illustrating the recruitment of cathepsin D (*D*) and of the V-ATPase (*E*) on phagosomes containing latex beads. Bar, 3 μm.

***L. donovani* promastigotes impair the phagosomal association of Syt V.**

Given their ability to inhibit phagosome maturation [16,17,24], we explored the impact of *L. donovani* promastigotes and their LPG on the phagosomal association of Syt V. Accordingly, we infected the mouse macrophage cell line RAW 264.7 stably expressing a Syt V-GFP fusion protein (Syt V-GFP RAW 264.7 cells) with either wild-type (WT) *L. donovani* promastigotes, the LPG-defective *lpg1*-KO mutant, the Galβ1,4Manα1-PO_4-defective *lpg2*-KO mutant or the *lpg2*-KO add-back (*lpg2*-KO+*LPG2*). We used Zym as a positive control for the recruitment of Syt V to phagosomes [40]. Our results show that Syt V-GFP was present on over 80% of phagosomes containing either *lpg1*-KO promastigotes, *lpg2*-KO promastigotes, or Zym (Figures 2A and B). In contrast, we detected Syt V-GFP on 54 to 65% of phagosomes containing either WT or *lpg2*-KO+*LPG2* promastigotes in three independent experiments. Quantification analyses revealed a three-fold reduction in the levels of Syt V-GFP present on those positive phagosomes with respect to phagosomes containing either *lpg1*-KO or *lpg2*-KO promastigotes (Figures 2C). These observations suggested that LPG impairs the phagosomal recruitment of Syt V.

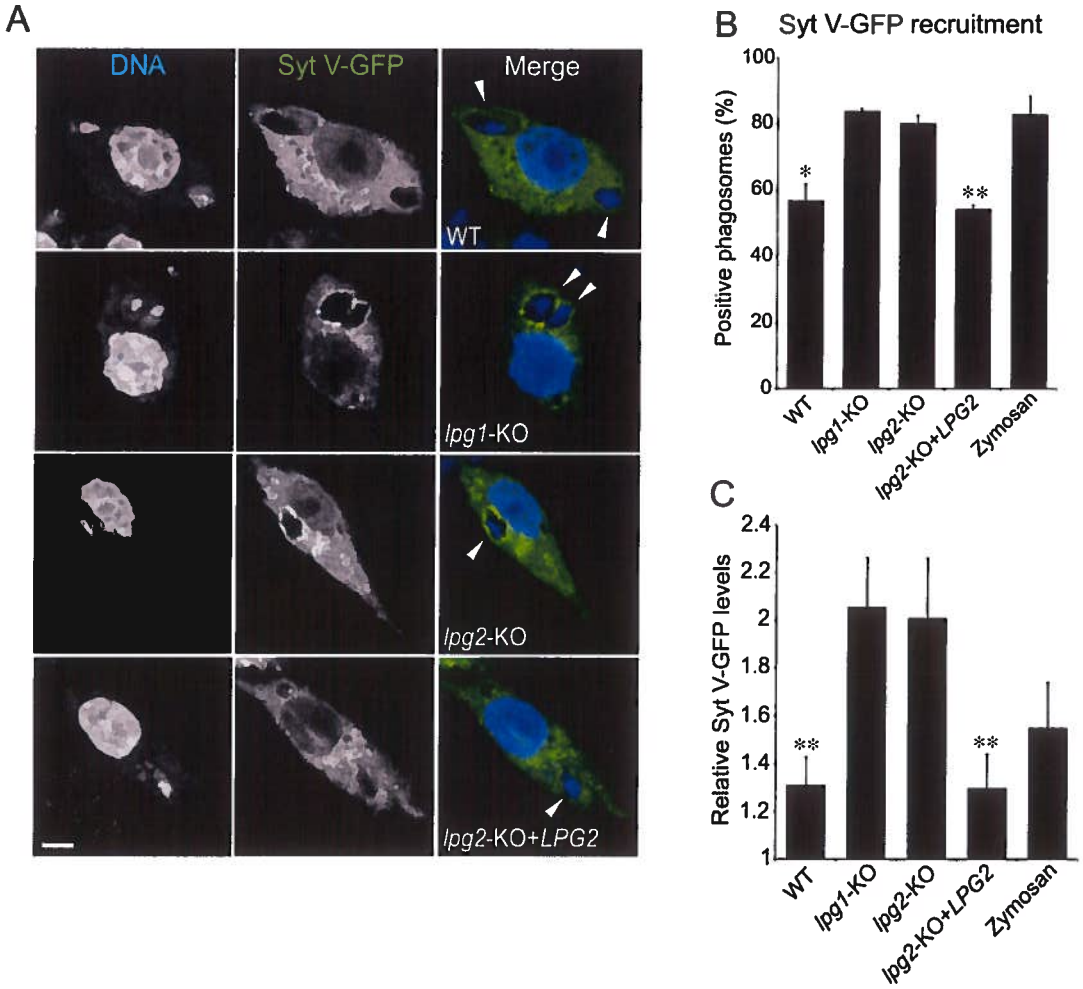

Figure 2. Syt V-GFP is excluded from *L. donovani* promastigote-containing phagosomes. Syt V-GFP RAW 264.7 cells were infected with either WT *lpg1*-KO, *lpg2*-KO, *lpg2*-KO+*LPG2 L. donovani* promastigotes or zymosan for 2 h, fixed and stained for DNA. *A*, Confocal images illustrating the presence of Syt V-GFP on parasite-containing phagosomes (shown by arrowheads). Presence (*B*) and relative levels (*C*) of Syt V-GFP were determined. Recruitment was determined on at least 100 phagosomes for each condition and expressed as a percentage of recruitment, and relative levels were determined as described in *Materials and Methods*. Three independent experiments were performed and the bars show the standard deviations of one representative triplicate (*, $p \leq 0.05$; **, $p \leq 0.005$; *B* and *C*, *p* values compare the presence and the accumulation of Syt V-GFP on phagosomes containing WT and *lpg2*-KO+*LPG2 vs lpg1*-KO and *lpg2*-KO parasites). Bar, 3μm.

To directly address the impact of LPG on the recruitment of Syt V to phagosomes, we fed bone marrow-derived macrophages (BMM) with either Zym or Zym coated with purified LPG (LPG-Zym) [22]. Consistent with previous observations [17,22], we found a reduced acquisition of LAMP-1 on phagosomes containing LPG-Zym, whereas the recruitment of EEA1 to phagosomes containing Zym or LPG-Zym was similar (Figure 3A and B). In the case of Syt V, we detected its presence on 24 to 30% of phagosomes containing LPG-Zym compared to over 60% of phagosomes containing Zym at all time points tested in three independent experiments (Figure 3C and D). Quantification analyses showed that the levels of Syt V present on those positive phagosomes containing LPG-Zym was significantly lower than the Syt V levels on phagosomes containing Zym (Figure 3C and D). We obtained similar results with the Syt V-GFP RAW 264.7 cells (Figure 3E and S2). Furthermore, the signals for Syt V (green) and LPG (red) rarely superimposed on the phagosome membrane (Figure 4A), and fluorescence intensity line scans acquired along the periphery of phagosomes showed that the most intense LPG and Syt V signals never overlapped, at both 30 min and 120 min after the initiation of phagocytosis (Figure 4B). We made similar observations in Syt V-GFP RAW 264.7 cells (Figure 4C and D). Collectively, these results established that insertion of LPG into the phagosomal membrane caused the exclusion of Syt V in a very localized manner.

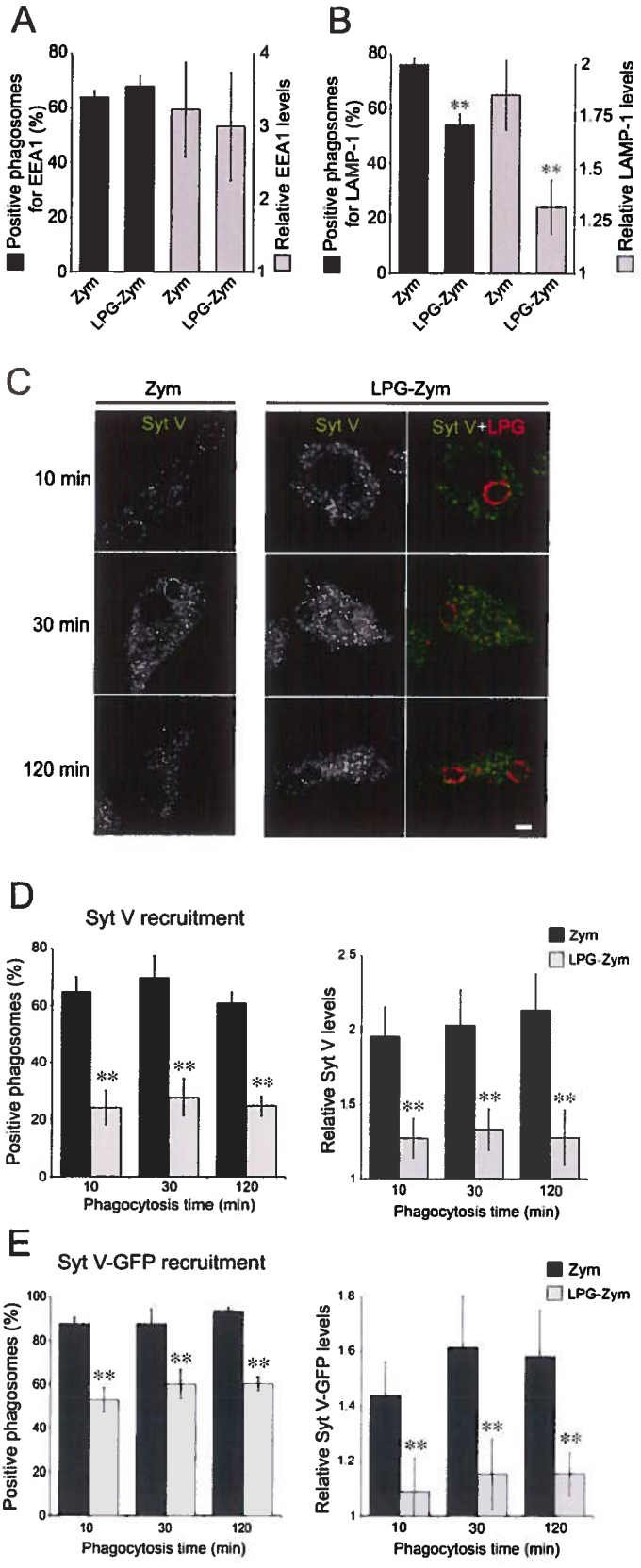
A
Positive phagosomes for EEA1 (%)
Relative EEA1 levels
Zym
LPG-Zym
B
Positive phagosomes for LAMP-1 (%)
Relative LAMP-1 levels
C
Zym
LPG-Zym
Syt V
Syt V+LPG
10 min
30 min
120 min
D
Syt V recruitment
Positive phagosomes (%)
Relative Syt V levels
Phagocytosis time (min)
E
Syt V-GFP recruitment
Positive phagosomes (%)
Relative Syt V-GFP levels
Phagocytosis time (min)

Figure 3. Recruitment of Syt V is impaired on phagosomes containing LPG-coated Zymosan. *A* and *B*, BMM were allowed to internalize Zym or LPG-Zym during 15 min (A) or 2 h (B), and prepared for confocal analysis. Presence (left y axis) and levels (right y axis) were determined for EEA1 (A) or LAMP-1 (B). *C* and *D*, BMM cells were allowed to internalize Zym or LPG-Zym for 10 min, 30 min or 2 h, fixed and stained for either endogenous Syt V (green) and LPG (red). The presence of Syt V and LPG on phagosomes is illustrated by confocal images (C). *D*. Quantification of Syt V recruitment (left panel) and relative Syt V levels on these phagosomes (right panel) were determined. *E*. Syt V-GFP cells were allowed to internalize Zym or LPG-Zym for 10 min, 30 min or 2 h, fixed and stained for LPG. Quantification of Syt V- recruitment (left panel) and relative Syt V levels on these phagosomes (right panel) were determined. The recruitment of EEA1, LAMP1 and Syt V was determined on at least 100 phagosomes for each condition, at least three independent experiments were performed and the bars show the standard deviations of one representative triplicate (*, $p \leq 0.05$; **, $p \leq 0.005$). Bar, 3μm

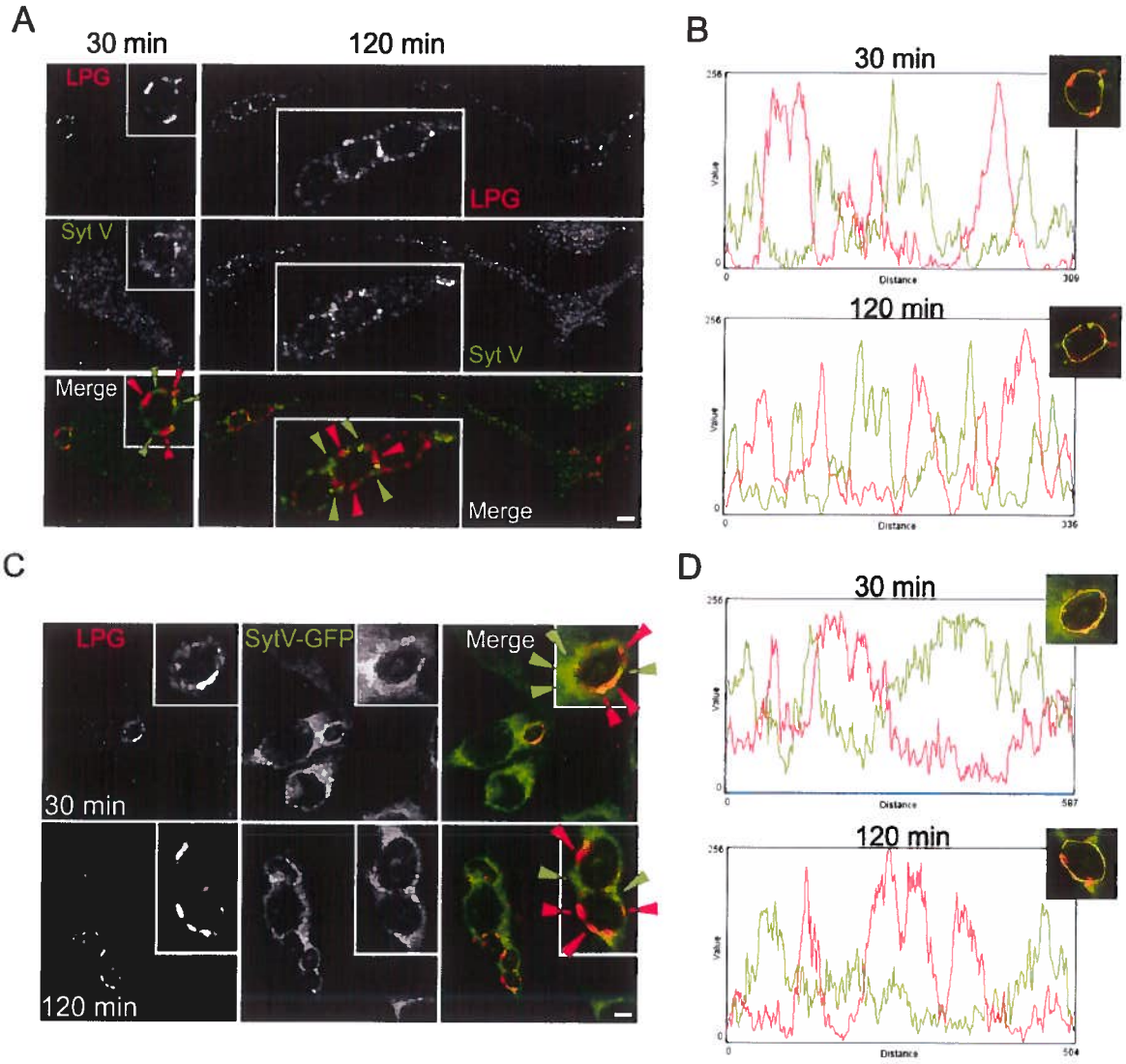
A
30 min
120 min
LPG
LPG
Syt V
Syt V
Merge
Merge
B
30 min
120 min
Value
Distance
C
LPG
SytV-GFP
Merge
30 min
120 min
D
30 min
120 min
Value
Distance

Figure 4. Exclusion of Syt V is restricted to the LPG insertion sites on the phagosome membrane. *A* and *B*, BMM were allowed to internalize Zym-LPG during 30 min or 2 h, and stained for Syt V (green) and LPG (red). Green arrowheads indicate a localized Syt V recruitment on phagosome membrane and red arrowheads indicate a localized LPG insertion into phagosome membrane (A). *C* and *D*, Syt V-GFP cells were allowed to internalize Zym-LPG for 30 min or 2 h, fixed and stained for LPG (red). Green arrowheads indicate a localized Syt V-GFP recruitment on phagosome membrane and red arrowheads indicate a localized LPG insertion into phagosome membrane (C). A rim around a representative phagosome formed in BMM (B) or in SytV-GFP cells (D) from *A* and *C* respectively, was manually traced with a one pixel width and fluorescence intensity profile of Syt V in green and LPG in red were represented in a graph for each phagocytosis time point. Bar, 3μm

Recruitment of Syt V to GM1-containing microdomains of phagosome membranes is prevented by LPG.

In rat brain synaptosomes, a fraction of Syt I and Syt II is present in lipid rafts [34]. To examine whether LPG-mediated exclusion of Syt V from phagosomes was related to the insertion of LPG into lipid microdomains [27,29] (Figure 5D), we first determined whether phagosome-associated Syt V was present in these microdomains. Our results clearly show that a fraction of Syt V colocalizes with GM1-microdomains on Zym-containing phagosomes (Figure 5A, arrowheads). Consistently, cholesterol depletion by methyl-β-cyclodextrin inhibited the recruitment of Syt V (Figure 5B and C). Having established that phagosomal Syt V associates with GM1-containing microdomains, we examined the localization of LPG, Syt V, and GM1 on phagosomes containing either Zym or LPG-Zym. For phagosomes containing Zym, the signals for Syt V (blue) and GM1 (red) superposed to a large extent and fluorescence intensity line scans acquired along the periphery of a representative phagosome showed that most of the Syt V and GM1 signals overlapped (Figure 5E and F, top panel). In contrast, on phagosomes containing LPG-Zym, the signals for LPG and GM1 colocalized, whereas most of the remaining Syt V signal was not associated with GM1 (representative phagosome, Figure 5E and F, bottom panel). These results established that association of LPG with GM1-containing microdomains resulted in the exclusion or dissociation of Syt V from the phagosome membrane.

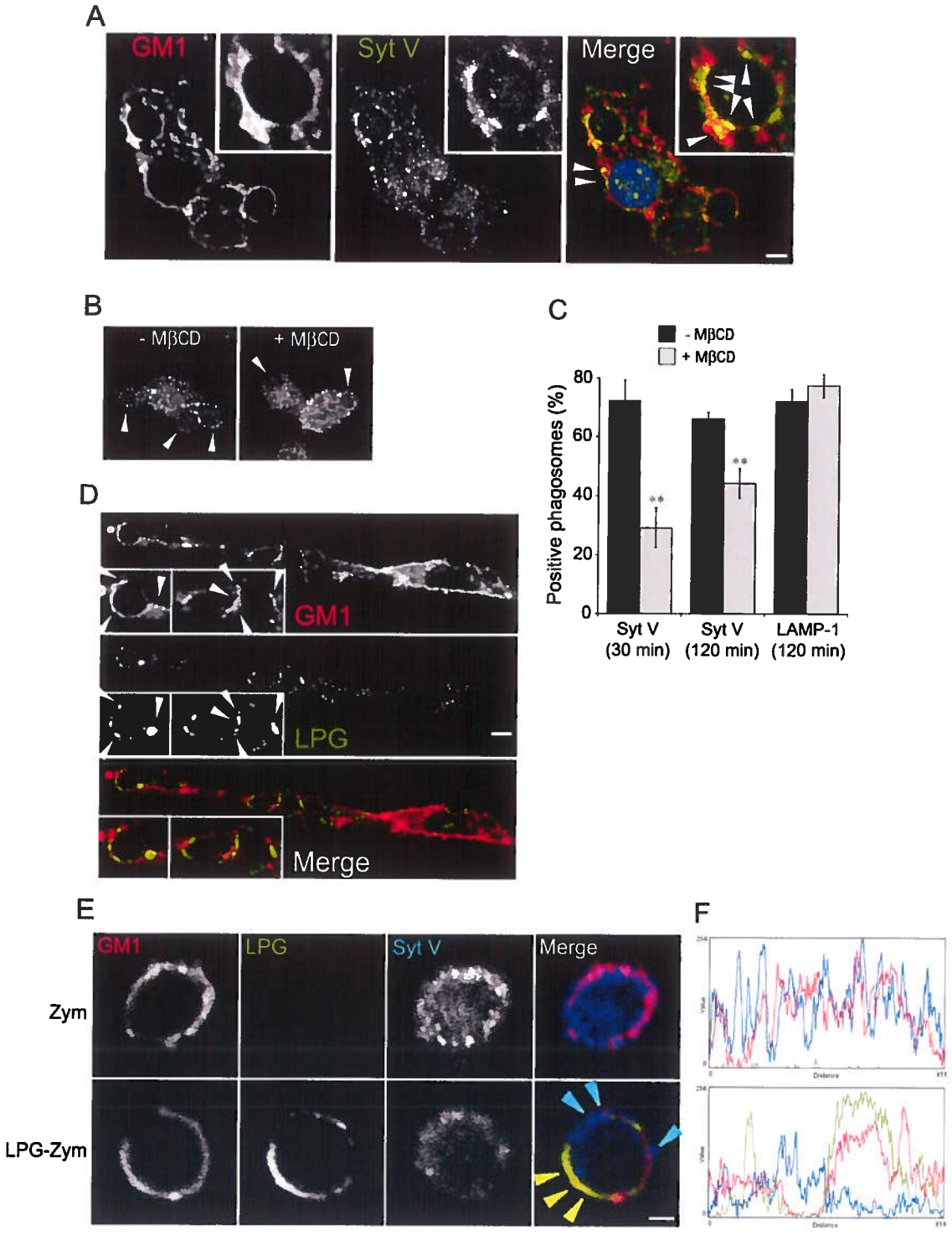
A
GM1
Syt V
Merge
B
- MβCD
+ MβCD
C
- MβCD
+ MβCD
Positive phagosomes (%)
80
60
40
20
0
**
**
Syt V (30 min)
Syt V (120 min)
LAMP-1 (120 min)
D
GM1
LPG
Merge
E
GM1
LPG
Syt V
Merge
Zym
LPG-Zym
F

Figure 5. Recruitment of Syt V to GM1-containing microdomains of phagosome membranes is prevented by LPG. *A*, BMM were allowed to internalize Zym for 30 min, fixed and stained for endogenous Syt V (green) and GM1 (red). White arrowheads indicate examples of colocalization between Syt V and GM1-positive microdomains, indicating a Syt V enrichment on these microdomains. *B* and *C*, BMM were either left untreated or treated with 10 mmol/L MβCD for 1 h before the internalization of Zym for 30 and 120 min. Cells were then fixed and stained for Syt V and LAMP-1. Representative confocal images of Syt V recruitment on cells with or without MβCD treatment is presented (*B*), white arrowheads indicate phagosomes. Syt V acquisition is expressed as a percentage of phagosome recruitment for Syt V. At least 100 phagosomes for each condition were assessed. Three independent experiments were performed and the bars show the standard deviations of one representative triplicate (*C*) (**, $p \leq 0.005$). *D*, BMM were allowed to internalize Zym-LPG for 30 min, fixed and stained for LPG (green) and GM1 (red). White arrowheads indicate a colocalization between LPG and GM1-positive rafts. BMM were allowed to internalize Zym (*E*, upper panel) or LPG-Zym (*E*, lower panel) for 30 min, fixed and stained for Syt V (blue), LPG (green) and GM1 (red). Blue arrowheads indicate a local Syt V acquisition on phagosome membrane and yellow arrowheads indicate a local colocalization between GM1 microdomains and LPG. A rim around each phagosome was manually traced with a one pixel width and fluorescence intensity profile of Syt V in blue, LPG in green and GM1 in red were represented in a graph (*F*). Bars, 3 μm (*A*, *B* and *D*) or 1μm (*E*).

***L. donovani* promastigotes exclude the V-ATPase from phagosomes via their LPG.**

The demonstration that Syt V regulates acquisition of the V-ATPase led us to verify the hypothesis that exclusion or dissociation of Syt V from phagosomes containing *L. donovani* promastigotes may impair the recruitment of the V-ATPase to these phagosomes. At 2 h after the initiation of phagocytosis, our results from three independent experiments showed a reduction in the recruitment of the V-ATPase *c* subunit on phagosomes containing WT promastigotes, ranging from 54 to 62% with respect to phagosomes containing either *lpg1*-KO or *lpg2*-KO promastigotes (Figures 6A and B). Co-localization of the V-ATPase *c* subunit with LAMP-1 on phagosomes containing *lpg1*-KO promastigotes showed that the V-ATPase *c* subunit was present on the phagosome membrane (Figure S3). As expected, phagosomes containing *lpg2*-KO+*LPG2* cells were similar to WT-phagosomes with respect to the presence of the V-ATPase. We next monitored the acidification of *L. donovani* promastigote-containing phagosomes using the lysosomotropic agent LysoTracker red as an indicator of phagosome pH. Our results showed a clear correlation between the presence of the V-ATPase *c* subunit and the association of LysoTracker red to phagosomes (Figure 6C). In Figure 1, we showed that silencing of Syt V inhibited recruitment of the V-ATPase *c* subunit to phagosomes containing Zym or latex beads. In Figure 6D, we show that silencing of Syt V abrogated recruitment of the V-ATPase *c* subunit to phagosomes containing *lpg1*-KO and *lpg2*-KO mutants. In the case of phagosomes containing either WT or *lpg2*-KO+*LPG2* promastigotes, Syt V silencing had the same effect as the presence of LPG on the recruitment of the V-ATPase *c* subunit (Figure 6D). Collectively, these results show that LPG enables *L. donovani* promatigotes to inhibit phagosomal recruitment of the V-ATPase by a Syt V-dependent mechanism and to prevent acidification. Remarkably, at 24 h after the initiation of phagocytosis, we detected the V-ATPase *c* subunit on only 10 to 17% of phagosomes containing *L. donovani* promastigotes in three independent experiments, consistent with LPG still being present (Figure 7A and C). At this time point, we detected LysoTracker red on only 20% of phagosomes containing WT promastigotes (not shown), indicating that promastigotes remodel their intracellular niche to establish infection in a compartment that fails to acidify, at a time when differentiation into amastigotes takes place. In

contrast, we detected the V-ATPase *c* subunit on 66 to 71% of phagosomes containing *L. donovani* amastigotes at both 2 h and 24 h after the initiation of phagocytosis (Figure 7B and C). This observation is consistent with the fact that amastigotes replicate in an acidic phagolysosomal compartment [14].

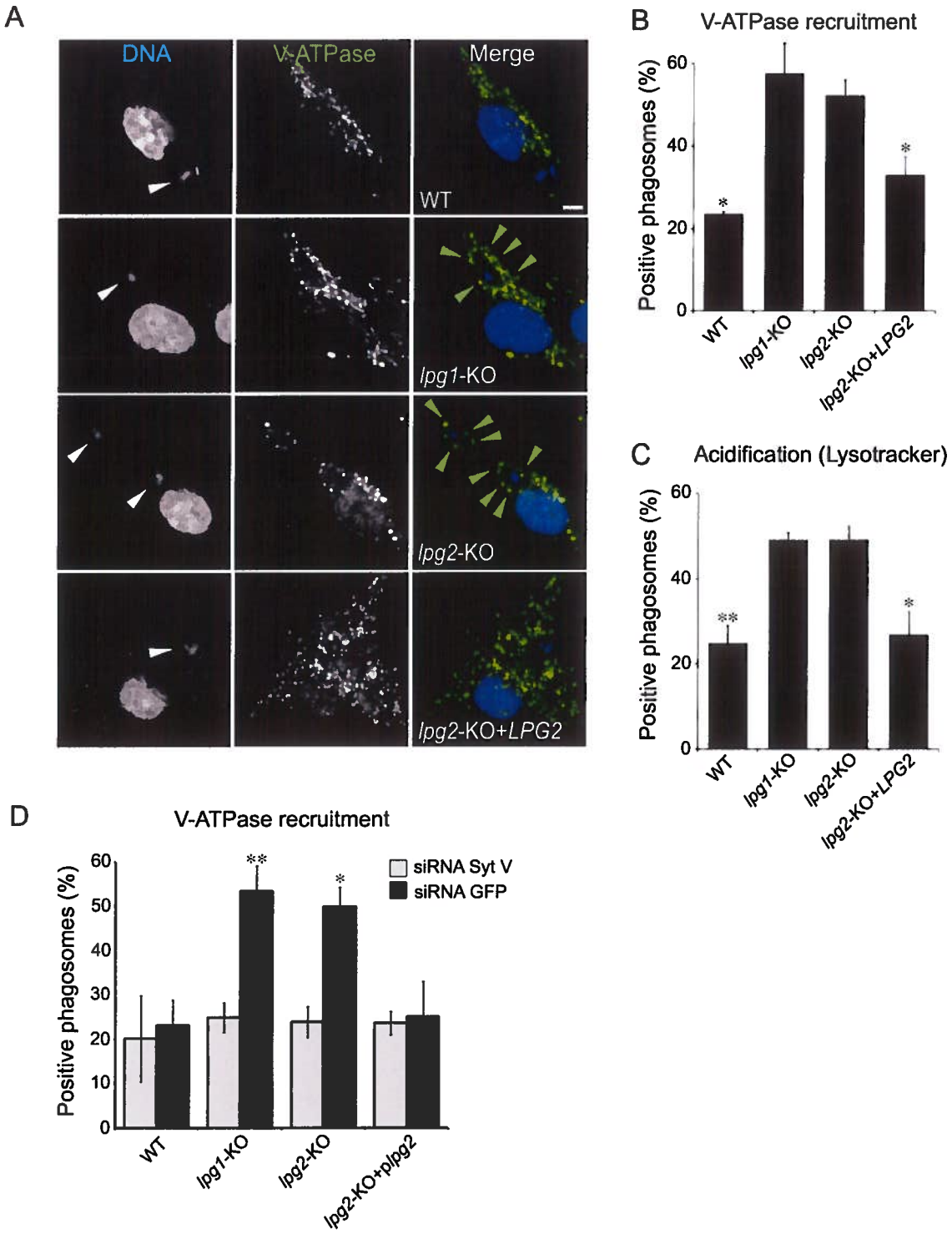
A
DNA
V-ATPase
Merge
WT
lpg1-KO
lpg2-KO
lpg2-KO+LPG2
B
V-ATPase recruitment
Positive phagosomes (%)
60
40
20
0
*
*
WT
lpg1-KO
lpg2-KO
lpg2-KO+LPG2
C
Acidification (Lysotracker)
Positive phagosomes (%)
60
40
20
0
**
*
WT
lpg1-KO
lpg2-KO
lpg2-KO+LPG2
D
V-ATPase recruitment
siRNA Syt V
siRNA GFP
Positive phagosomes (%)
60
50
40
30
20
10
0
**
*
WT
lpg1-KO
lpg2-KO
lpg2-KO+plpg2

Figure 6. LPG prevents delivery to phagosomes of the V-ATPase and acidification through a Syt V-dependent mechanism. *A* and *B*, BMM cells were infected with either WT, *lpg1*-KO, *lpg2*-KO, *lpg2*-KO+*LPG2* promastigotes for 2 h, fixed and stained for V-ATPase (green) and DNA (blue). *A*, Confocal images illustrating V-ATPase acquisition (green arrowheads) on parasite-containing phagosomes (white arrowheads). *B*, V-ATPase acquisition was determined on at least 100 phagosomes for each condition. Three independent experiments were performed and the bars show the standard deviations of one representative triplicate (*, $p \leq 0.05$; *p* values compare the presence and the relative levels of V-ATPase on phagosomes containing WT and *lpg2*-KO+*LPG2 vs lpg1*-KO and *lpg2*-KO parasites). *C*, BMM cells were incubated 2 h with Lysotracker red prior to infection with either WT, *lpg1*-KO, *lpg2*-KO, *lpg2*-KO+*LPG2* promastigotes for 2h and then fixed. *D*, RAW 264.7 cells were transfected with either a siRNA to Syt V or a siRNA to GFP, incubated for 24 h and infected with either WT, *lpg1*-KO, *lpg2*-KO, *lpg2*-KO+*LPG2* promastigotes for 2 h. Macrophages were then fixed and stained for DNA and the V-ATPase. Phagosomal recruitments were determined on at least 60 phagosomes for each condition. Two independent experiments were performed and the bars show the standard deviations of one representative triplicate. Data are shown as the percentage of recruitment (*, $p \leq 0.05$; **, $p \leq 0.005$; *p* values compare the acquisition of V-ATPase on phagosomes containing WT and *lpg2*-KO+*LPG2 vs lpg1*-KO and *lpg2*-KO parasites). Bar, 3μm.

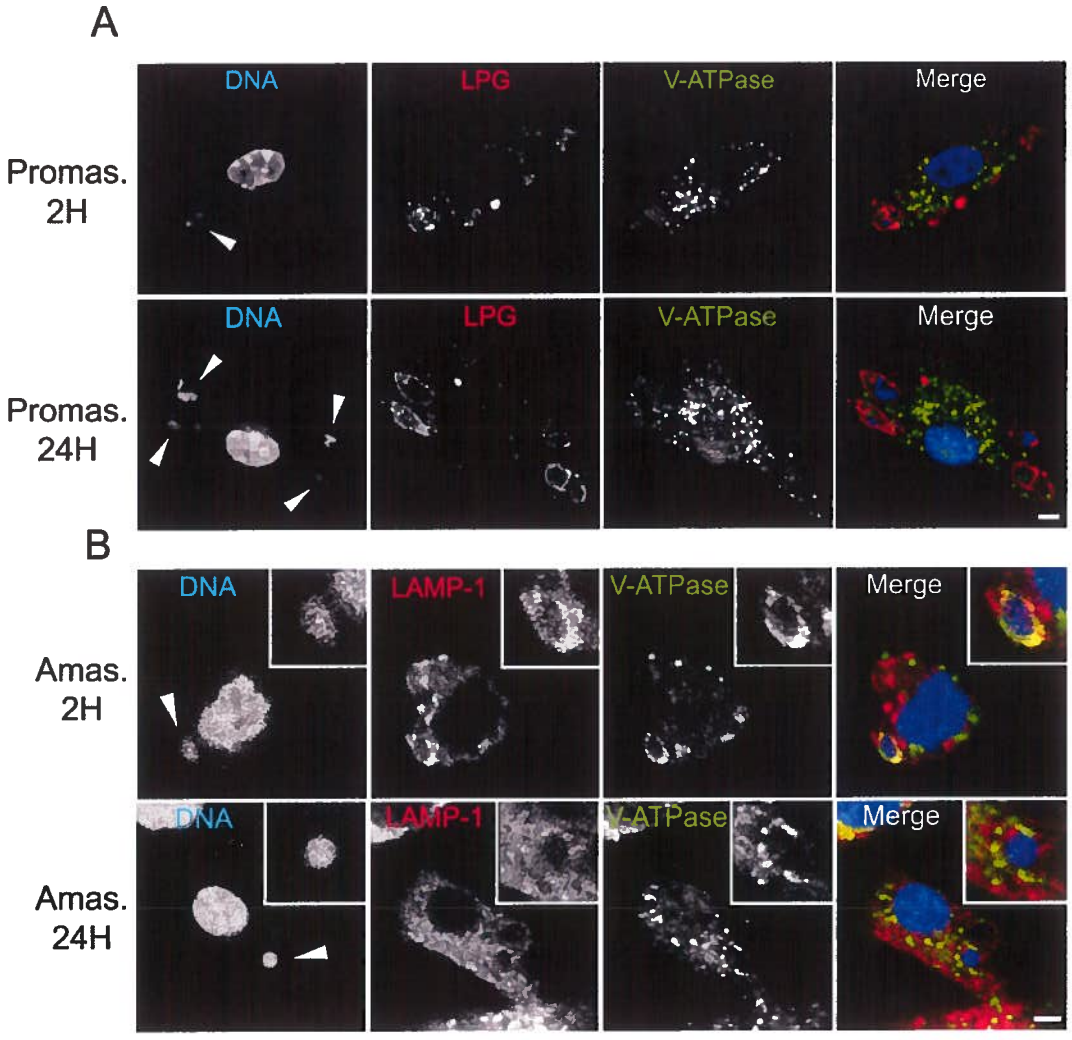
A
DNA
LPG
V-ATPase
Merge
Promas. 2H
Promas. 24H
B
LAMP-1
Amas. 2H
Amas. 24H
C
V-ATPase recruitment
Positive phagosomes (%)
80
60
40
20
0
**
**
Promas. 2H
Promas. 24H
Amas. 2H
Amas. 24H

Figure 7. The inhibition of the V-ATPase acquisition on phagosomes is specific for the promastigote stage. *A* - *C*, BMM cells were infected with either WT promastigotes or amastigotes for 2 h and 24 h, fixed and stained for V-ATPase (green), LPG (red) and DNA (blue) (A) or V-ATPase (green), LAMP-1 (red) and DNA (blue) (B). *A* and *B*, Confocal images illustrating V-ATPase acquisition on parasite-containing phagosomes (white arrowheads). *C*, V-ATPase acquisition was determined on at least 100 phagosomes for each condition and expressed as a percentage of recruitment. Three independent experiments were performed and the bars show the standard deviations of one representative triplicate (**, $p \leq 0.005$; p values compare the acquisition of V-ATPase on phagosomes containing promastigotes *vs* amastigotes parasites). Bar, 3μm.

Discussion

The exocytosis regulator Syt V is recruited to the nascent phagosome and remains associated throughout the maturation process [40], leading us to investigate its potential role in modulating interactions between the phagosome and endocytic organelles. Our results revealed that whereas silencing of Syt V had no effect on the recruitment of EEA1, LAMP-1, and cathepsin B, it inhibited the phagosomal acquisition of cathepsin D and of the V-ATPase c subunit. These findings indicated that Syt V plays a role in phagolysosome biogenesis, possibly by regulating the interaction between phagosomes and a subset of late endosomes or lysosomes enriched in cathepsin D and in the V-ATPase *c* subunit. Alternatively, Syt V may be needed to reach the level of phagosome maturation necessary to acquire the machinery that regulates the recruitment of cathepsin D and the V-ATPase *c* subunit. Our finding that acquisition of cathepsin B and cathepsin D is mediated by distinct mechanisms supports the demonstration that various hydrolases appear sequentially, at various time points during phagosome maturation [42]. This view is also consistent with evidence that various sub-populations of early endosomes, late endosomes, and lysosomes co-exist and that these compartments contain significant heterogeneity [43]. Together with previous findings [27], our results show that phagosomal acquisition of the V-ATPase and LAMP-1 are mediated through distinct mechanisms. Hence, the observations that LAMP-1 is recruited to phagosomes independently of Syt V and that *L. donovani* promastigotes (and LPG) impair the recruitment of LAMP-1 point to the existence of other inhibitory mechanisms and illustrate the complexity of phagolysosome biogenesis. The role of Syt V in regulating interactions between the phagosome and the endosomal compartments thus seems specific and further studies will be necessary to understand its precise role during phagosome maturation. Recent studies by Andrews and colleagues revealed that the lysosome-associated Syt VII, which controls membrane delivery to nascent phagosomes [9], is involved in phagolysosome fusion [9,10]. It will be of interest to determine whether Syt V and Syt VII use similar mechanisms to regulate phagolysosome biogenesis.

To establish infection inside macrophages, *L. donovani* promastigotes, the form of the parasite transmitted to mammals by the sand fly vector, create an intracellular niche by inhibiting phagolysosome biogenesis [16]. Genetic and biochemical approaches revealed that this inhibition is mediated by the parasite surface glycolipid LPG [16,17,22]. Insight into the mechanism of this inhibition came from the observations that LPG transfers from the parasite surface to the nascent phagosome membrane [26], where it disrupts existing lipid microdomains and alters the formation of these structures after promastigote internalization [28,29]. Whereas the precise mechanism remains to be elucidated, the current model is that LPG inserts into lipid microdomains via its GPI anchor, thereby allowing the negatively charged Galβ1,4Man-PO_4 polymer of LPG to directly interfere with the clusterization of molecules into these microdomains. This model is consistent with the demonstration that alteration of membrane properties is dependent on the length of the Galβ1,4Man-PO_4 polymer [16,44]. Because of their role in clustering specific sets of proteins, membrane lipid microdomains are central to a wide variety of cellular processes, including regulated exocytosis [45,46]. Our findings that Syt V was present in GM1-enriched phagosome microdomains and that LPG inserts into or associates with these structures to interfere with the phagosomal association of Syt V thus provides new insight into the mechanism of LPG-mediated inhibition of phagolysosome biogenesis.

Acquisition of an array of hydrolases and acidification of the phagosome enable the generation of a highly microbicidal environment [4] and the creation of a compartment competent for antigen processing and presentation [47]. To circumvent killing following uptake by macrophages, several intracellular microorganisms interfere with phagosome acidification and maturation [4,12,48]. The discovery that *L. donovani* promastigotes establish infection inside a compartment from which the V-ATPase is excluded may thus be favorable for parasite survival. Incidentally, a recent study showed that phagosome acidification is defective in Stat1-/- macrophages and this correlated with an increased survival of L. *major* promastigotes, suggesting a role for acidic pH in the control of intracellular *Leishmania* growth early during infection [49]. Furthermore, the finding that phagosomes containing *L. donovani* promastigotes fail to acquire the V-

ATPase and acidify even at 24 hours post-infection provides new insight on our undestanding of *Leishmania* biology. Indeed, in the absence of data on the pH of promastigote-containing phagosomes, it has been assumed that promastigotes initiate infection in an acidic environment and that differentiation of promastigotes into amastigotes is mainly triggered by a rapid exposure to an acidic environment and elevated temperature [50]. Exclusion of the V-ATPase raises the possibility that *L. donovani* promastigotes initiate the differentiation process in a non-acidified environment. Further studies will be required to fully address this point. An issue that remains unsolved pertains to the acquisition of phagolysosomal features and acidification of parasite-containing vacuoles upon completion of the differentiation of promastigotes into amastigotes. Indeed, previous work by Antoine and colleagues [14] established that *L. amazonensis* amastigotes reside within an acidic vacuole (pH 4.7-5.2), in agreement with the notion that *Leishmania* amastigotes are internalized within a vacuole that rapidly acquires lysosomal features and in which amastigotes proliferate [13,51]. Consistent with these previous reports, we showed the presence of LAMP-1 and the V-ATPase *c* subunit on phagosomes containing *L. donovani* amastigotes as early as 2 h after internalization. A possible explanation is that during the first few days post-infection, the presence of LPG in the phagosome membrane prevents acidification and maturation, allowing promastigote-to-amastigote differentiation to take place. The down-regulation of LPG biosynthesis below detectable levels in amastigotes [52] may enable phagosomes to gradually acquire lysosomal features and to acidify.

Little is known on the mechanisms that regulate recruitment of the V-ATPase to maturing phagosomes. The identification of Syt V as a regulator of this process and the fact that Syt V is present in microdomains of the phagosome membrane is consistent with the notion that these structures are important for the recruitment of the V-ATPase to the phagosome membrane [27]. Of interest, the V-ATPase *c* subunit has been previously identified in Triton X-100-resistant fractions from rat brain synaptic vesicles in association with synaptobrevin 2 and synaptophysin [53], leading the authors of that study to conclude that this interaction may play a role in recruiting the V-ATPase to

synaptic vesicles. Whether Syt V is part of such a SNARE complex on phagosomes and the characterization of this complex are important issues that await further investigation.

In this study, we provided novel findings into the mechanism of *Leishmania* pathogenesis, whereby targeting of Syt V, which plays a role in the acquisition of phagosome microbicidal properties, is part of the strategy used by *L. donovani* promastigotes to create a niche propitious to the establishment of infection within mammalian hosts (see working model, Figure 8). Interestingly, phagocytosis of either zymosan or *lpg2*-KO promastigotes coated with the virulence glycolipid lipoarabinomannan from *Mycobacterium tuberculosis*, impaired the phagosomal association of Syt V (Figure S4). Whether other intracellular microorganisms use a similar mechanism to remodel their intracellular niche remains to be investigated.

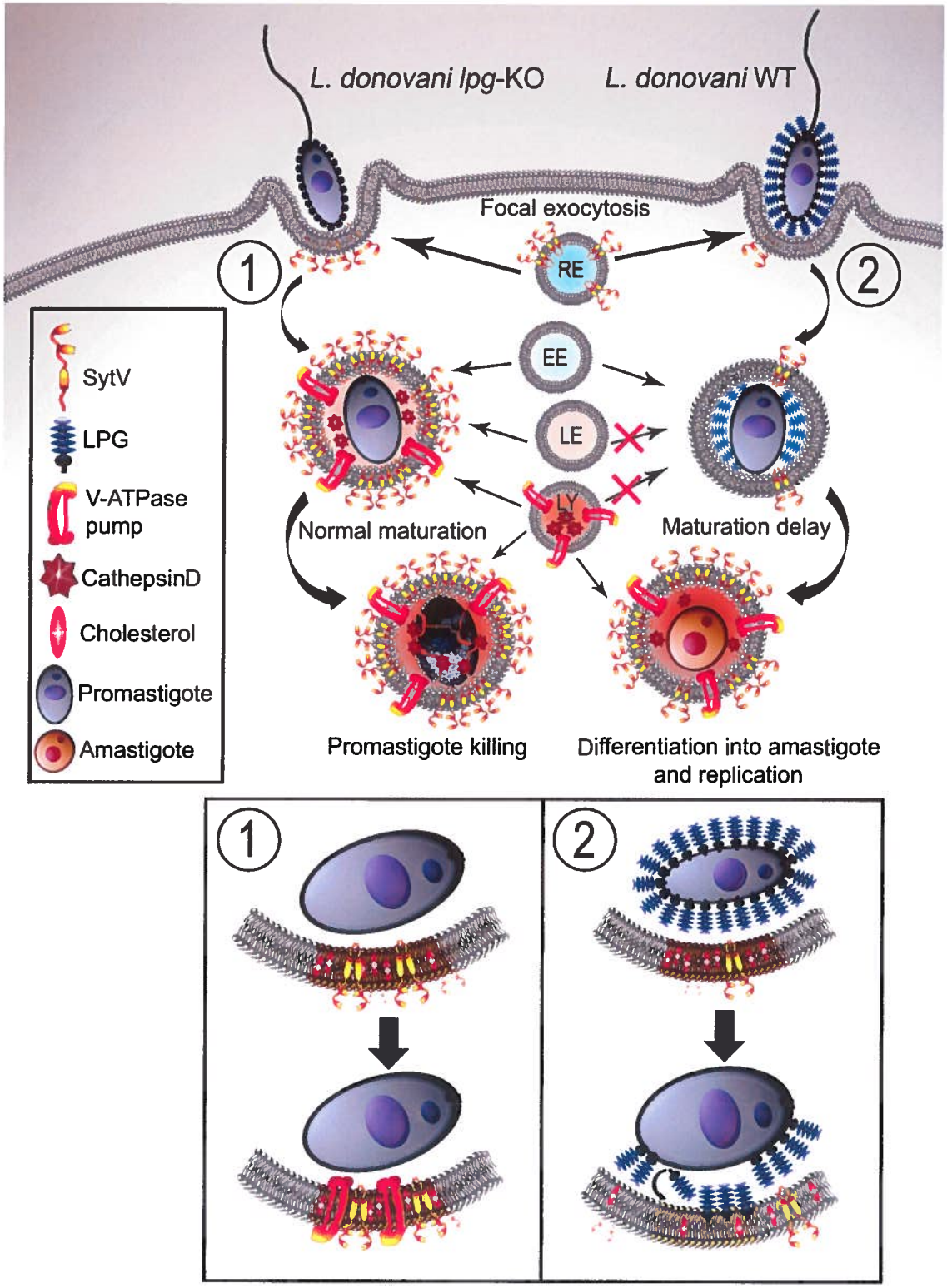
L. donovani lpg-KO
L. donovani WT
Focal exocytosis
RE
1
2
EE
LE
LY
Normal maturation
Maturation delay
SytV
LPG
V-ATPase pump
CathepsinD
Cholesterol
Promastigote
Amastigote
Promastigote killing
Differentiation into amastigote and replication
1
2

Figure 8. Working model for the exclusion of the V-ATPase from *L. donovani* promastigote-harboring phagosomes. Both WT and LPG-defective *L. donovani* promastigotes bind to macrophages, inducing the phagocytic process. During this step, membrane from internal vesicles such as recycling endosomes (RE) bearing Syt V participate to the membrane supply necessary for the formation of the nascent phagosome. LPG transfers to the phagosome membrane and inserts into lipid microdomains, excluding Syt V from the newly formed phagosome. Exclusion of Syt V impairs phagolysosome biogenesis, including acquisition of cathepsin D and V-ATPase (2) when compared to phagosomes harboring *L. donovani* promastigotes lacking LPG (1), which interact with the endosomal compartment (early endosomes, EE; late endosomes, LE; lysosomes, LY). This creates an intracellular niche that fails to acidify, at a time when promastigotes differentiate into amastigotes, which are resistant to the microbicidal properties of the phagolysosome. Mutants lacking LPG are degraded by the phagolysosomal environment

.

Materials and Methods

Macrophages

All animals were handled in strict accordance with good animal practice as defined by the Canadian Council on Animal Care, and all animal work was approved by the Comité institutionel de protection des animaux of INRS- Institut Armand-Frappier (protocol 0811-08). BMM were obtained by growing bone marrow cells from female BALB/c mice at 37°C in 5% CO2 for 7 days in Dulbecco Modified Eagle Medium with L-glutamine (Life Technologies) supplemented with 10% heat-inactivated FBS (Hyclone, Logan, UT), 10 mM Hepes (pH 7.4) and antibiotics (complete medium) in the presence of 15% (v/v) L929 cell-conditioned medium as a source of colony-stimulating factor (CSF)-1 [54]. BMM were made quiescent by culturing them in the absence of CSF-1 for 18 h prior to being used. The murine macrophage cell line RAW 264.7 was grown in complete medium in a 37°C incubator with 5% CO2. Stably transfected RAW264.7 cells expressing Syt V-GFP (Syt V-GFP RAW 264.7 cells) were previously described [40]. Transfectants were cultured in complete medium containing 500 μg/ml G418 (Life Technologies).

Parasites

Leishmania donovani promastigotes (Sudanese strain 1S) were grown at 26°C in RPMI 1640 medium supplemented with 20% heat-inactivated FBS, 100 μM adenine, 20 mM 2-[N-morpholino]ethanesulphonic acid (pH 5.5), 5 μM hemin, 3 μM biopterin, 1 μM biotin and antibiotics. The isogenic *L. donovani* LPG-defective mutants *lpg1*-KO and *lpg2*-KO were described previously [55]. The *lpg1*-KO mutant secretes repeating Galβ1,4Manα1-PO_4-containing molecules, but lacks the ability to assemble a functional LPG glycan core [56], precluding synthesis of LPG. The *lpg2*-KO mutant expresses the truncated LPG Gal(α1,6)Gal(α1,3)Gal$_f$(β1,3)[Glc(α1-P)]Man(α1,3)Man(α1,4)GN(α1,6)-PI, and does

not synthesize repeating Galβ1,4Manα1-PO_4 units [57]. The *lpg2*-KO+*LPG2* add-back was grown in the presence of 50 μg/ml G418. For infections, promastigotes were used in late stationary phase of growth. *L. donovani* amastigotes (Strain LV9) were isolated from the spleen of infected female LVG Golden Syrian hamsters (Charles River, St-Constant, QC, Canada), as described [58].

Reagents and antibodies

The rabbit anti-Syt V spacer antiserum was raised against the cytoplasmic region between the transmembrane and the C2 domain (aa 71–216) [37] and was affinity-purified. The rat monoclonal antibody against LAMP-1 developed by J. T. August (1D4B) was obtained through the Developmental Studies Hybridoma Bank at the University of Iowa, and the National Institute of Child Health and Human Development. The rabbit antiserum against the 16 kDa proteolipid subunit (*c* subunit) of the V0 sector of the V-ATPase was kindly provided by Dr. Mhairi Skinner (University of Guelph, ON, Canada) [59]. The mouse monoclonal antibody against EEA1 was from BD Transduction Laboratories. The rabbit antiserum against cathepsin B was from Millipore and the rabbit antiserum against cathepsin D was from Upstate. The mouse monoclonal anti-LPG (CA7AE) was prepared from hybridoma supernatant [60]. Methyl-β-cyclodextrin (MβCD) was from Sigma (St-Louis, MO, USA). LPG was isolated from the log phase cultures of *L. donovani* promastigotes as previously described [61,62]. Purified lipoarabinomannan (LAM) from H37Rv strain of *Mycobacterium tuberculosis* was from Colorado State University (Fort Collins, CO, USA).

RNA interference

Syt V silencing by RNAi was performed as previously described [40] using a small interfering RNA (siRNA) corresponding to nucleotides 94–112 of the Syt V cDNA [38], whereas a siRNA specific to GFP was used as a negative control [63]. Adherent RAW 264.7 cells were transfected with siRNA duplexes at a final concentration of 240 nM using OligoFectamine (Invitrogen) as described [63]. A BLAST search against the mouse

genome sequence database was performed to ensure that the chosen siRNA sequences targeted only the mRNA of interest.

Cholesterol depletion

Cholesterol depletion was achieved by incubating macrophages with 10 mmol/L methyl-β-cyclodextrin (MβCD) (Sigma) in serum-free medium at 37°C for 1 h. Cells were washed with PBS before particle internalization.

Coating and opsonization of the particles

Purified LPG and LAM were sonicated and added to the particles at a final concentration of 25 μM in PBS, pH 7.3, incubated at 37°C for 1 h. Particles were washed and resuspended in complete medium prior to phagocytosis experiments. The efficiency of LPG coating was assessed by immunofluorescence using the anti-repeating unit antibody CA7AE. Complement opsonization of *L. donovani* promastigotes was done as described [23] and complement opsonisation of beads and zymosan was carried out by incubating the particles in DMEM supplemented with 10% mouse serum for 30 min at 37°C prior to phagocytosis.

Phagocytosis assay

For synchronized phagocytosis assays, macrophages were incubated with particles at a particle-to-cell ratio of 15:1 (unless otherwise specified) for 15 min at 4°C. Excess particles were removed by several thorough washes with DMEM and phagocytosis was triggered by transferring the cells to 37°C for the indicated time points before processing for microscopy.

Immunofluorescence

Macrophages were fixed for 10 min in PBS containing 2% paraformaldehyde, permeabilized using 0.1% Triton X-100, and nonspecific binding to surface Fc?R was blocked using 1% BSA, 2% goat serum, 6% milk, and 50% FBS. For immunostaining, cells were labeled with the appropriate combinations of primary antibodies or antisera (anti-Syt V, LAMP-1, EEA1, cathepsin D, cathepsin B, V-ATPase, LPG), and secondary antibodies (anti-rabbit, anti-mouse or anti-rat AlexaFluor 488, 568 or 647; Molecular Probes). DRAQ5 (Biostatus, Leicestershire, UK) was used to visualize macrophage and parasite nuclei and CTX-B-568 or 647 (Molecular Probes) was used to visualize GM1-enriched rafts. Syt V-GFP RAW 264.7 cells were fixed and directly incubated with DRAQ5 before being mounted or subjected to immunofluorescence. Of note, we used Syt V-GFP RAW 264.7 cells to localize Syt V following infection with *L. donovani* promastigotes because our antiserum against Syt V cross-reacts with *Leishmania* epitopes. All coverslips were mounted on glass slides with Fluoromount-G (Southern Biotechnology Associates). Detailed analysis of protein presence and localization on the phagosome was performed using an oil immersion Nikon Plan Apo 100 (N.A. 1.4) objective mounted on a Nikon Eclipse E800 microscope equipped with a Bio-Rad Radiance 2000 confocal imaging system (Bio-Rad, Zeiss). Images were obtained using appropriate filters, through the sequential scanning mode of the LaserSharp software (Bio-Rad Laboratories, Zeiss) with a Kalman filter of at least 6.

Phagosome acidification

BMM were preloaded with the acidotropic dye LysoTracker Red (Molecular Probes, Eugene, OR) diluted in DMEM (1:1000) for 2 h at 37°C. Cells were washed and infected with promastigotes for 2 h at 37°C as described in Phagocytosis assay. Cells were then rinsed, fixed with 2% paraformaldehyde for 10 min, washed and directly incubated 20 min with DRAQ5 before being mounted for confocal analysis.

Quantification of phagocytosis and protein recruitment on phagosomes

To assess the recruitment of proteins of interest, 100 phagosomes containing *L. donovani* or Zym were randomly scanned. To quantify the levels of these proteins, we determined the relative staining intensity as follows. The 488 and 568 nm excitation channels (emission 515/30 and 600/40 respectively) were separated and the protein staining rim around each phagosome was manually traced with a one pixel width. The fluorescence intensity of individual pixels was determined using the software Image J and an average intensity was calculated for each fluorescence intensity profile. To normalize intensity values of all phagosomes, cytosol intensity next to the phagosome under study was also evaluated and final phagosome intensity was expressed as the ratio of phagosome intensity (P) on cytosol intensity (C), thus P/C. In all cases, we ensured that signal intensity was not at saturation and the 20 more intense staining for each condition were selected and the average compared for the intensity level of each protein.

Statistical analyses

Statistical analyses were performed using Student's two-tail two-sample unequal variance test.

Acknowledgments

We are grateful to Dr. Mhairi Skinner (University of Guelph, Canada) for the rabbit antiserum against the 16 kDa proteolipid subunit of the V-ATPase and Marcel Desrosiers for expert assistance with confocal microscopy. Lipoarabinomannan was obtained as part of NIH, NIAID Contract No. HHSN266200400091C, entitled "Tuberculosis Vaccine Testing and Research Materials," which was awarded to Colorado State University. We thank Dr. Michel Desjardins, Guillermo Arango-Duque, and Christine Matte for critical comments on this manuscript.

Supplemental data

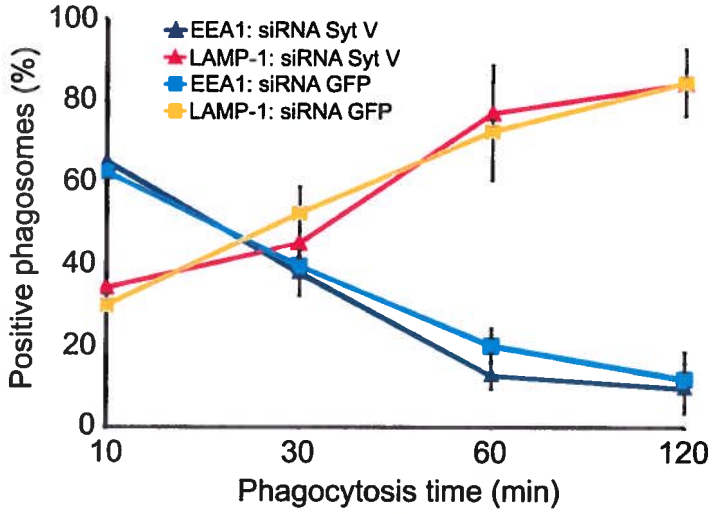

Figure S1. Kinetics of EEA1 and LAMP-1 phagosomal recruitment are normal in the absence of Syt V. RAW 264.7 cells were transfected with siRNAs to either Syt V or GFP, and incubated for 24 h. Cells were allowed to internalize Zym and phagosomal recruitments were determined at 10, 30, 60 and 120 min for EEA1 and LAMP1 on at least 100 phagosomes for each condition. Two independent experiments were performed and the bars show the standard deviations of one representative triplicate.

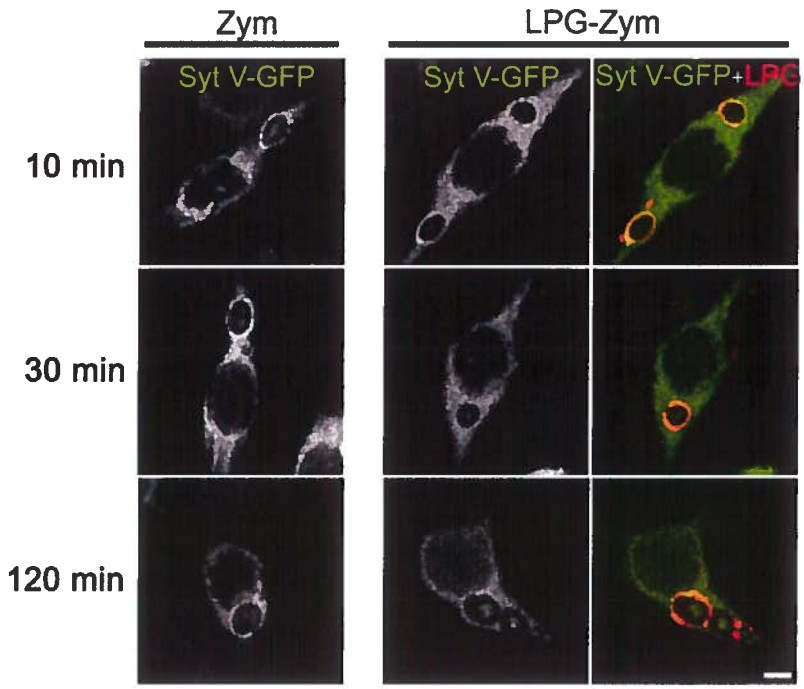

Figure S2. Recruitment of Syt V-GFP is reduced on phagosomes containing LPG-coated zymosan. Syt V-GFP cells were allowed to internalize Zym or LPG-Zym for 10 min, 30 min or 2 h, fixed and stained for LPG (red). Recruitment and relative levels of Syt V-GFP on phagosomes are illustrated by confocal images. Bar, 3μm.

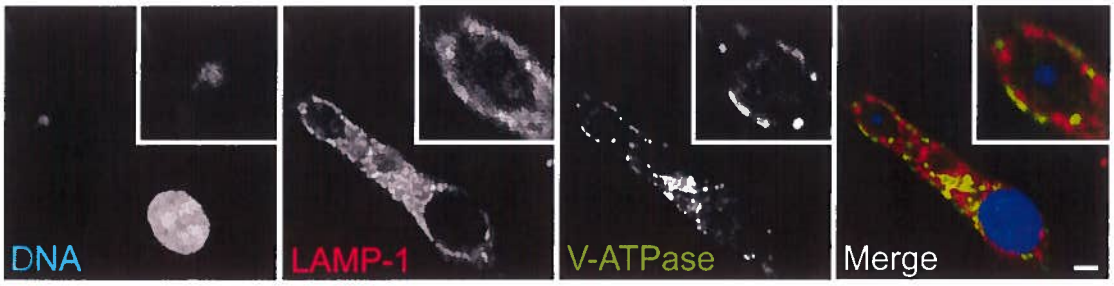

Figure S3. V-ATPase recruitment on phagosome membrane containing *lpg*-deficient promastigotes. BMM cells were infected with *lpg1*-KO promastigotes for 2 h, fixed and stained for the V-ATPase *c* subunit (green), LAMP-1 (red) ,and DNA (blue). The V-ATPase *c* subunit is present on the phagosome membrane, which is also positive for LAMP-1.

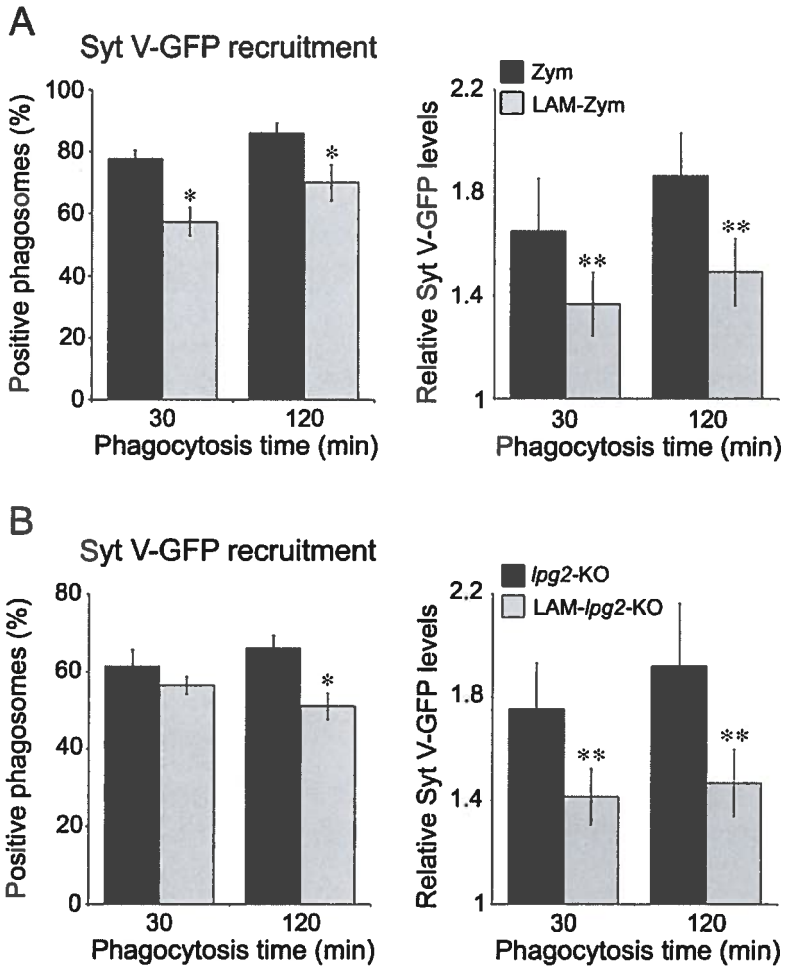

Figure S4. Recruitment of Syt V is prevented on phagosomes containing particles coated with the *Mycobacterium tuberculosis* lipoarabinomannan. *A* and *B*, SytV-GFP cells were allowed to internalized Zym or LAM-Zym (A), *lpg2*-KO or LAM-*lpg2*-KO (B) for 30 min or 2 h. The presence (*A* and *B*, left graph) and relative levels (*A* and *B*, right graph) of Syt V-GFP were determined. Three independent experiments were performed and the bars show the standard deviations of one representative triplicate (*, $p \leq 0.05$; **, $p \leq 0.005$).

References

1. Aderem A, Underhill DM (1999) Mechanisms of phagocytosis in macrophages. Annu Rev Immunol 17: 593-623.
2. Vieira OV, Botelho RJ, Grinstein S (2002) Phagosome maturation: aging gracefully. Biochem J 366: 689-704.
3. Jutras I, Desjardins M (2005) Phagocytosis: at the crossroads of innate and adaptive immunity. Annu Rev Cell Dev Biol 21: 511-527.
4. Haas A (2007) The phagosome: compartment with a license to kill. Traffic 8: 311-330.
5. Stow JL, Manderson AP, Murray RZ (2006) SNAREing immunity: the role of SNAREs in the immune system. Nat Rev Immunol 6: 919-929.
6. Bajno L, Peng XR, Schreiber AD, Moore HP, Trimble WS, et al. (2000) Focal exocytosis of VAMP3-containing vesicles at sites of phagosome formation. J Cell Biol 149: 697-706.
7. Collins RF, Schreiber AD, Grinstein S, Trimble WS (2002) Syntaxins 13 and 7 function at distinct steps during phagocytosis. J Immunol 169: 3250-3256.
8. Braun V, Fraisier V, Raposo G, Hurbain I, Sibarita JB, et al. (2004) TI-VAMP/VAMP7 is required for optimal phagocytosis of opsonised particles in macrophages. Embo J 23: 4166-4176.
9. Czibener C, Sherer NM, Becker SM, Pypaert M, Hui E, et al. (2006) Ca2+ and synaptotagmin VII-dependent delivery of lysosomal membrane to nascent phagosomes. J Cell Biol 174: 997-1007.
10. Roy D, Liston DR, Idone VJ, Di A, Nelson DJ, et al. (2004) A process for controlling intracellular bacterial infections induced by membrane injury. Science 304: 1515-1518.
11. Meresse S, Steele-Mortimer O, Moreno E, Desjardins M, Finlay B, et al. (1999) Controlling the maturation of pathogen-containing vacuoles: a matter of life and death. Nat Cell Biol 1: E183-188.
12. Gruenberg J, van der Goot FG (2006) Mechanisms of pathogen entry through the endosomal compartments. Nat Rev Mol Cell Biol 7: 495-504.

13. Chang KP, Dwyer DM (1976) Multiplication of a human parasite (*Leishmania donovani*) in phagolysosomes of hamster macrophages in vitro. Science 193: 678-680.

14. Antoine JC, Prina E, Jouanne C, Bongrand P (1990) Parasitophorous vacuoles of *Leishmania amazonensis*-infected macrophages maintain an acidic pH. Infect Immun 58: 779-787.

15. Antoine JC, Prina E, Lang T, Courret N (1998) The biogenesis and properties of the parasitophorous vacuoles that harbour *Leishmania* in murine macrophages. Trends Microbiol 6: 392-401.

16. Desjardins M, Descoteaux A (1997) Inhibition of phagolysosomal biogenesis by the *Leishmania* lipophosphoglycan. J Exp Med 185: 2061-2068.

17. Scianimanico S, Desrosiers M, Dermine JF, Meresse S, Descoteaux A, et al. (1999) Impaired recruitment of the small GTPase rab7 correlates with the inhibition of phagosome maturation by *Leishmania donovani* promastigotes. Cell Microbiol 1: 19-32.

18. Dermine JF, Scianimanico S, Prive C, Descoteaux A, Desjardins M (2000) *Leishmania* promastigotes require lipophosphoglycan to actively modulate the fusion properties of phagosomes at an early step of phagocytosis. Cell Microbiol 2: 115-126.

19. Späth GF, Garraway LA, Turco SJ, Beverley SM (2003) The role(s) of lipophosphoglycan (LPG) in the establishment of *Leishmania major* infections in mammalian hosts. Proc Natl Acad Sci U S A 100: 9536-9541.

20. Turco SJ, Descoteaux A (1992) The lipophosphoglycan of *Leishmania* parasites. Annu Rev Microbiol 46: 65-94.

21. Descoteaux A, Turco SJ (1999) Glycoconjugates in *Leishmania* infectivity. Biochim Biophys Acta 1455: 341-352.

22. Holm A, Tejle K, Magnusson KE, Descoteaux A, Rasmusson B (2001) *Leishmania donovani* lipophosphoglycan causes periphagosomal actin accumulation: correlation with impaired translocation of PKCα and defective phagosome maturation. Cell Microbiol 3: 439-447.

23. Lodge R, Descoteaux A (2005) *Leishmania donovani* promastigotes induce periphagosomal F-actin accumulation through retention of the GTPase Cdc42. Cell Microbiol 7: 1647-1658.

24. Lodge R, Diallo TO, Descoteaux A (2006) *Leishmania donovani* lipophosphoglycan blocks NADPH oxidase assembly at the phagosome membrane. Cell Microbiol 8: 1922-1931.

25. Späth GF, Epstein L, Leader B, Singer SM, Avila HA, et al. (2000) Lipophosphoglycan is a virulence factor distinct from related glycoconjugates in the protozoan parasite *Leishmania major*. Proc Natl Acad Sci U S A 97: 9258-9263.

26. Tolson DL, Turco SJ, Pearson TW (1990) Expression of a repeating phosphorylated disaccharide lipophosphoglycan epitope on the surface of macrophages infected with *Leishmania donovani*. Infect Immun 58: 3500-3507.

27. Dermine JF, Duclos S, Garin J, St-Louis F, Rea S, et al. (2001) Flotillin-1-enriched lipid raft domains accumulate on maturing phagosomes. J Biol Chem 276: 18507-18512.

28. Dermine JF, Goyette G, Houde M, Turco SJ, Desjardins M (2005) *Leishmania donovani* lipophosphoglycan disrupts phagosome microdomains in J774 macrophages. Cell Microbiol 7: 1263-1270.

29. Winberg ME, Holm A, Sarndahl E, Vinet AF, Descoteaux A, et al. (2009) *Leishmania donovani* lipophosphoglycan inhibits phagosomal maturation via action on membrane rafts. Microbes Infect 11: 215-222.

30. Shao D, Segal AW, Dekker LV (2003) Lipid rafts determine efficiency of NADPH oxidase activation in neutrophils. FEBS Lett 550: 101-106.

31. Vilhardt F, van Deurs B (2004) The phagocyte NADPH oxidase depends on cholesterol-enriched membrane microdomains for assembly. Embo J 23: 739-748.

32. Arellano-Reynoso B, Lapaque N, Salcedo S, Briones G, Ciocchini AE, et al. (2005) Cyclic β-1,2-glucan is a *Brucella* virulence factor required for intracellular survival. Nat Immunol 6: 618-625.

33. Welin A, Winberg ME, Abdalla H, Sarndahl E, Rasmusson B, et al. (2008) Incorporation of *Mycobacterium tuberculosis* lipoarabinomannan into macrophage membrane rafts is a prerequisite for the phagosomal maturation block. Infect Immun 76: 2882-2887.

34. Gil C, Soler-Jover A, Blasi J, Aguilera J (2005) Synaptic proteins and SNARE complexes are localized in lipid rafts from rat brain synaptosomes. Biochem Biophys Res Commun 329: 117-124.

35. Kay JG, Murray RZ, Pagan JK, Stow JL (2006) Cytokine secretion via cholesterol-rich lipid raft-associated SNAREs at the phagocytic cup. J Biol Chem 281: 11949-11954.

36. Li C, Ullrich B, Zhang JZ, Anderson RG, Brose N, et al. (1995) Ca^{2+}-dependent and -independent activities of neural and non-neural synaptotagmins. Nature 375: 594-599.

37. Saegusa C, Fukuda M, Mikoshiba K (2002) Synaptotagmin V is targeted to dense-core vesicles that undergo calcium-dependent exocytosis in PC12 cells. J Biol Chem 277: 24499-24505.

38. Iezzi M, Kouri G, Fukuda M, Wollheim CB (2004) Synaptotagmin V and IX isoforms control Ca^{2+} -dependent insulin exocytosis. J Cell Sci 117: 3119-3127.

39. Fukuda M, Sagi-Eisenberg R (2008) Confusion in the nomenclature of synaptotagmins V and IX: which is which? Calcium Binding Proteins 3: 1-4.

40. Vinet AF, Fukuda M, Descoteaux A (2008) The exocytosis regulator synaptotagmin V controls phagocytosis in macrophages. J Immunol 181: 5289-5295.

41. Desjardins M, Huber LA, Parton RG, Griffiths G (1994) Biogenesis of phagolysosomes proceeds through a sequential series of interactions with the endocytic apparatus. J Cell Biol 124: 677-688.

42. Garin J, Diez R, Kieffer S, Dermine JF, Duclos S, et al. (2001) The phagosome proteome: insight into phagosome functions. J Cell Biol 152: 165-180.

43. Rogers LD, Foster LJ (2007) The dynamic phagosomal proteome and the contribution of the endoplasmic reticulum. Proc Natl Acad Sci U S A 104: 18520-18525.

44. Miao L, Stafford A, Nir S, Turco SJ, Flanagan TD, et al. (1995) Potent inhibition of viral fusion by the lipophosphoglycan of *Leishmania donovani*. Biochemistry 34: 4676-4683.

45. Lang T (2007) SNARE proteins and 'membrane rafts'. J Physiol 585: 693-698.

46. Salaun C, James DJ, Chamberlain LH (2004) Lipid rafts and the regulation of exocytosis. Traffic 5: 255-264.

47. Ramachandra L, Song R, Harding CV (1999) Phagosomes are fully competent antigen-processing organelles that mediate the formation of peptide:class II MHC complexes. J Immunol 162: 3263-3272.

48. Huynh KK, Grinstein S (2007) Regulation of vacuolar pH and its modulation by some microbial species. Microbiol Mol Biol Rev 71: 452-462.

49. Späth GF, Schlesinger P, Schreiber R, Beverley SM (2009) A novel role for Stat1 in phagosome acidification and natural host resistance to intracellular infection by *Leishmania major*. PLoS Pathog 5: e1000381.

50. Zilberstein D, Shapira M (1994) The role of pH and temperature in the development of *Leishmania* parasites. Annu Rev Microbiol 48: 449-470.

51. Berman JD, Dwyer DM, Wyler DJ (1979) Multiplication of *Leishmania* in human macrophages in vitro. Infect Immun 26: 375-379.

52. McConville MJ, Blackwell JM (1991) Developmental changes in the glycosylated phosphatidylinositols of *Leishmania donovani*. Characterization of the promastigote and amastigote glycolipids. J Biol Chem 266: 15170-15179.

53. Galli T, McPherson PS, De Camilli P (1996) The V0 sector of the V-ATPase, synaptobrevin, and synaptophysin are associated on synaptic vesicles in a Triton X-100-resistant, freeze-thawing sensitive, complex. J Biol Chem 271: 2193-2198.

54. Descoteaux A, Matlashewski G (1989) c-fos and tumor necrosis factor gene expression in *Leishmania donovani*-infected macrophages. Mol Cell Biol 9: 5223-5227.

55. Privé C, Descoteaux A (2000) *Leishmania donovani* promastigotes evade the activation of mitogen-activated protein kinases p38, c-Jun N-terminal kinase, and extracellular signal-regulated kinase-1/2 during infection of naive macrophages. Eur J Immunol 30: 2235-2244.

56. Huang C, Turco SJ (1993) Defective galactofuranose addition in lipophosphoglycan biosynthesis in a mutant of *Leishmania donovani*. J Biol Chem 268: 24060-24066.

57. Descoteaux A, Luo Y, Turco SJ, Beverley SM (1995) A specialized pathway affecting virulence glycoconjugates of *Leishmania*. Science 269: 1869-1872.

58. Reiner NE (1982) Host-parasite relationship in murine Leishmaniasis: pathophysiological and immunological changes. Infect Immun 38(3): 1223-1230.

59. Skinner MA, MacLaren LA, Wildeman AG (1999) Stage-dependent redistribution of the V-ATPase during bovine implantation. J Histochem Cytochem 47: 1247-1254.

60. Tolson DL, Turco SJ, Beecroft RP, Pearson TW (1989) The immunochemical structure and surface arrangement of *Leishmania donovani* lipophosphoglycan determined using monoclonal antibodies. Mol Biochem Parasitol 35: 109-118.

61. Orlandi PA, Jr., Turco SJ (1987) Structure of the lipid moiety of the *Leishmania donovani* lipophosphoglycan. J Biol Chem 262: 10384-10391.

62. Russo DM, Turco SJ, Burns JM, Jr., Reed SG (1992) Stimulation of human T lymphocytes by *Leishmania* lipophosphoglycan-associated proteins. J Immunol 148: 202-207.

63. Flandin JF, Chano F, Descoteaux A (2006) RNA interference reveals a role for TLR2 and TLR3 in the recognition of *Leishmania donovani* promastigotes by interferon-?-primed macrophages. Eur J Immunol 36: 411-420.

Quatrième publication

(Le lipophosphoglycan de *Leishmania donovani* réduit le taux de phagocytose par un mécanisme dépendant de la Syt V)

Résumé de la quatrième publication

Vinet A.F., Fukuda M., Turco S.J. and Descoteaux A. (2008). The *Leishmania donovani* lipophosphoglycan reduces phagocytosis rate by a Synaptotagmin V-dependent process (Manuscript in preparation).

Le glycolipide de surface lipophosphoglycan du promastigote de *Leishmania donovani* bloque la maturation du phagosome et empêche ainsi la biogénèse du phagolysosome chez les macrophages. Un des mécanismes impliqués dans ce processus est l'exclusion du régulateur d'exocytose Synaptotagmine V (Syt V). En effet, nous avons récemment démontré que la Syt V régulait l'acquisition au phagosome de la Cathepsin D et de la pompe à proton V-ATPase, et l'exclusion de la Syt V des phagosomes contenant les promastigotes de *L. donovani* permettait au parasite de survivre à l'intérieur d'une vacuole non acidifiée. Le fait que la Syt V soit également impliquée dans l'apport membranaire issu de vésicules internes nous a amené à étudier l'effet du LPG sur cet apport membranaire durant les premières étapes de la formation du phagosome. Nos résultats ont tout d'abord confirmé les précédentes études observant un taux d'internalisation réduit des promastigotes WT comparés aux promastigotes mutants déficients pour l'expression du LPG. Les expériences menées avec des particules recouvertes de LPG ont démontré que cet effet était spécifique à ce glycolipide. De plus, nos résultats suggèrent que la réduction de phagocytose due au LPG implique un mécanisme dépendant de la Syt V puisque l'absence d'expression de la Syt V réduit le taux d'internalisation et élimine tout effet du LPG. L'ensemble de ces résultats révèle un effet précoce du LPG de *L. donovani* durant la formation du phagosome, et propose une explication aux observations d'un taux de phagocytose réduit des parasite WT par rapport aux promastigotes n'exprimant pas de LPG. Nous apportons aussi un nouvel élément de réponse concernant la régulation du recrutement de la Syt V sur les phagosomes par la PKC-α.

The *Leishmania donovani* lipophosphoglycan reduces phagocytosis rate by a Synaptotagmin V-dependent process.

Adrien F. Vinet[1], Mitsunori Fukuda[2], Salvatore J. Turco[3], and Albert Descoteaux[1]

[1]INRS-Institut Armand-Frappier and Centre for host-parasite interactions, Laval, QC, H7V 1B7 Canada,

[2]Department of Developmental Biology and Neurosciences, Tohoku University, Sendai, Miyagi 980-8578, Japan,

[3]Department of Biochemistry, University of Kentucky, KY, 40536, USA

Corresponding author: Albert Descoteaux, Tel: 450-687-5010 ext 4465, Fax: 450-686-5501, email: albert.descoteaux@iaf.inrs.ca

Running title: LPG reduces *L. donovani* phagocytosis

Keywords: Monocytes/Macrophages; Phagocytosis; *Leishmania*; lipophosphoglycan

Summary

The surface glycolipid lipophosphoglycan (LPG) of *Leishmania donovani* promastigotes blocks the phagosomal maturation and impairs the phagolysosome biogenesis in macrophages. A mechanism involved in this process is the exclusion of the exocytosis regulator Synaptotagmin V (Syt V). Indeed, we recently showed that Syt V regulates the Cathepsin D and the V-ATPase acquisition on phagosomes during its maturation, and the exclusion of Syt V by *L. donovani* LPG allows the promastigote to survive in a non-acidic vacuole. As Syt V was also showed to contribute to the membrane supply from internal vesicles during the phagosome formation, we decided in this study to investigate the effect of LPG on membrane supply during the first steps of the phagosome formation. Our results first confirmed previous report of a reduced internalization rate for WT *L. donovani* promastigotes regarding *lpg*-deficient mutants. Using LPG-coated particles, we showed that this effect is specific for the LPG. Furthermore, the reduction of phagocytosis mediated by LPG involved a Syt V-dependent mechanism since Syt V silencing reduced internalization rate of macrophages and abrogated any LPG effect. Taken together, these results highlight an early effect of *L. donovani* LPG during the formation of the phagosome, and propose an explanation to the reduced phagocytosis rate of WT parasites observed regarding promastigotes which don't express LPG. We also provided a new potential regulation of Syt V recruitment on phagosomes by PKC-α.

Introduction

Macrophages protect their host by a phagocytosis process, which enables the killing of pathogens. This internalization is initiated by the binding of opsonins or conserved motifs of the particle surface by specific phagocytic receptors, that trigger the phagosome formation via different pathways leading to actin remodelling [1,2]. The phagosome then acquires the ability to kill and degrade invading microorganism by a maturation process involving highly regulated and successive interactions with the endosomal compartment [3]. Visceral *Leishmania*sis (Kala-azar) is a disease caused by the intracellular protozoan parasite *Leishmania donovani* [4], which is inoculated into mammalian hosts by infected sand flies [5]. The promastigote form is phagocytosed by host macrophages, where it survives inside phagosomes and replicates within the phagolysosomal compartment as an amastigote form [6,7]. Evidences were provided that intraphagosomal survival of the promastigote is dependent on the presence of the *major* surface glycoconjugate, the lipophosphoglycan (LPG) [8-10], however the detailed mechanisms still remain largely unknown. LPG is an extracellular glycosylinositolphospholipid (GPI)-anchored polymer consisting of 16 to 36 repeating units of disaccharide-phosphate unit [Gal(β1,4)Man(α1-$PO_4 \rightarrow$ 6)] [11]. The requirement for LPG in the establishment of the infection inside the macrophage and the promastigote-to-amastigote conversion was demonstrated by LPG repeating units-defective mutants which are rapidly destroyed after phagocytosis [12]. When promastigotes attach to the macrophage surface, LPG is transferred from the parasite to the phagosomal membrane and is incorporated in lipid bilayers [13,14]. The insertion of LPG in membrane bilayer alters the biophysical properties of the entire membrane and studies demonstrated that among the anti-microbial mechanisms targeted by this glycan, a reduced fusogenic capacities of the phagosome was observed, leading to an inhibition of the phagolysosome biogenesis [13,15-18]. In phagosomes containing *L. donovani* promastigotes, we reported the exclusion of crucial factors of phagosome maturation such as the NADPH oxidase, the hydrolases Cath D or the vacuolar pump V-ATPase due to the action of LPG [12]. PKC-α is another signalling molecule whose activity and

phagosomal recruitment are impaired by LPG [19-22]. During phagocytosis, PKC-α is an early recruited protein on phagosome, implied in the regulation of periphagosomal depolymerisation of F-actin [23-26] and playing a role in the acquisition of phagolysosome features such as Cath D, Cath S, Rab-7 or LAMP-1 [27]. Although a direct connection between periphagosomal F-actin depolymerisation and phagosomal maturation remains to be clearly demonstrated, LPG has been proposed to act on PKC-α to prevent F-actin breakdown, forming a physical barrier and precluding further phagosome fusion with late endosomes/lysosomes [26,28].

The exocytosis of intracellular vesicles is necessary for phagocytosis from nascent phagosome formation to last steps of phagolysosome biogenesis. Despite that many membrane fusion processes extensively occur in macrophages during phagocytosis and cytokine secretion, regulators of membrane fusion such as Synaptotagmins are poorly studied. Among Syts family characterized by the presence of two Ca^{2+}-binding C2 domains on their cytoplasmic domain [29], Syt VII and Syt II have been shown to be involved in the regulation of vesicle released by phagocytes [30,31]. For instance, the former is required for a mechanism that promotes phagolysosomal fusion and intracellular growth of pathogenic bacteria in macrophages [32]. The transmembrane protein Syt V is a poorly studied Ca^{2+} sensor regulating membrane fusion in neuronal and pancreatic cells [33,34]. We previously demonstrated that in macrophages, Syt V is a recycling endosome associated protein recruited to forming phagosome, and that this exocytosis regulator controls the phagocytic process [35]. Furthermore, Syt V regulates phagolysosome biogenesis by the control of Cath D and the proton pump V-ATPase acquisition [Publication III, in press]. Analysis of the altered maturation of phagosomes containing *L. donovani* promastigotes revealed that LPG inserts into lipid microdomains of the phagosome membrane and impairs Syt V recruitment on phagosome, preventing their acidification [Publication III, in press].

L. donovani LPG are located on the parasite surface and are known to transfer into the membrane of host cells, so they constitute good candidates to modulate the initial step of entry into macrophages as phagocytosis of LPG-defective mutants is superior to that of

WT promastigotes [9,20,26]. Few hypothesis have been proposed to explain this reduced internalization rate of WT parasite, but no study addressed the mechanisms involved. In this study we investigated more precisely the effect of LPG on phagocytosis and proposed that LPG reduces internalization rate of the parasite by a Syt V-dependent mechanism. We also established a regulation of Syt V acquisition on phagosomes by PKC-α.

Materials and methods

Macrophages

Bone marrow-derived macrophages (BMM) were obtained as previously described [36]. Briefly, bone marrow cells from female BALB/c mice were grown at 37°C in 5% CO2 for 7 days in complete medium in the presence of 15% (v/v) L929 cell-conditioned medium as a source of colony-stimulating factor (CSF)-1 [36]. BMM were made quiescent by culturing them in the absence of CSF-1 for 18 h prior to being used. The murine macrophage cell line RAW 264.7 was grown in complete medium in a 37°C incubator with 5% CO2. Stably transfected RAW264.7 cells expressing Syt V-GFP (Syt V-GFP RAW 264.7 cells) were previously described [35]. The cell line RAW 264.7 transfected with the expression vector pCIN-4, and the DN PKC-overexpressing clones A2 and C2 [37] were cultured in a 37°C incubator with 5% CO2 in complete DMEM with 500 μg/ml G418 (Life Technologies).

Parasites

Leishmania donovani promastigotes (Sudanese strain 1S) were grown at 26°C in RPMI 1640 medium supplemented with 20% heat-inactivated FBS, 100 μM adenine, 20 mM 2-[N-morpholino]ethanesulphonic acid (pH 5.5), 5 μM hemin, 3 μM biopterin, 1 μM biotin and antibiotics. The isogenic *L. donovani* LPG-defective mutants *lpg1*-KO and *lpg2*-KO were described previously [38]. The *lpg1*-KO mutant secretes repeating Galβ1,4Manα1-PO_4-containing molecules, but lacks the ability to assemble a functional LPG glycan core [39], precluding synthesis of LPG. The *lpg2*-KO mutant expresses the truncated LPG Gal(α1,6)Gal(α1,3)Gal$_f$(β1,3)[Glc(α1-P)]Man(α1,3)Man(α1,4)GN(α1,6)-PI, and does not synthesize repeating Galβ1,4Manα1-PO4 units [7]. The *lpg2*-KO+LPG2 add-back was grown in the presence of 50 μg/ml G418. For infections, promastigotes were used in late stationary phase of growth.

Reagents and antibodies

The affinity-purified rabbit anti-Syt V was previously described [34]. The monoclonal anti-PKC-α was from Transduction Laboratories (Mississauga, Ont., Canada). The monoclonal anti-LPG (CA7AE) was prepared from hybridoma supernatant [40]. Methyl-β-cyclodextrin (MβCD) was from Sigma (St-Louis, MO, USA). LPG was isolated from the log phase cultures of *L. donovani* promastigotes as previously described [41,42].

RNA interference

Syt V silencing by RNAi was performed as previously described [35] by using a small interfering RNA (siRNA) corresponding to nucleotides 94–112 of Syt V cDNA [43], whereas a siRNA specific to GFP was used as a negative control [44]. Adherent RAW 264.7 cells were transfected with siRNA duplexes at a final concentration of 240 nM using OligoFectamine (Invitrogen) as described [44]. A BLAST search against the mouse genome sequence database was performed to ensure that the chosen siRNA sequences targeted only the mRNA of interest.

Cholesterol depletion

Cholesterol depletion was achieved by incubating macrophages with 10 mmol/L Methyl-β-cyclodextrin (MβCD) (Sigma) in serum-free medium at 37°C for 1 h and washed with PBS before particle internalization.

Coating and opsonization of the particles

Purified LPG was sonicated and added to the particles at a final concentration of 25 μM in PBS, pH 7.3, incubated at 37°C for 1 h, washed and resuspended in complete medium prior phagocytosis experiments. The efficiency of LPG coating was assessed by immunofluorescence using the anti-LPG antibody CA7AE. Complement opsonization of *L. donovani* promastigotes was done as described [28] and complement opsonisation of beads and zymosan was carried out by incubating the particles in DMEM supplemented with 10% mouse serum for 30 min at 37°C prior to phagocytosis.

Phagocytosis assay

For synchronized phagocytosis assays, macrophages were incubated with particles at a particle-to-cell ratio of 15:1 (unless otherwise specified) for 15 min at 4°C. Excess particles were removed by several thorough washes with DMEM and phagocytosis was triggered by transferring the cells to 37°C for the indicated time points before processing for microscopy.

Immunofluorescence

Macrophages were fixed 10 min using 2% paraformaldehyde in PBS, permeabilized using 0.1% Triton X-100, and nonspecific surface FcγR binding were blocked using 1% BSA, 2% goat serum, 6% milk, and 50% FBS. For immunostaining, cells were labelled with the appropriate combinations of primary antibodies or antisera (anti-Syt V, PKC-α, LPG), and secondary antibodies (anti-rabbit or anti-mouse AlexaFluor 488 or 568; Molecular Probes). Syt V-GFP cells were fixed and subjected to immunofluorescence. All coverslips were mounted on slides with Fluoromount-G (Southern Biotechnology Associates). Detailed analysis of protein presence and localization on the phagosome was performed using an oil immersion Nikon Plan Apo 100 (N.A. 1.4) objective mounted on a Nikon Eclipse E800 microscope equipped with a Bio-Rad Radiance 2000 confocal imaging system (Bio-Rad, Zeiss). Images were obtained using appropriate filters, through

the sequential scanning mode of the LaserSharp software (Bio-Rad Laboratories, Zeiss) with a Kalman filter of at least 6.

Statistical analyses

Statistical analyses were performed using Student's two-tail two-sample unequal variance test.

Results

***L. donovani* lipophosphoglycan reduces the phagocytosis rate of macrophages.**

Previous studies reported a reduced internalization of WT *L. donovani* with respect to the *lpg2*-KO mutant [9,20,26]. We first verified these findings and fed BMM with *L. donovani*. Accordingly, we observed that the phagocytosis rate of WT parasite at 10 min of infection was reduced with a phagocytic index of 200 parasites for 100 macrophages when compared to 350 parasites for 100 macrophages for *lpg2*-KO parasites (fig. 1A). Such as the *lpg2*-KO mutants, the LPG-defective *lpg1*-KO mutants infected more BMM than did the WT with a phagocytic index of 360 parasites per 100 macrophages. The phagocytosis rate of the *lpg2*-KO add-back (*lpg2*-KO+p*LPG2*) was similar with the WT with 230 parasites per 100 macrophages (fig. 1A). These results confirmed that *L. donovani* lacking LPG are more internalized than WT parasites.

To directly address the impact of LPG on phagocytosis, we performed the internalization of Zym or Zym coated with LPG (LPG-Zym) [22] and determined the phagocytic index for each condition. The phagocytosis rate of non-opsonized LPG-Zym was reduced 2.6 fold with respect to macrophages feeding Zym (fig. 1B). A reduced phagocytosis was also observed for LPG-Zym when particles were opsonized by serum (fig. 1C). To determine whether impaired phagocytosis was accentuated with an increased particle load, we performed phagocytosis of serum-opsonized Zym coated or not with LPG at different particle/cell ratio. Results indicated an increased phagocytosis impairment with a high particle/cell ratio, from 1.3 for the ratio 10/1 to 1.6 for the ratio 40/1 (fig. 1C). Moreover, the percentage of cell containing high particle load was superior for Zym than LPG-Zym. Indeed, distribution of the particle number per macrophage showed that most of the macrophages contain 5 Zym but only 1 LPG-zym (fig. 1D). These results indicate that LPG inhibits the internalization process mediated by both CR3 and non opsonin-dependant phagocytic receptors, and that effect is more important for a high particle load.

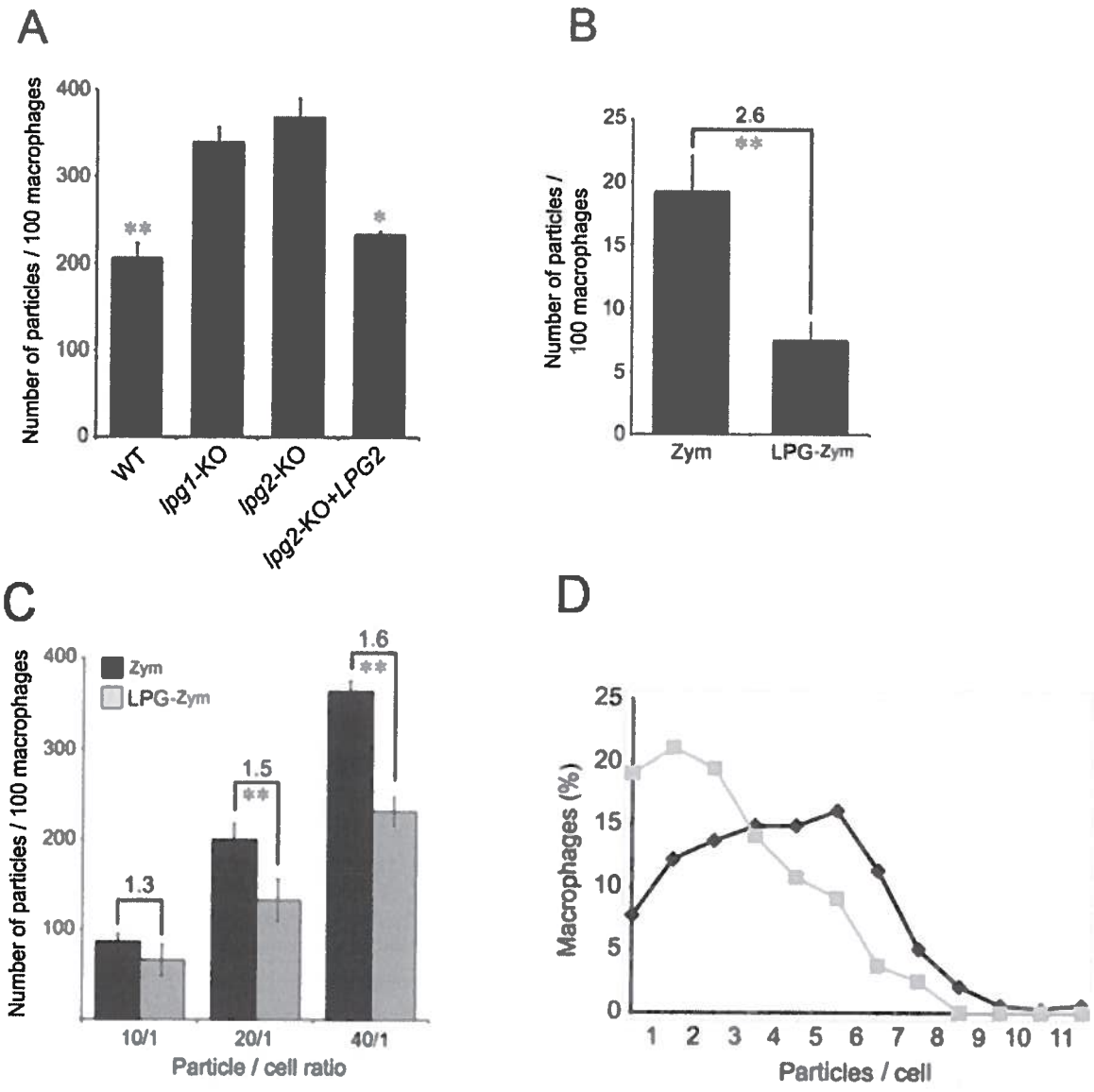
A
Number of particles / 100 macrophages
400
300
200
100
0
**
*
WT
lpg1-KO
lpg2-KO
lpg2-KO+LPG2
B
Number of particles / 100 macrophages
25
20
15
10
5
0
2.6
**
Zym
LPG-Zym
C
Number of particles / 100 macrophages
400
300
200
100
Zym
LPG-Zym
1.3
1.5
**
1.6
**
10/1
20/1
40/1
Particle / cell ratio
D
Macrophages (%)
25
20
15
10
5
0
1 2 3 4 5 6 7 8 9 10 11
Particles / cell

Figure 1. LPG decreases the phagocytosis rate of macrophages. *A*, BMM cells were infected with either WT, *lpg1*-KO, *lpg2*-KO, *lpg2*-KO+*LPG2 L. donovani* promastigotes for 10 min, fixed, and the number of parasites per 100 macrophages was determined. *B*, RAW 264.7 cells internalized non-opsonized Zym or LPG-Zym for 10 min and the number of particles per 100 macrophages was determined. *C* and *D*, RAW 264.7 cells were allowed to internalize serum-opsonized Zym or LPG-Zym for 10 min at different particles/cell ratios. The number of particles per 100 macrophages was determined (C) and the particle distribution in macrophages for the ratio 40/1 represented (D), grey square is for LPG-Zym; black rhombus is for Zym. For each condition, the phagocytic index was calculated on at least 100 cells in triplicate, at least three independent experiments were performed and the bars show the standard deviations of one representative triplicate (*A* - *C*) (*, $p \leq 0.005$; **, $p \leq 0.0005$; *A*, p values compare the phagocytic index of macrophages infected with WT and *lpg2*-KO+*LPG2 vs lpg1*-KO and *lpg2*-KO parasites).

LPG reduced phagocytosis is Syt V-dependent.

Having shown that Syt V is excluded from phagosome by LPG insertion on phagosome membrane during its maturation [Publication III, in press], we assumed that LPG could also have an inhibitory effect for Syt V recruitment on forming phagosomes. We fed RAW 264.7 cells stably transfected with the Syt V-GFP construction [35] with WT, LPG deficient mutants *lpg1*-KO and *lpg2*-KO or complemented *lpg2*-KO promastigotes. Accordingly, we observed an inhibition of Syt V-GFP recruitment at the phagocytic cup formed following binding of WT and *lpg2*-KO add-back parasites regarding the *lpg1*-KO and *lpg2*-KO mutants phagocytic cups (fig. 2). We verified this specific inhibition effect of LPG on Syt V-GFP recruitment with Zym or LPG-Zym and we observed a highly reduced Syt V-GFP recruitment on the phagocytic cup formed in the vicinity of LPG-positive particles (fig 3A). We made similar observations for endogenous Syt V in BMM cells (fig. 3A). Furthermore, this inhibition was specifically localized on phagosomes containing LPG-Zym since a Zym in a same macrophage showed an important accumulation of Syt V-GFP in the vicinity of the nascent phagosome (fig. 3B). These observations suggested that LPG locally impairs the phagosomal recruitment of Syt V at the phagocytic cup.

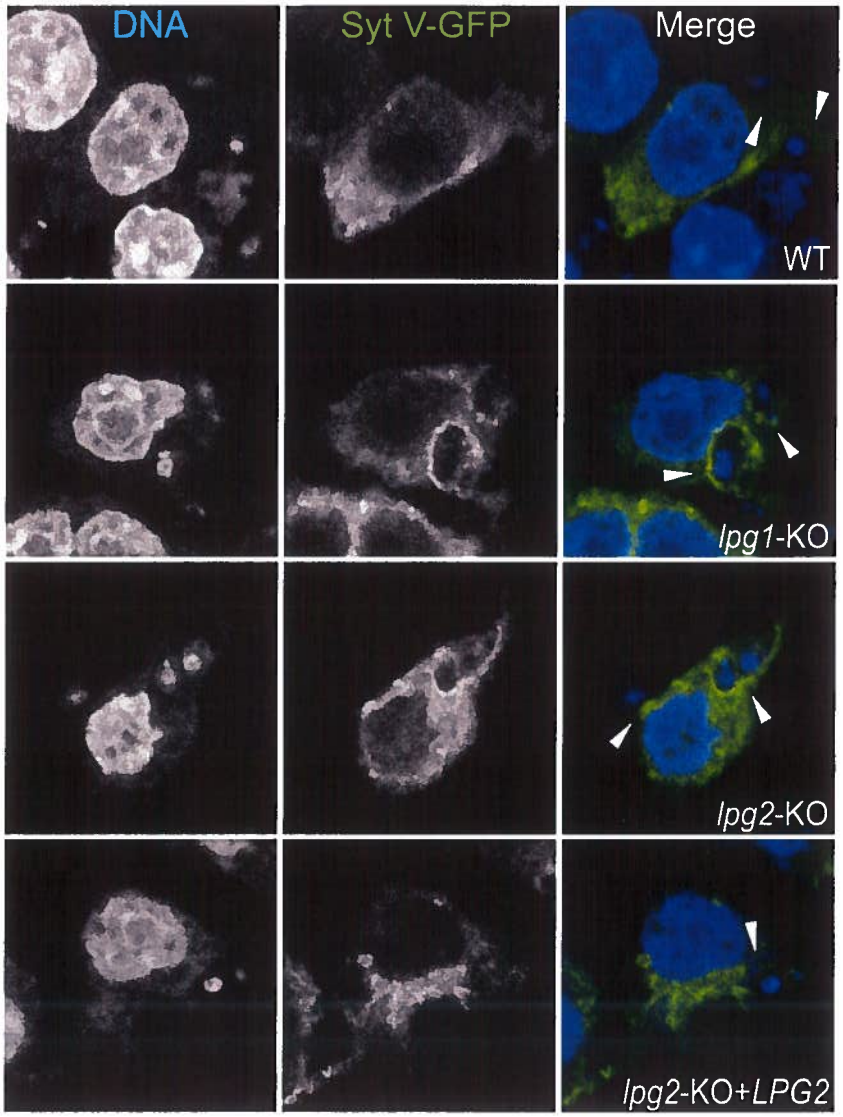

Figure 2. Syt V-GFP is not recruited on nascent phagosomes containing *L. donovani* promastigote. Syt V-GFP RAW 264.7 cells were infected with either WT, *lpg1*-KO, *lpg2*-KO, *lpg2*-KO+*LPG2 L. donovani* promastigotes for 10 min, fixed and stained for DNA. Representative confocal images illustrating the presence of Syt V-GFP on phagocytic cup containing parasites. Bar, 3µm.

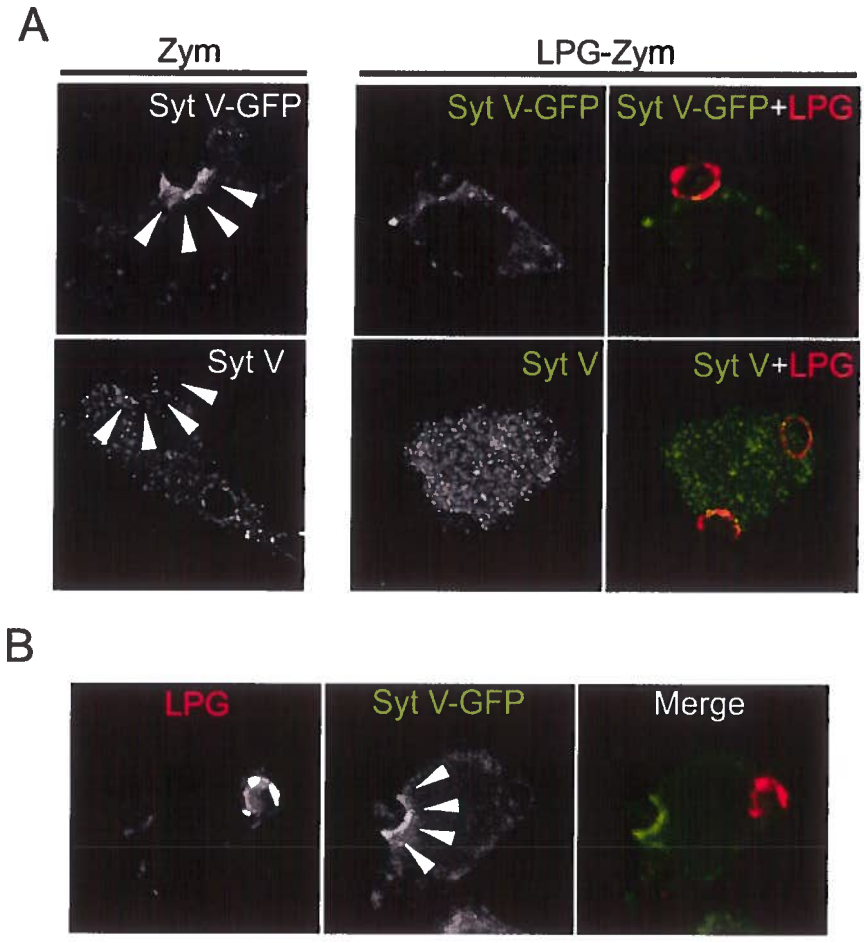

Figure 3. Syt V acquisition on phagocytic cup is locally impaired by LPG. *A* and *B*, Syt V-GFP RAW 264.7 cells (A, upper panel; B) or BMM cells (A, lower panel) were allowed to internalize Zym and/or LPG-Zym for 10 min and fixed. Cells were stained for Syt V and LPG (A, lower panel) or just for LPG (A, upper panel; B). Endogenous Syt V or Syt V-GFP recruitment is indicated by white arrowhead. Bar 3μm.

We provided evidence that in macrophages, Syt V plays a role in phagocytosis by the regulation of membrane supply during the first steps of the phagosome formation [35]. To further demonstrate that LPG effect on internalization rate is mainly dependent on Syt V, we performed Syt V silencing on RAW 264.7 cells and phagocytosis of Zym or LPG-Zym. We decided to increment the particle/cell ratio to mimic an increased membrane demand for infected cells. We first observed a reduced internalization rate for Syt V siRNA treated cells, whatever the ratio of particles per cell, as previously described [35]. Indeed, phagocytosis inhibition increased from 1.9 at the ratio 10/1 and 20/1 (fig. 3A, first and second panel respectively) to 2.3 for the ratio 40/1 (fig. 3A, third panel) with respect to the controls. Nevertheless, Syt V siRNA treatment had no significant effect on the internalization of LPG-Zym with respect to the controls GFP siRNA or Mock for all the tested ratios (fig 4). Moreover, the internalization of LPG-Zym whatever the conditions of transfection (e.g. Syt V siRNA, GFP siRNA or Mock transfected) was similar to the internalization of Zym by cells treated with Syt V siRNA (fig 4A). These results indicated that Syt V silencing and the effect of particles coated with LPG both impaired phagocytosis similarly, and these effects were not cumulative, suggesting a Syt V-dependent mechanism for the inhibition of phagocytosis by LPG.

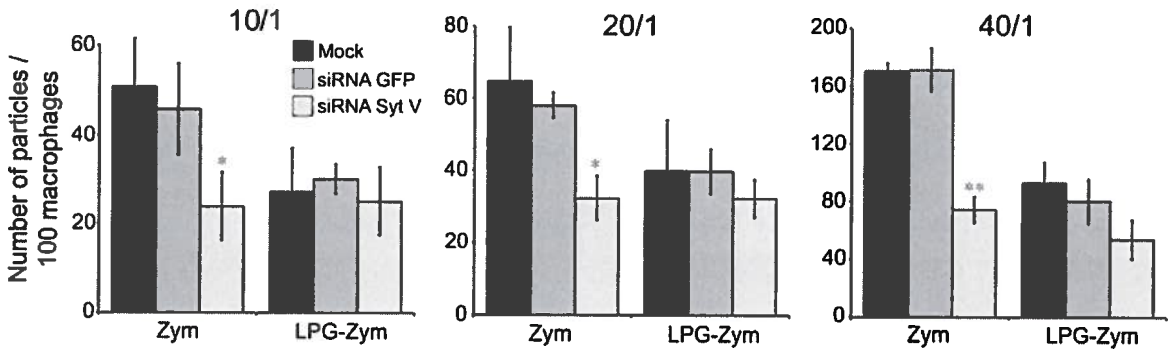

Figure 4. LPG reduces phagocytosis by a Syt V-dependent mechanism. RAW 264.7 cells were transfected with either a siRNA to Syt V or a siRNA to GFP, or only mock transfected (control), and incubated for 24 h. Cells were then allowed to internalize Zym or LPG-Zym for 10 min and fixed. The number of particles per 100 macrophages was determined for the ratios particles/cell ratio 10/1, 20/1 and 40/1. For each condition, the phagocytic index was calculated on at least 100 cells in triplicate, at least three independent experiments were performed and the bars show the standard deviations of one representative triplicate (*, $p \leq 0.005$; **, $p \leq 0.0005$).

Phagocytosis inhibition mediated by LPG affects cells with a high particle load.

We analysed the intracellular distribution of Zym at the ratio 40/1 in RAW 264.7 cells treated with Syt V siRNA, and results indicated that the reduction of the phagocytic index was actually due to a reduced percentage of cells containing 3 or more particles when compared to controls (fig 5A). This finding corroborates the requirement of Syt V for the internalization of a high number of particles. We investigated then the intracellular distribution of LPG-Zym in macrophages to state the effect of LPG during high particle load internalization. For GFP siRNA transfected RAW 264.7 cells and Mock transfected cells, macrophages which internalized LPG-Zym had a reduced number of cells containing 3 or more particles than macrophages feeding Zym (fig 5B, first and second graph). Interestingly, for Syt V siRNA transfected cells, the number of cells containing 3 or more Zym and Zym-LPG was similar although highly reduced with respect to controls GFP siRNA or Mock transfected cells. Nevertheless, a significant difference for the number of cells containing 1 to 2 Zym and LPG-Zym suggests that LPG could act to a lesser extent on an internalization process independent of Syt V under these conditions (fig 5B, third graph). Thus, these data show that LPG doesn't have any effect on the internalization of Syt V silenced cells containing a large number of particles and support the hypothesis that LPG's effect on internalization rate is mainly dependent on Syt V.

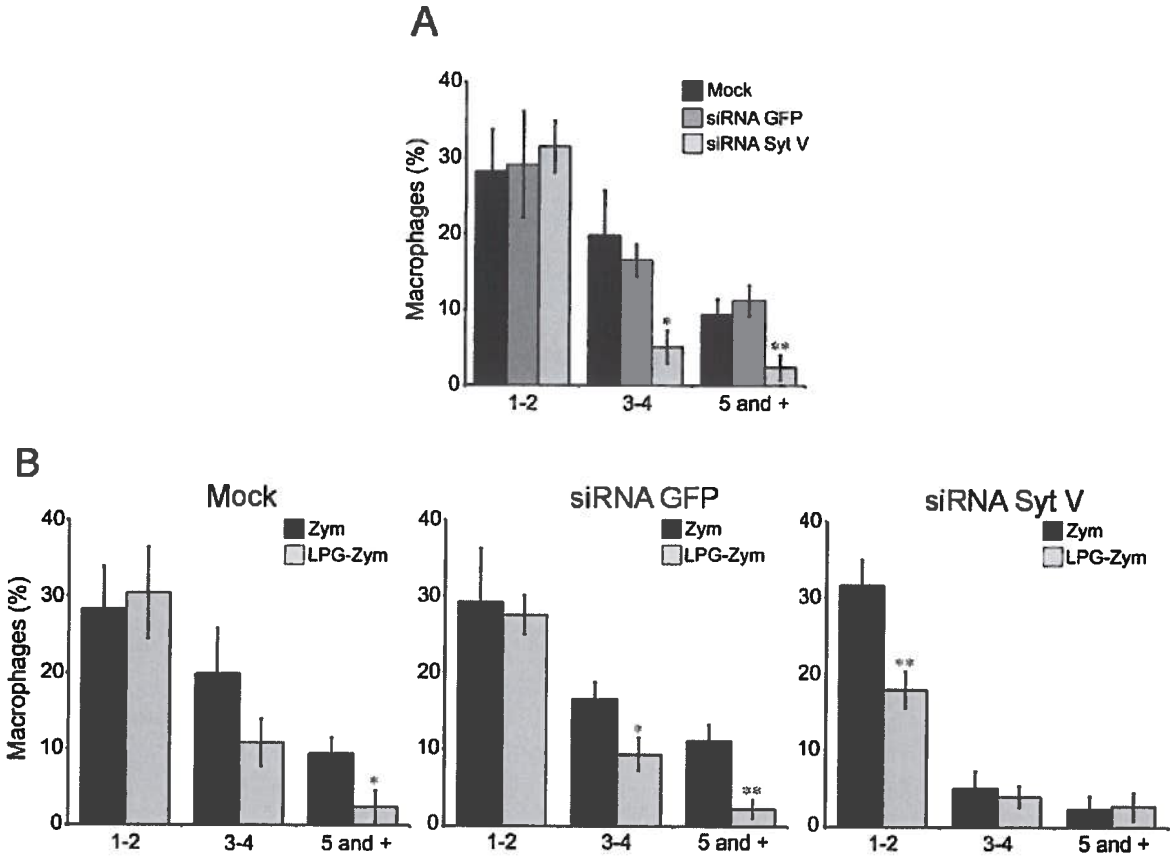

Figure 5. Phagocytosis inhibition mediated by LPG and Syt V silencing affects cells with a high particles load. *A* and *B*, RAW 264.7 cells were transfected with either a siRNA to Syt V or a siRNA to GFP, or only mock transfected, and incubated for 24 h. Cells were then allowed to internalize Zym or LPG-Zym for 10 min and fixed. The particle distribution per macrophage was determined for a particles/cell ratio of 40/1 and expressed as a percentage of macrophages containing 1-2, 3-4 or 5+ particles. For each condition, the particle distribution was calculated on at least 100 cells in triplicate, at least three independent experiments were performed and the bars show the standard deviations of one representative triplicate (*, $p \leq 0.005$; **, $p \leq 0.0005$).

Dominant-negative PKC-α expressing cells impair Syt V recruitment on phagosomes.

We sought to find out possible regulators of Syt V acquisition on phagosomes. We first identified Syt V in macrophages as a potential interacting protein with PKC-α (Vinet and Descoteaux, unpublished observations; [35]). Confocal analysis of Syt V and PKC-α distribution on 10 min aging phagosomes revealed a colocalization between these two proteins in RAW 264.7 cell line (fig 6A) and BMM primary cells (fig. 6B). To further determine the role of PKC-α in the Syt V regulation, we used two clones of the RAW 264.7 cell line overexpressing a dominant-negative (DN) mutant of PKC-α [37]. We first observed many correlations in the regulation of the phagocytosis process between Syt V silencing and DN-PKC-α expression. A study of Breton and Descoteaux showed an impaired internalization of IgG-SRBC for DN- PKC-α expressing cells, suggesting a role for PKC-α in the regulation of FcγR-induced phagocytosis [45]. We examined the phagocytosis of serum-opsonised zymosan and results clearly showed that such as the reduced phagocytosis of cells with a Syt V silencing, DN PKC-α expressing cells showed a 70% reduction of the Zym internalization (fig 6C). We also observed that similarly to Syt V [Publication III, in press], PKC-α needs intact lipid microdomains for its acquisition on phagosome membrane since a cholesterol depletion by the methyl-β-cyclodextrin drug inhibited the recruitment of PKC-α to Zym-containing phagosomes in a similar level to Syt V (fig 6D and 6E). We then focused on the phagosomal recruitment of Syt V in DN PKC-α expressing cells. It was interesting to note that Syt V recruitment was impaired by about 50% in DN-PKC-α expressing cells, indicating a regulating role of PKC-α in the Syt V phagosomal recruitment (fig. 7A and 7B).

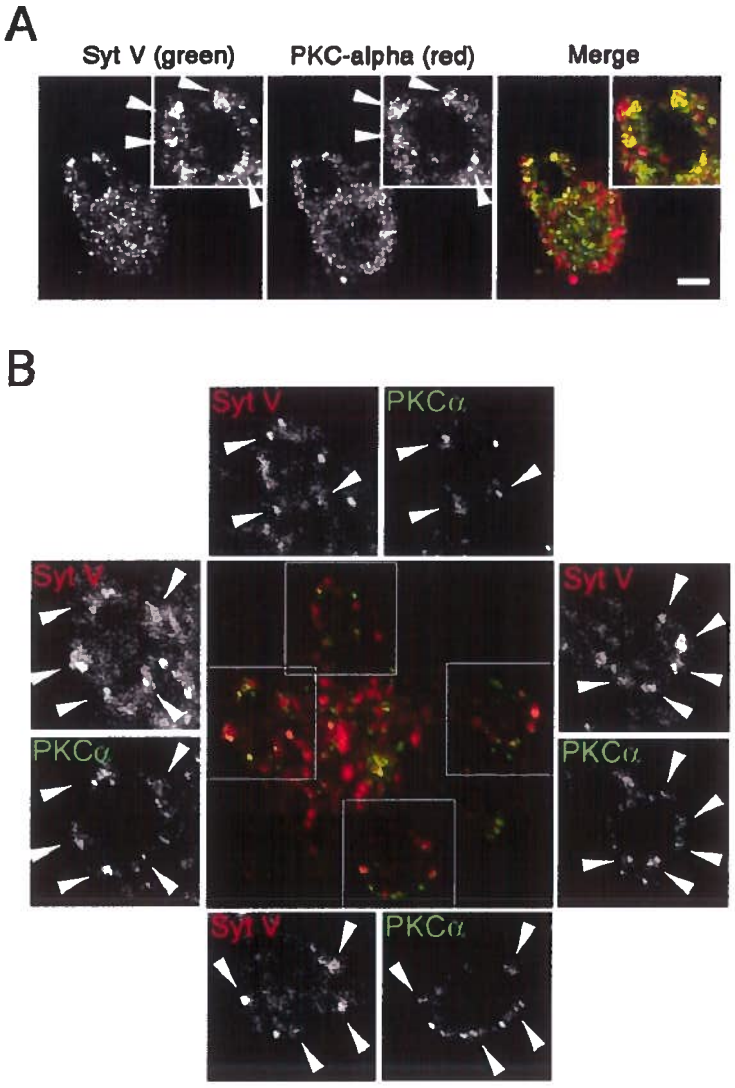

Figure 6. Syt V colocalizes with PKC-α on macrophage phagosomes. *A* and *B*, RAW 264.7 cells (A) or BMM cells (B) were allowed to internalize Zym during 30 min (A) or 10 min (B), fixed and stained for Syt V and PKC-α. White arrowheads show example of colocalization on phagosomes. Bar, 3μm.

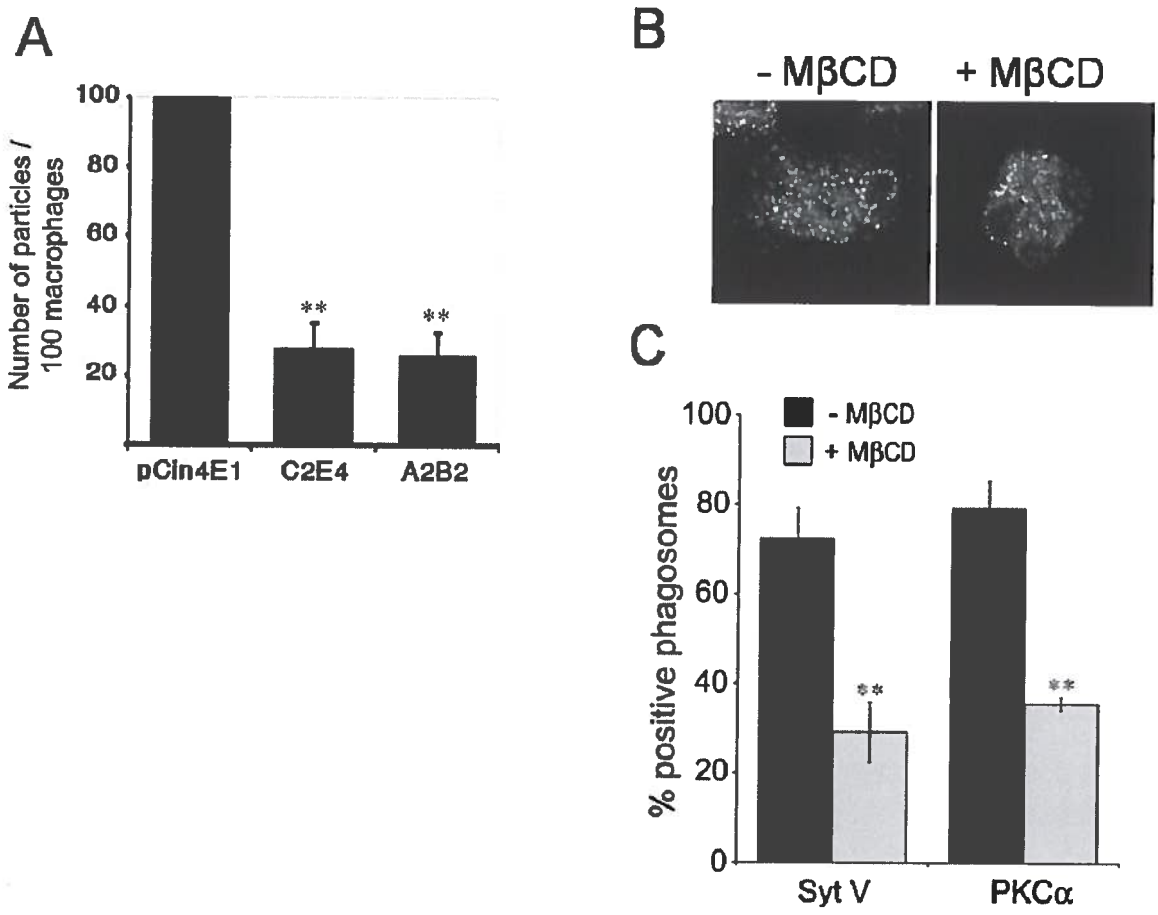

Figure 7. PKC-α is important for CR-mediated phagocytosis and is dependent on intact lipid microdomains for its recruitment on phagosome. *A*, Zym were internalized by control (pCin4E1 expressing vector alone) and RAW 264.7 cells expressing a DN-PKC-α (clones A2B2 and C2E4) for 30 min. Cells were then fixed, the number of particles per 100 macrophages was determined and expressed as a percentage of pCin4E1 control cells. *B* and *C*, BMM were either left untreated or treated with 10 mmol/L MβCD for 1 h before the internalization of Zym for 30 min. Cells were then fixed and stained for Syt V and PKC-α. Representative confocal images of PKC-α recruitment on cells treated or not with MβCD is presented (*B*). At least 100 phagosomes for each condition were assessed (A-C). Three independent experiments were performed and the bars show the standard deviations of one representative triplicate (**, $p \leq 0.005$).

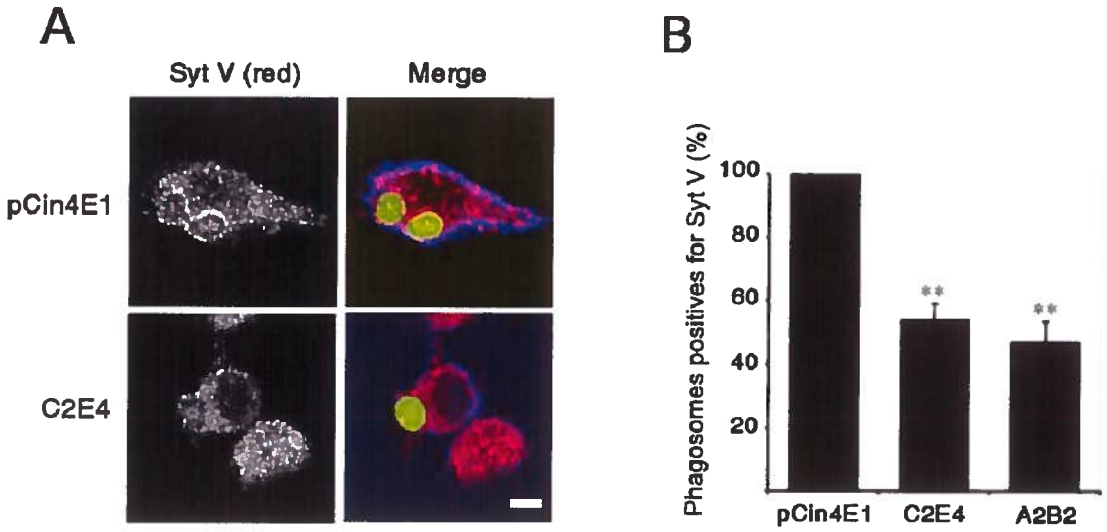

Figure 8. PKC-α activity mediates Syt V recruitment on phagosomes. *A* and *B*, 488-Zym were internalized by control (pCin4E1 expressing vector alone) and RAW 264.7 cells expressing a DN-PKC-α (clones A2B2 and C2E4) for 30 min. Cells were then fixed, Syt V recruitment was determined and expressed as a percentage of pCin4E1 control cells (B). At least 100 phagosomes for each condition were assessed. Three independent experiments were performed and the bars show the standard deviations of one representative triplicate (**, $p \leq 0.005$). Representative confocal images illustrating the presence of Syt V on phagosome membrane containing particles (A). Bar, 3μm.

Discussion

Several studies reported a reduced infection rate of WT *L. donovani* compared to *lpg2*-KO mutants in macrophages [9,20,26]. Given that opsonized *L. donovani* enters macrophages predominantly through CR3 [12], one proposed explanation was that lpg-deficient promastigotes infect macrophages more efficiently than WT as C3 deposition on *lpg2*-KO promastigotes is more important [12]. Indeed, the surface protein GP63 is known to act as a primary acceptor for C3 deposition [46,47] and a larger accessibility of this protein in the absence of LPG on *lpg2*-KO promastigote surface may be responsible for the superior C3 deposition. However, the finding of a reduced phagocytosis of LPG-Zym compared to Zym, mediated or not by C3 complement, suggests another mechanism directly related to the action of LPG on macrophages upon parasite attachment.

We have previously shown that LPG insertion into GM1-containing lipid microdomains impaired the association of Syt V to phagosome membranes during the maturation process [Publication III, in press]. We also showed the importance of Syt V for membrane supply during the early steps of the large particles phagocytosis [35]. We decided in this work to study more precisely the impact of the *L. donovani* LPG on the internalization process and to determinate whether the reduced internalization rate observed could be due to a Syt V-dependent mechanism. Syt V silencing or LPG-Zym phagocytosis both decreased the frequency of macrophages containing 3 or more particles under conditions of high membrane demand. Moreover, our results revealed that LPG didn't have any significant effects on the phagocytosis of Syt V siRNA treated cells, in opposition to GFP siRNA and Mock controls which showed a decreased phagocytosis of LPG-Zym compared to Zym particles. These data argue for an inhibition effect of LPG on the internalization process by a Syt V-dependent pathway. Thus, this work provides a new insight into a mechanism of LPG outcome on macrophage phagocytosis during the phagosome formation and strongly supports a model in which contact of *L. donovani* promastigotes with macrophage membrane is followed by the insertion of LPG into the membrane of the phagocytic cup. This insertion could then modify the biophysical

properties of this membrane, which consequently affects Syt V positive-endosomes interaction with the membrane of the nascent phagosome and prevents the membrane supply necessary for the internalization of a high particle load.

Lipid microdomains have been shown to function as signal transduction platforms [48-50] and have been proposed to play a crucial role in phagocytosis mediated by Fcγ receptors [51,52]. During the first contacts of the macrophage plasma membrane with pathogens, many authors observed an accumulation of microdomain-associated molecules at bacterial entry on the plasma membranes of phagocytes [53] indicating the involvement of membrane microdomains in the engulfment of pathogens by phagocytes. Further destruction of membrane microdomains by methyl-β-cyclodextrin, which extracts cholesterol, prevented the infection of target cells by microorganisms [54-57]. For instance, the association of the phagocytic receptor CR3 and a GPI protein, which has been shown to be located and dependent of intact cholesterol-rich domains, was important for the infection of *Mycobacterium Kansasii* [54]. Following *L. donovani* attachment on macrophages, LPG inserts and accumulates into lipid microdomains on macrophage membrane via its GPI anchor and disrupts membrane rafts to manipulate subsequent phagosome maturation [58] [14,59,60]. Nothing is currently known about the potential effects of LPG disruption on lipid microdomains during the formation of the phagosome. We observed that Syt V was enriched in lipid microdomains and dependent of intact microdomains for its phagosomal recruitment [Publication III, in press]. It is thus relevant that some LPG could insert into and disrupt lipid microdomains of the plasma membrane in the vicinity of the attached parasite. This insertion could interfere with the clustering of molecules necessary for the Syt V-dependent interaction of endosomes, resulting in Syt V exclusion from the phagocytic cup and a reduced membrane supply.

Syt V is also an important regulator of phagolysosome biogenesis. Indeed, Syt V mediates the interaction between phagosomes and a subset of late endosomes or lysosomes enriched in cathepsin D and in the V-ATPase *c* subunit [Publication III, in press]. To delay the phagosome maturation, we previously showed that LPG from *L. donovani* promastigotes impairs Syt V acquisition on maturing phagosome, preventing phagosome acidification [Publication III, in press]. Here, we observed that Syt V exclusion by LPG takes place as soon as the phagosome formation and, by this way, *L. donovani* promastigotes could alter the phagosome composition from the first minutes of the infection to establish afterward favourable conditions for its transformation into the amastigote form. LPG is essential for the promastigote to amastigote differentiation by inhibiting phagosome maturation, and highly increases the parasite survival [12]. However, our results strongly suggest that LPG also reduces the infection rate of the parasite at least in part by a focal exocytosis defect mediated by Syt V. This finding may appear surprising as intracellular pathogens should promote its internalization to reach their replication niche in their host cells. Nevertheless, in evolutionary terms, although an obligated fitness cost for the parasite to reach its niche into macrophages, LPG is a predominant factor to delay microbicidal activities and allows its differentiation. Thus, imposed cost associated to a lower number of parasite infection may largely be compensated by a dramatically improved survival rate and could lead to a greater fitness for the parasite.

In phagocytes, Syt regulation is completely unknown. However, for other cell types, several studies showed a Syt regulation by PKC. It has been proposed that the phosphorylation of the most studied member of this family, Syt I, by CaMKII and PKC contributes to the mechanism(s) by which these two kinases regulate neurotransmitter release [61]. Syt VI is phosphorylated by PKC on conserved threonines in the polybasic regions and regulates acrosomal exocytosis [62]. Another example was proposed with the internalization of the Syt IX from the plasma membrane and its delivery to the ERC by a mechanism dependent on phosphorylation by Ca^{2+}-dependent PKC-α or –β [63]. Here, we clearly showed that PKC-α regulates Syt V recruitment on phagosome using DN-PKC-α RAW 264.7 cells. Furthermore, many evidences indicate a good correlation of the

effect of a Syt V silencing and a DN expression of PKC-α. Indeed, besides the decrease of the internalization rate, Syt V silencing and expression of a DN-PKC-α both impair phagosome maturation by inhibiting acquisition of markers such as Cath D, Cath S, Rab-7, LAMP-1 for DN- PKC-α expressing cells [27] or Cath D and the vacuolar V-ATPase for Syt V silencing [Publication III, in press]. Moreover, LPG excludes both PKC-α and Syt V from phagosomes and this process could be imputable to lipid microdomains disruption for PKC-α as already described for Syt V [Publication III, in press], since a methyl-β-cyclodextrin treatment of BMM cells also impairs PKC-α recruitment on phagosome. Several studies reported that LPG inhibits PKC-α activity [19-21] and its recruitment on phagosome [22]. Thus, the inhibition of PKC-α activity and its impaired recruitment on phagosome by *L. donovani* LPG could also participate to the impaired acquisition of Syt V on phagosome as soon as the early steps of the phagocytosis.

Some lines of evidence suggest that PKC-α could directly interact with Syt V to regulate Syt V acquisition on phagosomes. First Syt V was identified in macrophage phagosomes by a PKC-α co-immunoprecipitation of phagosome lysates and a subsequent analysis by mass spectrometry of protein complex associated to PKC-α (Vinet and Descoteaux, unpublished). Second, we observed a colocalization between Syt V and PKC-α specifically on macrophage phagosomes, indicating that both proteins are present on same membrane areas. Nevertheless, a direct interaction of Syt V and PKC-α was not confirmed by co-immunoprecipitation and western blot analysis (data not shown). Thus, this point remains unclear and further investigations are necessary to precisely address whether their interaction is direct or indirect.

Taken together, our findings pointed out an early effect of LPG on the internalization process of *L. donovani* and proposed that LPG alteration of the membrane supply, mediated by Syt V, represents a possible mechanism responsible of the reduced phagocytosis rate observed of the WT *L. donovani* compared to their *lpg*-KO counterpart. Furthermore, we provided first evidences of a PKC-α regulation of Syt V acquisition on phagosome in macrophages.

References

1. Aderem A, Underhill DM (1999) Mechanisms of phagocytosis in macrophages. Annu Rev Immunol 17: 593-623.

2. May RC, Machesky LM (2001) Phagocytosis and the actin cytoskeleton. J Cell Sci 114: 1061-1077.

3. Desjardins M, Huber LA, Parton RG, Griffiths G (1994) Biogenesis of phagolysosomes proceeds through a sequential series of interactions with the endocytic apparatus. J Cell Biol 124: 677-688.

4. Lainson R, Shaw JJ (1978) Epidemiology and ecology of *Leishmania*sis in Latin-America. Nature 273: 595-600.

5. Pimenta PF, Turco SJ, McConville MJ, Lawyer PG, Perkins PV, et al. (1992) Stage-specific adhesion of *Leishmania* promastigotes to the sandfly midgut. Science 256: 1812-1815.

6. Chang KP, Dwyer DM (1976) Multiplication of a human parasite *Leishmania donovani* in phagolysosomes of hamster macrophages in vitro. Science 193: 678-680.

7. Descoteaux A, Luo Y, Turco SJ, Beverley SM (1995) A specialized pathway affecting virulence glycoconjugates of *Leishmania*. Science 269: 1869-1872.

8. Handman E, Schnur LF, Spithill TW, Mitchell GF (1986) Passive transfer of *Leishmania* lipopolysaccharide confers parasite survival in macrophages. J Immunol 137: 3608-3613.

9. McNeely TB, Turco SJ (1990) Requirement of lipophosphoglycan for intracellular survival of *Leishmania donovani* within human monocytes. J Immunol 144: 2745-2750.

10. Spath GF, Epstein L, Leader B, Singer SM, Avila HA, et al. (2000) Lipophosphoglycan is a virulence factor distinct from related glycoconjugates in the protozoan parasite *Leishmania major*. Proc Natl Acad Sci U S A 97: 9258-9263.

11. Turco SJ, Descoteaux A (1992) The lipophosphoglycan of *Leishmania* parasites. Annu Rev Microbiol 46: 65-94.

12. Lodge R, Diallo TO, Descoteaux A (2006) *Leishmania donovani* lipophosphoglycan blocks NADPH oxidase assembly at the phagosome membrane. Cell Microbiol 8: 1922-1931.

13. Miao L, Stafford A, Nir S, Turco SJ, Flanagan TD, et al. (1995) Potent inhibition of viral fusion by the lipophosphoglycan of *Leishmania donovani*. Biochemistry 34: 4676-4683.

14. Tolson DL, Turco SJ, Pearson TW (1990) Expression of a repeating phosphorylated disaccharide lipophosphoglycan epitope on the surface of macrophages infected with *Leishmania donovani*. Infect Immun 58: 3500-3507.

15. Desjardins M, Descoteaux A (1997) Inhibition of phagolysosomal biogenesis by the *Leishmania* lipophosphoglycan. J Exp Med 185: 2061-2068.

16. Dermine JF, Scianimanico S, Prive C, Descoteaux A, Desjardins M (2000) *Leishmania* promastigotes require lipophosphoglycan to actively modulate the fusion properties of phagosomes at an early step of phagocytosis. Cell Microbiol 2: 115-126.

17. Spath GF, Garraway LA, Turco SJ, Beverley SM (2003) The role(s) of lipophosphoglycan (LPG) in the establishment of *Leishmania major* infections in mammalian hosts. Proc Natl Acad Sci U S A 100: 9536-9541.

18. Scianimanico S, Desrosiers M, Dermine JF, Meresse S, Descoteaux A, et al. (1999) Impaired recruitment of the small GTPase rab7 correlates with the inhibition of phagosome maturation by *Leishmania donovani* promastigotes. Cell Microbiol 1: 19-32.

19. McNeely TB, Rosen G, Londner MV, Turco SJ (1989) Inhibitory effects on protein kinase C activity by lipophosphoglycan fragments and glycosylphosphatidylinositol antigens of the protozoan parasite *Leishmania*. Biochem J 259: 601-604.

20. Descoteaux A, Matlashewski G, Turco SJ (1992) Inhibition of macrophage protein kinase C-mediated protein phosphorylation by *Leishmania donovani* lipophosphoglycan. J Immunol 149: 3008-3015.

21. Giorgione JR, Turco SJ, Epand RM (1996) Transbilayer inhibition of protein kinase C by the lipophosphoglycan from *Leishmania donovani*. Proc Natl Acad Sci U S A 93: 11634-11639.

22. Holm A, Tejle K, Magnusson KE, Descoteaux A, Rasmusson B (2001) *Leishmania donovani* lipophosphoglycan causes periphagosomal actin accumulation: correlation with impaired translocation of PKCα and defective phagosome maturation. Cell Microbiol 3: 439-447.

23. Allen LA, Aderem A (1995) Protein kinase C regulates MARCKS cycling between the plasma membrane and lysosomes in fibroblasts. Embo J 14: 1109-1121.

24. Larsen EC, DiGennaro JA, Saito N, Mehta S, Loegering DJ, et al. (2000) Differential requirement for classic and novel PKC isoforms in respiratory burst and phagocytosis in RAW 264.7 cells. J Immunol 165: 2809-2817.

25. Allen LA, Aderem A (1996) Mechanisms of phagocytosis. Curr Opin Immunol 8: 36-40.

26. Holm A, Tejle K, Gunnarsson T, Magnusson KE, Descoteaux A, et al. (2003) Role of protein kinase C-α for uptake of unopsonized prey and phagosomal maturation in macrophages. Biochem Biophys Res Commun 302: 653-658.

27. Ng Yan Hing JD, Desjardins M, Descoteaux A (2004) Proteomic analysis reveals a role for protein kinase C-α in phagosome maturation. Biochem Biophys Res Commun 319: 810-816.

28. Lodge R, Descoteaux A (2005) *Leishmania donovani* promastigotes induce periphagosomal F-actin accumulation through retention of the GTPase Cdc42. Cell Microbiol 7: 1647-1658.

29. Chapman ER (2002) Synaptotagmin: a $Ca^{(2+)}$ sensor that triggers exocytosis? Nat Rev Mol Cell Biol 3: 498-508.

30. Czibener C, Sherer NM, Becker SM, Pypaert M, Hui E, et al. (2006) Ca^{2+} and synaptotagmin VII-dependent delivery of lysosomal membrane to nascent phagosomes. J Cell Biol 174: 997-1007.

31. Lindmark IM, Karlsson A, Serrander L, Francois P, Lew D, et al. (2002) Synaptotagmin II could confer $Ca^{(2+)}$ sensitivity to phagocytosis in human neutrophils. Biochim Biophys Acta 1590: 159-166.

32. Roy D, Liston DR, Idone VJ, Di A, Nelson DJ, et al. (2004) A process for controlling intracellular bacterial infections induced by membrane injury. Science 304: 1515-1518.

33. Iezzi M, Kouri G, Fukuda M, Wollheim CB (2004) Synaptotagmin V and IX isoforms control Ca^{2+} -dependent insulin exocytosis. J Cell Sci 117: 3119-3127.

34. Saegusa C, Fukuda M, Mikoshiba K (2002) Synaptotagmin V is targeted to dense-core vesicles that undergo calcium-dependent exocytosis in PC12 cells. J Biol Chem 277: 24499-24505.

35. Vinet AF, Fukuda M, Descoteaux A (2008) The exocytosis regulator synaptotagmin V controls phagocytosis in macrophages. J Immunol 181: 5289-5295.

36. Descoteaux A, Matlashewski G (1989) c-fos and tumor necrosis factor gene expression in *Leishmania donovani*-infected macrophages. Mol Cell Biol 9: 5223-5227.

37. St-Denis A, Chano F, Tremblay P, St-Pierre Y, Descoteaux A (1998) Protein kinase C-α modulates lipopolysaccharide-induced functions in a murine macrophage cell line. J Biol Chem 273: 32787-32792.

38. Prive C, Descoteaux A (2000) *Leishmania donovani* promastigotes evade the activation of mitogen-activated protein kinases p38, c-Jun N-terminal kinase, and extracellular signal-regulated kinase-1/2 during infection of naive macrophages. Eur J Immunol 30: 2235-2244.

39. Huang C, Turco SJ (1993) Defective galactofuranose addition in lipophosphoglycan biosynthesis in a mutant of *Leishmania donovani*. J Biol Chem. pp. 24060-24066.

40. Tolson DL, Turco SJ, Beecroft RP, Pearson TW (1989) The immunochemical structure and surface arrangement of *Leishmania donovani* lipophosphoglycan determined using monoclonal antibodies. Mol Biochem Parasitol 35: 109-118.

41. Orlandi PA, Jr., Turco SJ (1987) Structure of the lipid moiety of the *Leishmania donovani* lipophosphoglycan. J Biol Chem 262: 10384-10391.

42. Russo DM, Turco SJ, Burns JM, Jr., Reed SG (1992) Stimulation of human T lymphocytes by *Leishmania* lipophosphoglycan-associated proteins. J Immunol 148: 202-207.

43. Iezzi M, Eliasson L, Fukuda M, Wollheim CB (2005) Adenovirus-mediated silencing of synaptotagmin 9 inhibits Ca^{2+}-dependent insulin secretion in islets. FEBS Lett 579: 5241-5246.

44. Flandin JF, Chano F, Descoteaux A (2006) RNA interference reveals a role for TLR2 and TLR3 in the recognition of *Leishmania donovani* promastigotes by interferon-γ-primed macrophages. Eur J Immunol 36: 411-420.

45. Breton A, Descoteaux A (2000) Protein kinase C-α participates in FcγR-mediated phagocytosis in macrophages. Biochem Biophys Res Commun 276: 472-476.

46. Russell DG (1987) The macrophage-attachment glycoprotein gp63 is the predominant C3-acceptor site on *Leishmania mexicana* promastigotes. Eur J Biochem 164: 213-221.

47. Brittingham A, Morrison CJ, McMaster WR, McGwire BS, Chang KP, et al. (1995) Role of the *Leishmania* surface protease gp63 in complement fixation, cell adhesion, and resistance to complement-mediated lysis. J Immunol 155: 3102-3111.

48. Brown D (2002) Structure and function of membrane rafts. Int J Med Microbiol 291: 433-437.

49. Rajendran L, Simons K (2005) Lipid rafts and membrane dynamics. J Cell Sci 118: 1099-1102.

50. Del Pozo MA (2004) Integrin signaling and lipid rafts. Cell Cycle 3: 725-728.

51. Kwiatkowska K, Frey J, Sobota A (2003) Phosphorylation of FcγRIIA is required for the receptor-induced actin rearrangement and capping: the role of membrane rafts. J Cell Sci 116: 537-550.

52. Kono H, Suzuki T, Yamamoto K, Okada M, Yamamoto T, et al. (2002) Spatial raft coalescence represents an initial step in FcγR signaling. J Immunol 169: 193-203.

53. Gatfield J, Pieters J (2000) Essential role for cholesterol in entry of mycobacteria into macrophages. Science 288: 1647-1650.

54. Peyron P, Bordier C, N'Diaye EN, Maridonneau-Parini I (2000) Nonopsonic phagocytosis of *Mycobacterium kansasii* by human neutrophils depends on cholesterol and is mediated by CR3 associated with glycosylphosphatidylinositol-anchored proteins. J Immunol 165: 5186-5191.

55. Schneider B, Schueller C, Utermoehlen O, Haas A (2007) Lipid microdomain-dependent macropinocytosis determines compartmentation of *Afipia felis*. Traffic 8: 226-240.

56. Alfsen A, Iniguez P, Bouguyon E, Bomsel M (2001) Secretory IgA specific for a conserved epitope on gp41 envelope glycoprotein inhibits epithelial transcytosis of HIV-1. J Immunol 166: 6257-6265.

57. Grassme H, Jendrossek V, Riehle A, von Kurthy G, Berger J, et al. (2003) Host defense against *Pseudomonas aeruginosa* requires ceramide-rich membrane rafts. Nat Med 9: 322-330.

58. Winberg ME, Holm A, Sarndahl E, Vinet AF, Descoteaux A, et al. (2009) *Leishmania donovani* lipophosphoglycan inhibits phagosomal maturation via action on membrane rafts. Microbes Infect 11: 215-222.

59. Dermine JF, Duclos S, Garin J, St-Louis F, Rea S, et al. (2001) Flotillin-1-enriched lipid raft domains accumulate on maturing phagosomes. J Biol Chem 276: 18507-18512.

60. Dermine JF, Goyette G, Houde M, Turco SJ, Desjardins M (2005) *Leishmania donovani* lipophosphoglycan disrupts phagosome microdomains in J774 macrophages. Cell Microbiol 7: 1263-1270.

61. Hilfiker S, Pieribone VA, Nordstedt C, Greengard P, Czernik AJ (1999) Regulation of synaptotagmin I phosphorylation by multiple protein kinases. J Neurochem 73: 921-932.

62. Roggero CM, Tomes CN, De Blas GA, Castillo J, Michaut MA, et al. (2005) Protein kinase C-mediated phosphorylation of the two polybasic regions of synaptotagmin VI regulates their function in acrosomal exocytosis. Dev Biol 285: 422-435.

63. Haberman Y, Ziv I, Gorzalczany Y, Fukuda M, Sagi-Eisenberg R (2005) Classical protein kinase C(s) regulates targeting of synaptotagmin IX to the endocytic recycling compartment. J Cell Sci 118: 1641-1649.

Résultats Supplémentaires

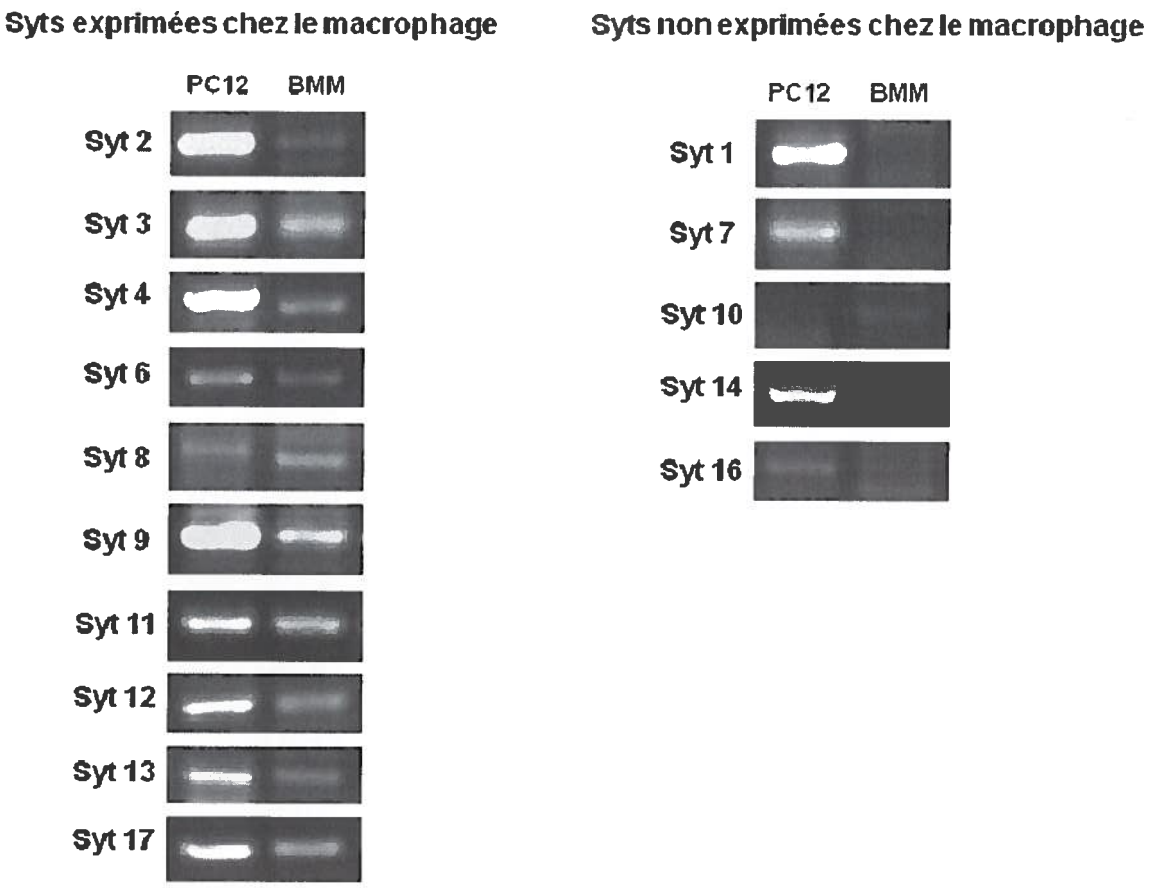

Figure S1: Expression de l'ARNm des different autres membres de la famille des Syts dans le macrophage. Les Syt 2, 3, 4, 6, 8, 9, 11, 12, 13 et 17 sont exprimées chez les macrophages dérivés de la moelle osseuse, tel que montré ici par RT-PCR. La lignée cellulaire PC12 issue de neurone fut utilisée comme contrôl.

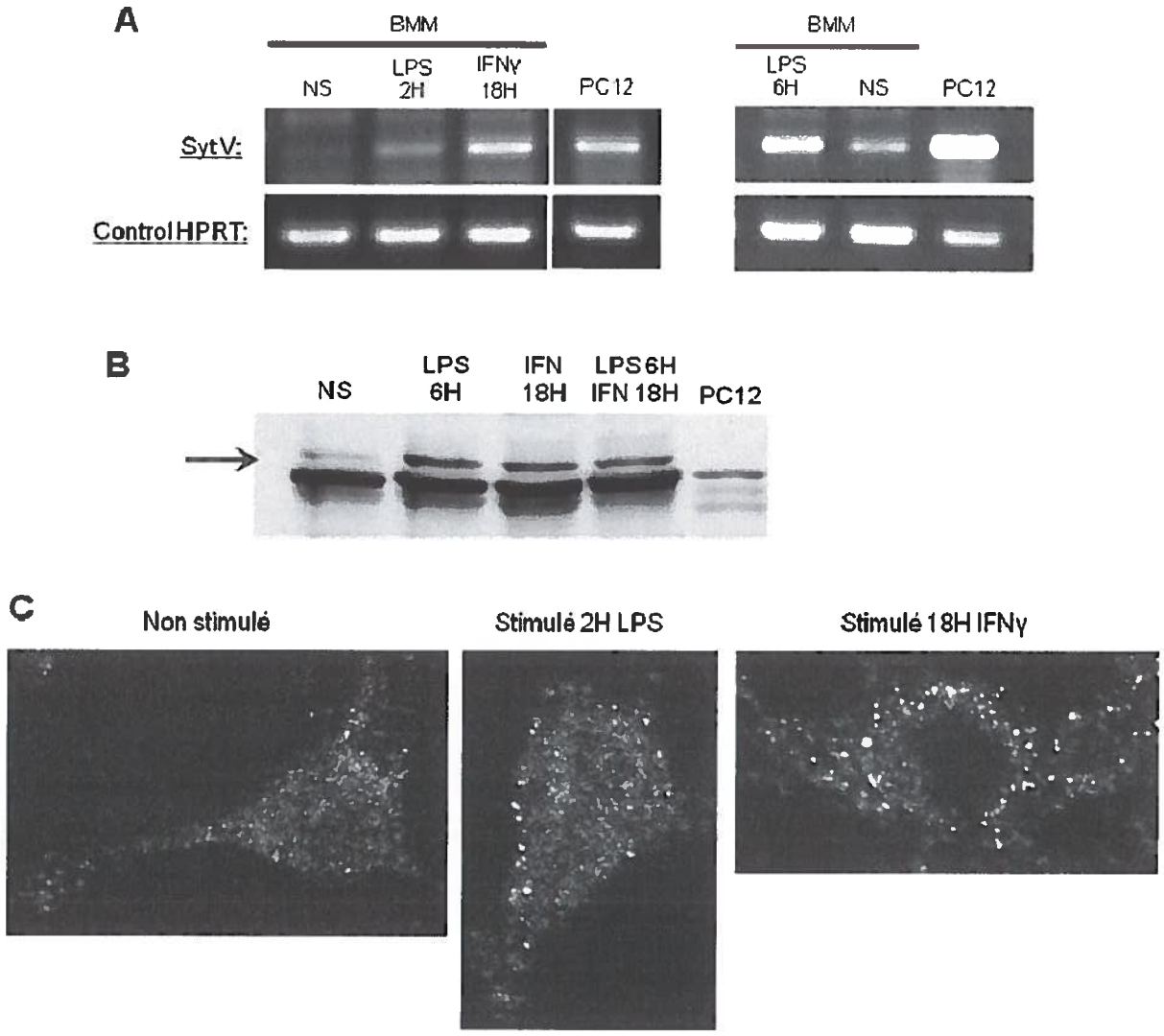

Figure S2: Augmentation de l'expression de la Syt V suite à une stimulation à l'IFNγ et au LPS. *A-C*, Les macrophages ont été traités avec l'IFN-γ (100 unités/ml) et/ou le LPS (0.5 µg/ml) durant les temps indiqués. *A*, L'expression de l'ARNm de la Syt V a été déterminé chez les macrophages issus de la moelle osseuse par RT-PCR. *B* et *C*, l'expression protéique a été déterminée par western blot sur 10µg de lysats cellulaires totaux (B) et par microscopie confocale (C) par l'anticorps anti-Syt V C2AB chez des macrophages péritonéaux. La lignée cellulaire PC12 issue de neurone fut utilisée comme contrôl (A, B).

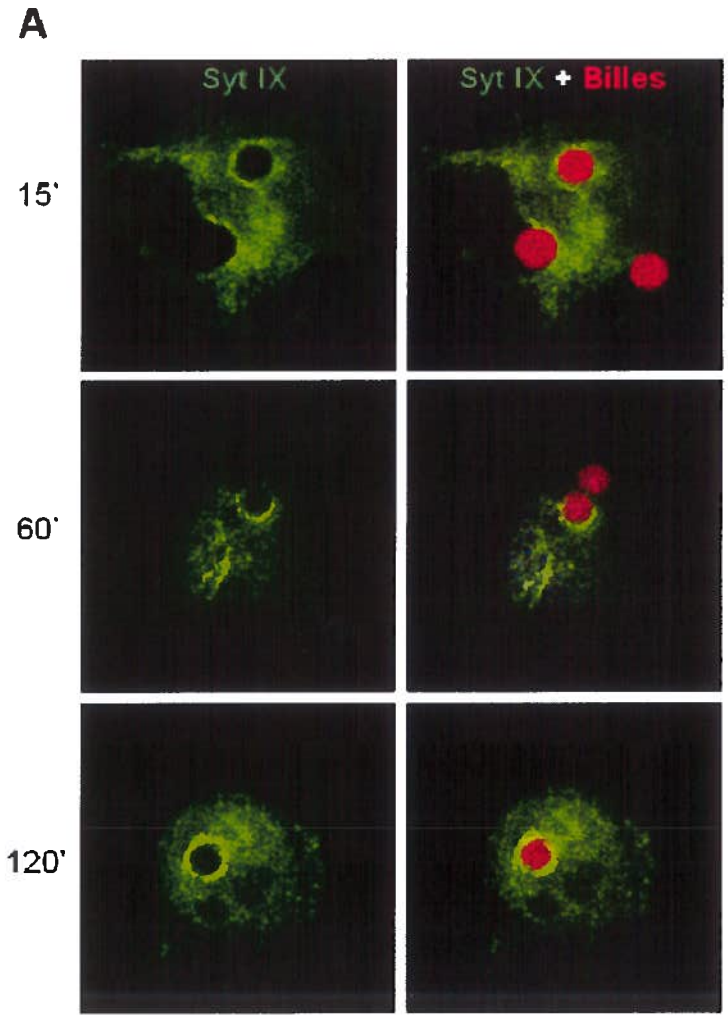

Figure S3: La Syt IX est recutée au phagosome de macrophages. Des billes de latex (rouge) ont été internalisées durant 15, 60 ou 120 min par des macrophages péritonéaux, puis les cellules ont été fixées et marquées pour la Syt IX (vert).

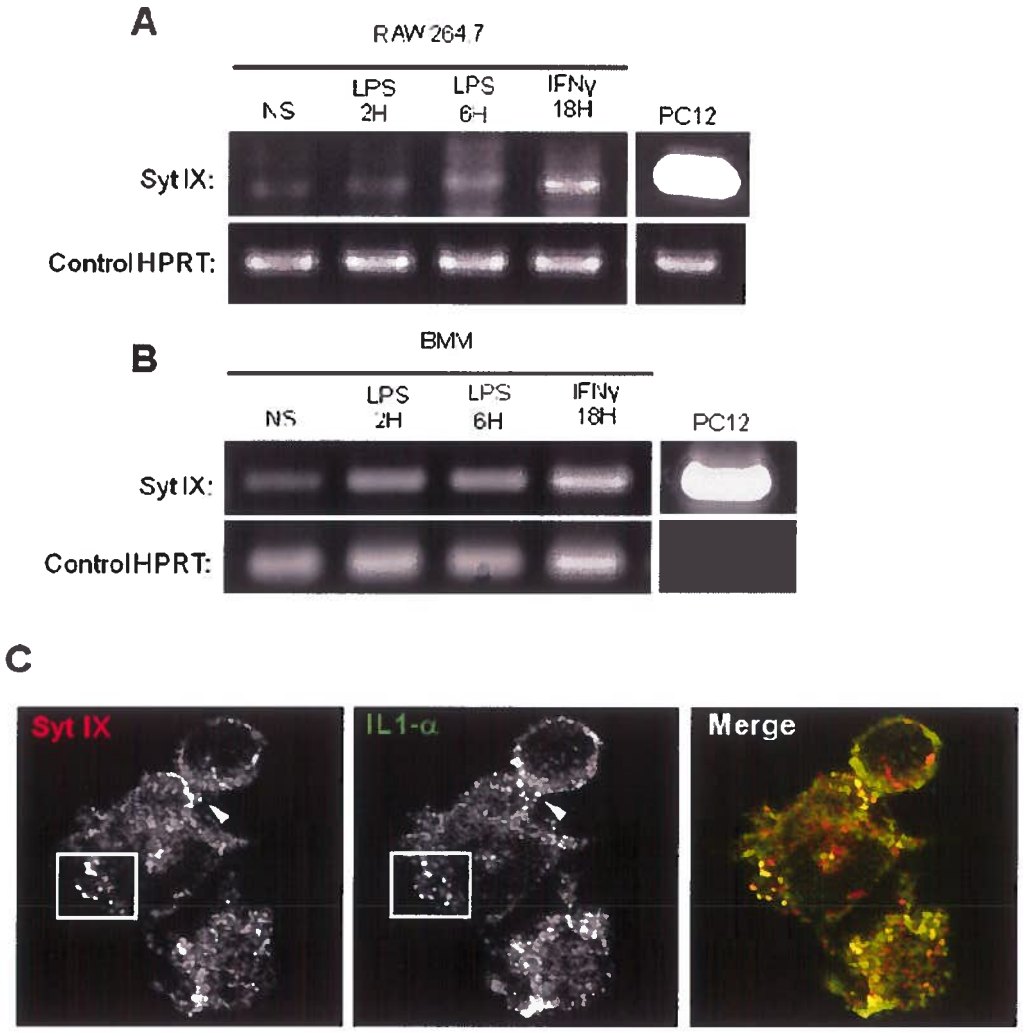

Figure S4: Augmentation de l'expression de la Syt IX après stimulation des macrophages et association avec les vésicules positives pour l'IL1-α. *A-B*, Les macrophages ont été traités avec l'IFN-γ (100 unités/ml) ou le LPS (0.5 µg/ml) durant les temps indiqués et l'expression de l'ARNm de la Syt IX a été déterminée chez les macrophages RAW 264.7 (A) ou issus de la moelle osseuse de souris (B) par RT-PCR. La lignée cellulaire PC12 issue de neurone fut utilisée comme contrôl (A, B). *C*, Co-marquage de la Syt IX et de l'IL1-α et visualisation par microscopie confocale de leur colocalisation chez des macrophages péritonéaux (voir cadre blanc et la flèche blanche).

DISCUSSION

1 La Syt V et la phagocytose

1.1 Les acteurs de la fusion membranaire lors de la phagocytose

De par leur très forte activité d'endocytose, d'exocytose et de phagocytose, les macrophages sont soumis à d'intenses évènements de fusions membranaires. Ces fusions sont indispensables à leur rôle dans l'immunité innée car elles sont absolument nécessaires à la régulation de processus tels que la sécrétion de cytokines ou la phagocytose, mais également pour l'immunité adaptative lors de la présentation antigénique. Ainsi, bien qu'il soit évident que les fusions membranaires soient cruciales à l'accomplissement des fonctions du macrophage, encore peu d'études se sont intéressées à l'identification des acteurs de ces fusions, et encore moins à l'identification des régulateurs de ces fusions membranaires. Le processus phagocytique fait intervenir un grand nombre de fusions membranaires dès la formation de la coupe phagocytique et tout au long de la maturation du phagosome, et quelques SNARE ont été identifiées au niveau du phagosome. Par exemple, les protéines endosomales SNARE VAMP-3 et VAMP-7 sont recrutées au phagosome naissant durant les premières étapes de la phagocytose (Bajno et al., 2000; Braun et al., 2004). Les syntaxines 7 et 13 sont nécessaires à diverses étapes de la maturation du phagosome car elles régulent la fusion du phagosome avec les endosomes précoces/tardifs et les lysosomes respectivement (Collins et al., 2002). Il a été démontré récemment que les SNARE associées au ER, la Syntaxine 18 et Sec22b, étaient impliquées dans la fusion membranaire entre le ER et la membrane plasmique durant la phagocytose des macrophages J774 (Hatsuzawa et al., 2006). Cependant, le mécanisme moléculaire n'est pas encore clair, et le rôle de Sec22b sur la phagocytose est parfois celui d'un régulateur positif (Becker, Volchuk, et Rothman, 2005), parfois celui d'un régulateur négatif (Hatsuzawa et al., 2009).

1.2 Les synaptotagmines et la phagocytose

Parmi les régulateurs de fusion membranaire, les synaptotagmines jouent un rôle clé dans la régulation dépendante du Ca^{2+}. Cependant, les études s'intéressant aux Syts se limitent principalement aux cellules neuronales et à quelques cellules sécrétrices pour lesquelles les Syts régulent l'exocytose. Très peu d'études se sont intéressées à l'implication potentielle des Syts au niveau de l'immunité et plus particulièrement chez le macrophage. La Syt la mieux caractérisée chez les cellules immunitaires est la Syt VII au niveau des macrophages, qui régule l'exocytose dépendante du calcium des lysosomes (Martinez et al., 2000). En l'absence de Syt VII, la phagocytose est inhibée et particulièrement sous condition de haute demande en membrane (Czibener et al., 2006). Chez les neutrophiles, la Syt II est présente au niveau des granules et est recrutée au phagosome, cependant son rôle reste inconnu (Lindmark et al., 2002).

1.3 Calcium et phagocytose

D'après les effets connus du calcium sur la fusion membranaire dans un grand nombre de systèmes, il est généralement supposé que la biogénèse du phagolysosme est dépendante du calcium (Jaconi et al., 1990). Cette supposition fut validée expérimentalement par le groupe de Krusner (Malik, Denning, et Kusner, 2000) qui montra que la maturation du phagosome était bloquée lorsque les changements du niveau d'ions calcium cytosoliques étaient empêchés via des agents tampons (Malik, Denning, et Kusner, 2000). Il a été décrit que l'élévation d'ions calcium accompagnant la phagocytose de bactéries ou de particules inertes était réduite ou absente dans le cas de certains microorganismes pathogènes. Cela fut par exemple décrit pour *Mycobacterium.* Ce phénomène fut attribué au glycolipide lipoarrabinomannan (Vergne, Chua, et Deretic, 2003) qui bloquerait la signalisation de la sphingosine kinase régulant potentiellement l'augmentation transitoire d'ions calcium normalement associée à la phagocytose de particule non virulentes (Malik et al., 2000). L'utilisation de particules recouvertes de LAM nous a permis d'observer une inhibition de l'accumulation de la Syt V au

phagosome. Si l'on considère que la Syt V possède un rôle de senseur calcique lors des évènements de fusions membranaires endosomales et phagosomales, cette observation pourrait alors s'expliquer par un blocage des interactions dépendantes de l'activité de Syt V entre le phagosome et les endosomes positifs pour Syt V (dû à l'activité anti-calcique du LAM). Ce processus aurait alors pour conséquence un défaut dans l'acquisition de la Syt V et de la maturation du phagosome tel qu'observé (Article III; (Fratti et al., 2003)).

1.4 La Syt V et la formation du phagosome

Les connaissances actuelles sur la Syt V sont très limitées. Une étude a démontré que la Syt V était spécifique aux vésicules à cœur dense des neurones et qu'elle régulait l'exocytose dépendante du Ca^{2+} (Saegusa, Fukuda, et Mikoshiba, 2002). Wolheim et ses collaborateurs ont démontré par RNAi que la Syt V régule l'exocytose d'insuline par les cellules pancréatiques β (Iezzi et al., 2004). Au cours de ce projet, nous avons identifié l'expression de la Syt V au niveau de son ARNm et au niveau protéique chez le macrophage. Nous avons pu observer son association aux endosomes de recyclage et son recrutement dès la formation de la coupe phagocytique. Par la méthode de l'ARN d'interférence nous avons mis en évidence un rôle critique de la Syt V lors de la phagocytose, particulièrement lorsque le macrophage se trouve en situation de forte demande membranaire (particules de forte taille et/ou grand nombre de particules par macrophage). Ainsi il est fort probable que la Syt V contrôle la mobilisation des endosomes de recyclage comme source intracellulaire de membrane lors de l'exocytose focale (Figure 13). Le rôle de la Syt V apparaît donc assez semblable à celui décrit pour la Syt VII par Andrews et collaborateurs (Czibener et al., 2006), bien qu'appartenant à des types d'endosomes différents. On peut d'ailleurs noter que l'importance de la Syt VII pendant l'apport membranaire au niveau du phagosome naissant semble plus spécifique aux particules de très grande taille ($\geq$ 6 µm) alors que l'importance de la Syt V concerne des particules $\geq$ 3 µm. Cette différence pourrait s'expliquer par une mobilisation séquentielle des vésicules intracellulaires selon la demande membranaire. Il est en effet possible que les endosomes précoces/de recyclage soient les premiers recrutés à la coupe

phagocytique pour l'internalisation de particules de taille moyenne. Puis, dans le cas d'une phagocytose de très grandes particules, représentant une condition de demande membranaire très importante, d'autres vésicules telles que les lysosomes pourraient être mobilisées. Cette supposition expliquerait également que la phagocytose de macrophages issus de souris VAMP-3$^{-/-}$ ne soient pas profondément altérée (Allen, Yang, et Pessin, 2002), dû à un effet compensatoire des lysosomes. Nos résultats démontrent d'ailleurs que l'inhibition de la phagocytose n'est pas totale et qu'une certaine compensation pourrait exister au cours du temps, puisqu'à 10 min d'internalisation l'inhibition de phagocytose peut atteindre 70% pour un très grand nombre de particules, alors qu'à 60 min d'internalisation, l'inhibition de phagocytose ne dépasse pas 50% pour des conditions similaires (Article I).

Les endosomes de recyclage représentent donc des vésicules très importantes pour la phagocytose. Outre leur rôle clé d'apport membranaire à la coupe phagocytique (Braun et Niedergang, 2006; Huynh et al., 2007), plusieurs molécules associées à ces endosomes de recyclage et impliquées dans la régulation de la fusion membranaire telles que VAMP-3, Rab-11 et Arf-6 sont recrutées au niveau du phagosome naissant et contribuent au processus d'internalisation (Allen, Yang, et Pessin, 2002; Bajno et al., 2000; Cox et al., 2000; Niedergang et al., 2003; Zhang et al., 1998). Le recrutement précoce de la Syt V au phagosome est cohérent avec sa localisation au niveau des endosomes de recyclage et représente un régulateur général puisque la phagocytose de particules impliquant divers récepteurs phagocytiques est inhibée suite à une RNAi Syt V. L'association de la Syt V avec des SNAREs connus telles que VAMP-3, Rab-11 ou Arf-6 est possible et reste à déterminer. La Syt V n'est pas seulement présente au niveau de la coupe phagocytique et des phagosomes mais également au niveau de structures de type filipode. Cette observation suggère que la Syt V qui est associée aux endosomes de recyclage est libérée au niveau de la membrane plasmique lorsque les endosomes de recyclage fusionnent avec celle-ci. Ainsi la Syt V pourrait avoir un rôle plus général encore puisqu'il a été démontré que l'apport membranaire a partir des endosomes de recyclage au niveau de la coupe phagocytique, permet également le relargage de TNF-α (Murray et al., 2005). En effet, suite à une activation du macrophage, il y a un accroissement de la circulation

endosomale afin de satisfaire la demande en sécrétion de cytokines et ce phénomène est relié à la régulation à la hausse de l'expression des SNARE impliquées (Murray et al., 2005; Stow, Manderson, et Murray, 2006). D'autres études seront nécessaires pour déterminer une potentielle implication de la Syt V dans ces évènements.

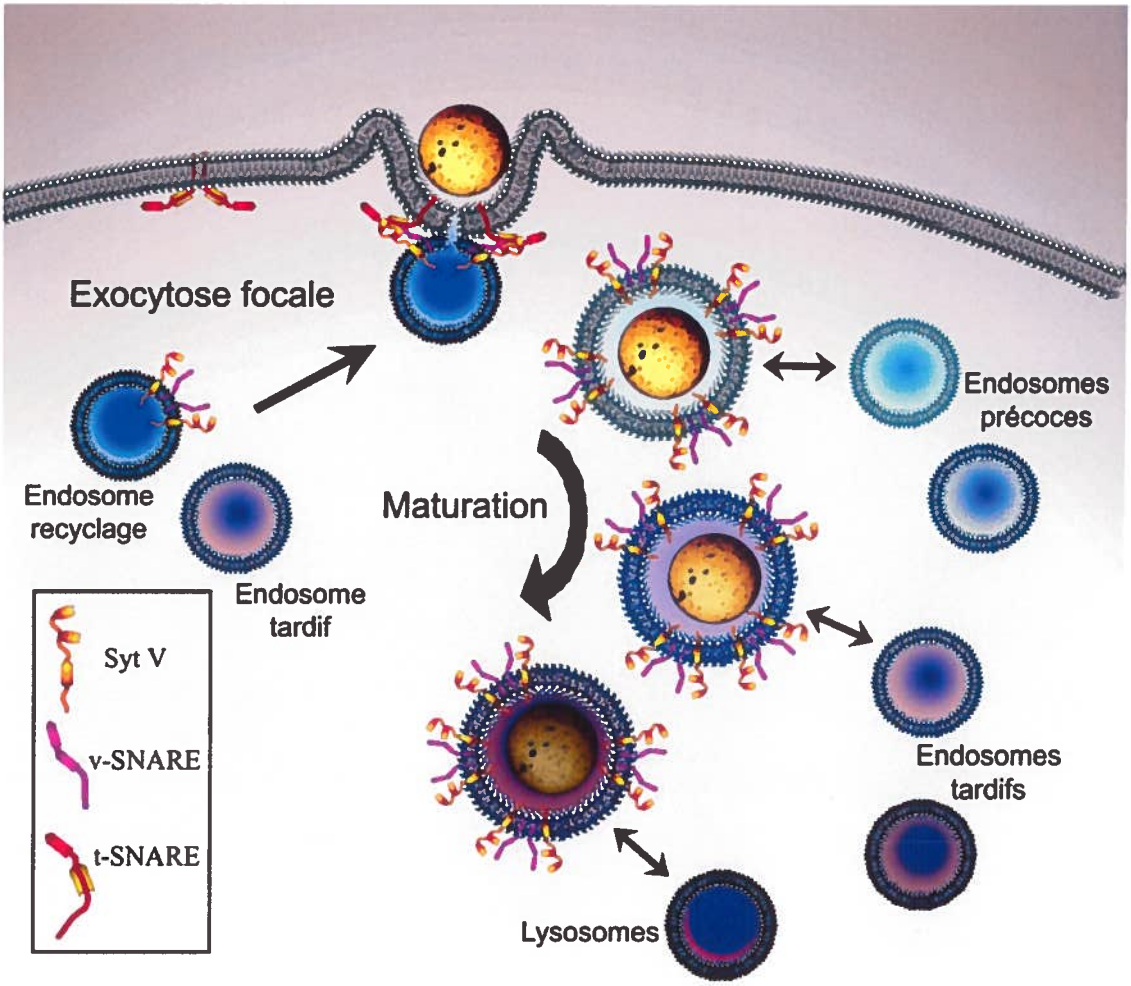

Figure 13: Proposition d'un modèle représentant le rôle de la Syt V lors de la formation du phagosome. La Syt V associée aux endosomes de recyclage régule l'apport membranaire issu de ces endosomes au niveau de la coupe phagocytique pendant l'exocytose focale provoquée par l'internalisation d'une particule de grande taille. La Syt V reste ensuite associée au phagosome durant le processus de maturation.

1.5 La Syt V et la maturation du phagosome : régulation de l'acquisition de la Cath D et de la V-ATPase au phagosome

Le fait que la Syt V reste associée au phagosome tout au long du processus de maturation (Article I et Figure 13) suggère qu'elle puisse jouer un rôle durant la biogenèse du phagolysosome en régulant la fusion membranaire entre le compartiment endosomal et le phagosome lors des interactions transitoires de type « Kiss and Run » (Desjardins et al., 1994). Nos expériences ont révélé que la Syt V régulait l'acquisition de la Cathepsine D et de la sous-unité *c* de la V-ATPase. Le fait que l'acquisition de ces deux facteurs essentiels à l'activité microbicide du phagosome soit régulée par la Syt V suggère un rôle primordial de ce régulateur de fusion membranaire durant la biogénèse du phagolysosome. En effet, durant ce processus, l'apparition séquentielle des hydrolases cathepsines permet un apprêtement et une présentation antigénique optimales (Garin et al., 2001; Honey et Rudensky, 2003; Villadangos et Ploegh, 2000) et l'acidification progressive du phagosome potentialise l'efficacité des mécanismes microbicides tels que les enzymes lytiques, les peptides cationiques et les FRO. Il est donc possible que la Syt V soit impliquée dans les processus de dégradation du contenu du phagolysosome menant à la présentation antigénique. Cependant, nos résultats montrent aussi que le recrutement de EEA1, LAMP-1 et de la cathepsine B ne sont pas altérés par une absence d'expression de la Syt V. Ceci indique que la Syt V fait partie de la machinerie de fusion qui régule les interactions entre le phagosome et des sous-populations spécifiques d'endosomes tardifs / lysosomes enrichis en cathepsine D et en sous-unité *c* de la V-ATPase. Ces résultats peuvent également indiquer que la Syt V pourrait être nécessaire pour atteindre un niveau de maturation du phagosome permettant l'acquisition de la cathepsine D et de la sous-unité *c* de la V-ATPase. Le fait que l'acquisition de la cathepsine B et D soit régulée par des mécanismes distincts supporte le modèle proposant que diverses hydrolases apparaissent séquentiellement durant la maturation du phagosome (Garin et al., 2001). Enfin, cette observation est également cohérente avec les indices montrant que diverses sous-populations d'endosomes précoces, tardifs et de lysosomes co-existent, et que ces

compartiments contiennent une certaine hétérogénéité (Rogers et Foster, 2007; Yates et al., 2007).

Bien que la présence de la V-ATPase à la membrane du phagosome soit établie (Lukacs, Rotstein, et Grinstein, 1990), le mécanisme d'acquisition de la V-ATPase au phagosome reste obscur. On considère que l'acidification du phagosome est la conséquence de fusions entre le phagosome et les lysosomes où la V-ATPase est enrichie. Cependant, l'acidification régulée par la V-ATPase est initiée durant les phases précoces de la formation du phagosome, c'est-à-dire bien avant l'acquisition des marqueurs lysosomaux (Lukacs, Rotstein, et Grinstein, 1990; Sun-Wada et al., 2009; Yates, Hermetter, et Russell, 2005). Par exemple, la V-ATPase et certaines protéinases lysosomales sont recrutées avec des cinétiques différentes (Tsang et al., 2000; Yates et al., 2007), notamment les protéases cystéines telles que les Cath B et L (Yates, Hermetter, et Russell, 2005). De plus, les phagosomes contenant *Mycobacterium* pourrait acquérir LAMP-1, mais la V-ATPase est absente de leur membrane (Deretic et al., 2006; Sturgill-Koszycki et al., 1994). Ces observations indiqueraient donc que la V-ATPase est recrutée au phagosome selon une voie différente de celles de LAMP-1 et de certaines cathepsines. L'identification de la Syt V comme régulateur de ce processus est donc tout à fait pertinent dû à la présence précoce de la Syt V au niveau de la membrane phagosomale, mais également dû au fait que la Syt V ne régule aucunement l'acquisition de LAMP-1 ou de la Cath B (Article III).

Le fait que la Syt V soit présente au niveau des microdomaines lipidiques de la membrane phagosomale confirme l'importance de ces domaines pour le recrutement de la V-ATPase à la membrane du phagosome (Dermine et al., 2001). Il a d'ailleurs été démontré précédemment que la sous-unité *c* de la V-ATPase est présente dans les fractions résistantes au Triton X-100 de vésicules synaptiques issues de cerveau de rat, en association avec la synaptobrevine 2 et la synaptophysine (Galli, McPherson, et De Camilli, 1996). Cette observation a amené les auteurs à conclure que cette interaction pourrait jouer un rôle dans le recrutement de la V-ATPase aux vésicules synaptiques. Étudier la formation d'un complexe entre la Syt V et de telles SNAREs ainsi que caractériser ce complexe représente un axe de recherche très intéressant et mérite d'être approfondi.

1.6 Régulation de l'acquisition de la Syt V au phagosome par PKC-α

Chez les phagocytes, les molécules régulant les Syts sont totalement inconnues. Toutefois, pour d'autres types cellulaires, plusieurs études ont démontré une régulation de l'activité des Syts par des PKC. Par exemple, il a été proposé que la phosphorylation de la Syt I par CaMKII et PKC contribuait aux mécanismes par lesquels ces deux kinases régulent le relargage de neurotransmetteur (Hilfiker et al., 1999). La Syt IV est aussi phosphorylée par PKC pour réguler l'exocytose acrosomale des spermatozoïdes (Roggero et al., 2005). Un autre exemple concerne la Syt IX dont l'internalisation à partir de la membrane plasmique jusqu'à son relargage au ERC dépend d'une phosphorylation par les PKC-α ou -β (Haberman et al., 2005). Nos résultats montrent que l'activité de la PKC-α est nécessaire au recrutement de la Syt V (Article IV). De plus, plusieurs effets similaires entre l'expression dominante d'une PKC-α inactive et une réduction de l'expression de la Syt V (notamment pour le taux d'internalisation et l'acquisition de la Cath D) tendent à confirmer une régulation de la Syt V par la PKC-α. Le LPG exclut aussi bien la Syt V que la PKC-α du phagosome (article III; (Holm et al., 2001)) et ce processus est fort probablement dépendant des microdomaines lipidiques puisque, tout comme la Syt V, la désorganisation des microdomaines lipidiques réduit l'acquisition de la PKC-α au phagosome (article IV). Cependant, même si la Syt V et la PKC-α colocalisent au niveau de la membrane des phagosomes de macrophages, on ne peut pas affirmer que l'interaction entre ces deux protéines est directe et une étude plus approfondie d'une potentielle phosphorylation de la Syt V par PKC-α sera nécessaire.

1.7 Expression à la hausse des Syts suite à une stimulation des macrophages

L'IFN-γ et le LPS issu de la paroi de bactéries gram⁻ sont deux puissants activateurs des macrophages, empruntant deux voies de signalisation bien distinctes: la voie JAK/STAT et des TLR respectivement. Ces molécules stimulatrices sont des facteurs extrêmement importants pour la résolution de la plupart des infections. Cependant, plusieurs microorganismes tels que le parasite *Leishmania donovani* ne provoquent pas de sécrétions de cytokines pro-inflammatoires, leur permettant une entrée dite « silencieuse » à l'intérieur du macrophage (Carrera et al., 1996; Descoteaux et Matlashewski, 1989; Hatzigeorgiou et al., 1996; Piedrafita et al., 1999; Reiner, 1987). De récentes études sur l'identification du protéome du phagosome ont permis de dresser un premier inventaire des protéines phagosomales régulées suite à une stimulation du macrophage par l'IFN-γ (Jutras et al., 2008). Ainsi, plusieurs sous-unités de la pompe à proton V-ATPase sont régulées à la hausse, de même que de nombreuses protéines impliquées dans la fusion du phagosome avec le compartiment endocytique. Nos résultats, montrant une expression de l'ARNm et une expression protéique à la hausse de la Syt V suite à une stimulation des macrophages par l'IFN-γ et le LPS, sont donc tout à fait pertinents (Figure S2). Ces résultats suggèrent que la Syt V pourrait donc participer à l'exacerbation de la réponse microbicide et inflammatoire, notamment via son rôle de régulateur de l'acquisition au phagosome de facteurs tels que la Cath D et la V-ATPase du macrophage activé.

1.8 Autres Syts impliquées dans la phagocytose

De nombreux membres de la famille des Syts semblent être exprimés dans le macrophage, au moins au niveau de leur ARNm (Figure S1). Les études portant sur les neurones et certains autres types cellulaires tels que les cellules pancréatiques, ont montré que diverses Syts étaient présentes sur un même organelle et pouvaient ainsi moduler l'exocytose, notamment par leur sensibilité différente au calcium (ces Syts pouvant même former des homo- ou des hétéromères). Il reste à démontrer si les mutiples isoformes de Syts fonctionnent indépendemment ou en coopération sur certains types de vésicules. Par exemple, il a été démontré une redondance partielle de la Syt I et la Syt II pour l'exocytose rapide et synchrone de neurotransmetteurs (Geppert et al., 1994; Nagy et al., 2006), tout comme une redondance semble également exister entre la Syt I et la Syt IX, notamment pour la dilatation du pore de fusion chez les cellules PC12 (Zhu et al., 2007). Le modèle proposant que les Syts coopéreraient avec les SNARE (ces dernières constituant la machinerie minimale de fusion membranaire) afin d'accélérer la fusion en se liant aux deux membranes pourrait se révéler minimaliste (Rizo, Chen, et Arac, 2006). En effet, ce modèle a été remis en question ces dernières années notamment grâce à la mise en évidence d'un impact plus important des Syts et d'autres régulateurs de fusion membranaires, ainsi que l'observation de nouvelles fonctions associées aux Syts. Il est donc fort probable qu'il en soit de même au niveau de la membrane du phagosome, et l'identification de nouvelles Syts permettrait d'avoir une meilleure compréhension des phénomènes de fusion phagosomale, notamment en ce qui concerne le choix de fusion entre le type « kiss and run », total, ou intermédiaire. Une meilleure connaissance des Syts impliquées pendant la phagocytose permettrait également de préciser le rôle du calcium au cours de cet évènement.

Certains de nos résultats ont montré le recrutement de la Syt IX à la membrane phagosomale (Figure S3). De plus, tout comme la Syt V, l'expression de la Syt IX est aussi régulée à la hausse suite à une stimulation des macrophages par l'INF-γ et le LPS (Figure S4A et B). Il serait fort intéressant d'étudier un potentiel rôle de la Syt IX lors du relargage de médiateurs pro-inflammatoires puisqu'elle semble associée aux vésicules contenant l'IL1-α (Figure S4C).

2 *La Syt V et l'altération de la phagocytose par Leishmania donovani*

2.1 Régulation des acteurs de la fusion membranaire par des microorganismes pathogènes

Il existe très peu d'études s'intéressant à l'impact des facteurs issus de microorganismes pathogènes sur l'expression ou la régulation des acteurs de la fusion membranaire. Les exemples les plus connus sont certainement la toxine botulique (BoNT) et la toxine tétanique (TeNT) de *Clostridium* qui sont des protéases clivant les protéines SNARE et empêchent ainsi le relargage de neurotransmetteur (Sakaba et al., 2005). Par exemple, BoNT-A, -C et –E clivent SNAP-25, BoNT-C clive également la syntaxine-1A et BoNT-B, -D, -F, -G et TeNT clivent VAMP-2 (Lalli et al., 2003). Bien que les effets des toxines clostridiales aient été d'abord étudiés au niveau neuronal, ils ont été récemment étudiés dans un contexte non neuronal et il a été démontré, par exemple, que BoNT-E clivait SNAP-23 au niveau de cellules issues du rein de souris et bloquait ainsi le processus exocytique régulé par la synaptotagmine VII (Rao et al., 2004).

De récentes études conduites par Andrews et collègues ont révélé que la Syt VII, qui est associée aux lysosomes, contrôle non seulement l'apport membranaire au niveau du phagosome naissant (Czibener et al., 2006) mais qu'elle est aussi impliquée dans les évènements de fusion membranaire du phagolysosome (Czibener et al., 2006; Roy et al., 2004). En effet, la Syt VII protège les cellules contre des microorganismes pathogènes provoquant une perméabilisation de la membrane tels que les bactéries *Salmonella* ou *Yersinia*, par un processus impliquant un phénomène de fusion des phagolysosomes dépendant du Ca^{2+}, analogue au phénomène de réparation membranaire (Roy et al., 2004). Cependant, cette étude représente à ce jour le seul autre exemple de l'implication d'un membre de la famille des Syts durant l'altération de la maturation du phagosome par un microorganisme.

En ce qui concerne *Leishmania donovani*, une récente étude s'intéressant à la phagocytose de promastigotes par les neutrophiles a mis en évidence l'existence de deux modes d'entrée du parasite (Gueirard et al., 2008). Le premier, qui concerne environ 75-80 % des phagosomes contenant les promastigotes, implique les lysosomes et mène à la formation d'un phagosome « spacieux » à l'intérieur duquel le parasite est rapidement dégradé. Ce type de phagosome est également caractérisé par une absence du marqueur du ER, le G-6-P. Le second se caractérise par la formation d'un phagosome resserré dont la membrane est fortement positive pour le G-6-P et pour lequel les *Leishmania* phagocytés survivent même après 48H d'infection. Ce second type de phagosome pourrait donc faire intervenir le ER comme source de membrane lors de sa formation. Bien que le LPG ne semble pas impliqué dans le choix du type d'entrée, il semble néanmoins important pour maintenir le promastigote dans un compartiment non lytique dont la membrane dérive du ER. Cette étude supporte donc le modèle selon lequel les promastigotes de *Leishmania donovani* sont capables d'éviter la biogénèse d'un phagolysosome. Les auteurs proposent que les promastigotes favoriseraient les interactions entre le phagosome et le ER afin de créer une niche permettant sa survie, le neutrophile étant ensuite internalisé par les macrophages. Il serait très intéressant d'étudier si un mécanisme similaire intervient chez les macrophages puisque, bien que controversée, la participation du ER lors de la formation du phagosome a été observée lors de plusieurs travaux (Gagnon et al., 2002; Garin et al., 2001; Guermonprez et al., 2003).

2.2 La Syt V est ciblée par le LPG de *L. donovani*

Comme nous l'avons vu, l'acquisition de diverses hydrolases et l'acidification du phagosome génèrent un environnement fortement microbicide (Haas, 2007) et permet ainsi la création d'un compartiment compétent pour l'apprêtement puis la présentation antigénique (Ramachandra, Song, et Harding, 1999). Afin d'éviter d'être éliminés suite à leur internalisation par les macrophages, de nombreux microorganismes intracellulaires interfèrent avec la maturation du phagosome et son acidification (Gruenberg et van der Goot, 2006; Haas, 2007; Huynh et Grinstein, 2007). La forme promastigote du parasite *Leishmania donovani* crée une niche intracellulaire à l'intérieur du macrophage en inhibant la biogénèse du phagolysosome (Desjardins et Descoteaux, 1997). Cette inhibition est provoquée par le glycolipide LPG à la surface du parasite (Desjardins et Descoteaux, 1997; Holm et al., 2001; Scianimanico et al., 1999) et se caractérise par une exclusion des composants cytosoliques de la NADPH oxydase de la membrane phagosomale (Lodge, Diallo, et Descoteaux, 2006). Ainsi, la désorganisation du phagosome par le LPG permet aux promastigotes de *L. donovani* d'établir une infection dans un environnement dépourvu d'oxydants (Lodge, Diallo, et Descoteaux, 2006), ce qui pourrait être propice à leur différenciation en amastigotes.

Un des évènements les plus précoces observés durant la phagocytose du promastigote de *L. donovani* est le transfert de son LPG à la surface de la membrane de la cellule hôte (Tolson, Turco, et Pearson, 1990), causant une modification de leurs propriétés biophysiques (Miao et al., 1995; Rasmusson et al., 1998). Au niveau du phagosome naissant, le LPG s'insère à l'intérieur de la membrane, désorganise les microdomaines lipidiques existants et altère la formation de ces structures suite à l'internalisation du promastigote ((Dermine et al., 2005); Article II). Bien que les mécanismes précis ne soient pas entièrement compris, le modèle en vigueur propose que le LPG s'insère à l'intérieur des microdomaines lipidiques via leur ancre GPI, permettant ainsi aux charges négatives du polymère Galβ1,4Man-PO_4 du LPG d'interférer directement avec l'organisation des molécules appartenant aux microdomaines lipidiques. Ce modèle est cohérent avec la démonstration de l'altération des propriétés membranaires en fonction de la longueur du polymère Galβ1,4Man-PO_4 (Desjardins et Descoteaux,

1997; Miao et al., 1995). De par leur rôle organisationnel très spécifique pour certaines protéines, les microdomaines lipidiques sont essentiels à de nombreux processus incluant l'exocytose (Lang, 2007; Salaun, James, et Chamberlain, 2004). Notre étude montre qu'une fraction de la Syt V est associée aux microdomaines enrichis en GM1 sur la membrane du phagosome. De plus, une forte réduction du cholestérol inhibe cette association et démontre l'importance de microdomaines lipidiques intacts pour le recrutement de Syt V au phagosome (Article III). Ainsi, nous avons pu observer que la Syt V était exclue des sites d'insertion du LPG au niveau des microdomaines lipidiques. Par cette étude, nous proposons un nouveau mécanisme de pathogénèse de *L. donovani* en démontrant que l'insertion du LPG au niveau des microdomaines lipidiques du phagosome empêche le recrutement de la Syt V, causant l'exclusion de la sous-unité c de la V-ATPase du phagosome.

2.3 Importance de l'acidification du phagosome sur la survie de *L. donovani*

Un rôle potentiel du pH acide comme activité anti-*Leishmania* avait été évoqué par Desjardins et collègues basé sur l'observation que les promastigotes résident de manière transitoire dans des phagosomes non fusogéniques (Dermine et al., 2000; Desjardins et Descoteaux, 1997; Scianimanico et al., 1999), cet effet étant dû au relargage de LPG par le parasite. Ainsi, les promastigotes de *Leishmania* pourraient avoir développé une stratégie de survie intracellulaire consistant à éviter le contact avec le contenu lysosomal, stratégie partagée par d'autres microorganismes pathogènes (via d'autres facteurs de virulence) tels que *Toxoplasma* (Mordue et Sibley, 1997), *Legionella* (Horwitz, 1983), et *Mycobacterium* (Malo et al., 1994; Sturgill-Koszycki et al., 1994). Cependant cette hypothèse n'est pas partagée par tous les auteurs. En effet, une étude portant sur le défaut d'acidification de macrophages issus de souris Stat1$^{-/-}$ a amené Berverley et collègues à étudier le rôle du pH phagosomal sur la survie et la croissance de *L. major* (Spath et al., 2009). Leurs résultats semblent tout d'abord confirmer l'hypothèse du rôle de l'acidification phagosomale comme activité leishmanicide par l'observation

d'une augmentation de la survie intracellulaire de *L. major* dans les cellules hôtes déficientes en Stat1. Cependant, la charge intracellulaire de parasites était similaire durant les premières 48H de l'infection, alors qu'une différence dans le pH phagosomal était notable durant cette même période. La survie des parasites WT et *lpg-* avait augmenté de la même façon dans les macrophages entre 2 et 5 jours suivant l'infection, suggérant que l'activité leishmanicide dépendante du pH chez les cellules $Stat^{-/-}$ agissait indépendamment du LPG. Les mécanismes responsables du défaut d'acidification chez les cellules déficientes en Stat-1 restent toutefois totalement inconnus, tout comme le rôle de la V-ATPase lors de ce phénomène.

D'autres études démontrèrent que les promastigotes de *Leishmania* peuvent survivre et croître *in vitro* dans un milieu acide (Zakai, Chance, et Bates, 1998), leur glycocalix conférant une résistance aux hydrolases lysosomales de l'insecte vecteur et de l'hôte vertébré (Sacks et al., 2000; Spath et al., 2003b). La survie intracellulaire des mutants déficients en LPG fut restaurée au niveau du wild-type dans les cellules hôtes $phox^{-/-}$ déficientes en oxydase, bien que les phénomènes de fusion entre le phagosome contenant le parasite et les lysosomes de la cellule hôte semblent normaux (Spath et al., 2003a). Ainsi l'importance de l'inhibition des fusions membranaires entre phagosome et endosome, celle de l'acidification et le rôle du LPG sur la survie du parasite ne sont pas clairement établis et semblent parfois contradictoires.

Nos résultats nous ont permis de mettre en évidence les liens qui existent entre la présence du LPG à la surface du parasite et l'acidification du phagosome en révélant un impact négatif du LPG sur l'acquisition de la V-ATPase et sur l'acidification du phagosome. De plus, ils semblent confirmer une réduction de l'activité fusogénique du phagosome contenant la forme promastigote de *L. donovani* dû au LPG puisque l'on peut observer une réduction du recrutement du régulateur positif de fusion Syt V, ainsi que de la pompe à proton V-ATPase. Enfin, certains résultats préliminaires sur la survie des promastigotes de *L. donovani* dans le cas d'une absence de l'expression de Syt V semblent montrer l'importance de ce régulateur de fusion pour le contrôle de l'infection et suggèrent que le pH phagosomal pourrait avoir un impact sur la survie du parasite.

2.4 Acidification et différenciation de la forme promastigote en amastigote

Le fait que le promastigote de *L. donovani* établisse l'infection dans un compartiment pour lequel la V-ATPase est exclue pourrait donc favoriser la survie du parasite. Nos résultats démontrant que les phagosomes contenant les promastigotes de *L. donovani* ne s'acidifient pas, même après 24H d'infection (Article III), apportent un nouvel élément à notre compréhension de la biologie des *Leishmania*. En effet, malgré l'absence de données sur le pH des phagosomes contenant la forme promastigote, les auteurs supposent que les promastigotes initient l'infection dans un environnement acide et que la différenciation de la forme promastigote en amastigote est principalement déclenchée par une rapide exposition à un environnement acide et une température de 37°C (Zilberstein et Shapira, 1994). Cependant, nos données indiquent que des facteurs de l'hôte, autres que le pH acide, pourraient initier le processus de différenciation. Une question qui reste sans réponse concerne l'acquisition des propriétés spécifiques au phagolysosome ainsi que l'acidification des vacuoles contenant le parasite immédiatement après la différenciation du promastigote en amastigote. En effet, les travaux d'Antoine et collègues (Antoine et al., 1990) ont établi que les amastigotes de *L. amazoniensis* demeurent à l'intérieur d'une vacuole acide (pH 4.7-5.2), confirmant ainsi que les amastigotes de *Leishmania* sont internalisés à l'intérieur de vacuoles qui acquièrent rapidement les propriétés lysosomales et dans lesquelles ils prolifèrent (Berman, Dwyer, et Wyler, 1979; Chang et Dwyer, 1976). En accord avec cette observation, nous avons montré la présence de LAMP-1 et de la sous-unité *c* de la V-ATPase au phagosome contenant l'amastigote de *L. donovani* à 2H d'infection (Article III). Une explication possible serait que durant les premiers jours d'infection, la présence du LPG dans la membrane des phagosomes prévient l'acidification et la maturation du phagosome, permettant ainsi la différenciation de la forme promastigote en une forme amastigote. La très faible expression du LPG, en dessous des niveaux détectables, chez l'amastigote (McConville et Blackwell, 1991) pourrait permettre alors au phagosome d'acquérir les propriétés lysosomales et de s'acidifier.

2.5 Impact du LPG sur l'exocytose focale et l'internalisation du parasite

Nos résultats suggèrent que l'exclusion de la Syt V de la membrane du phagosome par le LPG est un phénomène très précoce puisque visible dès la formation du phagosome (article IV). Cette exclusion pourrait alors s'expliquer par une inhibition des fusions membranaires, régulées par la Syt V associée aux endosomes de recyclage, avec la membrane plasmique de la coupe phagocytique, ayant pour conséquence un apport réduit de membrane intra-vésiculaire. Ce phénomène expliquerait ainsi la réduction du nombre de parasites WT internalisés comparés aux parasites déficients pour le LPG (Holm et al., 2003; McNeely et Turco, 1990). Une explication concernant la diminution de la phagocytose de parasites WT avait été proposée auparavant. En effet, les promastigotes déficients en LPG lieraient une plus grande quantité de C3 dû au fait que le C3 aurait plus facilement accès au GP63 qui est connu pour être un bon accepteur primaire du complément (Brittingham et al., 1995; Russell, 1987). Ainsi, étant donné que les *L. donovani* opsonisés stimulent principalement les CR3 de la surface du macrophage lors de leur entrée (Lodge et Descoteaux, 2006), les promastigotes déficients en LPG seraient alors plus facilement internalisés que les promastigotes WT. Cependant, le fait d'avoir observé une réduction de l'internalisation de Zym recouvert de LPG comparé au Zym seul en absence d'opsonine suggère l'existence d'un autre phénomène qui pourrait être plus spécifique au LPG. C'est pourquoi nous avons démontré que la réduction de l'activité phagocytique des macrophages par le LPG était, du moins en partie, un processus dépendant de l'expression de la Syt V. Le modèle que nous proposons est le suivant: suite au contact du promastigote avec la membrane du macrophage, la formation de la coupe phagocytique s'amorce et le LPG s'insérerait au niveau de cette zone de contact. Cette insertion modifierait alors les propriétés biophysiques de la membrane et affecterait par conséquent les interactions des endosomes régulés par la Syt V avec la membrane de la coupe phagocytique. Ainsi l'apport membranaire nécessaire pour l'internalisation du parasite serait réduit, limitant le nombre de parasites pouvant être phagocytés.

Évidemment nos expériences portant sur l'exclusion de la Syt V durant la maturation du phagosome suggèrent fortement qu'un mécanisme similaire, dépendant des microdomaines lipidiques, s'effectue dès la formation du phagosome. L'implication des microdomaines lipidiques lors de l'entrée de microorganismes pathogènes a été décrite à de nombreuses reprises (Alfsen et al., 2001; Gatfield et Pieters, 2000; Grassme et al., 2003; Kannan et al., 2006; Peyron et al., 2000; Schneider et al., 2007). Par exemple, l'association du récepteur CR3 avec un GPI de *Mycobacterium Kansasii* est cruciale pour son internalisation (Peyron et al., 2000). Il est donc tout à fait possible qu'une partie du LPG du promastigote s'insère spécifiquement au niveau de microdomaines lipidiques et interfère avec l'organisation des molécules nécessaires aux interactions endosome / coupe phagocytique dépendantes de la Syt V, excluant cette dernière de la membrane du phagosome naissant.

Le LPG est essentiel pour l'établissement de l'infection de *L. donovani* et notamment pour la différenciation de la forme promastigote en forme amastigote en retardant la maturation du phagosome. Le LPG permet ainsi de grandement améliorer la survie du parasite (Lodge et Descoteaux, 2006). Le fait que nos résultats montrent que le LPG réduit le taux de phagocytose du parasite pourrait paraître surprenant puisque les microorganismes intracellulaires devraient au contraire favoriser leur internalisation afin d'établir leur niche de réplication dans la cellule hôte. Néanmoins, d'un point de vue évolutionniste, bien qu'il y ait un coût associé à un nombre inférieur de parasites internalisés lors d'une infection, cette perte pourrait être largement compensée par une forte amélioration du taux de survie et aboutirait à une meilleure valeur sélective du parasite.

CONCLUSION

Au cours de ces travaux, la caractérisation des rôles de la Syt V pendant la phagocytose nous a apporté une meilleure compréhension des mécanismes de fusion membranaire responsables de l'exocytose focale lors de la formation du phagosome, et de l'acquisition de la Cathepsin D et de la pompe à proton V-ATPase durant la maturation phagosomale. De plus, cette étude a permis d'identifier un nouveau mécanisme impliqué dans la pathogénèse de *Leishmania donovani*. En effet, le ciblage de la Syt V fait partie de la stratégie utilisée par les promastigotes de *L. donovani* pour créer une niche propice à l'établissement de l'infection à l'intérieur des cellules hôtes, en réduisant notamment l'acidification du phagosome. Il est intéressant de noter que la phagocytose de particules zymosan ou de promastigotes *lpg2*-KO recouverts du glycolipide lipoarabinomannan de *Mycobacterium tuberculosis*, diminue également l'acquisition de Syt V au phagosome. L'utilisation de mécanismes similaires à celui de *L. donovani* par d'autres microorganismes intracellulaires afin de remodeler leur niche intracellulaire reste à explorer.

Outre le rôle clé de la Syt V, cette thèse présente également quelques résultats concernant la présence d'autres membres des synaptotagmines au niveau des phagosomes et pourrait ouvrir la voie à de nombreuses autres études. En effet, les synaptotagmines peuvent former des homo-/hétéro-dimères et l'étude de leur fonction et de leurs interactions avec les SNARE reste un domaine quasi vierge chez les phagocytes. Ces régulateurs de fusion membranaire peuvent être ciblés spécifiquement par des facteurs de virulence de microorganismes pathogènes et devraient être pris en considération lors de la mise au point de stratégies visant à contrôler l'établissement de l'infection chez des patients.

Enfin, il est important de noter que ces travaux démontrent pour la première fois un défaut de l'acidification des phagosomes contenant la forme promastigote des *Leishmania donovani*. Il serait peut-être nécessaire de compléter le concept selon lequel seuls la température et le pH seraient importants pour la différenciation en une forme amastigote. D'autre facteurs spécifiques aux conditions retrouvées à l'intérieur du phagosome pourraient participer à l'initiation de cette transformation et pourraient alors ne pas être négligeables lors de la culture axénique de ces parasites afin de mieux mimer les conditions favorables à leur virulence.

Remerciements

Nombreuses furent les personnes et personnages croisés au cours de ces 5 dernières années, qui participèrent de manière directe ou plus indirecte à l'harmonie nécessaire à l'achèvement de ce projet doctoral. Tout d'abord, je remercie mon directeur de recherche Albert Descoteaux pour la confiance et l'accueil qu'il m'a accordé lors de mon arrivée sur le sol québécois. Durant le développement de mon projet de thèse, la pertinence des conseils d'Albert et sa rigueur ont été une aide précieuse et m'ont permis de beaucoup apprendre. J'ai particulièrement apprécié ses encouragements et la liberté qu'il m'a laissée pour mener ce projet et tester, parfois de manière fructueuse et d'autres non, de nouvelles avenues possibles.

Merci à la fondation Armand Frappier pour le financement qu'elle m'a accordé la première année et au CHPI pour les bourses de voyage afin de participer aux congrès.

Je n'oublie pas Marcel et son excellente expertise en microscopie qui a été une aide considérable.

Bien évidemment, l'environnement de travail est très important. Les membres passés et présents ont grandement participé à la bonne conduite de mes travaux. La dynamique change mais c'est toujours aussi agréable de pouvoir compter sur le support et l'amitié de ces compagnon(e)s, que je n'appellerai pas d'infortune. Christelle, complice depuis le quasi-commencement, lorsque la testostérone dominait encore le lab et jusqu'à l'avènement du « girl power ». Je n'oublie pas Tamsir et ses questionnements métaphysiques sur la condition féminine, PO et l'impertinence du degré ultime, Jean-Frou et son martelage musical(!?!), Franky et ses messages masqués, Roro et sa couleur écarlate, John qui m'initia aux techniques du lab et pas seulement, Christine et son fier caractère québécois que j'ai vraiment appris à apprécier. Et bien sûr merci aussi pour vos discussions constructives…

Au cours de ces années, plusieurs étudiants et stagiaires passèrent plus rapidement par le lab, mais faire leur connaissance fut aussi un grand plaisir. Christine T., qui repoussa les limites du concept de diminution exponentiel du potentiel cognitif avec l'augmentation du nombre de cerveaux (expériences menées avec Stéphanie...). Mireille PM et Geneviève... Vous avez apporté beaucoup de vie et de spontanéïté. Aurélie à qui je souhaite une belle réussite pour l'avenir. Louise et sa gentilesse. Et puis les « petits nouveaux » du lab: Julia (heu, pas si nouvelle en fait...), Neda (Chocolate junkie), Lydie et Guillermo, bonne chance pour la suite.

Aussi je n'oublie pas ces personnes des autres lab, qui ont bien souvent permis de passer des lunch bien animés: Syl, Mériam, Houda, Ronan, Caro, Héctor, Benoît, Olivier, Phillipe... et j'en oublie sûrement.

S'il y a une personne qui mérite que je la remercie humblement, c'est bien ma douce et tendre qui m'a offert un soutien inconditionnel ainsi qu'une aide directe notamment dans la relecture orthographique et grammaticale (tout en récoltant une bonne migraine).

Enfin un merci aux membres de ma famille qui, même si l'océan nous séparait, m'ont toujours soutenu dans mes projets.

BIBLIOGRAPHIE

Aderem, A., and Underhill, D. M. (1999). Mechanisms of phagocytosis in macrophages. *Annu Rev Immunol* **17,** 593-623.

Alexander, J., and Vickerman, K. (1975). Fusion of host cell secondary lysosomes with the parasitophorous vacuoles of *Leishmania mexicana*-infected macrophages. *J Protozool* **22**(4), 502-8.

Alfsen, A., Iniguez, P., Bouguyon, E., and Bomsel, M. (2001). Secretory IgA specific for a conserved epitope on gp41 envelope glycoprotein inhibits epithelial transcytosis of HIV-1. *J Immunol* **166**(10), 6257-65.

Allen, L.-A. H., Yang, C., and Pessin, J. E. (2002). Rate and extent of phagocytosis in macrophages lacking vamp3. *J Leukoc Biol* **72**(1), 217-221.

Allen, L. A., and Aderem, A. (1995a). Protein kinase C regulates MARCKS cycling between the plasma membrane and lysosomes in fibroblasts. *Embo J* **14**(6), 1109-21.

Allen, L. A., and Allgood, J. A. (2002). Atypical protein kinase C-ζ is essential for delayed phagocytosis of *Helicobacter pylori*. *Curr Biol* **12**(20), 1762-6.

Allen, L. H., and Aderem, A. (1995b). A role for MARCKS, the α isozyme of protein kinase C and myosin I in zymosan phagocytosis by macrophages. *J Exp Med* **182**(3), 829-40.

Aniento, F., Gu, F., Parton, R. G., and Gruenberg, J. (1996). An endosomal β COP is involved in the pH-dependent formation of transport vesicles destined for late endosomes. *J Cell Biol* **133**(1), 29-41.

Antoine, J. C., Prina, E., Jouanne, C., and Bongrand, P. (1990). Parasitophorous vacuoles of *Leishmania amazonensis*-infected macrophages maintain an acidic pH. *Infect Immun* **58**(3), 779-87.

Antoine, J. C., Prina, E., Lang, T., and Courret, N. (1998). The biogenesis and properties of the parasitophorous vacuoles that harbour *Leishmania* in murine macrophages. *Trends Microbiol* **6**(10), 392-401.

Antonin, W., Holroyd, C., Fasshauer, D., Pabst, S., Von Mollard, G. F., and Jahn, R. (2000). A SNARE complex mediating fusion of late endosomes defines conserved properties of SNARE structure and function. *Embo J* **19**(23), 6453-64.

Areschoug, T., and Gordon, S. (2008). Pattern recognition receptors and their role in innate immunity: focus on microbial protein ligands. *Contrib Microbiol* **15**, 45-60.

Arredouani, M., Yang, Z., Ning, Y., Qin, G., Soininen, R., Tryggvason, K., and Kobzik, L. (2004). The scavenger receptor MARCO is required for lung defense against pneumococcal pneumonia and inhaled particles. *J Exp Med* **200**(2), 267-72.

Ashery, U., Varoqueaux, F., Voets, T., Betz, A., Thakur, P., Koch, H., Neher, E., Brose, N., and Rettig, J. (2000). Munc13-1 acts as a priming factor for large dense-core vesicles in bovine chromaffin cells. *Embo J* **19**(14), 3586-96.

Atiya-Nasagi, Y., Cohen, H., Medalia, O., Fukudan, M., and Sagi-Eisenberg, R. (2005). O-glycosylation is essential for intracellular targeting of synaptotagmins I and II in non-neuronal specialized secretory cells. *J Cell Sci* **118**(Pt 7), 1363-72.

Axline, S. G., and Reaven, E. P. (1974). Inhibition of phagocytosis and plasma membrane mobility of the cultivated macrophage by cytochalasin B. Role of subplasmalemmal microfilaments. *J Cell Biol* **62**(3), 647-59.

Babior, B. M. (2004). NADPH oxidase. *Curr Opin Immunol* **16**(1), 42-7.

Bai, J., Tucker, W. C., and Chapman, E. R. (2004). PIP_2 increases the speed of response of synaptotagmin and steers its membrane-penetration activity toward the plasma membrane. *Nat Struct Mol Biol* **11**(1), 36-44.

Bajno, L., Peng, X. R., Schreiber, A. D., Moore, H. P., Trimble, W. S., and Grinstein, S. (2000). Focal exocytosis of VAMP3-containing vesicles at sites of phagosome formation. *J Cell Biol* **149**(3), 697-706.

Becker, T., Volchuk, A., and Rothman, J. E. (2005). Differential use of endoplasmic reticulum membrane for phagocytosis in J774 macrophages. *Proc Natl Acad Sci U S A* **102**(11), 4022-6.

Berman, J. D., Dwyer, D. M., and Wyler, D. J. (1979). Multiplication of *Leishmania* in human macrophages in vitro. *Infect Immun* **26**(1), 375-9.

Bertholet, S., Dickensheets, H. L., Sheikh, F., Gam, A. A., Donnelly, R. P., and Kenney, R. T. (2003). *Leishmania donovani*-induced expression of suppressor of cytokine signaling 3 in human macrophages: a novel mechanism for intracellular parasite suppression of activation. *Infect Immun* **71**(4), 2095-101.

Bevec, T., Stoka, V., Pungercic, G., Dolenc, I., and Turk, V. (1996). Major histocompatibility complex class II-associated p41 invariant chain fragment is a strong inhibitor of lysosomal cathepsin L. *J Exp Med* **183**(4), 1331-8.

Beyenbach, K. W., and Wieczorek, H. (2006). The V-type H^+ ATPase: molecular structure and function, physiological roles and regulation. *J Exp Biol* **209**(Pt 4), 577-89.

Bianchi, M. E. (2007). DAMPs, PAMPs and alarmins: all we need to know about danger. *J Leukoc Biol* **81**(1), 1-5.

Blackwell, J. M. (1985). Receptors and recognition mechanisms of *Leishmania* species. *Trans R Soc Trop Med Hyg* **79**(5), 606-12.

Blanchette, J., Racette, N., Faure, R., Siminovitch, K. A., and Olivier, M. (1999). *Leishmania*-induced increases in activation of macrophage SHP-1 tyrosine phosphatase

are associated with impaired IFN-γ-triggered JAK2 activation. *Eur J Immunol* **29**(11), 3737-44.

Blander, J. M. (2007). Signalling and phagocytosis in the orchestration of host defence. *Cell Microbiol* **9**(2), 290-9.

Blander, J. M., and Medzhitov, R. (2004). Regulation of phagosome maturation by signals from toll-like receptors. *Science* **304**(5673), 1014-8.

Blander, J. M., and Medzhitov, R. (2006a). On regulation of phagosome maturation and antigen presentation. *Nat Immunol* **7**(10), 1029-35.

Blander, J. M., and Medzhitov, R. (2006b). Toll-dependent selection of microbial antigens for presentation by dendritic cells. *Nature* **440**(7085), 808-12.

Bokoch, G. M., and Diebold, B. A. (2002). Current molecular models for NADPH oxidase regulation by Rac GTPase. *Blood* **100**(8), 2692-6.

Booth, J. W., Trimble, W. S., and Grinstein, S. (2001). Membrane dynamics in phagocytosis. *Semin Immunol* **13**(6), 357-64.

Borregaard, N., Kjeldsen, L., Lollike, K., and Sengelov, H. (1993). Granules and vesicles of human neutrophils. The role of endomembranes as source of plasma membrane proteins. *Eur J Haematol* **51**(5), 318-22.

Botelho, R. J., Hackam, D. J., Schreiber, A. D., and Grinstein, S. (2000). Role of COPI in phagosome maturation. *J Biol Chem* **275**(21), 15717-27.

Braun, V., Fraisier, V., Raposo, G., Hurbain, I., Sibarita, J. B., Chavrier, P., Galli, T., and Niedergang, F. (2004). TI-VAMP/VAMP7 is required for optimal phagocytosis of opsonised particles in macrophages. *Embo J* **23**(21), 4166-76.

Braun, V., and Niedergang, F. (2006). Linking exocytosis and endocytosis during phagocytosis. *Biol Cell* **98**(3), 195-201.

Breton, A., and Descoteaux, A. (2000). Protein kinase C-α participates in FcγR-mediated phagocytosis in macrophages. *Biochem Biophys Res Commun* **276**(2), 472-6.

Brittingham, A., Morrison, C. J., McMaster, W. R., McGwire, B. S., Chang, K. P., and Mosser, D. M. (1995). Role of the *Leishmania* surface protease gp63 in complement fixation, cell adhesion, and resistance to complement-mediated lysis. *J Immunol* **155**(6), 3102-11.

Brittingham, A., and Mosser, D. M. (1996). Exploitation of the complement system by *Leishmania* promastigotes. *Parasitol Today* **12**(11), 444-7.

Brown, G. E., Stewart, M. Q., Liu, H., Ha, V. L., and Yaffe, M. B. (2003). A novel assay system implicates PtdIns(3,4)P(2), PtdIns(3)P, and PKC-δ in intracellular production of reactive oxygen species by the NADPH oxidase. *Mol Cell* **11**(1), 35-47.

Brumell, J. H., Howard, J. C., Craig, K., Grinstein, S., Schreiber, A. D., and Tyers, M. (1999). Expression of the protein kinase C substrate pleckstrin in macrophages: association with phagosomal membranes. *J Immunol* **163**(6), 3388-95.

Bryant, P. W., Lennon-Dumenil, A. M., Fiebiger, E., Lagaudriere-Gesbert, C., and Ploegh, H. L. (2002). Proteolysis and antigen presentation by MHC class II molecules. *Adv Immunol* **80**, 71-114.

Bucci, C., Parton, R. G., Mather, I. H., Stunnenberg, H., Simons, K., Hoflack, B., and Zerial, M. (1992). The small GTPase rab5 functions as a regulatory factor in the early endocytic pathway. *Cell* **70**(5), 715-28.

Bucci, C., Thomsen, P., Nicoziani, P., McCarthy, J., and van Deurs, B. (2000). Rab7: a key to lysosome biogenesis. *Mol Biol Cell* **11**(2), 467-80.

Callaghan, J., Nixon, S., Bucci, C., Toh, B. H., and Stenmark, H. (1999). Direct interaction of EEA1 with Rab5b. *Eur J Biochem* **265**(1), 361-6.

Caron, E., and Hall, A. (1998). Identification of two distinct mechanisms of phagocytosis controlled by different Rho GTPases. *Science* **282**(5394), 1717-1721.

Carrera, L., Gazzinelli, R. T., Badolato, R., Hieny, S., Muller, W., Kuhn, R., and Sacks, D. L. (1996). *Leishmania* promastigotes selectively inhibit interleukin 12 induction in bone marrow-derived macrophages from susceptible and resistant mice. *J Exp Med* **183**(2), 515-26.

Cellier, M. F., Courville, P., and Campion, C. (2007). Nramp1 phagocyte intracellular metal withdrawal defense. *Microbes Infect* **9**(14-15), 1662-70.

Chang, K. P., and Dwyer, D. M. (1976). Multiplication of a human parasite (*Leishmania donovani*) in phagolysosomes of hamster macrophages in vitro. *Science* **193**(4254), 678-80.

Chapman, E. R. (2002). Synaptotagmin: a $Ca^{(2+)}$ sensor that triggers exocytosis? *Nat Rev Mol Cell Biol* **3**(7), 498-508.

Chatelain, R., Varkila, K., and Coffman, R. L. (1992). IL-4 induces a Th2 response in *Leishmania major*-infected mice. *J Immunol* **148**(4), 1182-7.

Chia, J. K., and McManus, E. J. (1990). In vitro tumor necrosis factor induction assay for analysis of febrile toxicity associated with amphotericin B preparations. *Antimicrob Agents Chemother* **34**(5), 906-8.

Chimini, G., and Chavrier, P. (2000). Function of Rho family proteins in actin dynamics during phagocytosis and engulfment. *Nat Cell Biol* **2**(10), E191-6.

Christoforidis, S., McBride, H. M., Burgoyne, R. D., and Zerial, M. (1999). The Rab5 effector EEA1 is a core component of endosome docking. *Nature* **397**(6720), 621-5.

Claus, V., Jahraus, A., Tjelle, T., Berg, T., Kirschke, H., Faulstich, H., and Griffiths, G. (1998). Lysosomal enzyme trafficking between phagosomes, endosomes, and lysosomes in J774 macrophages. Enrichment of cathepsin H in early endosomes. *J Biol Chem* **273**(16), 9842-51.

Cohen, J. (1992). AIDS vaccines. Trials set in high-risk populations. *Science* **258**(5089), 1729.

Collins, R. F., Schreiber, A. D., Grinstein, S., and Trimble, W. S. (2002). Syntaxins 13 and 7 function at distinct steps during phagocytosis. *J Immunol* **169**(6), 3250-6.

Courret, N., Frehel, C., Gouhier, N., Pouchelet, M., Prina, E., Roux, P., and Antoine, J. C. (2002). Biogenesis of *Leishmania*-harbouring parasitophorous vacuoles following phagocytosis of the metacyclic promastigote or amastigote stages of the parasites. *J Cell Sci* **115**(Pt 11), 2303-16.

Cox, D., Lee, D. J., Dale, B. M., Calafat, J., and Greenberg, S. (2000). A Rab11-containing rapidly recycling compartment in macrophages that promotes phagocytosis. *Proc Natl Acad Sci U S A* **97**(2), 680-5.

Craxton, M. (2001). Genomic analysis of synaptotagmin genes. *Genomics* **77**(1-2), 43-9.

Craxton, M. (2004). Synaptotagmin gene content of the sequenced genomes. *BMC Genomics* **5**(1), 43.

Craxton, M., and Goedert, M. (1995). Synaptotagmin V: a novel synaptotagmin isoform expressed in rat brain. *FEBS Lett* **361**(2-3), 196-200.

Craxton, M., Olsen, A., and Goedert, M. (1997). Human synaptotagmin V (SYT5): sequence, genomic structure, and chromosomal location. *Genomics* **42**(1), 165-9.

Croft, S. L., Seifert, K., and Yardley, V. (2006). Current scenario of drug development for leishmaniasis. *Indian J Med Res* **123**(3), 399-410.

Croft, S. L., and Yardley, V. (2002). Chemotherapy of leishmaniasis. *Curr Pharm Des* **8**(4), 319-42.

Crowley, M. T., Costello, P. S., Fitzer-Attas, C. J., Turner, M., Meng, F., Lowell, C., Tybulewicz, V. L., and DeFranco, A. L. (1997). A critical role for Syk in signal transduction and phagocytosis mediated by Fcγ receptors on macrophages. *J Exp Med* **186**(7), 1027-39.

Czibener, C., Sherer, N. M., Becker, S. M., Pypaert, M., Hui, E., Chapman, E. R., Mothes, W., and Andrews, N. W. (2006). Ca^{2+} and synaptotagmin VII-dependent delivery of lysosomal membrane to nascent phagosomes. *J Cell Biol* **174**(7), 997-1007.

Davis, A. F., Bai, J., Fasshauer, D., Wolowick, M. J., Lewis, J. L., and Chapman, E. R. (1999). Kinetics of synaptotagmin responses to Ca^{2+} and assembly with the core SNARE complex onto membranes. *Neuron* **24**(2), 363-76.

De Veer, M. J., Curtis, J. M., Baldwin, T. M., DiDonato, J. A., Sexton, A., McConville, M. J., Handman, E., and Schofield, L. (2003). MyD88 is essential for clearance of *Leishmania major*: possible role for lipophosphoglycan and Toll-like receptor 2 signaling. *Eur J Immunol* **33**(10), 2822-31.

Deretic, V., Singh, S., Master, S., Harris, J., Roberts, E., Kyei, G., Davis, A., de Haro, S., Naylor, J., Lee, H. H., and Vergne, I. (2006). *Mycobacterium tuberculosis* inhibition of phagolysosome biogenesis and autophagy as a host defence mechanism. *Cell Microbiol* **8**(5), 719-27.

Dermine, J. F., Duclos, S., Garin, J., St-Louis, F., Rea, S., Parton, R. G., and Desjardins, M. (2001). Flotillin-1-enriched lipid raft domains accumulate on maturing phagosomes. *J Biol Chem* **276**(21), 18507-12.

Dermine, J. F., Goyette, G., Houde, M., Turco, S. J., and Desjardins, M. (2005). *Leishmania donovani* lipophosphoglycan disrupts phagosome microdomains in J774 macrophages. *Cell Microbiol* **7**(9), 1263-70.

Dermine, J. F., Scianimanico, S., Prive, C., Descoteaux, A., and Desjardins, M. (2000). *Leishmania* promastigotes require lipophosphoglycan to actively modulate the fusion properties of phagosomes at an early step of phagocytosis. *Cell Microbiol* **2**(2), 115-26.

Descoteaux, A., Luo, Y., Turco, S. J., and Beverley, S. M. (1995). A specialized pathway affecting virulence glycoconjugates of *Leishmania*. *Science* **269**(5232), 1869-72.

Descoteaux, A., and Matlashewski, G. (1989). c-fos and tumor necrosis factor gene expression in *Leishmania donovani*-infected macrophages. *Mol Cell Biol* **9**(11), 5223-7.

Descoteaux, A., Matlashewski, G., and Turco, S. J. (1992). Inhibition of macrophage protein kinase C-mediated protein phosphorylation by *Leishmania donovani* lipophosphoglycan. *J Immunol* **149**(9), 3008-15.

Desjardins, M. (2003). ER-mediated phagocytosis: a new membrane for new functions. *Nat Rev Immunol* **3**(4), 280-91.

Desjardins, M., and Descoteaux, A. (1997). Inhibition of phagolysosomal biogenesis by the *Leishmania* lipophosphoglycan. *J Exp Med* **185**(12), 2061-8.

Desjardins, M., Houde, M., and Gagnon, E. (2005). Phagocytosis: the convoluted way from nutrition to adaptive immunity. *Immunol Rev* **207**, 158-65.

Desjardins, M., Huber, L. A., Parton, R. G., and Griffiths, G. (1994). Biogenesis of phagolysosomes proceeds through a sequential series of interactions with the endocytic apparatus. *J Cell Biol* **124**(5), 677-88.

Desjardins, M., Nzala, N. N., Corsini, R., and Rondeau, C. (1997). Maturation of phagosomes is accompanied by changes in their fusion properties and size-selective acquisition of solute materials from endosomes. *J Cell Sci* **110 (Pt 18)**, 2303-14.

Desjeux, P. (2004). Leishmaniasis: current situation and new perspectives. *Comp Immunol Microbiol Infect Dis* **27**(5), 305-18.

Diefenbach, A., Schindler, H., Donhauser, N., Lorenz, E., Laskay, T., MacMicking, J., Rollinghoff, M., Gresser, I., and Bogdan, C. (1998). Type 1 interferon (IFNα/β) and type 2 nitric oxide synthase regulate the innate immune response to a protozoan parasite. *Immunity* **8**(1), 77-87.

Doyle, S. L., and O'Neill, L. A. (2006). Toll-like receptors: from the discovery of NFκB to new insights into transcriptional regulations in innate immunity. *Biochem Pharmacol* **72**(9), 1102-13.

Dubuisson, J., Helle, F., and Cocquerel, L. (2008). Early steps of the hepatitis C virus life cycle. *Cell Microbiol* **10**(4), 821-7.

Emil, R. U. (2002). Perspective on antigen processing and presentation. *Immunological Reviews* **185**(1), 86-102.

Etienne-Manneville, S., and Hall, A. (2002). Rho GTPases in cell biology. *Nature* **420**(6916), 629-35.

Eze, M. O., Yuan, L., Crawford, R. M., Paranavitana, C. M., Hadfield, T. L., Bhattacharjee, A. K., Warren, R. L., and Hoover, D. L. (2000). Effects of opsonization

and γ interferon on growth of *Brucella melitensis* 16M in mouse peritoneal macrophages in vitro. *Infect Immun* **68**(1), 257-63.

Fadok, V. A., Bratton, D. L., Rose, D. M., Pearson, A., Ezekewitz, R. A., and Henson, P. M. (2000). A receptor for phosphatidylserine-specific clearance of apoptotic cells. *Nature* **405**(6782), 85-90.

Fang, F. C. (2004). Antimicrobial reactive oxygen and nitrogen species: concepts and controversies. *Nat Rev Microbiol* **2**(10), 820-32.

Fernandez-Chacon, R., Konigstorfer, A., Gerber, S. H., Garcia, J., Matos, M. F., Stevens, C. F., Brose, N., Rizo, J., Rosenmund, C., and Sudhof, T. C. (2001). Synaptotagmin I functions as a calcium regulator of release probability. *Nature* **410**(6824), 41-9.

Fernandez, I., Arac, D., Ubach, J., Gerber, S. H., Shin, O., Gao, Y., Anderson, R. G., Sudhof, T. C., and Rizo, J. (2001). Three-dimensional structure of the synaptotagmin 1 C2B-domain: synaptotagmin 1 as a phospholipid binding machine. *Neuron* **32**(6), 1057-69.

Finger, F. P., and Novick, P. (1998). Spatial regulation of exocytosis: lessons from yeast. *J Cell Biol* **142**(3), 609-12.

Fitzer-Attas, C. J., Lowry, M., Crowley, M. T., Finn, A. J., Meng, F., DeFranco, A. L., and Lowell, C. A. (2000). Fcγ receptor-mediated phagocytosis in macrophages lacking the Src family tyrosine kinases Hck, Fgr, and Lyn. *J Exp Med* **191**(4), 669-82.

Flannagan, R. S., Cosio, G., and Grinstein, S. (2009). Antimicrobial mechanisms of phagocytes and bacterial evasion strategies. *Nat Rev Microbiol* **7**(5), 355-66.

Forget, G., Gregory, D. J., and Olivier, M. (2005). Proteasome-mediated degradation of STAT1α following infection of macrophages with *Leishmania donovani*. *J Biol Chem* **280**(34), 30542-9.

Forget, G., Siminovitch, K. A., Brochu, S., Rivest, S., Radzioch, D., and Olivier, M. (2001). Role of host phosphotyrosine phosphatase SHP-1 in the development of murine leishmaniasis. *Eur J Immunol* **31**(11), 3185-96.

Fratti, R. A., Chua, J., Vergne, I., and Deretic, V. (2003). *Mycobacterium tuberculosis* glycosylated phosphatidylinositol causes phagosome maturation arrest. *Proc Natl Acad Sci U S A* **100**(9), 5437-42.

Fukuda, M. (2002). Vesicle-associated membrane protein-2/synaptobrevin binding to synaptotagmin I promotes O-glycosylation of synaptotagmin I. *J Biol Chem* **277**(33), 30351-8.

Fukuda, M. (2003a). Molecular cloning and characterization of human, rat, and mouse synaptotagmin XV. *Biochem Biophys Res Commun* **306**(1), 64-71.

Fukuda, M. (2003b). Molecular cloning, expression, and characterization of a novel class of synaptotagmin (Syt XIV) conserved from Drosophila to humans. *J Biochem* **133**(5), 641-9.

Fukuda, M. (2004). RNA interference-mediated silencing of synaptotagmin IX, but not synaptotagmin I, inhibits dense-core vesicle exocytosis in PC12 cells. *Biochem J* **380**(Pt 3), 875-9.

Fukuda, M. (2006). Distinct developmental expression of synaptotagmin I and IX in the mouse brain. *Neuroreport* **17**(2), 179-82.

Fukuda, M., Kanno, E., and Mikoshiba, K. (1999). Conserved N-terminal cysteine motif is essential for homo- and heterodimer formation of synaptotagmins III, V, VI, and X. *J Biol Chem* **274**(44), 31421-7.

Fukuda, M., Kanno, E., Ogata, Y., and Mikoshiba, K. (2001). Mechanism of the SDS-resistant synaptotagmin clustering mediated by the cysteine cluster at the interface between the transmembrane and spacer domains. *J Biol Chem* **276**(43), 40319-25.

Fukuda, M., Kowalchyk, J. A., Zhang, X., Martin, T. F., and Mikoshiba, K. (2002). Synaptotagmin IX regulates Ca^{2+}-dependent secretion in PC12 cells. *J Biol Chem* **277**(7), 4601-4.

Fukuda, M., and Mikoshiba, K. (1997). The function of inositol high polyphosphate binding proteins. *Bioessays* **19**(7), 593-603.

Fukuda, M., and Mikoshiba, K. (2000). Calcium-dependent and -independent hetero-oligomerization in the synaptotagmin family. *J Biochem* **128**(4), 637-45.

Fukuda, M., Moreira, J. E., Liu, V., Sugimori, M., Mikoshiba, K., and Llinas, R. R. (2000). Role of the conserved WHXL motif in the C terminus of synaptotagmin in synaptic vesicle docking. *Proc Natl Acad Sci U S A* **97**(26), 14715-9.

Fukuda, M., and Sagi-Eisenberg, R. (2008). Confusion in the nomenclature of synaptotagmins V and IX: which is which? *Calcium Binding Proteins* **3**, 1-4.

Gagnon, E., Duclos, S., Rondeau, C., Chevet, E., Cameron, P. H., Steele-Mortimer, O., Paiement, J., Bergeron, J. J., and Desjardins, M. (2002). Endoplasmic reticulum-mediated phagocytosis is a mechanism of entry into macrophages. *Cell* **110**(1), 119-31.

Galli, T., McPherson, P. S., and De Camilli, P. (1996). The V_0 sector of the V-ATPase, synaptobrevin, and synaptophysin are associated on synaptic vesicles in a Triton X-100-resistant, freeze-thawing sensitive, complex. *J Biol Chem* **271**(4), 2193-8.

Garin, J., Diez, R., Kieffer, S., Dermine, J. F., Duclos, S., Gagnon, E., Sadoul, R., Rondeau, C., and Desjardins, M. (2001). The phagosome proteome: insight into phagosome functions. *J Cell Biol* **152**(1), 165-80.

Gatfield, J., and Pieters, J. (2000). Essential role for cholesterol in entry of mycobacteria into macrophages. *Science* **288**(5471), 1647-50.

Gaullier, J. M., Simonsen, A., D'Arrigo, A., Bremnes, B., Stenmark, H., and Aasland, R. (1998). FYVE fingers bind PtdIns(3)P. *Nature* **394**(6692), 432-3.

Geppert, M., Goda, Y., Hammer, R. E., Li, C., Rosahl, T. W., Stevens, C. F., and Sudhof, T. C. (1994). Synaptotagmin I: a major Ca^{2+} sensor for transmitter release at a central synapse. *Cell* **79**(4), 717-27.

Gerold, G., Zychlinsky, A., and de Diego, J. L. (2007). What is the role of Toll-like receptors in bacterial infections? *Semin Immunol* **19**(1), 41-7.

Ghazizadeh, S., Bolen, J. B., and Fleit, H. B. (1994). Physical and functional association of Src-related protein tyrosine kinases with FcγRII in monocytic THP-1 cells. *J Biol Chem* **269**(12), 8878-84.

Gil, C., Soler-Jover, A., Blasi, J., and Aguilera, J. (2005). Synaptic proteins and SNARE complexes are localized in lipid rafts from rat brain synaptosomes. *Biochem Biophys Res Commun* **329**(1), 117-24.

Gillooly, D. J., Morrow, I. C., Lindsay, M., Gould, R., Bryant, N. J., Gaullier, J. M., Parton, R. G., and Stenmark, H. (2000). Localization of phosphatidylinositol 3-phosphate in yeast and mammalian cells. *Embo J* **19**(17), 4577-88.

Giorgione, J. R., Turco, S. J., and Epand, R. M. (1996). Transbilayer inhibition of protein kinase C by the lipophosphoglycan from *Leishmania donovani*. *Proc Natl Acad Sci U S A* **93**(21), 11634-9.

Goldstein, J. L., Ho, Y. K., Basu, S. K., and Brown, M. S. (1979). Binding site on macrophages that mediates uptake and degradation of acetylated low density lipoprotein, producing massive cholesterol deposition. *Proc Natl Acad Sci U S A* **76**(1), 333-7.

Gomez, C. R., Boehmer, E. D., and Kovacs, E. J. (2005). The aging innate immune system. *Current Opinion in Immunology* **17**(5), 457-462.

Gordon, A. H., Hart, P. D., and Young, M. R. (1980). Ammonia inhibits phagosome-lysosome fusion in macrophages. *Nature* **286**(5768), 79-80.

Gordon, S., and Taylor, P. R. (2005). Monocyte and macrophage heterogeneity. *Nat Rev Immunol* **5**(12), 953-64.

Gough, P. J., and Gordon, S. (2000). The role of scavenger receptors in the innate immune system. *Microbes Infect* **2**(3), 305-11.

Grassme, H., Jendrossek, V., Riehle, A., von Kurthy, G., Berger, J., Schwarz, H., Weller, M., Kolesnick, R., and Gulbins, E. (2003). Host defense against *Pseudomonas aeruginosa* requires ceramide-rich membrane rafts. *Nat Med* **9**(3), 322-30.

Green, P. J., Feizi, T., Stoll, M. S., Thiel, S., Prescott, A., and McConville, M. J. (1994). Recognition of the major cell surface glycoconjugates of *Leishmania* parasites by the human serum mannan-binding protein. *Mol Biochem Parasitol* **66**(2), 319-28.

Greenberg, S. (1995). Signal transduction of phagocytosis. *Trends Cell Biol* **5**(3), 93-9.

Greenberg, S., el Khoury, J., di Virgilio, F., Kaplan, E. M., and Silverstein, S. C. (1991). $Ca^{(2+)}$-independent F-actin assembly and disassembly during Fc receptor-mediated phagocytosis in mouse macrophages. *J Cell Biol* **113**(4), 757-67.

Gresham, H. D., Dale, B. M., Potter, J. W., Chang, P. W., Vines, C. M., Lowell, C. A., Lagenaur, C. F., and Willman, C. L. (2000). Negative regulation of phagocytosis in murine macrophages by the Src kinase family member, Fgr. *J Exp Med* **191**(3), 515-28.

Griffin, F. M., Jr., and Mullinax, P. J. (1985). In vivo activation of macrophage C3 receptors for phagocytosis. *J Exp Med* **162**(1), 352-7.

Griffiths, G., Hoflack, B., Simons, K., Mellman, I., and Kornfeld, S. (1988). The mannose 6-phosphate receptor and the biogenesis of lysosomes. *Cell* **52**(3), 329-41.

Grise, F., Taib, N., Monterrat, C., Lagree, V., and Lang, J. (2007). Distinct roles of the C2A and the C2B domain of the vesicular Ca^{2+} sensor synaptotagmin 9 in endocrine β-cells. *Biochem J* **403**(3), 483-92.

Gruenberg, J., and van der Goot, F. G. (2006). Mechanisms of pathogen entry through the endosomal compartments. *Nat Rev Mol Cell Biol* **7**(7), 495-504.

Gueirard, P., Laplante, A., Rondeau, C., Milon, G., and Desjardins, M. (2008). Trafficking of *Leishmania donovani* promastigotes in non-lytic compartments in neutrophils enables the subsequent transfer of parasites to macrophages. *Cell Microbiol* **10**(1), 100-11.

Guermonprez, P., Saveanu, L., Kleijmeer, M., Davoust, J., Van Endert, P., and Amigorena, S. (2003). ER-phagosome fusion defines an MHC class I cross-presentation compartment in dendritic cells. *Nature* **425**(6956), 397-402.

Haas, A. (2007). The phagosome: compartment with a license to kill. *Traffic* **8**(4), 311-30.

Haberman, Y., Grimberg, E., Fukuda, M., and Sagi-Eisenberg, R. (2003). Synaptotagmin IX, a possible linker between the perinuclear endocytic recycling compartment and the microtubules. *J Cell Sci* **116**(Pt 21), 4307-18.

Haberman, Y., Ziv, I., Gorzalczany, Y., Fukuda, M., and Sagi-Eisenberg, R. (2005). Classical protein kinase C(s) regulates targeting of synaptotagmin IX to the endocytic recycling compartment. *J Cell Sci* **118**(Pt 8), 1641-9.

Haberman, Y., Ziv, I., Gorzalczany, Y., Hirschberg, K., Mittleman, L., Fukuda, M., and Sagi-Eisenberg, R. (2007). Synaptotagmin (Syt) IX is an essential determinant for protein sorting to secretory granules in mast cells. *Blood* **109**(8), 3385-92.

Hackam, D. J., Rotstein, O. D., Bennett, M. K., Klip, A., Grinstein, S., and Manolson, M. F. (1996). Characterization and subcellular localization of target membrane soluble NSF attachment protein receptors (t-SNAREs) in macrophages. Syntaxins 2, 3, and 4 are present on phagosomal membranes. *J Immunol* **156**(11), 4377-83.

Hackam, D. J., Rotstein, O. D., Zhang, W. J., Demaurex, N., Woodside, M., Tsai, O., and Grinstein, S. (1997). Regulation of phagosomal acidification. Differential targeting of Na^+/H^+ exchangers, Na^+/K^+-ATPases, and vacuolar-type H^+-atpases. *J Biol Chem* **272**(47), 29810-20.

Han, W., Rhee, J. S., Maximov, A., Lao, Y., Mashimo, T., Rosenmund, C., and Sudhof, T. C. (2004). N-glycosylation is essential for vesicular targeting of synaptotagmin 1. *Neuron* **41**(1), 85-99.

Hanson, P. I., Roth, R., Lin, Y., and Heuser, J. E. (2008). Plasma membrane deformation by circular arrays of ESCRT-III protein filaments. *J Cell Biol* **180**(2), 389-402.

Harrison, R. E., Bucci, C., Vieira, O. V., Schroer, T. A., and Grinstein, S. (2003). Phagosomes fuse with late endosomes and/or lysosomes by extension of membrane protrusions along microtubules: role of Rab7 and RILP. *Mol Cell Biol* **23**(18), 6494-506.

Hatsuzawa, K., Hashimoto, H., Hashimoto, H., Arai, S., Tamura, T., Higa-Nishiyama, A., and Wada, I. (2009). Sec22b is a negative regulator of phagocytosis in macrophages. *Mol Biol Cell.*

Hatsuzawa, K., Tamura, T., Hashimoto, H., Hashimoto, H., Yokoya, S., Miura, M., Nagaya, H., and Wada, I. (2006). Involvement of syntaxin 18, an endoplasmic reticulum (ER)-localized SNARE protein, in ER-mediated phagocytosis. *Mol. Biol. Cell* **17**(9), 3964-3977.

Hatzigeorgiou, D. E., Geng, J., Zhu, B., Zhang, Y., Liu, K., Rom, W. N., Fenton, M. J., Turco, S. J., and Ho, J. L. (1996). Lipophosphoglycan from *Leishmania* suppresses agonist-induced interleukin-1-β gene expression in human monocytes via a unique promoter sequence. *Proc Natl Acad Sci U S A* **93**(25), 14708-13.

Henry, R. M., Hoppe, A. D., Joshi, N., and Swanson, J. A. (2004). The uniformity of phagosome maturation in macrophages. *J Cell Biol* **164**(2), 185-94.

Herrick, D. Z., Sterbling, S., Rasch, K. A., Hinderliter, A., and Cafiso, D. S. (2006). Position of synaptotagmin I at the membrane interface: cooperative interactions of tandem C2 domains. *Biochemistry* **45**(32), 9668-74.

Heyworth, P. G., Cross, A. R., and Curnutte, J. T. (2003). Chronic granulomatous disease. *Curr Opin Immunol* **15**(5), 578-84.

Hilfiker, S., Pieribone, V. A., Nordstedt, C., Greengard, P., and Czernik, A. J. (1999). Regulation of synaptotagmin I phosphorylation by multiple protein kinases. *J Neurochem* **73**(3), 921-32.

Hoebe, K., Georgel, P., Rutschmann, S., Du, X., Mudd, S., Crozat, K., Sovath, S., Shamel, L., Hartung, T., Zahringer, U., and Beutler, B. (2005). CD36 is a sensor of diacylglycerides. *Nature* **433**(7025), 523-7.

Hoeppner, D. J., Hengartner, M. O., and Schnabel, R. (2001). Engulfment genes cooperate with ced-3 to promote cell death in *Caenorhabditis elegans*. *Nature* **412**(6843), 202-206.

Holm, A., Tejle, K., Gunnarsson, T., Magnusson, K. E., Descoteaux, A., and Rasmusson, B. (2003). Role of protein kinase C α for uptake of unopsonized prey and phagosomal maturation in macrophages. *Biochem Biophys Res Commun* **302**(4), 653-8.

Holm, A., Tejle, K., Magnusson, K. E., Descoteaux, A., and Rasmusson, B. (2001). *Leishmania donovani* lipophosphoglycan causes periphagosomal actin accumulation: correlation with impaired translocation of PKCα and defective phagosome maturation. *Cell Microbiol* **3**(7), 439-47.

Honey, K., and Rudensky, A. Y. (2003). Lysosomal cysteine proteases regulate antigen presentation. *Nat Rev Immunol* **3**(6), 472-82.

Hoppe, A. D., and Swanson, J. A. (2004). Cdc42, Rac1, and Rac2 display distinct patterns of activation during phagocytosis. *Mol Biol Cell* **15**(8), 3509-19.

Horikoshi, T., Arany, I., Rajaraman, S., Chen, S. H., Brysk, H., Lei, G., Tyring, S. K., and Brysk, M. M. (1998). Isoforms of cathepsin D and human epidermal differentiation. *Biochimie* **80**(7), 605-12.

Horwitz, M. A. (1983). The Legionnaires' disease bacterium (*Legionella pneumophila*) inhibits phagosome-lysosome fusion in human monocytes. *J Exp Med* **158**(6), 2108-26.

Huang, C., and Turco, S. J. (1993). Defective galactofuranose addition in lipophosphoglycan biosynthesis in a mutant of *Leishmania donovani*. *J Biol Chem* **268**(32), 24060-24066.

Hudson, A. W., and Birnbaum, M. J. (1995). Identification of a nonneuronal isoform of synaptotagmin. *Proc Natl Acad Sci U S A* **92**(13), 5895-9.

Hughes, P. E., and Pfaff, M. (1998). Integrin affinity modulation. *Trends Cell Biol* **8**(9), 359-64.

Hui, E., Bai, J., Wang, P., Sugimori, M., Llinas, R. R., and Chapman, E. R. (2005). Three distinct kinetic groupings of the synaptotagmin family: candidate sensors for rapid and delayed exocytosis. *Proc Natl Acad Sci U S A* **102**(14), 5210-4.

Hui, E., Bai, J., and Chapman, E. R. (2006). Ca^{2+}-triggered simultaneous membrane penetration of the tandem C2-domains of synaptotagmin I. *Biophys J* **91**(5), 1767-77.

Hurtado-Lorenzo, A., Skinner, M., El Annan, J., Futai, M., Sun-Wada, G. H., Bourgoin, S., Casanova, J., Wildeman, A., Bechoua, S., Ausiello, D. A., Brown, D., and Marshansky, V. (2006). V-ATPase interacts with ARNO and Arf6 in early endosomes and regulates the protein degradative pathway. *Nat Cell Biol* **8**(2), 124-36.

Huynh, K. K., and Grinstein, S. (2007). Regulation of vacuolar pH and its modulation by some microbial species. *Microbiol Mol Biol Rev* **71**(3), 452-62.

Huynh, K. K., Kay, J. G., Stow, J. L., and Grinstein, S. (2007). Fusion, fission, and secretion during phagocytosis. *Physiology (Bethesda)* **22**, 366-72.

Iezzi, M., Eliasson, L., Fukuda, M., and Wollheim, C. B. (2005). Adenovirus-mediated silencing of synaptotagmin 9 inhibits Ca^{2+}-dependent insulin secretion in islets. *FEBS Lett* **579**(23), 5241-6.

Iezzi, M., Kouri, G., Fukuda, M., and Wollheim, C. B. (2004). Synaptotagmin V and IX isoforms control Ca^{2+} -dependent insulin exocytosis. *J Cell Sci* **117**(Pt 15), 3119-27.

Ilg, T., Demar, M., and Harbecke, D. (2001). Phosphoglycan repeat-deficient *Leishmania mexicana* parasites remain infectious to macrophages and mice. *J Biol Chem* **276**(7), 4988-97.

Jaconi, M. E., Lew, D. P., Carpentier, J. L., Magnusson, K. E., Sjogren, M., and Stendahl, O. (1990). Cytosolic free calcium elevation mediates the phagosome-lysosome fusion during phagocytosis in human neutrophils. *J Cell Biol* **110**(5), 1555-64.

Jahraus, A., Storrie, B., Griffiths, G., and Desjardins, M. (1994). Evidence for retrograde traffic between terminal lysosomes and the prelysosomal/late endosome compartment. *J Cell Sci* **107 (Pt 1)**, 145-57.

Jha, T. K., Sundar, S., Thakur, C. P., Felton, J. M., Sabin, A. J., and Horton, J. (2005). A phase II dose-ranging study of sitamaquine for the treatment of visceral leishmaniasis in India. *Am J Trop Med Hyg* **73**(6), 1005-11.

Jordens, I., Fernandez-Borja, M., Marsman, M., Dusseljee, S., Janssen, L., Calafat, J., Janssen, H., Wubbolts, R., and Neefjes, J. (2001). The Rab7 effector protein RILP controls lysosomal transport by inducing the recruitment of dynein-dynactin motors. *Curr Biol* **11**(21), 1680-5.

Joshi, P. B., Kelly, B. L., Kamhawi, S., Sacks, D. L., and McMaster, W. R. (2002). Targeted gene deletion in *Leishmania major* identifies leishmanolysin (GP63) as a virulence factor. *Mol Biochem Parasitol* **120**(1), 33-40.

Jutras, I., and Desjardins, M. (2005). Phagocytosis: at the crossroads of innate and adaptive immunity. *Annual Review of Cell and Developmental Biology* **21**(1), 511-527.

Jutras, I., Houde, M., Currier, N., Boulais, J., Duclos, S., LaBoissiere, S., Bonneil, E., Kearney, P., Thibault, P., Paramithiotis, E., Hugo, P., and Desjardins, M. (2008). Modulation of the phagosome proteome by interferon-γ. *Mol Cell Proteomics* **7**(4), 697-715.

Kanai, F., Liu, H., Field, S. J., Akbary, H., Matsuo, T., Brown, G. E., Cantley, L. C., and Yaffe, M. B. (2001). The PX domains of $p47^{phox}$ and $p40^{phox}$ bind to lipid products of PI(3)K. *Nat Cell Biol* **3**(7), 675-8.

Kane, M. M., and Mosser, D. M. (2000). *Leishmania* parasites and their ploys to disrupt macrophage activation. *Curr Opin Hematol* **7**(1), 26-31.

Kane, M. M., and Mosser, D. M. (2001). The role of IL-10 in promoting disease progression in leishmaniasis. *J Immunol* **166**(2), 1141-7.

Kang, R., Swayze, R., Lise, M. F., Gerrow, K., Mullard, A., Honer, W. G., and El-Husseini, A. (2004). Presynaptic trafficking of synaptotagmin I is regulated by protein palmitoylation. *J Biol Chem* **279**(48), 50524-36.

Kang, Y. S., Kim, Y. M., Park, K. I., Kim Cho, S., Choi, K. S., and Cho, M. (2006). Analysis of EST and lectin expressions in hemocytes of Manila clams (*Ruditapes philippinarum*) (Bivalvia: Mollusca) infected with *Perkinsus olseni*. *Dev Comp Immunol* **30**(12), 1119-31.

Kannan, S., Audet, A., Knittel, J., Mullegama, S., Gao, G. F., and Wu, M. (2006). Src kinase Lyn is crucial for Pseudomonas aeruginosa internalization into lung cells. *Eur J Immunol* **36**(7), 1739-52.

Kay, J. G., Murray, R. Z., Pagan, J. K., and Stow, J. L. (2006). Cytokine secretion via cholesterol-rich lipid raft-associated SNAREs at the phagocytic cup. *J Biol Chem* **281**(17), 11949-54.

Kiefer, F., Brumell, J., Al-Alawi, N., Latour, S., Cheng, A., Veillette, A., Grinstein, S., and Pawson, T. (1998). The Syk protein tyrosine kinase is essential for Fcγ receptor signaling in macrophages and neutrophils. *Mol Cell Biol* **18**(7), 4209-20.

Kobayashi, T., Stang, E., Fang, K. S., de Moerloose, P., Parton, R. G., and Gruenberg, J. (1998). A lipid associated with the antiphospholipid syndrome regulates endosome structure and function. *Nature* **392**(6672), 193-7.

Konduri, S. D., Yanamandra, N., Siddique, K., Joseph, A., Dinh, D. H., Olivero, W. C., Gujrati, M., Kouraklis, G., Swaroop, A., Kyritsis, A. P., and Rao, J. S. (2002). Modulation of cystatin C expression impairs the invasive and tumorigenic potential of human glioblastoma cells. *Oncogene* **21**(57), 8705-12.

Kopf, M., Brombacher, F., Kohler, G., Kienzle, G., Widmann, K. H., Lefrang, K., Humborg, C., Ledermann, B., and Solbach, W. (1996). IL-4-deficient Balb/c mice resist infection with *Leishmania major*. *J Exp Med* **184**(3), 1127-36.

Kurzchalia, T. V., and Parton, R. G. (1999). Membrane microdomains and caveolae. *Curr Opin Cell Biol* **11**(4), 424-31.

Lafont, F., Verkade, P., Galli, T., Wimmer, C., Louvard, D., and Simons, K. (1999). Raft association of SNAP receptors acting in apical trafficking in Madin-Darby canine kidney cells. *Proc Natl Acad Sci U S A* **96**(7), 3734-8.

Lalli, G., Bohnert, S., Deinhardt, K., Verastegui, C., and Schiavo, G. (2003). The journey of tetanus and botulinum neurotoxins in neurons. *Trends Microbiol* **11**(9), 431-7.

Lang, T. (2007). SNARE proteins and 'membrane rafts'. *J Physiol* **585**(Pt 3), 693-8.

Larsen, E. C., DiGennaro, J. A., Saito, N., Mehta, S., Loegering, D. J., Mazurkiewicz, J. E., and Lennartz, M. R. (2000). Differential requirement for classic and novel PKC isoforms in respiratory burst and phagocytosis in RAW 264.7 cells. *J Immunol* **165**(5), 2809-17.

Larsen, E. C., Ueyama, T., Brannock, P. M., Shirai, Y., Saito, N., Larsson, C., Loegering, D., Weber, P. B., and Lennartz, M. R. (2002). A role for PKC-ε in FcγR-mediated phagocytosis by RAW 264.7 cells. *J Cell Biol* **159**(6), 939-44.

Larsson, M., Fonteneau, J. F., and Bhardwaj, N. (2001). Dendritic cells resurrect antigens from dead cells. *Trends in Immunology* **22**(3), 141-148.

Lawe, D. C., Patki, V., Heller-Harrison, R., Lambright, D., and Corvera, S. (2000). The FYVE domain of early endosome antigen 1 is required for both phosphatidylinositol 3-phosphate and Rab5 binding. Critical role of this dual interaction for endosomal localization. *J Biol Chem* **275**(5), 3699-705.

Le Cabec, V., Cols, C., and Maridonneau-Parini, I. (2000). Nonopsonic phagocytosis of zymosan and *Mycobacterium kansasii* by CR3 (CD11b/CD18) involves distinct molecular determinants and is or is not coupled with NADPH oxidase activation. *Infect Immun* **68**(8), 4736-45.

Lee, W. L., Kim, M. K., Schreiber, A. D., and Grinstein, S. (2005). Role of ubiquitin and proteasomes in phagosome maturation. *Mol Biol Cell* **16**(4), 2077-90.

Lehrer, R. I., Lichtenstein, A. K., and Ganz, T. (1993). Defensins: antimicrobial and cytotoxic peptides of mammalian cells. *Annu Rev Immunol* **11**, 105-28.

Leiva, N., Pavarotti, M., Colombo, M. I., and Damiani, M. T. (2006). Reconstitution of recycling from the phagosomal compartment in streptolysin O-permeabilized macrophages: role of Rab11. *Exp Cell Res* **312**(10), 1843-55.

Lennon-Dumenil, A. M., Bakker, A. H., Maehr, R., Fiebiger, E., Overkleeft, H. S., Rosemblatt, M., Ploegh, H. L., and Lagaudriere-Gesbert, C. (2002). Analysis of protease activity in live antigen-presenting cells shows regulation of the phagosomal proteolytic contents during dendritic cell activation. *J Exp Med* **196**(4), 529-40.

Lew, P. D., Monod, A., Waldvogel, F. A., Dewald, B., Baggiolini, M., and Pozzan, T. (1986). Quantitative analysis of the cytosolic free calcium dependency of exocytosis from three subcellular compartments in intact human neutrophils. *J Cell Biol* **102**(6), 2197-204.

Li, C., Ullrich, B., Zhang, J. Z., Anderson, R. G., Brose, N., and Sudhof, T. C. (1995). $Ca^{(2+)}$-dependent and -independent activities of neural and non-neural synaptotagmins. *Nature* **375**(6532), 594-9.

Lindmark, I. M., Karlsson, A., Serrander, L., Francois, P., Lew, D., Rasmusson, B., Stendahl, O., and Nusse, O. (2002). Synaptotagmin II could confer $Ca^{(2+)}$ sensitivity to phagocytosis in human neutrophils. *Biochim Biophys Acta* **1590**(1-3), 159-66.

Littleton, J. T., Barnard, R. J., Titus, S. A., Slind, J., Chapman, E. R., and Ganetzky, B. (2001). SNARE-complex disassembly by NSF follows synaptic-vesicle fusion. *Proc Natl Acad Sci U S A* **98**(21), 12233-8.

Lodge, R., and Descoteaux, A. (2005a). *Leishmania donovani* promastigotes induce periphagosomal F-actin accumulation through retention of the GTPase Cdc42. *Cell Microbiol* **7**(11), 1647-58.

Lodge, R., and Descoteaux, A. (2005b). Modulation of phagolysosome biogenesis by the lipophosphoglycan of *Leishmania*. *Clin Immunol* **114**(3), 256-65.

Lodge, R., and Descoteaux, A. (2006). Phagocytosis of *Leishmania donovani* amastigotes is Rac1 dependent and occurs in the absence of NADPH oxidase activation. *Eur J Immunol* **36**(10), 2735-44.

Lodge, R., Diallo, T. O., and Descoteaux, A. (2006). *Leishmania donovani* lipophosphoglycan blocks NADPH oxidase assembly at the phagosome membrane. *Cell Microbiol* **8**(12), 1922-31.

Love, D. C., Mentink Kane, M., and Mosser, D. M. (1998). *Leishmania amazonensis*: the phagocytosis of amastigotes by macrophages. *Exp Parasitol* **88**(3), 161-71.

Lukacs, G. L., Rotstein, O. D., and Grinstein, S. (1990). Phagosomal acidification is mediated by a vacuolar-type $H^{(+)}$-ATPase in murine macrophages. *J Biol Chem* **265**(34), 21099-107.

Lynch, K. L., and Martin, T. F. (2007). Synaptotagmins I and IX function redundantly in regulated exocytosis but not endocytosis in PC12 cells. *J Cell Sci* **120**(Pt 4), 617-27.

Mackler, J. M., Drummond, J. A., Loewen, C. A., Robinson, I. M., and Reist, N. E. (2002). The C(2)B $Ca^{(2+)}$-binding motif of synaptotagmin is required for synaptic transmission in vivo. *Nature* **418**(6895), 340-4.

Malik, Z. A., Denning, G. M., and Kusner, D. J. (2000). Inhibition of $Ca^{(2+)}$ signaling by *Mycobacterium tuberculosis* is associated with reduced phagosome-lysosome fusion and increased survival within human macrophages. *J Exp Med* **191**(2), 287-302.

Malo, D., Vogan, K., Vidal, S., Hu, J., Cellier, M., Schurr, E., Fuks, A., Bumstead, N., Morgan, K., and Gros, P. (1994). Haplotype mapping and sequence analysis of the mouse Nramp gene predict susceptibility to infection with intracellular parasites. *Genomics* **23**(1), 51-61.

Maniak, M., Rauchenberger, R., Albrecht, R., Murphy, J., and Gerisch, G. (1995). Coronin involved in phagocytosis: dynamics of particle-induced relocalization visualized by a green fluorescent protein Tag. *Cell* **83**(6), 915-24.

Marcinkiewicz, J., Grabowska, A., and Chain, B. (1995). Nitric oxide up-regulates the release of inflammatory mediators by mouse macrophages. *Eur J Immunol* **25**(4), 947-51.

Martens, S., and McMahon, H. T. (2008). Mechanisms of membrane fusion: disparate players and common principles. *Nat Rev Mol Cell Biol* **9**(7), 543-56.

Martinez, I., Chakrabarti, S., Hellevik, T., Morehead, J., Fowler, K., and Andrews, N. W. (2000). Synaptotagmin VII Regulates Ca^{2+}-dependent Exocytosis of Lysosomes in Fibroblasts. *J. Cell Biol.* **148**(6), 1141-1150.

Masson, P. L., Heremans, J. F., and Schonne, E. (1969). Lactoferrin, an iron-binding protein in neutrophilic leukocytes. *J Exp Med* **130**(3), 643-58.

Mayer, A., Wickner, W., and Haas, A. (1996). Sec18p (NSF)-driven release of Sec17p (α-SNAP) can precede docking and fusion of yeast vacuoles. *Cell* **85**(1), 83-94.

Mayorga, L. S., Bertini, F., and Stahl, P. D. (1991). Fusion of newly formed phagosomes with endosomes in intact cells and in a cell-free system. *J Biol Chem* **266**(10), 6511-7.

McBride, H. M., Rybin, V., Murphy, C., Giner, A., Teasdale, R., and Zerial, M. (1999). Oligomeric complexes link Rab5 effectors with NSF and drive membrane fusion via interactions between EEA1 and syntaxin 13. *Cell* **98**(3), 377-86.

McConville, M. J., and Blackwell, J. M. (1991). Developmental changes in the glycosylated phosphatidylinositols of *Leishmania donovani*. Characterization of the promastigote and amastigote glycolipids. *J Biol Chem* **266**(23), 15170-9.

McGuire, T. R., Trickler, W. J., Smith, L., Hoie, E. B., and Miller, D. W. (2005). Release of TNF-α and IL-1β from porcine brain endothelium corresponds to the

pyrogenic potential of three marketed formulations of amphotericin. *Inflamm Res* **54**(9), 375-9.

McNeely, T. B., Rosen, G., Londner, M. V., and Turco, S. J. (1989). Inhibitory effects on protein kinase C activity by lipophosphoglycan fragments and glycosylphosphatidylinositol antigens of the protozoan parasite *Leishmania. Biochem J* **259**(2), 601-4.

McNeely, T. B., and Turco, S. J. (1990). Requirement of lipophosphoglycan for intracellular survival of *Leishmania donovani* within human monocytes. *J Immunol* **144**(7), 2745-50.

Metcalf, D. (1971). Transformation of granulocytes to macrophages in bone marrow colonies in vitro. *J Cell Physiol* **77**(2), 277-80.

Miao, L., Stafford, A., Nir, S., Turco, S. J., Flanagan, T. D., and Epand, R. M. (1995). Potent inhibition of viral fusion by the lipophosphoglycan of *Leishmania donovani. Biochemistry* **34**(14), 4676-83.

Mills, I. G., Urbe, S., and Clague, M. J. (2001). Relationships between EEA1 binding partners and their role in endosome fusion. *J Cell Sci* **114**(Pt 10), 1959-65.

Misura, K. M., Scheller, R. H., and Weis, W. I. (2000). Three-dimensional structure of the neuronal-Sec1-syntaxin 1a complex. *Nature* **404**(6776), 355-62.

Miyake, K. (2007). Innate immune sensing of pathogens and danger signals by cell surface Toll-like receptors. *Semin Immunol* **19**(1), 3-10.

Mordue, D. G., and Sibley, L. D. (1997). Intracellular fate of vacuoles containing *Toxoplasma gondii* is determined at the time of formation and depends on the mechanism of entry. *J Immunol* **159**(9), 4452-9.

Morehead, J., Coppens, I., and Andrews, N. W. (2002). Opsonization modulates Rac-1 activation during cell entry by *Leishmania amazonensis*. *Infect Immun* **70**(8), 4571-80.

Mukherjee, S., Ghosh, R. N., and Maxfield, F. R. (1997). Endocytosis. *Physiol Rev* **77**(3), 759-803.

Mukhopadhyay, S., Chen, Y., Sankala, M., Peiser, L., Pikkarainen, T., Kraal, G., Tryggvason, K., and Gordon, S. (2006). MARCO, an innate activation marker of macrophages, is a class A scavenger receptor for Neisseria meningitidis. *Eur J Immunol* **36**(4), 940-9.

Mukhopadhyay, S., and Gordon, S. (2004). The role of scavenger receptors in pathogen recognition and innate immunity. *Immunobiology* **209**(1-2), 39-49.

Murray, R. Z., Kay, J. G., Sangermani, D. G., and Stow, J. L. (2005). A role for the phagosome in cytokine secretion. *Science* **310**(5753), 1492-5.

Muziol, T., Pineda-Molina, E., Ravelli, R. B., Zamborlini, A., Usami, Y., Gottlinger, H., and Weissenhorn, W. (2006). Structural basis for budding by the ESCRT-III factor CHMP3. *Dev Cell* **10**(6), 821-30.

Nagy, G., Kim, J. H., Pang, Z. P., Matti, U., Rettig, J., Sudhof, T. C., and Sorensen, J. B. (2006). Different effects on fast exocytosis induced by synaptotagmin 1 and 2 isoforms and abundance but not by phosphorylation. *J Neurosci* **26**(2), 632-43.

Nakagawa, T. Y., and Rudensky, A. Y. (1999). The role of lysosomal proteinases in MHC class II-mediated antigen processing and presentation. *Immunol Rev* **172**, 121-9.

Nalefski, E. A., and Falke, J. J. (1996). The C2 domain calcium-binding motif: structural and functional diversity. *Protein Sci* **5**(12), 2375-90.

Naroeni, A., and Porte, F. (2002). Role of cholesterol and the ganglioside GM(1) in entry and short-term survival of *Brucella suis* in murine macrophages. *Infect Immun* **70**(3), 1640-4.

Nauseef, W. M. (2004). Assembly of the phagocyte NADPH oxidase. *Histochem Cell Biol* **122**(4), 277-91.

Ng Yan Hing, J. D., Desjardins, M., and Descoteaux, A. (2004). Proteomic analysis reveals a role for protein kinase C-α in phagosome maturation. *Biochem Biophys Res Commun* **319**(3), 810-6.

Niedergang, F., Colucci-Guyon, E., Dubois, T., Raposo, G., and Chavrier, P. (2003). ADP ribosylation factor 6 is activated and controls membrane delivery during phagocytosis in macrophages. *J Cell Biol* **161**(6), 1143-50.

Nishiki, T., and Augustine, G. J. (2004). Dual roles of the C2B domain of synaptotagmin I in synchronizing Ca^{2+}-dependent neurotransmitter release. *J Neurosci* **24**(39), 8542-50.

Nusse, O., Serrander, L., Lew, D. P., and Krause, K. H. (1998). Ca^{2+}-induced exocytosis in individual human neutrophils: high- and low-affinity granule populations and submaximal responses. *Embo J* **17**(5), 1279-88.

Odorizzi, G. (2006). The multiple personalities of Alix. *J Cell Sci* **119**(Pt 15), 3025-32.

Olazabal, I. M., Caron, E., May, R. C., Schilling, K., Knecht, D. A., and Machesky, L. M. (2002). Rho-kinase and myosin-II control phagocytic cup formation during CR, but not FcγR, phagocytosis. *Curr Biol* **12**(16), 1413-18.

Paclet, M. H., Coleman, A. W., Vergnaud, S., and Morel, F. (2000). $P67^{phox}$-mediated NADPH oxidase assembly: imaging of cytochrome b_{558} liposomes by atomic force microscopy. *Biochemistry* **39**(31), 9302-10.

Pang, Z. P., Shin, O. H., Meyer, A. C., Rosenmund, C., and Sudhof, T. C. (2006). A gain-of-function mutation in synaptotagmin-1 reveals a critical role of Ca^{2+}-dependent soluble N-ethylmaleimide-sensitive factor attachment protein receptor complex binding in synaptic exocytosis. *J Neurosci* **26**(48), 12556-65.

Pelletier, I., Hashidate, T., Urashima, T., Nishi, N., Nakamura, T., Futai, M., Arata, Y., Kasai, K., Hirashima, M., Hirabayashi, J., and Sato, S. (2003). Specific recognition of *Leishmania major* poly-β-galactosyl epitopes by galectin-9: possible implication of galectin-9 in interaction between *L. major* and host cells. *J Biol Chem* **278**(25), 22223-30.

Pelletier, I., and Sato, S. (2002). Specific recognition and cleavage of galectin-3 by *Leishmania major* through species-specific polygalactose epitope. *J Biol Chem* **277**(20), 17663-70.

Perez-Victoria, F. J., Castanys, S., and Gamarro, F. (2003). *Leishmania donovani* resistance to miltefosine involves a defective inward translocation of the drug. *Antimicrob Agents Chemother* **47**(8), 2397-403.

Perin, M. S., Fried, V. A., Mignery, G. A., Jahn, R., and Sudhof, T. C. (1990). Phospholipid binding by a synaptic vesicle protein homologous to the regulatory region of protein kinase C. *Nature* **345**(6272), 260-3.

Peterson, M. R., and Emr, S. D. (2001). The class C Vps complex functions at multiple stages of the vacuolar transport pathway. *Traffic* **2**(7), 476-86.

Peyron, P., Bordier, C., N'Diaye, E. N., and Maridonneau-Parini, I. (2000). Nonopsonic phagocytosis of *Mycobacterium kansasii* by human neutrophils depends on

cholesterol and is mediated by CR3 associated with glycosylphosphatidylinositol-anchored proteins. *J Immunol* **165**(9), 5186-91.

Phillip, D. S., Christina, O.-J., and Lesley, E. S. (2005). Intestinal macrophages: unique effector cells of the innate immune system. *Immunological Reviews* **206**(1), 149-159.

Piedrafita, D., Proudfoot, L., Nikolaev, A. V., Xu, D., Sands, W., Feng, G. J., Thomas, E., Brewer, J., Ferguson, M. A., Alexander, J., and Liew, F. Y. (1999). Regulation of macrophage IL-12 synthesis by *Leishmania* phosphoglycans. *Eur J Immunol* **29**(1), 235-44.

Pierre, P., and Mellman, I. (1998). Developmental regulation of invariant chain proteolysis controls MHC class II trafficking in mouse dendritic cells. *Cell* **93**(7), 1135-45.

Pillay, C. S., Elliott, E., and Dennison, C. (2002). Endolysosomal proteolysis and its regulation. *Biochem J* **363**(Pt 3), 417-29.

Platt, N., Suzuki, H., Kurihara, Y., Kodama, T., and Gordon, S. (1996). Role for the class A macrophage scavenger receptor in the phagocytosis of apoptotic thymocytes in vitro. *Proc Natl Acad Sci U S A* **93**(22), 12456-60.

Pluddemann, A., Neyen, C., and Gordon, S. (2007). Macrophage scavenger receptors and host-derived ligands. *Methods* **43**(3), 207-17.

Poupon, V., Stewart, A., Gray, S. R., Piper, R. C., and Luzio, J. P. (2003). The role of mVps18p in clustering, fusion, and intracellular localization of late endocytic organelles. *Mol Biol Cell* **14**(10), 4015-27.

Prive, C., and Descoteaux, A. (2000). *Leishmania donovani* promastigotes evade the activation of mitogen-activated protein kinases p38, c-Jun N-terminal kinase, and

extracellular signal-regulated kinase-1/2 during infection of naive macrophages. *Eur J Immunol* **30**(8), 2235-44.

Proudfoot, L., Nikolaev, A. V., Feng, G. J., Wei, W. Q., Ferguson, M. A., Brimacombe, J. S., and Liew, F. Y. (1996). Regulation of the expression of nitric oxide synthase and leishmanicidal activity by glycoconjugates of *Leishmania* lipophosphoglycan in murine macrophages. *Proc Natl Acad Sci U S A* **93**(20), 10984-9.

Proudfoot, L., O'Donnell, C. A., and Liew, F. Y. (1995). Glycoinositolphospholipids of *Leishmania major* inhibit nitric oxide synthesis and reduce leishmanicidal activity in murine macrophages. *Eur J Immunol* **25**(3), 745-50.

Puentes, S. M., Da Silva, R. P., Sacks, D. L., Hammer, C. H., and Joiner, K. A. (1990). Serum resistance of metacyclic stage *Leishmania major* promastigotes is due to release of C5b-9. *J Immunol* **145**(12), 4311-6.

Qualmann, B., and Mellor, H. (2003). Regulation of endocytic traffic by Rho GTPases. *Biochem J* **371**(Pt 2), 233-41.

Quraishi, O., Nagler, D. K., Fox, T., Sivaraman, J., Cygler, M., Mort, J. S., and Storer, A. C. (1999). The occluding loop in cathepsin B defines the pH dependence of inhibition by its propeptide. *Biochemistry* **38**(16), 5017-23.

Ramachandra, L., Boom, W. H., and Harding, C. V. (2008). Class II MHC antigen processing in phagosomes. *Methods Mol Biol* **445**, 353-77.

Ramachandra, L., Song, R., and Harding, C. V. (1999). Phagosomes are fully competent antigen-processing organelles that mediate the formation of peptide:class II MHC complexes. *J Immunol* **162**(6), 3263-72.

Rao, S. K., Huynh, C., Proux-Gillardeaux, V., Galli, T., and Andrews, N. W. (2004). Identification of SNAREs involved in synaptotagmin VII-regulated lysosomal exocytosis. *J Biol Chem* **279**(19), 20471-9.

Rasmusson, B. J., Flanagan, T. D., Turco, S. J., Epand, R. M., and Petersen, N. O. (1998). Fusion of Sendai virus and individual host cells and inhibition of fusion by lipophosphoglycan measured with image correlation spectroscopy. *Biochim Biophys Acta* **1404**(3), 338-52.

Reddien, P. W., Cameron, S., and Horvitz, H. R. (2001). Phagocytosis promotes programmed cell death in *C. elegans*. *Nature* **412**(6843), 198-202.

Reddy, A., Caler, E. V., and Andrews, N. W. (2001). Plasma membrane repair is mediated by $Ca^{(2+)}$-regulated exocytosis of lysosomes. *Cell* **106**(2), 157-69.

Reiner, N. E. (1987). Parasite accessory cell interactions in murine leishmaniasis. I. Evasion and stimulus-dependent suppression of the macrophage interleukin 1 response by *Leishmania donovani*. *J Immunol* **138**(6), 1919-25.

Rickman, C., Archer, D. A., Meunier, F. A., Craxton, M., Fukuda, M., Burgoyne, R. D., and Davletov, B. (2004a). Synaptotagmin interaction with the syntaxin/SNAP-25 dimer is mediated by an evolutionarily conserved motif and is sensitive to inositol hexakisphosphate. *J Biol Chem* **279**(13), 12574-9.

Rickman, C., Craxton, M., Osborne, S., and Davletov, B. (2004b). Comparative analysis of tandem C2 domains from the mammalian synaptotagmin family. *Biochem J* **378**(Pt 2), 681-6.

Rink, J., Ghigo, E., Kalaidzidis, Y., and Zerial, M. (2005). Rab conversion as a mechanism of progression from early to late endosomes. *Cell* **122**(5), 735-49.

Rizo, J., Chen, X., and Arac, D. (2006). Unraveling the mechanisms of synaptotagmin and SNARE function in neurotransmitter release. *Trends Cell Biol* **16**(7), 339-50.

Rodrigues, C. D., Hannus, M., Prudencio, M., Martin, C., Goncalves, L. A., Portugal, S., Epiphanio, S., Akinc, A., Hadwiger, P., Jahn-Hofmann, K., Rohl, I., van Gemert, G. J., Franetich, J. F., Luty, A. J., Sauerwein, R., Mazier, D., Koteliansky, V., Vornlocher, H. P., Echeverri, C. J., and Mota, M. M. (2008). Host scavenger receptor SR-BI plays a dual role in the establishment of malaria parasite liver infection. *Cell Host Microbe* **4**(3), 271-82.

Rodrigues, V., Jr., Santana da Silva, J., and Campos-Neto, A. (1998). Transforming growth factor β and immunosuppression in experimental visceral leishmaniasis. *Infect Immun* **66**(3), 1233-6.

Rogers, L. D., and Foster, L. J. (2007). The dynamic phagosomal proteome and the contribution of the endoplasmic reticulum. *Proc Natl Acad Sci U S A* **104**(47), 18520-5.

Roggero, C. M., Tomes, C. N., De Blas, G. A., Castillo, J., Michaut, M. A., Fukuda, M., and Mayorga, L. S. (2005). Protein kinase C-mediated phosphorylation of the two polybasic regions of synaptotagmin VI regulates their function in acrosomal exocytosis. *Dev Biol* **285**(2), 422-35.

Rosales, J. L., and Ernst, J. D. (1997). Calcium-dependent neutrophil secretion: characterization and regulation by annexins. *J Immunol* **159**(12), 6195-202.

Ross, G. D., and Vetvicka, V. (1993). CR3 (CD11b, CD18): a phagocyte and NK cell membrane receptor with multiple ligand specificities and functions. *Clin Exp Immunol* **92**(2), 181-4.

Roy, D., Liston, D. R., Idone, V. J., Di, A., Nelson, D. J., Pujol, C., Bliska, J. B., Chakrabarti, S., and Andrews, N. W. (2004). A process for controlling intracellular bacterial infections induced by membrane injury. *Science* **304**(5676), 1515-8.

Russell, D. G. (1987). The macrophage-attachment glycoprotein gp63 is the predominant C3-acceptor site on *Leishmania mexicana* promastigotes. *Eur J Biochem* **164**(1), 213-21.

Russell, D. G., and Yates, R. M. (2007a). TLR signalling and phagosome maturation: an alternative viewpoint. *Cell Microbiol* **9**(4), 849-50.

Russell, D. G., and Yates, R. M. (2007b). Toll-like receptors and phagosome maturation. *Nat Immunol* **8**(3), 217; author reply 217-8.

Sacks, D., and Kamhawi, S. (2001). Molecular aspects of parasite-vector and vector-host interactions in leishmaniasis. *Annu Rev Microbiol* **55**, 453-83.

Sacks, D. L. (1989). Metacyclogenesis in *Leishmania* promastigotes. *Exp Parasitol* **69**(1), 100-3.

Sacks, D. L., Modi, G., Rowton, E., Spath, G., Epstein, L., Turco, S. J., and Beverley, S. M. (2000). The role of phosphoglycans in *Leishmania*-sand fly interactions. *Proc Natl Acad Sci U S A* **97**(1), 406-11.

Saegusa, C., Fukuda, M., and Mikoshiba, K. (2002). Synaptotagmin V is targeted to dense-core vesicles that undergo calcium-dependent exocytosis in PC12 cells. *J Biol Chem* **277**(27), 24499-505.

Saito, T., and Gale, M., Jr. (2007). Principles of intracellular viral recognition. *Curr Opin Immunol* **19**(1), 17-23.

Sakaba, T., Stein, A., Jahn, R., and Neher, E. (2005). Distinct kinetic changes in neurotransmitter release after SNARE protein cleavage. *Science* **309**(5733), 491-4.

Salaun, C., James, D. J., and Chamberlain, L. H. (2004). Lipid rafts and the regulation of exocytosis. *Traffic* **5**(4), 255-64.

Sankaranarayanan, S., and Ryan, T. A. (2001). Calcium accelerates endocytosis of vSNAREs at hippocampal synapses. *Nat Neurosci* **4**(2), 129-36.

Savill, J., Fadok, V., Henson, P., and Haslett, C. (1993). Phagocyte recognition of cells undergoing apoptosis. *Immunol Today* **14**(3), 131-6.

Schiavo, G., Gu, Q. M., Prestwich, G. D., Sollner, T. H., and Rothman, J. E. (1996). Calcium-dependent switching of the specificity of phosphoinositide binding to synaptotagmin. *Proc Natl Acad Sci U S A* **93**(23), 13327-32.

Schmidt, A., Caron, E., and Hall, A. (2001). Lipopolysaccharide-induced activation of β2-integrin function in macrophages requires Irak kinase activity, p38 mitogen-activated protein kinase, and the Rap1 GTPase. *Mol Cell Biol* **21**(2), 438-48.

Schmidt, A., and Hall, M. N. (1998). Signaling to the actin cytoskeleton. *Annu Rev Cell Dev Biol* **14**, 305-38.

Schneider, B., Schueller, C., Utermoehlen, O., and Haas, A. (2007). Lipid microdomain-dependent macropinocytosis determines compartmentation of *Afipia felis*. *Traffic* **8**(3), 226-40.

Scianimanico, S., Desrosiers, M., Dermine, J. F., Meresse, S., Descoteaux, A., and Desjardins, M. (1999). Impaired recruitment of the small GTPase rab7 correlates with the inhibition of phagosome maturation by *Leishmania donovani* promastigotes. *Cell Microbiol* **1**(1), 19-32.

Scott, C. C., Dobson, W., Botelho, R. J., Coady-Osberg, N., Chavrier, P., Knecht, D. A., Heath, C., Stahl, P., and Grinstein, S. (2005). Phosphatidylinositol-4,5-bisphosphate hydrolysis directs actin remodeling during phagocytosis. *J Cell Biol* **169**(1), 139-49.

Scott, P. (2003). Development and regulation of cell-mediated immunity in experimental leishmaniasis. *Immunol Res* **27**(2-3), 489-98.

Shin, O. H., Maximov, A., Lim, B. K., Rizo, J., and Sudhof, T. C. (2004). Unexpected Ca^{2+}-binding properties of synaptotagmin 9. *Proc Natl Acad Sci U S A* **101**(8), 2554-9.

Singh, S., and Sivakumar, R. (2004). Challenges and new discoveries in the treatment of leishmaniasis. *J Infect Chemother* **10**(6), 307-15.

Skoberne, M., Somersan, S., Almodovar, W., Truong, T., Petrova, K., Henson, P. M., and Bhardwaj, N. (2006). The apoptotic-cell receptor CR3, but not {α}vβ5, is a regulator of human dendritic-cell immunostimulatory function. *Blood* **108**(3), 947-955.

Sollner, T., Whiteheart, S. W., Brunner, M., Erdjument-Bromage, H., Geromanos, S., Tempst, P., and Rothman, J. E. (1993). SNAP receptors implicated in vesicle targeting and fusion. *Nature* **362**(6418), 318-24.

Soto, J., Arana, B. A., Toledo, J., Rizzo, N., Vega, J. C., Diaz, A., Luz, M., Gutierrez, P., Arboleda, M., Berman, J. D., Junge, K., Engel, J., and Sindermann, H. (2004). Miltefosine for new world cutaneous leishmaniasis. *Clin Infect Dis* **38**(9), 1266-72.

Southwick, F. S., and Stossel, T. P. (1983). Contractile proteins in leukocyte function. *Semin Hematol* **20**(4), 305-21.

Spath, G. F., Epstein, L., Leader, B., Singer, S. M., Avila, H. A., Turco, S. J., and Beverley, S. M. (2000). Lipophosphoglycan is a virulence factor distinct from related glycoconjugates in the protozoan parasite *Leishmania major*. *Proc Natl Acad Sci U S A* **97**(16), 9258-63.

Spath, G. F., Garraway, L. A., Turco, S. J., and Beverley, S. M. (2003a). The role(s) of lipophosphoglycan (LPG) in the establishment of *Leishmania major* infections in mammalian hosts. *Proc Natl Acad Sci U S A* **100**(16), 9536-41.

Spath, G. F., Lye, L. F., Segawa, H., Sacks, D. L., Turco, S. J., and Beverley, S. M. (2003b). Persistence without pathology in phosphoglycan-deficient *Leishmania major*. *Science* **301**(5637), 1241-3.

Spath, G. F., Schlesinger, P., Schreiber, R., and Beverley, S. M. (2009). A novel role for Stat1 in phagosome acidification and natural host resistance to intracellular infection by *Leishmania major*. *PLoS Pathog* **5**(4), e1000381.

Stevens, C. F., and Sullivan, J. M. (2003). The synaptotagmin C2A domain is part of the calcium sensor controlling fast synaptic transmission. *Neuron* **39**(2), 299-308.

Stow, J. L., Manderson, A. P., and Murray, R. Z. (2006). SNAREing immunity: the role of SNAREs in the immune system. *Nat Rev Immunol* **6**(12), 919-29.

Strzelecka-Kiliszek, A., Kwiatkowska, K., and Sobota, A. (2002). Lyn and Syk kinases are sequentially engaged in phagocytosis mediated by FcγR. *J Immunol* **169**(12), 6787-94.

Stuart, L. M., and Ezekowitz, R. A. B. (2005). Phagocytosis: Elegant Complexity. *Immunity* **22**(5), 539-550.

Stuehr, D. J. (1999). Mammalian nitric oxide synthases. *Biochim Biophys Acta* **1411**(2-3), 217-30.

Sturgill-Koszycki, S., Schlesinger, P. H., Chakraborty, P., Haddix, P. L., Collins, H. L., Fok, A. K., Allen, R. D., Gluck, S. L., Heuser, J., and Russell, D. G. (1994). Lack of acidification in *Mycobacterium* phagosomes produced by exclusion of the vesicular proton-ATPase. *Science* **263**(5147), 678-81.

Sudhof, T. C. (2002). Synaptotagmins: why so many? *J Biol Chem* **277**(10), 7629-32.

Sugita, S., Shin, O. H., Han, W., Lao, Y., and Sudhof, T. C. (2002). Synaptotagmins form a hierarchy of exocytotic $Ca^{(2+)}$ sensors with distinct $Ca^{(2+)}$ affinities. *Embo J* **21**(3), 270-80.

Sun-Wada, G. H., Tabata, H., Kawamura, N., Aoyama, M., and Wada, Y. (2009). Direct recruitment of H^+-ATPase from lysosomes for phagosomal acidification. *J Cell Sci* **122**(Pt 14), 2504-13.

Sutton, R. B., Davletov, B. A., Berghuis, A. M., Sudhof, T. C., and Sprang, S. R. (1995). Structure of the first C2 domain of synaptotagmin I: a novel Ca^{2+}/phospholipid-binding fold. *Cell* **80**(6), 929-38.

Sutton, R. B., Ernst, J. A., and Brunger, A. T. (1999). Crystal structure of the cytosolic C2A-C2B domains of synaptotagmin III. Implications for $Ca^{(+2)}$-independent snare complex interaction. *J Cell Biol* **147**(3), 589-98.

Sutton, R. B., and Sprang, S. R. (1998). Structure of the protein kinase Cβ phospholipid-binding C2 domain complexed with Ca^{2+}. *Structure* **6**(11), 1395-405.

Swanson, J. A., and Baer, S. C. (1995). Phagocytosis by zippers and triggers. *Trends Cell Biol* **5**(3), 89-93.

Swanson, J. A., and Hoppe, A. D. (2004). The coordination of signaling during Fc receptor-mediated phagocytosis. *J Leukoc Biol* **76**(6), 1093-1103.

Tauber, A. I. (2003). Metchnikoff and the phagocytosis theory. *Nat Rev Mol Cell Biol* **4**(11), 897-901.

Tjelle, T. E., Lovdal, T., and Berg, T. (2000). Phagosome dynamics and function. *Bioessays* **22**(3), 255-63.

Tolson, D. L., Turco, S. J., and Pearson, T. W. (1990). Expression of a repeating phosphorylated disaccharide lipophosphoglycan epitope on the surface of macrophages infected with *Leishmania donovani*. *Infect Immun* **58**(11), 3500-7.

Touret, N., Paroutis, P., Terebiznik, M., Harrison, R. E., Trombetta, S., Pypaert, M., Chow, A., Jiang, A., Shaw, J., Yip, C., Moore, H. P., van der Wel, N., Houben, D., Peters, P. J., de Chastellier, C., Mellman, I., and Grinstein, S. (2005). Quantitative and dynamic assessment of the contribution of the ER to phagosome formation. *Cell* **123**(1), 157-70.

Triantafilou, M., Gamper, F. G., Haston, R. M., Mouratis, M. A., Morath, S., Hartung, T., and Triantafilou, K. (2006). Membrane sorting of toll-like receptor (TLR)-2/6 and TLR2/1 heterodimers at the cell surface determines heterotypic associations with CD36 and intracellular targeting. *J Biol Chem* **281**(41), 31002-11.

Tripathi, A., and Gupta, C. M. (2003). Transbilayer translocation of membrane phosphatidylserine and its role in macrophage invasion in *Leishmania* promastigotes. *Mol Biochem Parasitol* **128**(1), 1-9.

Trombetta, E. S., and Mellman, I. (2005). Cell biology of antigen processing in vitro and in vivo. *Annu Rev Immunol* **23**, 975-1028.

Tsang, A. W., Oestergaard, K., Myers, J. T., and Swanson, J. A. (2000). Altered membrane trafficking in activated bone marrow-derived macrophages. *J Leukoc Biol* **68**(4), 487-94.

Tucker, W. C., Edwardson, J. M., Bai, J., Kim, H. J., Martin, T. F., and Chapman, E. R. (2003). Identification of synaptotagmin effectors via acute inhibition of secretion from cracked PC12 cells. *J Cell Biol* **162**(2), 199-209.

Tucker, W. C., Weber, T., and Chapman, E. R. (2004). Reconstitution of Ca^{2+}-regulated membrane fusion by synaptotagmin and SNAREs. *Science* **304**(5669), 435-8.

Turco, S. J., and Descoteaux, A. (1992). The lipophosphoglycan of *Leishmania* parasites. *Annu Rev Microbiol* **46**, 65-94.

Turco, S. J., Spath, G. F., and Beverley, S. M. (2001). Is lipophosphoglycan a virulence factor? A surprising diversity between *Leishmania* species. *Trends Parasitol* **17**(5), 223-6.

Turk, B., Dolenc, I., Lenarcic, B., Krizaj, I., Turk, V., Bieth, J. G., and Bjork, I. (1999). Acidic pH as a physiological regulator of human cathepsin L activity. *Eur J Biochem* **259**(3), 926-32.

Ullrich, H. J., Beatty, W. L., and Russell, D. G. (1999). Direct delivery of procathepsin D to phagosomes: implications for phagosome biogenesis and parasitism by *Mycobacterium*. *Eur J Cell Biol* **78**(10), 739-48.

Underhill, D. M., and Ozinsky, A. (2002). Phagocytosis of microbes: complexity in action. *Annu Rev Immunol* **20**, 825-52.

van Furth, R., and Cohn, Z. A. (1968). The origin and kinetics of mononuclear phagocytes. *J Exp Med* **128**(3), 415-35.

van Furth, R., Cohn, Z. A., Hirsch, J. G., Humphrey, J. H., Spector, W. G., and Langevoort, H. L. (1972). The mononuclear phagocyte system: a new classification of macrophages, monocytes, and their precursor cells. *Bull World Health Organ* **46**(6), 845-52.

van Kooyk, Y., and Figdor, C. G. (2000). Avidity regulation of integrins: the driving force in leukocyte adhesion. *Curr Opin Cell Biol* **12**(5), 542-7.

van Zandbergen, G., Klinger, M., Mueller, A., Dannenberg, S., Gebert, A., Solbach, W., and Laskay, T. (2004). Cutting edge: neutrophil granulocyte serves as a vector for *Leishmania* entry into macrophages. *J Immunol* **173**(11), 6521-5.

Vergne, I., Chua, J., and Deretic, V. (2003). Tuberculosis toxin blocking phagosome maturation inhibits a novel Ca^{2+}/calmodulin-PI3K hVPS34 cascade. *J Exp Med* **198**(4), 653-9.

Verhage, M., Maia, A. S., Plomp, J. J., Brussaard, A. B., Heeroma, J. H., Vermeer, H., Toonen, R. F., Hammer, R. E., van den Berg, T. K., Missler, M., Geuze, H. J., and Sudhof, T. C. (2000). Synaptic assembly of the brain in the absence of neurotransmitter secretion. *Science* **287**(5454), 864-9.

Vieira, O. V., Botelho, R. J., and Grinstein, S. (2002). Phagosome maturation: aging gracefully. *Biochem J* **366**(Pt 3), 689-704.

Vieira, O. V., Botelho, R. J., Rameh, L., Brachmann, S. M., Matsuo, T., Davidson, H. W., Schreiber, A., Backer, J. M., Cantley, L. C., and Grinstein, S. (2001). Distinct roles of class I and class III phosphatidylinositol 3-kinases in phagosome formation and maturation. *J Cell Biol* **155**(1), 19-25.

Vieira, O. V., Bucci, C., Harrison, R. E., Trimble, W. S., Lanzetti, L., Gruenberg, J., Schreiber, A. D., Stahl, P. D., and Grinstein, S. (2003). Modulation of Rab5 and Rab7 recruitment to phagosomes by phosphatidylinositol 3-kinase. *Mol Cell Biol* **23**(7), 2501-14.

Vilhardt, F., and van Deurs, B. (2004). The phagocyte NADPH oxidase depends on cholesterol-enriched membrane microdomains for assembly. *Embo J* **23**(4), 739-48.

Villadangos, J. A., and Ploegh, H. L. (2000). Proteolysis in MHC class II antigen presentation: who's in charge? *Immunity* **12**(3), 233-9.

Vray, B., Hartmann, S., and Hoebeke, J. (2002). Immunomodulatory properties of cystatins. *Cell Mol Life Sci* **59**(9), 1503-12.

Wade, N., Bryant, N. J., Connolly, L. M., Simpson, R. J., Luzio, J. P., Piper, R. C., and James, D. E. (2001). Syntaxin 7 complexes with mouse Vps10p tail interactor 1b, syntaxin 6, vesicle-associated membrane protein VAMP8, and VAMP7 in b16 melanoma cells. *J Biol Chem* **276**(23), 19820-7.

Walther, K., Diril, M. K., Jung, N., and Haucke, V. (2004). Functional dissection of the interactions of stonin 2 with the adaptor complex AP-2 and synaptotagmin. *Proc Natl Acad Sci U S A* **101**(4), 964-9.

Wanderley, J. L., Benjamin, A., Real, F., Bonomo, A., Moreira, M. E., and Barcinski, M. A. (2005). Apoptotic mimicry: an altruistic behavior in host/*Leishmania* interplay. *Braz J Med Biol Res* **38**(6), 807-12.

Wang, C. T., Bai, J., Chang, P. Y., Chapman, E. R., and Jackson, M. B. (2006). Synaptotagmin-Ca^{2+} triggers two sequential steps in regulated exocytosis in rat PC12 cells: fusion pore opening and fusion pore dilation. *J Physiol* **570**(Pt 2), 295-307.

Wang, C. T., Grishanin, R., Earles, C. A., Chang, P. Y., Martin, T. F., Chapman, E. R., and Jackson, M. B. (2001). Synaptotagmin modulation of fusion pore kinetics in regulated exocytosis of dense-core vesicles. *Science* **294**(5544), 1111-5.

Wang, C. T., Lu, J. C., Bai, J., Chang, P. Y., Martin, T. F., Chapman, E. R., and Jackson, M. B. (2003). Different domains of synaptotagmin control the choice between kiss-and-run and full fusion. *Nature* **424**(6951), 943-7.

Webb, J. L., Harvey, M. W., Holden, D. W., and Evans, T. J. (2001). Macrophage nitric oxide synthase associates with cortical actin but is not recruited to phagosomes. *Infect Immun* **69**(10), 6391-400.

Whyte, J. R., and Munro, S. (2001). The Sec34/35 Golgi transport complex is related to the exocyst, defining a family of complexes involved in multiple steps of membrane traffic. *Dev Cell* **1**(4), 527-37.

Williams, M. A., and Solomkin, J. S. (1999). Integrin-mediated signaling in human neutrophil functioning. *J Leukoc Biol* **65**(6), 725-36.

Winberg, M. E., Holm, A., Sarndahl, E., Vinet, A. F., Descoteaux, A., Magnusson, K. E., Rasmusson, B., and Lerm, M. (2009). *Leishmania donovani* lipophosphoglycan inhibits phagosomal maturation via action on membrane rafts. *Microbes Infect* **11**(2), 215-22.

Woods, J. A., Lu, Q., and Lowder, T. (2000). Exercise-induced modulation of macrophage function. *Immunol Cell Biol* **78**(5), 545-553.

Wright, S. D., and Griffin, F. M., Jr. (1985). Activation of phagocytic cells' C3 receptors for phagocytosis. *J Leukoc Biol* **38**(2), 327-39.

Wright, S. D., and Silverstein, S. C. (1982). Tumor-promoting phorbol esters stimulate C3b and C3b' receptor-mediated phagocytosis in cultured human monocytes. *J Exp Med* **156**(4), 1149-64.

Yalaoui, S., Huby, T., Franetich, J. F., Gego, A., Rametti, A., Moreau, M., Collet, X., Siau, A., van Gemert, G. J., Sauerwein, R. W., Luty, A. J., Vaillant, J. C., Hannoun, L., Chapman, J., Mazier, D., and Froissard, P. (2008). Scavenger receptor BI boosts hepatocyte permissiveness to *Plasmodium* infection. *Cell Host Microbe* **4**(3), 283-92.

Yates, R. M., Hermetter, A., and Russell, D. G. (2005). The kinetics of phagosome maturation as a function of phagosome/lysosome fusion and acquisition of hydrolytic activity. *Traffic* **6**(5), 413-20.

Yates, R. M., Hermetter, A., and Russell, D. G. (2009). Recording phagosome maturation through the real-time, spectrofluorometric measurement of hydrolytic activities. *Methods Mol Biol* **531**, 157-71.

Yates, R. M., Hermetter, A., Taylor, G. A., and Russell, D. G. (2007). Macrophage activation downregulates the degradative capacity of the phagosome. *Traffic* **8**(3), 241-50.

Yates, R. M., and Russell, D. G. (2005). Phagosome maturation proceeds independently of stimulation of toll-like receptors 2 and 4. *Immunity* **23**(4), 409-17.

Yoshinaka, K., Kumanogoh, H., Nakamura, S., and Maekawa, S. (2004). Identification of V-ATPase as a major component in the raft fraction prepared from the synaptic plasma membrane and the synaptic vesicle of rat brain. *Neurosci Lett* **363**(2), 168-72.

Zakai, H. A., Chance, M. L., and Bates, P. A. (1998). In vitro stimulation of metacyclogenesis in *Leishmania braziliensis*, *L. donovani*, *L. major* and *L. mexicana*. *Parasitology* **116 (Pt 4)**, 305-9.

Zanetti, M. (2005). The role of cathelicidins in the innate host defenses of mammals. *Curr Issues Mol Biol* **7**(2), 179-96.

Zhang, Q., Cox, D., Tseng, C. C., Donaldson, J. G., and Greenberg, S. (1998). A requirement for ARF6 in Fcγ receptor-mediated phagocytosis in macrophages. *J Biol Chem* **273**(32), 19977-81.

Zhang, X., Kim-Miller, M. J., Fukuda, M., Kowalchyk, J. A., and Martin, T. F. (2002). Ca^{2+}-dependent synaptotagmin binding to SNAP-25 is essential for Ca^{2+}-triggered exocytosis. *Neuron* **34**(4), 599-611.

Zheleznyak, A., and Brown, E. J. (1992). Immunoglobulin-mediated phagocytosis by human monocytes requires protein kinase C activation. Evidence for protein kinase C translocation to phagosomes. *J Biol Chem* **267**(17), 12042-8.

Zhu, D., Zhou, W., Liang, T., Yang, F., Zhang, R. Y., Wu, Z. X., and Xu, T. (2007). Synaptotagmin I and IX function redundantly in controlling fusion pore of large dense core vesicles. *Biochem Biophys Res Commun* **361**(4), 922-7.

Zigmond, S. H., and Hirsch, J. G. (1972). Effects of cytochalasin B on polymorphonuclear leucocyte locomotion, phagocytosis and glycolysis. *Exp Cell Res* **73**(2), 383-93.

Zilberstein, D., and Shapira, M. (1994). The role of pH and temperature in the development of *Leishmania* parasites. *Annu Rev Microbiol* **48**, 449-70.

ANNEXE 1

Large Scale Phagosome Preparation

Adrien F. Vinet[1] and Albert Descoteaux[1]

(1) Immunology and Parasitology, INRS-Institut Armand Frappier, Université du Québec, 531 des Prairies Boulevard, Laval, QC, Canada, H7V 1B7

Methods in Molecular Biology

Methods and Protocols Macrophages and Dendritic Cells

Methods and Protocols Humana Press 2009 10.1007/978-1-59745-396-7_20

Summary

Phagocytosis is the process by which cells engulf and destroy large particles such as pathogens or apoptotic cells. In this way, macrophages play a pivotal role in the resolution of microbial infections. However, many microorganisms have evolved efficient strategies to preempt the weaponry of macrophages. A better understanding of the components engaged in the phagosome formation and maturation is necessary to devise novel approaches aimed at counteracting these microbial strategies. Recently, large-scale approaches have been used to improve our understanding of phagosome functional properties by the identification of hundreds of proteins and by studying each of them.

Presently, purification of pathogen-containing phagosomes presents several technical challenges, whereas the use of latex beads to isolate phagosomes presents many advantages because this system can mimic host–pathogen interactions during phagocytosis. This system thus remains the best approach to advance our knowledge of phagosome biology, notably when used in conjunction with functional approaches. In this chapter, we outline an approach for the isolation of large-scale phagosome preparations with high degrees of purity.

Keywords Phagosome - Phagocytosis - Proteome - Isolation

Introduction

Phagocytosis by specialized cells is an efficient process for the uptake and degradation of particles larger than 0.5 μm. Newly formed phagosomes, whose membranes originate from the plasma membrane and from internal vesicles (*1*–*3*), undergo compositional modifications through a maturation process. Acquisition of microbicidal properties by maturing phagosomes requires highly regulated sequential interactions with endosomes and lysosomes, allowing for the recruitment of molecules conferring new functions to these maturing phagosomes (*4*, *5*). Despite recent major advances in the identification of phagosomal proteins, many remain to be identified and their roles remain largely unknown.

To study recruitment kinetics to phagosomes of specific effectors, a method for isolation of phagosomes was needed. A method introduced by Wetzel and Korn (*6*) and "re-discovered" by Desjardins and colleagues allowed new advances in phagosome biology. Thus latex-bead-containing phagosomes can be isolated by taking advantage of the low density of the beads, thereby permitting subsequent immunochemistry or biochemical assays. These phagosome preparations, which are devoid of major contaminants from other organelles (*7*, *8*), possess several of the functional properties required to generate a microbicidal phagolysosome (*8*, *9*), as they mature into phagolysosomes (*10*) and display degradative molecules such as hydrolases (*11*), reflecting the high level of complexity of the cellular processes involved in phagolysosome biogenesis (*7*, *8*).

Using this approach, we previously showed that PKC-α plays a role during phagosome maturation by regulating the acquisition of molecules associated with microbicidal properties (*12*). Phagosome preparations can be used to identify new proteins not previously known to be associated with these organelles and to demonstrate their role in regulating phagosome biology (*12*, *13*). Multiprotein complexes can also be isolated by immunoprecipitation and analyzed subsequently by 2D-gel electrophoresis.

Ultimately, data obtained with these approaches need to be validated by current immunochemical or biochemical methods such as western blot or confocal immunofluorescence. In this chapter, we describe methods for the large-scale isolation of phagosome preparations with high degrees of purity.

Materials

2.1 Cell Culture

1. Dulbecco's modified Eagle's medium with glutamine (DMEM).
2. DMEM is supplemented with 10% heat-inactivated (56°C, 30 min) fetal bovine serum.
3. 1% Streptamycin/penicillin from Invitrogen and 10% 10 mM HEPES, pH 7.3, from Bioshop are added.
4. Cells are grown in 100 × 15 mm dishes in a 37-°C incubator with 5% CO_2.

2.2 Phagosome Isolation and Immunoprecipitation

1. Deionized, distilled water should be used throughout these protocols (ddH_2O).
2. Tissue culture dishes of 150 × 20 mm.
3. Latex beads: 0.8 μm diameter, 10% suspension, blue dyed.
4. Protease Inhibitor Cocktail Tablets. Prepare a 25× solution by dissolving one tablet in 2 mL ddH_2O. Store at –20°C.
5. Sucrose solutions: 8.55%, 10%, 25%, 35%, and 62% (w/v), add Imidazol to each solution at a final concentration of 3 mM and 1× protease inhibitor solution. Solutions can be heated to dissolve sucrose crystals. Adjust pH to 7.4 and filter on Millipor 0.45 μm (except the 62% sucrose solution). Store at 4°C.
6. 1% NP-40 lysis buffer: 150 mM NaCl, 20 mM Tris–HCl, EDTA 10 mM, 1% (v/v) NP-40 and without protease and phosphatase inhibitors. Complete with ddH_2O and adjust pH to 7.5.
7. 1% NP-40 lysis buffer containing protease and phosphatase inhibitors: NP-40 lysis buffer with the same composition as in **item 6** but with the addition of 50 mM NaF, 10 mM $Na_4P_2O_7$, 1 mM Na_3VO_4, 1.5 mM EGTA, and 1× protease inhibitor.
8. 0.1% NP-40 lysis buffer without protease and phosphatase inhibitors: Tris–HCl,

EDTA 10 mM, 0.1% (v/v) NP-40. Complete with ddH_2O and adjust pH to 7.5.

9. Immobilized Protein A IPA300.

2.3 SDS–Polyacrylamide Gel Electrophoresis (SDS–PAGE)

1. 30.8% acrylamide/bis solution: 30% (w/v) acrylamide, 0.8% (w/v) bisacrylamide, adjust with ddH_2O. Store at 4°C.
2. 10% (w/v) SDS in ddH_2O.
3. Separating gel solution (4×): Tris–HCl 1.5 M, pH 8.8, 0.1% SDS. Complete with ddH_2O. Store at room temperature.
4. Stacking buffer (4×): 0.5 Tris–HCl M, pH 6.8, 0.1% SDS. Complete with ddH_2O. Store at room temperature.
5. Ammonium persulfate: prepare 10% (w/v) solution in ddH_2O aliquot, and freeze at –20°C. APS can be stored at 4°C several weeks.
6. N,N,N,N′-Tetramethyl-ethylenediamine (TEMED).
7. Running buffer (5×): 1.5% (w/v) Tris base, 7.2% (w/v) glycine, 0.5% SDS. Complete with ddH_2O. Store at room temperature.
8. 2× SDS-loading buffer: 60 mM Tris–HCl, pH 7.5, 2 mM EDTA, 0.2 M DTT, 20% glycerol (v/v), 2% SDS (v/v from a 10% SDS stock w/v in ddH_2O), and 0.1 mg/mL bromophenol blue (The dye allows the investigator to track the progress of the electrophoresis). Complete with ddH_2O.

2.4 Western Blotting

1. Transfer buffer: 25 mM Tris, 250 mM glycine, 20% methanol. Complete with ddH_2O. Store at room temperature.
2. Nitrocellulose membrane, 3-MM paper.
3. Ponceau S solution: 0.5% (v/v) Ponceau S, 1% (v/v) acetic acid, adjusts with ddH_2O. Store at room temperature.
4. Phosphate-buffered saline (PBS) 10×: 1.37 mM NaCl, 27 mM KCl, 100 mM Na_2HPO_4, 15 mM KH_2PO_4 (adjust to pH 7.4 if necessary). Autoclave before storage at

room temperature. Working solution is prepared by diluting one part with nine parts ddH_2O.

5. Enhanced chemiluminescent (ECL) reagents.

2.5 Two-Dimension Gels

1. Rehydration/lysis buffer: 8 M urea, 2 M thiourea, 4% (w/v) CHAPS, 40 mM DTE, 20 mM Tris, 2% (v/v) IPG buffer, 0.0025% bromophenol blue, complete with ddH_2O.
2. Agarose solution 1%: 0.188 M Tris–HCl, pH 8.8, 0.1% (w/v) SDS, 9% (v/v) glycerol, 1% (w/v) agarose, 0.005% (v/v) bromophenol blue, complete with ddH2O.
3. Equilibration buffer: 6 M urea, 2% (w/v) SDS, 30% (v/v) glycerol, and 0.1 M Tris–HCl, pH 8.8.
4. Equilibration buffer I: Equilibration buffer, 13 mM DTE.
5. Equilibration buffer II: Equilibration buffer, 2.5% (w/v) iodoacetamide.
6. After silver staining, the gel is scanned, and the protein pattern is analyzed with the Image Master 2D software (Amersham–Pharmacia Biotech).

2.6 Synchronized Phagocytosis

1. Microscope coverslips (Circles No. 1 – 0.13–0.17 mm thick; Size: 12 mm) and microscope slides (25 × 75 × 1 mm).
2. 3 μm polybeads dyed microparticles. Prepare a diluted solution by adding 0.5 mL of the stock solution in 4.5 mL of cold PBS, NaN3 0.1%. Particle number can be counted to determine concentration. Store at 4°C for several months.
3. Zymosan. Prepare a diluted solution by adding 4 mL of the stock solution in 36 mL of cold PBS 0.1% NaN3. Particle number can be counted to determine concentration. Store at 4°C during several month.
4. Sheep Red Blood Cells. Store at 4°C during 1 month. Prepare a diluted solution by adding 1 mL of the stock solution in 9 mL of cold PBS. Particle concentration should be determined. Store at 4°C up to several days.

2.7 Confocal Immunofluorescence

1. Paraformaldehyde: prepare a fresh 2% (v/v) solution in PBS for each experiment. Store at room temperature before use.
2. Blocking/permeabilization solution: 0.1% (v/v) Triton X-100, 1% (w/v) BSA, and 20% (v/v) normal goat serum, 6% (w/v) milk, 50% (v/v) fetal bovine serum. This solution must be prepared fresh for each experiment.
3. Antimouse or antirabbit AlexaFluor 488 or 568. DRAQ-5 5 mM.
4. Fluoromount-G.
5. Detailed analysis of protein localization on phagosomes is performed using an oil immersion Nikon Plan Apo 100X (N.A. 1.4) objective mounted on a Nikon Eclipse E800 microscope equipped with a Bio-Rad Radiance 2000 confocal imaging system.
6. Fluorochrome excitation is achieved using a 10-mW Argon-Krypton laser for 488 nm (Alexa488) and 568 nm (Alexa568), and a 10-mW diode laser for 638 nm (Alexa647). Images are obtained using appropriate filters, through the sequential scanning mode of the LaserSharp software (Bio-Rad Laboratories) with a Kalman filter of at least 4, and converted using MRCtoM 1.9.3 and AdobePhotoshop 6.0.

Methods

A simple technique can be used to isolate pure preparations of phagosomes from macrophage cell lines such as RAW264.7 or J774 cells (**Fig.** 1). Enrichment of specific phagosome components associated with the microbicidal activity of phagosomes, such as hydrolases (e.g., cathepsin D and S) or LAMP-1, can easily be assessed by Western blot (**Fig.** 2). Phagosome isolation has been used to identify new phagosome-associated proteins as well as to study protein modifications during phagosome maturation (*14*). After phagosome isolation and lysis, components can be separated by two-dimension gel electrophoresis, enabling the identification of proteins according to their isoelectric point on immobilized pH gradients 4–7 and their molecular weight (standard SDS–PAGE). A global view of the compositional changes that occur during phagolysosome biogenesis can be obtained by comparing proteomic patterns of samples from phagosomes isolated at various time points. More specific studies on protein complex formation can be achieved by immunoprecipitation of a known component of the phagosome proteome. Obviously, these methods are not sufficient to clearly demonstrate the presence of these newly identify components, and others methods (e.g., Western blotting and confocal microscopy) must be used to confirm and validate the proteomic data. Ultimately, it is important to determine the functions of these components during phagocytosis and phagolysosome biogenesis.

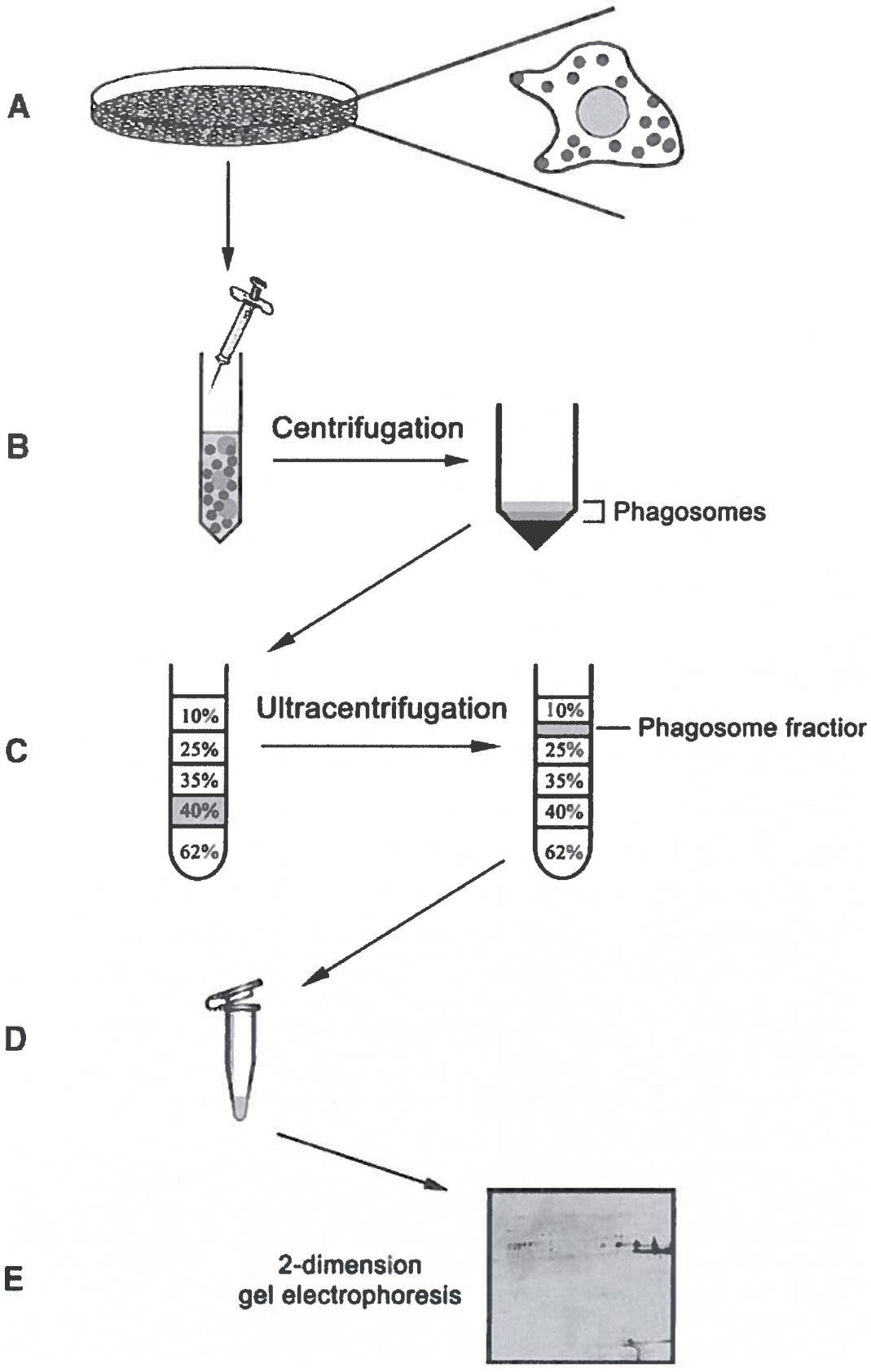
A
B
Centrifugation
Phagosomes
C
10%
25%
35%
40%
62%
Ultracentrifugation
10%
25%
35%
40%
62%
Phagosome fractior
D
E
2-dimension
gel electrophoresis

Figure 1. Scheme of phagosome purification. (**a**) *Phagocytosis.* Macrophages are allowed to internalize a large amount of latex beads. (**b**) *Homogenization.* Cells are scrapped in PBS and homogenized by vigorously ejecting the cell suspension through a needle on the wall of the tube. After centrifugation, the phagosome layer corresponding to the two clearer phases is mixed with 62% sucrose solution in order to obtain a 40% sucrose solution containing phagosomes. (**c**) *Purification.* The 40% sucrose solution containing phagosomes is laid down on a 62% sucrose solution and covered up by the sucrose solutions as shown. Ultracentrifugation allows purification of latex-beads-containing phagosomes by migration according to beads density, at the interface between the 10 and the 25% sucrose solution. (**d**) *Lysis.* Phagosome solution is then mixed with PBS and ultracentrifugation allows phagosome precipitation at the bottom of the tube. Phagosomes can be lysed. (**e**) *Analysis.* Immunoprecipitation of a protein known to be involved in complex formation is possible on phagosome lysates and separation of protein complexes can be realized by two-dimension gel electrophoresis

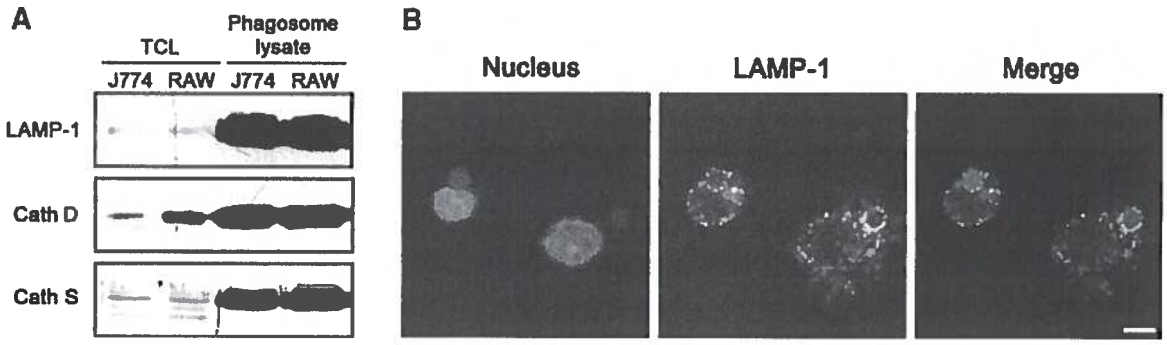

Figure 2. Enrichment of proteins in the phagosomal compartment. The lysosomal marker LAMP-1 and the hydrolases Cathepsin D and S are massively acquired during the late steps of phagosomal maturation. (**a**) Phagosomes were obtained after a 90-min phagocytosis. 15 μg of total cell lysate (TCL) and 30 μg of phagosome lysate from RAW264.7 and J774 cell lines were loaded on a 10% acrylamide gel, transferred, and blotted with an anti-LAMP-1, an anti-Cath D, and an anti-Cath S antibody. (**b**) Immunofluorescence analysis by confocal microscopy shows recruitment of LAMP-1 on phagosomes. RAW264.7 cells were allowed to internalize fluorescent latex beads for 90 min before fixation. Cells were stained with an anti-LAMP-1 antibody and an antirat coupled with a 488 fluorochrome (Molecular Probes). Nuclei were stained using DRAQ-5 reagent (Biostatus, Leicestershire). Bar, 3 μm

3.1 Phagosome Isolation

1. Adherent macrophages (5 × 107 per 150 × 20 mm tissue culture dish) are incubated 24 h, reaching confluence between 70 and 80%.
2. Vortex latex beads vigorously before use to disrupt aggregates. Prior to initiating internalization, medium is gently removed and cells are incubated at 4°C for 10 min in the presence of 0.8-μm-diameter latex beads diluted 1:50 in 10 mL of complete medium, to allow beads to make contact with the cell monolayer. Cells and beads are then transferred to 37°C and incubated for 90 min to allow internalization to take place (*see* **Note 1**).
3. Gently wash cells three times with warm medium to remove noninternalized beads. During washes, dishes are put on a shaker. After this step, cells can be observed by light microscopy to verify the presence of a high number of bead containing phagosomes (black points in cells).
4. To obtain mature phagolysosomes, cells are further incubated for a chase period of 60 min in fresh medium at 37°C. Cells are then washed (3 × 5 min) in PBS at 4°C on a shaker, scraped with a rubber policeman in 4 mL of ice-cold PBS, and transferred to a 15-mL Falcon tube (one Falcon tube can accommodate cells from two dishes).
5. Cells are washed twice in 8 mL ice-cold PBS (centrifugation at 1,500 rpm for 3 min) to remove noninternalized beads. A third wash is performed in 2 mL of homogenization buffer (8.5% sucrose).
6. Cells are pelleted in 1 mL homogenization buffer and homogenized on ice with a 1 mL syringe using a 22-G needle (12–15 strokes) in the 15-mL Falcon tube.
7. Homogenization is carried out until about 90% of cells are broken without major breakage of nuclei, as monitored by light microscopy.
8. Cell extracts are pelleted in a 15-mL Falcon tube at 2,000 rpm for 5 min at 4°C. The supernatant (about 1 mL) contains the phagosomes (**Fig.** 1). The phagosome suspension is carefully removed and is brought to 40% sucrose by adding an equal volume of a 62% sucrose solution in a 2-mL microfuge tube. Mix thoroughly with a pipet.

9. This 40% sucrose phagosome suspension is gently loaded on top of a 3-mL cushion of 62% sucrose, followed by the addition of solutions of 2 mL of 35% sucrose, 2 mL of 25% sucrose, and 2 mL of 10% sucrose.
10. Centrifugation is performed at 4°C in a swinging bucket rotor (SW41; Beckman Instruments) for 1 h at 100,000 × *g*.
11. Phagosomes (a band colored in blue) are carefully collected at the interface of the 10% and 25% sucrose layers and resuspended in 12 mL cold PBS containing 1× protease inhibitors. Phagosomes from two tubes can be pooled for the next centrifugation.
12. The phagosomes are pelleted at 4°C by a 15-min centrifugation at 40,000 × *g* in an SW41 rotor.
13. Supernatant is removed and the phagosome pellet is resuspended in 40–50 µL of ice-cold 1% NP-40 lysis buffer containing protease and phosphatase inhibitors (*see* **Note 2**). It is important to dry out the wall of the tube before adding lysis buffer to remove PBS 1×. Place on ice for 10 min and store at –20°C. The protein concentration of the phagosome preparations can be determined using the Pierce BCA protein assay reagent or any other standardized protein assay system.

3.2 Immunoprecipitation

1. Aliquot 50 µL of immobilized Protein A into four separate 1.5-mL microfuge tubes (tubes 1, 2, 3, and 4) and equilibrate three times with 500 µL 1% NP-40 lysis buffer without protease and phosphatase inhibitors (i.e., add lysis buffer; mix gently, spin down, and remove supernatant).
2. Tubes 1 and 2 are used for antibody binding: add 500 µL of 1% NP-40 lysis buffer without protease and phosphatase inhibitors and 5 µg of the antibody. Incubate for 3–4 h at 4°C in a rotary shaker.
3. Tubes 3 and 4 are used for preclearing phagosome extracts: add 700 µg per tube of phagosome extract in 0.5 mL total (adjust with 1% NP-40 lysis buffer with protease and phosphatase inhibitors if necessary) to equilibrated beads and incubate for 1 h at 4°C in a rotary shaker in order to eliminate nonspecific binding.

4. After incubation with the antibody, beads from tubes 1 and 2 are washed three times in 500 µL of 1% NP-40 lysis buffer without protease and phosphatase inhibitors by mixing gently, spinning down, and removing supernatant.
5. Transfer precleared phagosome extracts from tubes 3 and 4 into tubes 1 and 2 containing antibody linked to beads. Incubate overnight at 4°C in a rotary shaker.
6. Spin tubes 1 and 2 down and remove supernatants; wash the beads twice with 1% NP-40 lysis buffer without protease and phosphatase inhibitors and twice with lysis buffer 0.1% NP-40 without protease and phosphatase inhibitors.
7. Resuspend the beads in a small volume of rehydration/lysis buffer (cf. **Subheading 2.5 , step 1**), pool the contents of the two microfuge tubes, spin down and resuspend beads in 450 µL of rehydration/lysis buffer.
8. Vortex 1 h at room temperature before loading the samples for two-dimensional gel electrophoresis.

3.3 Two-Dimensional Gel Electrophoresis

1. Proteins are first separated according to their isoelectric points on 24-cm linear immobilized pH-gradient strips. Remove a dry strip of pH 4–7 from –20°C and allow to equilibrate at room temperature for 15 min.
2. Load the sample into the rehydration tray, leave about 1 cm at each end.
3. Note the basic end of the strip and position it at the left side of the tray.
4. Place the IPG strip gel-side down on the top of the sample; verify that there are no bubbles.
5. Completely overlay with mineral oil, cover the tray with lid, and leave at room temperature overnight.
6. Cut two electrode papers of 1.5 cm and wet with ddH_2O. Mop up until the papers become semidry.
7. Take out IPG strip and lay it down on the filter paper gel-side at top to remove oil excess.

8. Place the IPG strip in a strip holder gel-side on top and the acid side (+) at the positive side. The strip must be placed between the electrodes.
9. Lay down electrode papers lengthwise at 0.5 cm of the gel end for both sides, and gently lay down electrodes on the last 0.5 cm of the electrode paper in order that they are aligned properly.
10. Place strip holder cover and close the apparatus to test the voltage for 500 V. If voltage fails, verify that electrode papers are on the strip and that the electrode papers are not too dry.
11. Remove cap and completely cover the strip with mineral oil.
12. First dimension separation according to the isoelectric point.
13. Replace strip holder cover, close the apparatus, and proceed with the migration. At this step, voltage time volt-hours (Vh) will total approximately 106,000 Vh according to the following program:

500 V	**15 min**
1,000 V	30 min
2,000 V	30 min
3,000 V	30 min
4,000 V	30 min
5,000 V	60 min
6,000 V	60 min
8,000 V	Overnight

14. The strip is then rapidly taken out and after excess oil is drained out on filter paper, is placed in a glass tube containing Equilibration Buffer I. Incubate 10 min on a shaker at room temperature.
15. Remove the strip and place it in a glass tube containing Equilibration buffer II for 5 min at room temperature on a shaker. During this step, melt agarose solution which can be stored in a boiling hot beaker to keep it liquid.

16. Second dimension separation according to molecular weight:

    Prepare a 10% SDS–polyacrylamide gel (cf. **Subheading 3.5**) before the equilibration steps so that it can polymerize during the equilibration steps. Mix 7.9 mL H_2O, 6.7 mL 30.8% acrylamide/bis, 5 mL 1.5 M Tris–HCl, pH 8.8, 200 µL 10% SDS, 200 µL 10% ammonium persulfate, and 10 µL TEMED. Leave about 1.5 cm from the top for the strip.

17. Overlay with 0.1% SDS to avoid drying of the gel and the gel should polymerize in about 20–30 min.

18. Remove the 0.1% SDS solution and rinse the top of the gel twice with ddH_2O. Mop up remaining water with a filter paper.

19. Place the strip on the top of the gel, leaving space for agarose. Place the acid side on the left. Add two small filter papers saturated with molecular weight marker at both ends of the gel.

20. Add the agarose solution and quickly and with care push the strip in until it touches the polyacrylamide separation gel. Take care that the plastic-side of the gel remains pressed on the glass. Avoid bubbles between the strip and the separation gel. Let the agarose solidify.

21. Add running buffer and proceed with the migration by running the gel at 200 V. This step takes several hours.

22. Stop the migration as soon as the colorimetric marker leaves the gel. Disassemble the migration system, remove the agarose and the strip, take the gel out, and identify the pH by piercing at both ends.

3.4 Coomassie Blue Coloration, Nonfixing Silver Stain, and Protein Extraction

3.4.1 Coomassie Blue (see Note 3)

1. Wash the gel three times with ddH_2O (5 min each).
2. Proceed as described for the Colloidal Blue Staining Kit.

3.4.2 Nonfixing silver stain.

1. Always use freshly prepared solutions and perform all steps at room temperature with constant gentle agitation. Place the polyacrylamide gel in a plastic container.
2. Incubate the gel for 30 min in fixation solution consisting of 125 mL ethanol, 12.5 mL glacial acetic acid, and 112.5 mL ddH_2O. For a double fixation, repeat this step for an additional 30 min.
3. Pour out fixing solution and wash the gel for 10 min in a mixed solution of 125 mL ethanol and 125 mL ddH_2O. Then wash twice with ddH_2O (10 min each wash).
4. Incubate the gel for 5 min in a sensitizing solution: 0.02 g sodium thiosulfate in 250 mL ddH_2O.
5. Pour out sensitizing solution and wash the gel three times with ddH_2O (5 min each wash).
6. For the silver reaction, incubate the gel for 30 min in silver solution: 0.25 g silver nitrate and ddH_2O to a volume of 250 mL.
7. Pour out silver solution and wash the gel once with ddH_2O for 1 min.
8. Incubate the gel in developing solution: 5 g sodium carbonate, 0.25 mL formaldehyde (37% w/v) and ddH_2O until 250 mL. Do not allow the gel to overstain, and once the gel spots become visible, stop the reaction.
9. Briefly wash the gel in ddH_2O and stop the reaction by incubating the gel in a solution of 12.5 mL acetic acid and 237.5 mL ddH_2O for 5 min. The gel can be stored in a solution of 2.5 mL acetic acid and 247.5 mL ddH_2O for several days.

3.4.2 Extraction of protein spots.

1. For the following steps, it is absolutely necessary to work with latex gloves, bonnet, mask, and any additional protection to prevent keratin contamination of the samples. Wash all components with ethanol.
2. Put the gel between two acetate sheets wetted with ultrapure water.

3. Scan the gel and number the protein spots.
4. Lay down the gel between acetate sheets on a plexiglass tray
5. Add ultrapure water on the gel.
6. Extract each protein spot with a scalpel. Wash the scalpel between each extraction with ethanol and ultrapure H_2O. Place pieces of gel containing proteins in wells of a 96-well plate. The plate should be prepared beforehand by filling wells with 0.2 mL of ultrapure H_2O, 1% acetic acid.
7. Cover and seal the plate with parafilm. Samples can be stored at 4°C for several days.
8. The samples are now suitable to be analyzed by matrix-assisted laser desorption/ionization-time-of-flight mass spectrometry.

3.5 SDS–Polyacrylamide Mini-Gel Electrophoresis (SDS–PAGE)

1. Prepare a 10% separating gel by mixing 4 mL H_2O, 3.3 mL 30.8% acrylamide/bis, 2.5 mL 4× separating gel solution, 100 µL 10% ammonium persulfate, and 5 µL TEMED. Let about 1.5 cm from the top for the stacking gel.
2. Overlay with 0.1% SDS to avoid drying of the gel which should polymerize in 20–30 min.
3. Remove the 0.1% SDS solution and rinse the top of the gel twice with ddH_2O.
4. Prepare the stacking gel by mixing 3 mL H_2O, 650 µL 30.8% acrylamide/bis, 1.25 mL 4× Tris stacking buffer, 25 µL 10% ammonium persulfate, and 5 µL TEMED. Rinse the top of the separating gel a final time with 0.5 mL of the stacking gel solution, then add the stacking solution over the separating gel, and insert the comb. The gel should polymerize in about 20–30 min.
5. Prepare the running buffer by diluting 160 mL of the 5× running buffer with 640 mL H_2O and mix.
6. When the stacking gel has set, remove the comb and assemble the gel unit.
7. Add running buffer. It is important to carefully wash twice the wells with running buffer by using a 25-G needle before loading of the samples.
8. The protein concentration of each sample has to be known and adjusted to have the

same amount of protein in all samples. Adjustment may be done by adding lysis buffer. Be careful not to add too much lysis buffer because the protein sample is subsequently diluted 1:1 (v/v) with 2× SDS-loading buffer, and the final volume should not exceed 15 µL for loading.

9. Incubate samples for 5 min at 100°C, perform a quick spin, mix and load 15 µL of each sample in a well. One well must include molecular weight markers prepared according to the supplier's instructions.
10. Complete the assembly of the gel unit and connect to a power supply. The gel can be run at 100 V.
11. When the dye front reaches the bottom of the gel, transfer to the nitrocellulose membrane may be carried out (the dye fronts can be run off the gel if desired).

3.6 Western Blotting

1. Make sure that all parts of the apparatus are clean.
2. Cut three pieces of Whatman 3-MM filter paper barely larger than the gel and prewet with transfer buffer. Lay down the three pieces on the transfer apparatus. A sheet of the nitrocellulose barely larger than the separating gel size is laid on the surface of the 3-MM paper to wet the membrane. Pour transfer buffer onto the membrane and remove any air bubbles.
3. After the samples have been separated by SDS–PAGE, the gel unit is disassembled. The stacking gel is removed and one corner of the separating gel is cut to track its orientation. The separating gel is then laid on the top of the nitrocellulose membrane and the gel surface is moistened with transfer buffer.
4. Three additional pieces of 3-MM paper of the appropriate size are submerged in the transfer buffer and carefully laid on top of the gel. It is also extremely important to make sure of the proper orientation of the resulting sandwich, or proteins will be lost into the buffer (components must be placed in the following order: three pieces of 3-MM paper, nitrocellulose membrane, polyacrylamide gel, and finally three other pieces of 3-MM paper. Remove any bubbles after each step). Close the transfer

system.

5. Set the power supply at 15 V for 30 min.
6. After the transfer, the gel and the membrane are disassembled from the apparatus and the membrane is promptly rinsed with ddH_2O.
7. The membrane is then stained with Ponceau S for 1 min at room temperature to visualize the sample proteins and to assess the efficiency of the transfer. Red protein bands should become visible after removing excess dye with ddH_2O. The positions of the lanes and the markers are marked by gently pricking the membrane with the point of a needle.
8. Destain the membrane completely by rinsing in PBS on a shaker for about 10 min (*see* **Note 4**).
9. Block with blocking buffer (PBS-0.1% Tween, 5% BSA) for 2 h at room temperature or overnight at 4°C on a shaker (*see* **Note 5**).
10. Wash with PBS-0.1% Tween four times for 15 min each on a shaker.
11. Incubate the membrane with primary antibody diluted in 15 mL PBS + 5%BSA for 3 h at room temperature on a shaker or overnight at 4°C.
12. Wash with PBS-0.1% Tween four times for 15 min each on a shaker.
13. Incubate the membrane with the secondary antibody diluted in 15 mL PBS + 5% BSA for 45 min at room temperature on a shaker.
14. Wash with PBS-0.1% Tween four times for 15 min each on a shaker.
15. Following the instructions provided with the ECL kit, mix 5 mL Solution 1 and 5 mL Solution 2 immediately before use and incubate the blot for exactly 1 min (two blots can successively be developed with same solution) which is rotated by hand to ensure entire coverage of the membrane (*see* **Note 6**).
16. The blot is placed on an acetate sheet and promptly covered up with Saran wrap to avoid drying of the membrane. Keep out of light.
17. In the darkroom, the acetate-containing membrane is placed immediately in an autoradiography cassette with a medical film for a suitable exposure time (start from 30-s exposures to 45 min).

3.7 Preparation of Samples for Immunofluorescence

3.7.1 Synchronized Phagocytosis

1. Place round coverslips into wells of a 24-well tissue culture plate. The coverslips are sterilized or kept in alcohol until required. Coverslips kept in alcohol are dried in a sterile environment and dropped into each well with sterile forceps.
2. Harvest and resuspend macrophages in complete DMEM at 1–4 × 105 cells/mL. Seed 0.5 mL into each well of the 24-well plate and incubate at least 2 h or overnight at 37°C in 5% CO2 to allow cells to adhere to the coverslip.
3. During cell adherence, particles to be internalized are opsonized if necessary. Usually, the particle-to-cell ratio is 10:1 or 20:1.
4. Zymosan particles are laid down in a microfuge tube, spun 1 min at 14,000 × *g*, and resuspended in cold, sterile PBS 1× solution twice for washing (aspirate the supernatant carefully using a 26-G needle). Particles can be opsonized in 150 μL of pure mouse serum or in 0.3–0.5 mL of diluted mouse serum in sterile PBS 1× solution. Do not dilute the serum to less than 10%. Incubate 40 min to 1 h at 37°C for complement opsonization. The tube is shaken by inversion three or four times during incubation to allow optimal particle opsonization.
5. For IgG opsonization, sheep red blood cells (SRBC) or beads can be used.
6. SRBC are laid down in a 15-mL Falcon tube and centrifugated at 1,000 rpm for 5 min at 4°C and resuspended twice in cold sterile PBS for washing. After the last wash, SRBC are suspended in 7 mL sterile cold PBS and 7 μL of SRBC-specific IgG at 1 μg/μL (from mouse or rabbit) is added. Incubate SRBC 30 min in a rotary shaker at 4°C.
7. Beads are added to a microfuge tube, centrifugated 1 min at 14,000 × *g*, and resuspended in sterile cold PBS twice for washing (aspirate the supernatant carefully with a 26-G needle). After the last wash, beads are suspended in 1 mL 50 mM Tris–HCl, pH 9, and 1 μl of IgG at 1 μg/μL (from mouse or rabbit) is added. Incubate beads for 40 min in a rotary shaker at 4°C.

8. After opsonization, wash three times with cold sterile PBS 1× solution. For SRBC, gently shake the tube after centrifugation to avoid cell lysis. For zymosan and latex beads, particles can be vigorously shaken after centrifugation to avoid aggregate formation. Resuspend particles in an appropriate volume of complete DMEM and keep at 4°C until phagocytosis (keeping in mind that a volume of 300 μL will be added to each well for phagocytosis).
9. Once macrophages are ready for phagocytosis, remove the medium by gently aspirating the contents of each well. Wash cells twice with 0.5 mL cold DMEM. Keep plates at 4°C for 5 min before adding particles.
10. Remove medium and gently add 300 μL of the cold particle suspension. Keep the plates at 4°C during 10 min to allow particle deposition and their binding to the cells.
11. Remove unbound particles by three washes with cold DMEM and incubate cells at 37°C for 90 min for internalization.
12. Coverslips are then washed three times with PBS to eliminate noninternalized particles and cells are fixed in PBS2% paraformaldehyde for 10 min at room temperature.
13. Wash coverslips twice with PBS and incubate at room temperature for 10 min before a final wash (see **Note 8**).
14. Plates containing coverslips can be stored at 4°C for 1 month before immunofluorescence staining. Be careful that coverslips are always covered with cold PBS.

3.7.2 Confocal Immunofluorescence

1. For each subsequent step involving incubation of coverslips containing adherent cells (i.e., blocking/permeabilization, first and second antibody incubation), place a piece of parafilm in the bottom of a 150 × 20 mm dish (Sarstedt). The outside of the dish (both top and bottom) must be fully covered beforehand with aluminum foil. Place 50–80 μL of the incubation solution (e.g., blocking/permeabilization solution, first antibody solution, or second antibody solution) into the dish, and using forceps gently place

each coverslip with the cells face down in the desired solution. Do not press on coverslips. After incubation, carefully remove coverslips with forceps, and immerse them in wells containing PBS 1× solution. Keep the cell-side face up.

2. To permeabilize cells and block nonspecific surface Fcγ-receptors, promptly drain excess PBS and incubate in the blocking/permeabilization buffer at room temperature for 15–20 min.
3. Coverslips are then dipped in PBS and washed three times. Washes have to be gentle to maintain cell attachment.
4. Excess PBS is promptly drained from the coverslips, and the primary antibody solution (usually at a dilution of 1/1,000 to 1/100 in PBS) is added for 1 h at room temperature.
5. Cells are gently washed three times in PBS.
6. Coverslips are promptly drained for excess PBS and incubated with a solution containing the secondary antibody (1/500 dilution) coupled to an Alexa fluorochrome (Alexa 488, 568, or 647 for example) for 30 min at room temperature. A nuclear stain such as DRAQ 5 can be used and is diluted at 1/400 in the secondary antibody solution. From this step, be careful to protect samples from direct light to avoid bleaching.
7. Samples are gently washed three times and are ready to be mounted.
8. Coverslips are promptly drained for excess PBS and are mounted on glass slides with Fluoromount-G. Drops of Fluoromount-G are placed on glass slides and coverslips are laid down cell-face in contact with fluoromount. Excess fluoromount is removed and slides are then sealed with nail polish on the edges of coverslips.
9. Freshly mounted slides must be dried at room temperature and protected from light for 24 h before use. Slides can be stored for up a month at 4°C in the dark.

Notes

1. Depending on the experiments, various internalization time points are possible during phagosome isolation, and the chase period must be adapted to the protein component of interest, which may be recruited to phagosomes at early or later time points after initiation of phagocytosis. Internalization between 30 and 120 min is often used, and the chase period can cover a period from 30 min to more than 2 h. For example, to observe the early recruitment of a specific protein on phagosomes, cells and medium containing beads can be kept at 4°C for 20 min and then placed at 37°C for 30 min before phagosome isolation.
2. Phagosomes can be resuspended in ice-cold lysis buffer containing 150 mM NaCl, 20 mM Tris–HCl, pH 7.5, and 1% NP-40, but 1% Triton X-100 can be used instead of NP-40.
3. Coomassie blue staining is preferable if proteins are visible on acrylamide gel before sample isolation and mass spectrometry identification.
4. TBS can be used instead of PBS according to the manufacturer providing the first antibody.
5. Nitrocellulose membranes can be blocked with blocking buffer containing milk (PBS 0.1% Tween, 5% (w/v) milk) for 2 h at room temperature or overnight at 4°C on a shaker.
6. If the signal is too strong during exposure, the ECL solutions can be diluted (from 1/2 to 1/20) in ddH_2O as long as solutions 1 and 2 remain at the ratio of 1:1.
7. If the silver stain is not sufficient, the gel can be incubated in the silver solution overnight at room temperature with agitation.
8. During preparation of coverslips for immunofluorescence, observation by light microscopy after washing is advised in order to verify that cells have not detached during washing. Do not expose samples to light after incubation with the secondary antibody.

Acknowledgments

We are grateful to John Derek Ng Yan Hing for developing phagosome isolation procedures in our laboratory. This work was supported by the Canadian Institutes for Health Research. AD is the holder of a Canada Research Chair. AV was partly supported by a fellowship from the Fondation Armand-Frappier.

References

1. Bajno L, Peng XR, Schreiber AD, Moore HP, Trimble WS, Grinstein S. (2000). Focal exocytosis of VAMP3-containing vesicles at sites of phagosome formation. J Cell Biol; 149(3):697–706

2. Braun V, Fraisier V, Raposo G, (2004). TI-VAMP/VAMP7 is required for optimal phagocytosis of opsonised particles in macrophages. EMBO J; 23(21):4166–4176

3. Gagnon E, Duclos S, Rondeau C, (2002). Endoplasmic reticulum-mediated phagocytosis is a mechanism of entry into macrophages. Cell; 110(1):119–131

4. Jahraus A, Tjelle TE, Berg T, (1998). In vitro fusion of phagosomes with different endocytic organelles from J774 macrophages. J Biol Chem; 273(46):30379–30390

5. Vieira OV, Botelho RJ, Grinstein S. (2002). Phagosome maturation: aging gracefully. Biochem J; 366(Pt 3):689–704

6. Wetzel MG, Korn ED. (1969). Phagocytosis of latex beads by *Acahamoeba castellanii* (Neff). 3. Isolation of the phagocytic vesicles and their membranes. J Cell Biol; 43(1):90–104

7. Desjardins M, Huber L, Parton R, Griffiths G. (1994) Biogenesis of phagolysosomes proceeds through a sequential series of interactions with the endocytic apparatus. J Cell Biol; 124(5):677–688

8. Desjardins M, Celis J, van Meer G, (1994). Molecular characterization of phagosomes. J Biol Chem; 269(51):32194–32200

9. Desjardins M, Nzala N, Corsini R, Rondeau C. (1997) Maturation of phagosomes is accompanied by changes in their fusion properties and size-selective acquisition of solute materials from endosomes. J Cell Sci; 110(18):2303–2314

10. Desjardins M. Biogenesis of phagolysosomes: the 'kiss and run' hypothesis. (1995). Trends Cell Biol; 5(5):183–186

11. Claus V, Jahraus A, Tjelle T, (1998). Lysosomal enzyme trafficking between phagosomes, endosomes, and lysosomes in J774 macrophages. Enrichment of cathepsin H in early endosomes. J Biol Chem; 273(16):9842–9851

12. Ng Yan Hing JD, Desjardins M, Descoteaux A. (2004) Proteomic analysis reveals a role for protein kinase C-α in phagosome maturation. Biochem Biophys Res Commun; 319(3):810–816

13. Garin J, Diez R, Kieffer S, (2001). The phagosome proteome: insight into phagosome functions. J Cell Biol; 152(1):165–180

14. Defacque H, Bos E, Garvalov B, (2002). Phosphoinositides regulate membrane-dependent actin assembly by latex bead phagosomes. Mol Biol Cell; 13(4):1190–1202

Chapter 20

Large-Scale Phagosome Preparation

Adrien F. Vinet and Albert Descoteaux

Summary

Phagocytosis is the process by which cells engulf and destroy large particles such as pathogens or apoptotic cells. In this way, macrophages play a pivotal role in the resolution of microbial infections. However, many microorganisms have evolved efficient strategies to preempt the weaponry of macrophages. A better understanding of the components engaged in the phagosome formation and maturation is necessary to devise novel approaches aimed at counteracting these microbial strategies. Recently, large-scale approaches have been used to improve our understanding of phagosome functional properties by the identification of hundreds of proteins and by studying each of them.

Presently, purification of pathogen-containing phagosomes presents several technical challenges, whereas the use of latex beads to isolate phagosomes presents many advantages because this system can mimic host–pathogen interactions during phagocytosis. This system thus remains the best approach to advance our knowledge of phagosome biology, notably when used in conjunction with functional approaches. In this chapter, we outline an approach for the isolation of large-scale phagosome preparations with high degrees of purity.

Key words: Phagosome, Phagocytosis, Proteome, Isolation.

1. Introduction

Phagocytosis by specialized cells is an efficient process for the uptake and degradation of particles larger than 0.5 μm. Newly formed phagosomes, whose membranes originate from the plasma membrane and from internal vesicles *(1–3)*, undergo compositional modifications through a maturation process. Acquisition of microbicidal properties by maturing phagosomes requires highly regulated sequential interactions with endosomes and lysosomes, allowing for the recruitment of molecules conferring new functions to these maturing phagosomes *(4, 5)*. Despite recent major

Neil E. Reiner (ed.), *Macrophages and Dendritic Cells*, Methods In Molecular Biology, vol. 531

DOI: 10.1007/978-1-59745-396-7_20

advances in the identification of phagosomal proteins, many remain to be identified and their roles remain largely unknown.

To study recruitment kinetics to phagosomes of specific effectors, a method for isolation of phagosomes was needed. A method introduced by Wetzel and Korn *(6)* and "re-discovered" by Desjardins and colleagues allowed new advances in phagosome biology. Thus latex-bead-containing phagosomes can be isolated by taking advantage of the low density of the beads, thereby permitting subsequent immunochemistry or biochemical assays. These phagosome preparations, which are devoid of major contaminants from other organelles *(7, 8)*, possess several of the functional properties required to generate a microbicidal phagolysosome *(8, 9)*, as they mature into phagolysosomes *(10)* and display degradative molecules such as hydrolases *(11)*, reflecting the high level of complexity of the cellular processes involved in phagolysosome biogenesis *(7, 8)*.

Using this approach, we previously showed that PKC-α plays a role during phagosome maturation by regulating the acquisition of molecules associated with microbicidal properties *(12)*. Phagosome preparations can be used to identify new proteins not previously known to be associated with these organelles and to demonstrate their role in regulating phagosome biology *(12, 13)*. Multiprotein complexes can also be isolated by immunoprecipitation and analyzed subsequently by 2D-gel electrophoresis. Ultimately, data obtained with these approaches need to be validated by current immunochemical or biochemical methods such as western blot or confocal immunofluorescence. In this chapter, we describe methods for the large-scale isolation of phagosome preparations with high degrees of purity.

2. Materials

2.1. Cell Culture

1. Dulbecco's modified Eagle's medium with glutamine (DMEM).
2. DMEM is supplemented with 10% heat-inactivated (56°C, 30 min) fetal bovine serum.
3. 1% Streptamycin/penicillin from Invitrogen and 10% 10 mM HEPES, pH 7.3, from Bioshop are added.
4. Cells are grown in 100 × 15 mm dishes in a 37-°C incubator with 5% CO_2.

2.2. Phagosome Isolation and Immunoprecipitation

1. Deionized, distilled water should be used throughout these protocols (ddH_2O).
2. Tissue culture dishes of 150 × 20 mm.

3. Latex beads: 0.8 µm diameter, 10% suspension, blue dyed.
4. Protease Inhibitor Cocktail Tablets. Prepare a 25× solution by dissolving one tablet in 2 mL ddH_2O. Store at –20°C.
5. Sucrose solutions: 8.55%, 10%, 25%, 35%, and 62% (w/v), add Imidazol to each solution at a final concentration of 3 mM and 1× protease inhibitor solution. Solutions can be heated to dissolve sucrose crystals. Adjust pH to 7.4 and filter on Millipor 0.45 µm (except the 62% sucrose solution). Store at 4°C.
6. 1% NP-40 lysis buffer: 150 mM NaCl, 20 mM Tris–HCl, EDTA 10 mM, 1% (v/v) NP-40 and without protease and phosphatase inhibitors. Complete with ddH_2O and adjust pH to 7.5.
7. 1% NP-40 lysis buffer containing protease and phosphatase inhibitors: NP-40 lysis buffer with the same composition as in **item 6** but with the addition of 50 mM NaF, 10 mM $Na_4P_2O_7$, 1 mM Na_3VO_4, 1.5 mM EGTA, and 1× protease inhibitor.
8. 0.1% NP-40 lysis buffer without protease and phosphatase inhibitors: Tris–HCl, EDTA 10 mM, 0.1% (v/v) NP-40. Complete with ddH_2O and adjust pH to 7.5.
9. Immobilized Protein A IPA300.

2.3. SDS–Polyacrylamide Gel Electrophoresis (SDS–PAGE)

1. 30.8% acrylamide/bis solution: 30% (w/v) acrylamide, 0.8% (w/v) bisacrylamide, adjust with ddH_2O. Store at 4°C.
2. 10% (w/v) SDS in ddH_2O.
3. Separating gel solution (4×): Tris–HCl 1.5 M, pH 8.8, 0.4% SDS. Complete with ddH_2O. Store at room temperature.
4. Stacking buffer (4×): 0.5 Tris–HCl M, pH 6.8, 0.4% SDS. Complete with ddH_2O. Store at room temperature.
5. Ammonium persulfate: prepare 10% (w/v) solution in ddH_2O aliquot, and freeze at –20°C. APS can be stored at 4°C several weeks.
6. N,N,N,N′-Tetramethyl-ethylenediamine (TEMED).
7. Running buffer (5×): 1.5% (w/v) Tris base, 7.2% (w/v) glycine, 0.5% SDS. Complete with ddH_2O. Store at room temperature.
8. 2× SDS-loading buffer: 60 mM Tris–HCl, pH 7.5, 2 mM EDTA, 0.2 M DTT, 20% glycerol (v/v), 2% SDS (v/v from a 10% SDS stock w/v in ddH_2O), and 0.1 mg/mL bromophenol blue (The dye allows the investigator to track the progress of the electrophoresis). Complete with ddH_2O.

2.4. Western Blotting

1. Transfer buffer: 25 mM Tris, 250 mM glycine, 20% methanol. Complete with ddH_2O. Store at room temperature.

2. Nitrocellulose membrane, 3-MM paper.
3. Ponceau S solution: 0.5% (v/v) Ponceau S, 1% (v/v) acetic acid, adjusts with ddH_2O. Store at room temperature.
4. Phosphate-buffered saline (PBS) 10×: 1.37 mM NaCl, 27 mM KCl, 100 mM Na_2HPO_4, 15 mM KH_2PO_4 (adjust to pH 7.4 if necessary). Autoclave before storage at room temperature. Working solution is prepared by diluting one part with nine parts ddH_2O.
5. Enhanced chemiluminescence (ECL) reagents.

2.5. Two-Dimension Gels

1. Rehydration/lysis buffer: 8 M urea, 2 M thiourea, 4% (w/v) CHAPS, 40 mM DTE, 20 mM Tris, 2% (v/v) IPG buffer, 0.0025% bromophenol blue, complete with ddH_2O.
2. Agarose solution 1%: 0.188 M Tris–HCl, pH 8.8, 0.1% (w/v) SDS, 9% (v/v) glycerol, 1% (w/v) agarose, 0.005% (v/v) bromophenol blue, complete with ddH2O.
3. Equilibration buffer: 6 M urea, 2% (w/v) SDS, 30% (v/v) glycerol, and 0.1 M Tris–HCl, pH 8.8.
4. Equilibration buffer I: Equilibration buffer, 13 mM DTE.
5. Equilibration buffer II: Equilibration buffer, 2.5% (w/v) iodoacetamide.
6. After silver staining, the gel is scanned, and the protein pattern is analyzed with the Image Master 2D software (Amersham–Pharmacia Biotech).

2.6. Synchronized Phagocytosis

1. Microscope coverslips (Circles No. 1 – 0.13–0.17 mm thick; Size: 12 mm) and microscope slides (25 × 75 × 1 mm).
2. 3 μm polybeads dyed microparticles. Prepare a diluted solution by adding 0.5 mL of the stock solution in 4.5 mL of cold PBS, NaN3 0.1%. Particle number can be counted to determine concentration. Store at 4°C for several months.
3. Zymosan. Prepare a diluted solution by adding 4 mL of the stock solution in 36 mL of cold PBS 0.1% NaN3. Particle number can be counted to determine concentration. Store at 4°C during several month.
4. Sheep Red Blood Cells. Store at 4°C during 1 month. Prepare a diluted solution by adding 1 mL of the stock solution in 9 mL of cold PBS. Particle concentration should be determined. Store at 4°C up to several days.

2.7. Confocal Immunofluorescence

1. Paraformaldehyde: prepare a fresh 2% (v/v) solution in PBS for each experiment. Store at room temperature before use.
2. Blocking/permeabilization solution: 0.1% (v/v) Triton X-100, 1% (w/v) BSA, and 20% (v/v) normal goat serum,

6% (w/v) milk, 50% (v/v) fetal bovine serum. This solution must be freshly prepared for each experiment.

3. Anti-mouse or Anti-rabbit AlexaFluor 488 or 568. DRAQ-5 5 mM.
4. Fluoromount-G.
5. Detailed analysis of protein localization on phagosomes is performed using an oil immersion Nikon Plan Apo 100X (N.A. 1.4) objective mounted on a Nikon Eclipse E800 microscope equipped with a Bio-Rad Radiance 2000 confocal imaging system.
6. Fluorochrome excitation is achieved using a 10-mW Argon-Krypton laser for 488 nm (Alexa488) and 568 nm (Alexa568), and a 10-mW diode laser for 638 nm (Alexa647). Images are obtained using appropriate filters, through the sequential scanning mode of the LaserSharp software (Bio-Rad Laboratories) with a Kalman filter of at least 4, and converted using MRCtoM 1.9.3 and AdobePhotoshop 6.0.

3. Methods

A simple technique can be used to isolate pure preparations of phagosomes from macrophage cell lines such as RAW264.7 or J774 cells (**Fig. 1**). Enrichment of specific phagosome components associated with the microbicidal activity of phagosomes, such as hydrolases (e.g., cathepsin D and S) or LAMP-1, can easily be assessed by Western blot (**Fig. 2**). Phagosome isolation has been used to identify new phagosome-associated proteins as well as to study protein modifications during phagosome maturation *(14)*. After phagosome isolation and lysis, components can be separated by two-dimension gel electrophoresis, enabling the identification of proteins according to their isoelectric point on immobilized pH gradients 4–7 and their molecular weight (standard SDS–PAGE).

A global view of the compositional changes that occur during phagolysosome biogenesis can be obtained by comparing proteomic patterns of samples from phagosomes isolated at various time points. More specific studies on protein complex formation can be achieved by immunoprecipitation of a known component of the phagosome proteome. Obviously, these methods are not sufficient to clearly demonstrate the presence of these newly identified components, and other methods (e.g., Western blotting and confocal microscopy) must be used to confirm and validate the proteomic data. Ultimately, it is important to

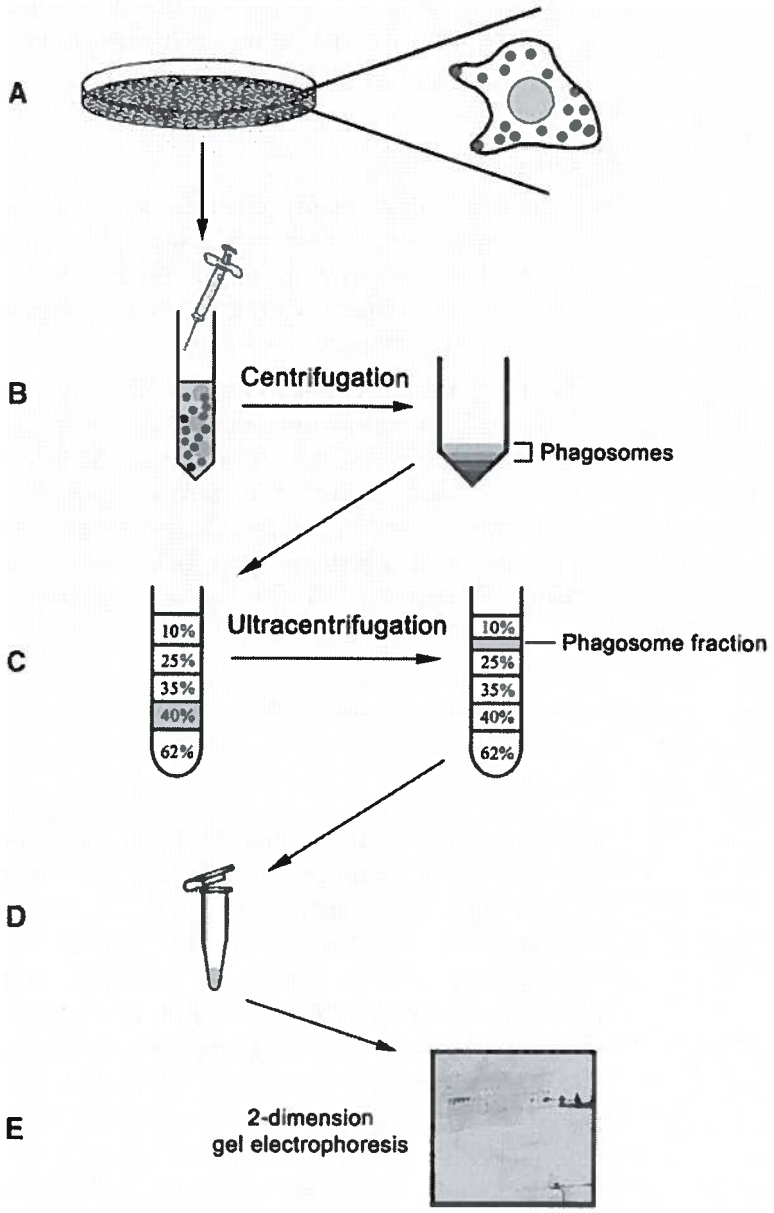

Fig. 1. Scheme of phagosome purification. (**A**) *Phagocytosis*. Macrophages are allowed to internalize a large amount of latex beads. (**B**) *Homogenization*. Cells are scrapped in PBS and homogenized by vigorously ejecting the cell suspension through a needle on the wall of the tube. After centrifugation, the phagosome layer corresponding to the two clearer phases is mixed with 62% sucrose solution in order to obtain a 40% sucrose solution containing phagosomes. (**C**) *Purification*. The 40% sucrose solution containing phagosomes is laid down on a 62% sucrose solution and covered up by the sucrose solutions as shown. Ultracentrifugation allows purification of latex-beads-containing phagosomes by migration according to beads density, at the interface between the 10 and the 25% sucrose solution. (**D**) *Lysis*. Phagosome solution is then mixed with PBS and ultracentrifugation allows phagosome precipitation at the bottom of the tube. Phagosomes can be lysed. (**E**) *Analysis*. Immunoprecipitation of a protein known to be involved in complex formation is possible on phagosome lysates and separation of protein complexes can be realized by two-dimension gel electrophoresis.

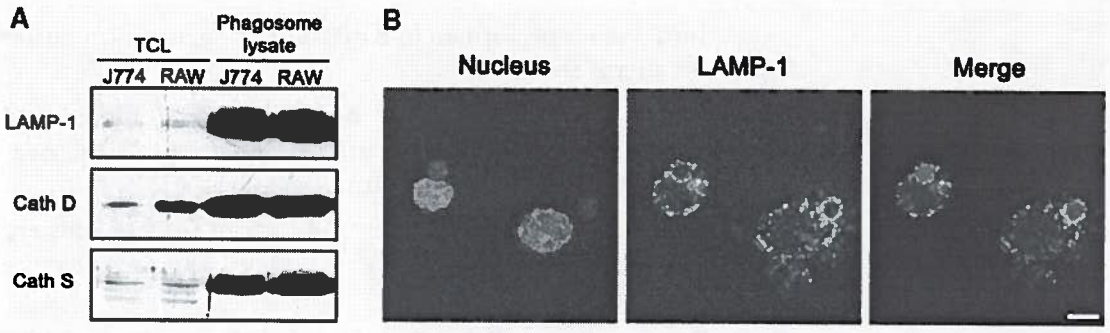

Fig. 2. Enrichment of proteins in the phagosomal compartment. The lysosomal marker LAMP-1 and the hydrolases Cathepsin D and S are massively acquired during the late steps of phagosomal maturation. (**A**) Phagosomes were obtained after a 90-min phagocytosis. 15 μg of total cell lysate (TCL) and 30 μg of phagosome lysate from RAW264.7 and J774 cell lines were loaded on a 10% acrylamide gel, transferred, and blotted with an anti-LAMP-1, an anti-Cath D, and an anti-Cath S antibody. (**B**) Immunofluorescence analysis by confocal microscopy shows recruitment of LAMP-1 on phagosomes. RAW264.7 cells were allowed to internalize fluorescent latex beads for 90 min before fixation. Cells were stained with an anti-LAMP-1 antibody and an anti-rat coupled with a 488 fluorochrome (Molecular Probes). Nuclei were stained using DRAQ-5 reagent (Biostatus, Leicestershire). Bar, 3 μm.

determine the functions of these components during phagocytosis and phagolysosome biogenesis.

3.1. Phagosome Isolation

1. Adherent macrophages (5×10^7 per 150 × 20 mm tissue culture dish) are incubated 24 h, reaching confluence between 70 and 80%.
2. Vortex latex beads vigorously before use to disrupt aggregates. Prior to initiating internalization, medium is gently removed and cells are incubated at 4°C for 10 min in the presence of 0.8 μm-diameter latex beads diluted 1:50 in 10 mL of complete medium, to allow beads to make contact with the cell monolayer. Cells and beads are then transferred to 37°C and incubated for 90 min to allow internalization to take place (*see* **Note 1**).
3. Gently wash cells three times with warm medium to remove non-internalized beads. During washes, dishes are put on a shaker. After this step, cells can be observed by light microscopy to verify the presence of a high number of bead containing phagosomes (black points in cells).
4. To obtain mature phagolysosomes, cells are further incubated for a chase period of 60 min in fresh medium at 37°C. Cells are then washed (3 × 5 min) in PBS at 4°C on a shaker, scraped with a rubber policeman in 4 mL of ice-cold PBS, and transferred to a 15-mL Falcon tube (one Falcon tube can accommodate cells from two dishes).
5. Cells are washed twice in 8 mL ice-cold PBS (centrifugation at 1,500 rpm for 3 min) to remove noninternalized beads.

A third wash is performed in 2 mL of homogenization buffer (8.5% sucrose).

6. Cells are pelleted in 1 mL homogenization buffer and homogenized on ice with a 1 mL syringe using a 22-G needle (12–15 strokes) in the 15-mL Falcon tube.
7. Homogenization is carried out until about 90% of cells are broken without major breakage of nuclei, as monitored by light microscopy.
8. Cell extracts are pelleted in a 15-mL Falcon tube at 2,000 rpm for 5 min at 4°C. The supernatant (about 1 mL) contains the phagosomes (**Fig.** 1). The phagosome suspension is carefully removed and is brought to 40% sucrose by adding an equal volume of a 62% sucrose solution in a 2-mL microfuge tube. Mix thoroughly with a pipet.
9. This 40% sucrose phagosome suspension is gently loaded on top of a 3-mL cushion of 62% sucrose, followed by the addition of solutions of 2 mL of 35% sucrose, 2 mL of 25% sucrose, and 2 mL of 10% sucrose.
10. Centrifugation is performed at 4°C in a swinging bucket rotor (SW41; Beckman Instruments) for 1 h at 100,000 × *g*.
11. Phagosomes (a band colored in blue) are carefully collected at the interface of the 10% and 25% sucrose layers and resuspended in 12 mL cold PBS containing 1× protease inhibitors. Phagosomes from two tubes can be pooled for the next centrifugation.
12. The phagosomes are pelleted at 4°C by a 15-min centrifugation at 40,000 × *g* in an SW41 rotor.
13. Supernatant is removed and the phagosome pellet is resuspended in 40–50 µL of ice-cold 1% NP-40 lysis buffer containing protease and phosphatase inhibitors (*see* **Note 2**). It is important to dry out the wall of the tube before adding lysis buffer to remove PBS 1×. Place on ice for 10 min and store at −20°C. The protein concentration of the phagosome preparations can be determined using the Pierce BCA protein assay reagent or any other standardized protein assay system.

3.2. Immunoprecipitation

1. Aliquot 50 µL of immobilized Protein A into four separate 1.5-mL microfuge tubes (tubes 1, 2, 3, and 4) and equilibrate three times with 500 µL 1% NP-40 lysis buffer without protease and phosphatase inhibitors (i.e., add lysis buffer; mix gently, spin down, and remove supernatant).
2. Tubes 1 and 2 are used for antibody binding: add 500 µL of 1% NP-40 lysis buffer without protease and phosphatase inhibitors and 5 µg of the antibody. Incubate for 3–4 h at 4°C in a rotary shaker.

3. Tubes 3 and 4 are used for preclearing phagosome extracts: add 700 µg per tube of phagosome extract in 0.5 mL total (adjust with 1% NP-40 lysis buffer with protease and phosphatase inhibitors if necessary) to equilibrate beads and incubate for 1 h at 4°C in a rotary shaker in order to eliminate non-specific binding.
4. After incubation with the antibody, beads from tubes 1 and 2 are washed three times in 500 µL of 1% NP-40 lysis buffer without protease and phosphatase inhibitors by mixing gently, spinning down, and removing supernatant.
5. Transfer precleared phagosome extracts from tubes 3 and 4 into tubes 1 and 2 containing antibody linked to beads. Incubate overnight at 4°C in a rotary shaker.
6. Spin tubes 1 and 2 down and remove supernatants; wash the beads twice with 1% NP-40 lysis buffer without protease and phosphatase inhibitors and twice with lysis buffer 0.1% NP-40 without protease and phosphatase inhibitors.
7. Resuspend the beads in a small volume of rehydration/lysis buffer (cf. **Subheading 2.5, step 1**), pool the contents of the two microfuge tubes, spin down and resuspend beads in 450 µL of rehydration/lysis buffer.
8. Vortex 1 h at room temperature before loading the samples for two-dimensional gel electrophoresis.

3.3. Two-Dimensional Gel Electrophoresis

1. Proteins are first separated according to their isoelectric points on 24-cm linear immobilized pH-gradient strips. Remove a dry strip of pH 4–7 from –20°C and allow to equilibrate at room temperature for 15 min.
2. Load the sample into the rehydration tray, leave about 1 cm at each end.
3. Note the basic end of the strip and position it at the left side of the tray.
4. Place the IPG strip gel-side down on the top of the sample; verify that there are no bubbles.
5. Completely overlay with mineral oil, cover the tray with lid, and leave at room temperature overnight.
6. Cut two electrode papers of 1.5 cm and wet with ddH_2O. Mop up until the papers become semi-dry.
7. Take out IPG strip and lay it down on the filter paper gel-side at top to remove oil excess.
8. Place the IPG strip in a strip holder gel-side on top and the acid side (+) at the positive side. The strip must be placed between the electrodes.
9. Lay down electrode papers lengthwise at 0.5 cm of the gel end for both sides, and gently lay down electrodes on the last

0.5 cm of the electrode paper in order that they are aligned properly.

10. Place strip holder cover and close the apparatus to test the voltage for 500 V. If voltage fails, verify that electrode papers are on the strip and that the electrode papers are not too dry.
11. Remove cap and completely cover the strip with mineral oil.
12. First dimension separation according to the isoelectric point.
13. Replace strip holder cover, close the apparatus, and proceed with the migration. At this step, voltage time volt-hours (Vh) will total approximately 106,000 Vh according to the following program:

500 V	15 min
1,000 V	30 min
2,000 V	30 min
3,000 V	30 min
4,000 V	30 min
5,000 V	60 min
6,000 V	60 min
8,000 V	Overnight

14. The strip is then rapidly taken out and after excess oil is drained out on filter paper, is placed in a glass tube containing Equilibration Buffer I. Incubate 10 min on a shaker at room temperature.
15. Remove the strip and place it in a glass tube containing Equilibration buffer II for 5 min at room temperature on a shaker. During this step, melt agarose solution which can be stored in a boiling hot beaker to keep it liquid.
16. Second dimension separation according to molecular weight: Prepare a 10% SDS–polyacrylamide gel (cf. **Subheading 3.5**) before the equilibration steps so that it can polymerize during the equilibration steps. Mix 7.9 mL H_2O, 6.7 mL 30.8% acrylamide/bis, 5 mL 1.5 M Tris–HCl, pH 8.8, 200 µL 10% SDS, 200 µL 10% ammonium persulfate, and 10 µL TEMED. Leave about 1.5 cm from the top for the strip.
17. Overlay with 0.1% SDS to avoid the drying of the gel and the gel should polymerize in about 20–30 min.
18. Remove the 0.1% SDS solution and rinse the top of the gel twice with ddH_2O. Mop up remaining water with a filter paper.
19. Place the strip on the top of the gel, leaving space for agarose. Place the acid side on the left. Add two small filter papers saturated with molecular weight marker at both ends of the gel.

20. Add the agarose solution and with care, quickly push the strip in until it touches the polyacrylamide separation gel. Make sure that the plastic-side of the gel remains pressed on the glass. Avoid bubbles between the strip and the separation gel. Let the agarose solidify.
21. Add running buffer and proceed with the migration by running the gel at 200 V. This step takes several hours.
22. Stop the migration as soon as the colorimetric marker leaves the gel. Disassemble the migration system, remove the agarose and the strip, take the gel out, and identify the pH by piercing at both ends.

3.4. Coomassie Blue Coloration, Nonfixing Silver Stain, and Protein Extraction

3.4.1. Coomassie Blue (see Note 3)

1. Wash the gel three times with ddH_2O (5 min each).
2. Proceed as described for the Colloidal Blue Staining Kit.
3. Non-fixing silver stain.
4. Always use freshly prepared solutions and perform all steps at room temperature with constant gentle agitation. Place the polyacrylamide gel in a plastic container.
5. Incubate the gel for 30 min in fixation solution consisting of 125 mL ethanol, 12.5 mL glacial acetic acid, and 112.5 mL ddH_2O. For a double fixation, repeat this step for an additional 30 min.
6. Pour out fixing solution and wash the gel for 10 min in a mixed solution of 125 mL ethanol and 125 mL ddH_2O. Then wash twice with ddH_2O (10 min each wash).
7. Incubate the gel for 5 min in a sensitizing solution: 0.02 g sodium thiosulfate in 250 mL ddH_2O.
8. Pour out sensitizing solution and wash the gel three times with ddH_2O (5 min each wash).
9. For the silver reaction, incubate the gel for 30 min in silver solution: 0.25 g silver nitrate and ddH_2O to a volume of 250 mL.
10. Pour out silver solution and wash the gel once with ddH_2O for 1 min.
11. Incubate the gel in developing solution: 5 g sodium carbonate, 0.25 mL formaldehyde (37% w/v) and ddH_2O until 250 mL. Do not allow the gel to overstain, and once the gel spots become visible, stop the reaction.
12. Briefly wash the gel in ddH_2O and stop the reaction by incubating the gel in a solution of 12.5 mL acetic acid and 237.5 mL ddH_2O for 5 min. The gel can be stored in a solution of 2.5 mL acetic acid and 247.5 mL ddH_2O for several days.
13. Extraction of protein spots. For the following steps, it is absolutely necessary to work with latex gloves, bonnet, mask,

and any additional protection to prevent keratin contamination of the samples. Wash all components with ethanol.

14. Put the gel between two acetate sheets wetted with ultrapure water.
15. Scan the gel and number the protein spots.
16. Lay down the gel between acetate sheets on a plexiglass tray.
17. Add ultrapure water on the gel.
18. Extract each protein spot with a scalpel. Wash the scalpel between each extraction with ethanol and ultrapure H_2O. Place pieces of gel containing proteins in wells of a 96-well plate. The plate should be prepared beforehand by filling wells with 0.2 mL of ultrapure H_2O, 1% acetic acid.
19. Cover and seal the plate with parafilm. Samples can be stored at 4°C for several days.
20. The samples are now suitable to be analyzed by matrix-assisted laser desorption/ionization-time-of-flight mass spectrometry.

3.5. SDS–Polyacrylamide Mini-Gel Electrophoresis (SDS–PAGE)

1. Prepare a 10% separating gel by mixing 4 mL H_2O, 3.3 mL 30.8% acrylamide/bis, 2.5 mL 4× separating gel solution, 100 µL 10% ammonium persulfate, and 5 µL TEMED. Let about 1.5 cm from the top for the stacking gel.
2. Overlay with 0.1% SDS to avoid the drying of the gel which should polymerize in 20–30 min.
3. Remove the 0.1% SDS solution and rinse the top of the gel twice with ddH_2O.
4. Prepare the stacking gel by mixing 3 mL H_2O, 650 µL 30.8% acrylamide/bis, 1.25 mL 4× Tris stacking buffer, 25 µL 10% ammonium persulfate, and 5 µL TEMED. Rinse the top of the separating gel a final time with 0.5 mL of the stacking gel solution, then add the stacking solution over the separating gel, and insert the comb. The gel should polymerize in about 20–30 min.
5. Prepare the running buffer by diluting 160 mL of the 5× running buffer with 640 mL H_2O and mix.
6. When the stacking gel has set, remove the comb and assemble the gel unit.
7. Add running buffer. It is important to carefully wash twice the wells with running buffer by using a 25-G needle before loading the samples.
8. The protein concentration of each sample has to be known and adjusted to have the same amount of protein in all samples. Adjustment may be done by adding lysis buffer. Be careful not to add too much lysis buffer because the protein

sample is subsequently diluted 1:1 (v/v) with 2× SDS-loading buffer, and the final volume should not exceed 15 µL for loading.

9. Incubate samples for 5 min at 100°C, perform a quick spin, mix and load 15 µL of each sample in a well. One well must include molecular weight markers prepared according to the supplier's instructions.
10. Complete the assembly of the gel unit and connect to a power supply. The gel can be run at 100 V.
11. When the dye front reaches the bottom of the gel, transfer to the nitrocellulose membrane may be carried out (the dye fronts can be run off the gel if desired).

3.6. Western Blotting

1. Make sure that all parts of the apparatus are clean.
2. Cut three pieces of Whatman 3-MM filter paper barely larger than the gel and pre-wet with transfer buffer. Lay down the three pieces on the transfer apparatus. A sheet of the nitrocellulose barely larger than the separating gel size is laid on the surface of the 3-MM paper to wet the membrane. Pour transfer buffer onto the membrane and remove any air bubbles.
3. After the samples have been separated by SDS–PAGE, the gel unit is disassembled. The stacking gel is removed and one corner of the separating gel is cut to track its orientation. The separating gel is then laid on the top of the nitrocellulose membrane and the gel surface is moistened with transfer buffer.
4. Three additional pieces of 3-MM paper of the appropriate size are submerged in the transfer buffer and carefully laid on top of the gel. It is also extremely important to make sure of the proper orientation of the resulting sandwich, or proteins will be lost into the buffer (components must be placed in the following order: three pieces of 3-MM paper, nitrocellulose membrane, polyacrylamide gel, and finally three other pieces of 3-MM paper. Remove any bubbles after each step). Close the transfer system.
5. Set the power supply at 15 V for 30 min.
6. After the transfer, the gel and the membrane are disassembled from the apparatus and the membrane is promptly rinsed with ddH_2O.
7. The membrane is then stained with Ponceau S for 1 min at room temperature to visualize the sample proteins and to assess the efficiency of the transfer. Red protein bands should become visible after removing excess dye with ddH_2O. The positions of the lanes and the markers are marked by gently pricking the membrane with the point of a needle.

8. Destain the membrane completely by rinsing in PBS on a shaker for about 10 min (*see* **Note 4**).
9. Block with blocking buffer (PBS-0.1% Tween, 5% BSA) for 2 h at room temperature or overnight at 4°C on a shaker (*see* **Note 5**).
10. Wash with PBS-0.1% Tween four times for 15 min each on a shaker.
11. Incubate the membrane with primary antibody diluted in 15 mL PBS + 5%BSA for 3 h at room temperature on a shaker or overnight at 4°C.
12. Wash with PBS-0.1% Tween four times for 15 min each on a shaker.
13. Incubate the membrane with the secondary antibody diluted in 15 mL PBS + 5% BSA for 45 min at room temperature on a shaker.
14. Wash with PBS-0.1% Tween four times for 15 min each on a shaker.
15. Following the instructions provided with the ECL kit, mix 5 mL Solution 1 and 5 mL Solution 2 immediately before use and incubate the blot for exactly 1 min (two blots can successively be developed with the same solution) which is rotated by hand to ensure the entire coverage of the membrane (*see* **Note 6**).
16. The blot is placed on an acetate sheet and promptly covered up with Saran wrap to avoid drying of the membrane. Keep out of light.
17. In the darkroom, the acetate-containing membrane is placed immediately in an autoradiography cassette with a medical film for a suitable exposure time (start from 30-s exposures to 45 min).

3.7. Preparation of Samples for Immunofluorescence

3.7.1. Synchronized Phagocytosis

1. Place round coverslips into wells of a 24-well tissue culture plate. The coverslips are sterilized or kept in alcohol until required. Coverslips kept in alcohol are dried in a sterile environment and dropped into each well with sterile forceps.
2. Harvest and resuspend macrophages in complete DMEM at 1–4 × 10^5 cells/mL. Seed 0.5 mL into each well of the 24-well plate and incubate at least 2 h or overnight at 37°C in 5% CO2 to allow cells to adhere to the coverslip.
3. During cell adherence, particles to be internalized are opsonized if necessary. Usually, the particle-to-cell ratio is 10:1 or 20:1.
4. Zymosan particles are laid down in a microfuge tube, spun 1 min at 14,000 × *g*, and resuspended in cold, sterile PBS 1× solution twice for washing (aspirate the supernatant carefully

using a 26-G needle). Particles can be opsonized in 150 µL of pure mouse serum or in 0.3–0.5 mL of diluted mouse serum in sterile PBS 1× solution. Do not dilute the serum to less than 10%. Incubate 40 min to 1 h at 37°C for complement opsonization. The tube is shaken by inversion three or four times during incubation to allow optimal particle opsonization.

5. For IgG opsonization, sheep red blood cells (SRBC) or beads can be used.
6. SRBC are laid down in a 15-mL Falcon tube and centrifugated at 200 × *g* for 5 min at 4°C and resuspended twice in cold sterile PBS for washing. After the last wash, SRBC are suspended in 7 mL sterile cold PBS and 7 µL of SRBC-specific IgG at 1 µg/µL (from mouse or rabbit) is added. Incubate SRBC 30 min in a rotary shaker at 4°C.
7. Beads are added to a microfuge tube, centrifugated 1 min at 14,000 × *g*, and resuspended in sterile cold PBS twice for washing (aspirate the supernatant carefully with a 26-G needle). After the last wash, beads are suspended in 1 mL 50 mM Tris–HCl, pH 9, and 1 µl of IgG at 1 µg/µL (from mouse or rabbit) is added. Incubate beads for 40 min in a rotary shaker at 4°C.
8. After opsonization, wash three times with cold sterile PBS 1× solution. For SRBC, gently shake the tube after centrifugation to avoid cell lysis. For zymosan and latex beads, particles can be vigorously shaken after centrifugation to avoid aggregate formation. Resuspend particles in an appropriate volume of complete DMEM and keep at 4°C until phagocytosis (keeping in mind that a volume of 300 µL will be added to each well for phagocytosis).
9. Once macrophages are ready for phagocytosis, remove the medium by gently aspirating the contents of each well. Wash cells twice with 0.5 mL cold DMEM. Keep plates at 4°C for 5 min before adding particles.
10. Remove medium and gently add 300 µL of the cold particle suspension. Keep the plates at 4°C during 10 min to allow particle deposition and their binding to the cells.
11. Remove unbound particles by three washes with cold DMEM and incubate cells at 37°C for 90 min for internalization.
12. Coverslips are then washed three times with PBS to eliminate non-internalized particles and cells are fixed in PBS 1×+2% paraformaldehyde for 10 min at room temperature.
13. Wash coverslips twice with PBS 1× and incubate at room temperature for 10 min before a final wash (see **Note 8**).

14. Plates containing coverslips can be stored at 4°C for 1 month before immunofluorescence staining. Be careful that coverslips are always covered with cold PBS.

3.7.2. Confocal Immunofluorescence

1. For each subsequent step involving incubation of coverslips containing adherent cells (i.e., blocking/permeabilization, first and second antibody incubation), place a piece of parafilm in the bottom of a 150 × 20 mm dish. The outside of the dish (both top and bottom) must be fully covered beforehand with aluminium foil. Place 50–80 µL of the incubation solution (e.g., blocking/permeabilization solution, first antibody solution, or second antibody solution) into the dish, and using forceps gently place each coverslip with the cells face down in the desired solution. Do not press on coverslips. After incubation, carefully remove coverslips with forceps, and immerse them in wells containing PBS 1× solution. Keep the cell-side face up.
2. To permeabilize cells and block nonspecific surface Fcγ-receptors, promptly drain excess PBS 1× and incubate in the blocking/permeabilization buffer at room temperature for 15–20 min.
3. Coverslips are then dipped in PBS 1× and washed three times. Washes have to be gentle to maintain cell attachment.
4. Excess PBS is promptly drained from the coverslips, and the primary antibody solution (usually at a dilution of 1/1,000 to 1/100 in PBS) is added for 1 h at room temperature.
5. Cells are gently washed three times in PBS 1×.
6. Coverslips are promptly drained for excess PBS and incubated with a solution containing the secondary antibody (1/500 dilution) coupled to an Alexa fluorochrome (Alexa 488, 568, or 647 for example) for 30 min at room temperature. A nuclear stain such as DRAQ 5 can be used and is diluted at 1/400 in the secondary antibody solution. From this step, be careful to protect samples from direct light to avoid bleaching.
7. Samples are gently washed three times and are ready to be mounted.
8. Coverslips are promptly drained for excess PBS and are mounted on glass slides with Fluoromount-G. Drops of Fluoromount-G are placed on glass slides and coverslips are laid down cell-face in contact with fluoromount. Excess fluoromount is removed and slides are then sealed with nail polish on the edges of coverslips.
9. Freshly mounted slides must be dried at room temperature and protected from light for 24 h before use. Slides can be stored for up to a month at 4°C in the dark.

4. Notes

1. Depending on the experiments, various internalization time points are possible during phagosome isolation, and the chase period must be adapted to the protein component of interest, which may be recruited to phagosomes at early or later time points after initiation of phagocytosis. Internalization between 30 and 120 min is often used, and the chase period can cover a period from 30 min to more than 2 h. For example, to observe the early recruitment of a specific protein on phagosomes, cells and medium containing beads can be kept at 4°C for 20 min and then placed at 37°C for 30 min before phagosome isolation.
2. Phagosomes can be resuspended in ice-cold lysis buffer containing 150 mM NaCl, 20 mM Tris–HCl, pH 7.5, and 1% NP-40, but 1% Triton X-100 can be used instead of NP-40.
3. Coomassie blue staining is preferable if proteins are visible on acrylamide gel before sample isolation and mass spectrometry identification.
4. TBS can be used instead of PBS according to the manufacturer providing the first antibody.
5. Nitrocellulose membranes can be blocked with blocking buffer containing milk (PBS 0.1% Tween, 5% (w/v) milk) for 2 h at room temperature or overnight at 4°C on a shaker.
6. If the signal is too strong during exposure, the ECL solutions can be diluted (from 1/2 to 1/20) in ddH_2O as long as solutions 1 and 2 remain at the ratio of 1:1.
7. If the silver stain is not sufficient, the gel can be incubated in the silver solution overnight at room temperature with agitation.
8. During preparation of coverslips for immunofluorescence, observation by light microscopy after washing is advised in order to verify that cells have not detached during washing. Do not expose samples to light after incubation with the secondary antibody.

Acknowledgments

We are grateful to John Derek Ng Yan Hing for developing phagosome isolation procedures in our laboratory. This work was supported by the Canadian Institutes for Health Research. AD is the holder of a Canada Research Chair. AFV was partly supported by a fellowship from the Fondation Armand-Frappier.

References

1. Bajno L, Peng XR, Schreiber AD, Moore HP, Trimble WS, Grinstein S. (2000). Focal exocytosis of VAMP3-containing vesicles at sites of phagosome formation. *J Cell Biol*; 149(3):697–706
2. Braun V, Fraisier V, Raposo G, et al. (2004). TI-VAMP/VAMP7 is required for optimal phagocytosis of opsonised particles in macrophages. *EMBO J*; 23(21):4166–4176
3. Gagnon E, Duclos S, Rondeau C, et al. (2002). Endoplasmic reticulum-mediated phagocytosis is a mechanism of entry into macrophages. *Cell*; 110(1):119–131
4. Jahraus A, Tjelle TE, Berg T, et al. (1998). In vitro fusion of phagosomes with different endocytic organelles from J774 macrophages. *J Biol Chem*; 273(46):30379–30390
5. Vieira OV, Botelho RJ, Grinstein S. (2002). Phagosome maturation: aging gracefully. *Biochem J*; 366(Pt 3):689–704
6. Wetzel MG, Korn ED. (1969). Phagocytosis of latex beads by *Acahamoeba castellanii* (Neff). 3. Isolation of the phagocytic vesicles and their membranes. *J Cell Biol*; 43(1):90–104
7. Desjardins M, Huber L, Parton R, Griffiths G. (1994) Biogenesis of phagolysosomes proceeds through a sequential series of interactions with the endocytic apparatus. *J Cell Biol*; 124(5):677–688
8. Desjardins M, Celis J, van Meer G, et al. (1994). Molecular characterization of phagosomes. *J Biol Chem*; 269(51):32194–32200
9. Desjardins M, Nzala N, Corsini R, Rondeau C. (1997) Maturation of phagosomes is accompanied by changes in their fusion properties and size-selective acquisition of solute materials from endosomes. *J Cell Sci*; 110(18):2303–2314
10. Desjardins M. Biogenesis of phagolysosomes: the 'kiss and run' hypothesis. (1995). *Trends Cell Biol*; 5(5):183–186
11. Claus V, Jahraus A, Tjelle T, et al. (1998). Lysosomal enzyme trafficking between phagosomes, endosomes, and lysosomes in J774 macrophages. Enrichment of cathepsin H in early endosomes. *J Biol Chem*; 273(16):9842–9851
12. Ng Yan Hing JD, Desjardins M, Descoteaux A. (2004) Proteomic analysis reveals a role for protein kinase C-alpha in phagosome maturation. *Biochem Biophys Res Commun*; 319(3):810–816
13. Garin J, Diez R, Kieffer S, et al. (2001). The phagosome proteome: insight into phagosome functions. *J Cell Biol*; 152(1):165–180
14. Defacque H, Bos E, Garvalov B, et al. (2002). Phosphoinositides regulate membrane-dependent actin assembly by latex bead phagosomes. *Mol Biol Cell*; 13(4):1190–1202

ANNEXE 2

The exocytosis regulator Synaptotagmin V controls phagocytosis

Adrien F. Vinet, Mitsunori Fukuda and Albert Descoteaux

The Journal of Immunology, 181(8):5289-95

The Exocytosis Regulator Synaptotagmin V Controls Phagocytosis in Macrophages[1]

Adrien F. Vinet,* Mitsunori Fukuda,† and Albert Descoteaux[2]*

Synaptotagmins (Syts) play a key role in the regulation of Ca^{2+}-triggered exocytosis and membrane fusion events, two crucial events associated to the phagocytic process. In the present study, we investigated the role of Syt V, a regulator of focal exocytosis, in phagocytosis. In macrophages, Syt V is localized on recycling endosomes and on filopodia-like structures and is recruited to the nascent phagosomes independently of the phagocytic receptor engaged. Silencing of Syt V by RNA interference revealed a role for this protein for phagocytosis, particularly under conditions of high membrane demand. In contrast, silencing of Syt V had no effect on the recruitment of the lysosomal marker LAMP1 to phagosomes, indicating that phagosome maturation is not regulated by Syt V. Collectively, these results illustrate the importance of Syt V in the regulation of an important innate function of macrophages. Furthermore, our results are consistent with the concept that focal exocytosis of endocytic organelles is a key event in phagocytosis and suggest that Syt V regulates this process. ***The Journal of Immunology,*** **2008, 181: 5289–5295.**

Phagocytosis is an essential arm of the innate response against infections, as it represents the process by which professional phagocytes internalize and destroy invading microorganisms (1, 2). During internalization, target particles are surrounded by pseudopods and are engulfed in a vacuole, the phagosome, which rapidly matures into a microbicidal phagolysosome. Whereas the nascent phagosome is formed to a large extent by invagination of the plasma membrane (3), the membrane surface required to internalize multiple or large targets may represent an area equivalent to the entire cell surface (4). Such a requirement suggests that membrane from intracellular sources contributes to the phagocytic process. Indeed, phagosome formation is accompanied by the exocytosis of endomembranes into the plasmalemma (4). Two compartments contribute to focal exocytosis during phagocytosis: the VAMP3- and Rab11-positive recycling endosomes (5–7) and the TI-VAMP/VAMP7-positive late endosomes/lysosomes (8). Evidence that soluble *N*-ethylmaleimide-sensitive factor attachment protein receptors (SNAREs)[3] associated to the endoplasmic reticulum are required for phagocytosis support a role for this organelle during phagocytosis (9, 10). However, this remains controversial (11). Nevertheless, the fact that both vesicle- and plasma-membrane associated SNAREs are essential for focal exocytosis and particle internalization (4, 5, 8, 10) illustrates the importance of membrane fusion regulators during phagocytosis.

Synaptotagmins (Syts) are a large family of transmembrane proteins characterized by the presence of tandem C2 domains which act as Ca^{2+} sensor, and regulate membrane fusion during exocytosis via interaction with SNAREs and membrane lipids (12, 13). Although several SNAREs modulate phagocytosis by controlling membrane fusion during focal exocytosis, little is known concerning the potential roles of Syts in phagocytosis. This is an important issue because for the SNARE complex to drive rapid membrane fusion in response to Ca^{2+} influx, additional factors, including a Ca^{2+} sensor(s), are required. In this regard, a recent study revealed that consistent with its role as a regulator of lysosomal exocytosis (14–16), Syt VII plays a key role in the delivery of lysosomal membrane to the phagosome (17), possibly acting in concert with VAMP7 (8). In neutrophils, the presence of Syt II on phagosomes suggested a role for this Ca^{2+} sensor during phagocytosis and secretion (18).

Several signaling molecules, including members of the protein kinase C (PKC) family of protein serine/threonine kinases, are activated during phagocytosis and associate to the phagosome during the maturation process (19–23). We previously obtained evidence that PKC-α plays a role in phagolysosome biogenesis (24), and, while investigating the mechanisms by which PKC-α modulates phagocytosis, we identified Syt V (25) as a molecule potentially interacting with PKC-α in phagosomes preparations (A.F.V. and A.D., unpublished observations). Syt V is predominantly associated to dense-core vesicles in neuronal cells (26) and pancreatic β cells where it regulates vesicle exocytosis (27, 28). In this study, we provide evidence that, in macrophages, Syt V plays a role in the regulation of phagocytosis.

Materials and Methods

Cell culture

Peritoneal exudate macrophages (PEM) were obtained from peritoneal lavages of 8- to 10-wk-old female C57BL/6 mice (Charles River Laboratories). PEM and the mouse macrophage cell lines J774 and RAW 264.7 were cultured in DMEM with L-glutamine (Life Technologies) supplemented with 10% heat-inactivated FBS (HyClone), 10 mM HEPES (pH 7.4), and antibiotics (complete medium) in a 37°C incubator with 5% CO_2. *Leishmania donovani* promastigotes (strain 1S) were grown as described (29).

*Institut National de la Recherche Scientifique-Institut Armand-Frappier, Université du Québec, Laval, Quebec, Canada; and †Department of Developmental Biology and Neurosciences, Graduate School of Life Sciences, Tohoku University, Sendai, Miyagi, Japan

Received for publication March 12, 2008. Accepted for publication August 15, 2008.

The costs of publication of this article were defrayed in part by the payment of page charges. This article must therefore be hereby marked *advertisement* in accordance with 18 U.S.C. Section 1734 solely to indicate this fact.

[1] This work was supported by Canadian Institutes of Health Research Grant MT-29033. A.D. is a chercheur-boursier of the Fonds de la recherche en santé du Québec and the holder of a Canada Research Chair. A.F.V. was partly supported by a doctoral fellowship from the Fondation Armand-Frappier.

[2] Address correspondence and reprint requests to Dr. Albert Descoteaux, Institut National de la Recherche Scientifique-Institut Armand-Frappier, 531 boul des Prairies, Laval, Quebec, Canada H7V 1B7. E-mail address: albert.descoteaux@iaf.inrs.ca

[3] Abbreviations used in this paper: SNARE, soluble *N*-ethylmaleimide-sensitive factor attachment protein receptor; IgG-SRBC, IgG-opsonized SRBC; PEM, peritoneal exudate macrophage; PKC, protein kinase C; siRNA, small interfering RNA; RNAi, RNA interference; Syt, synaptotagmin.

 0022-1767/08/$2.00

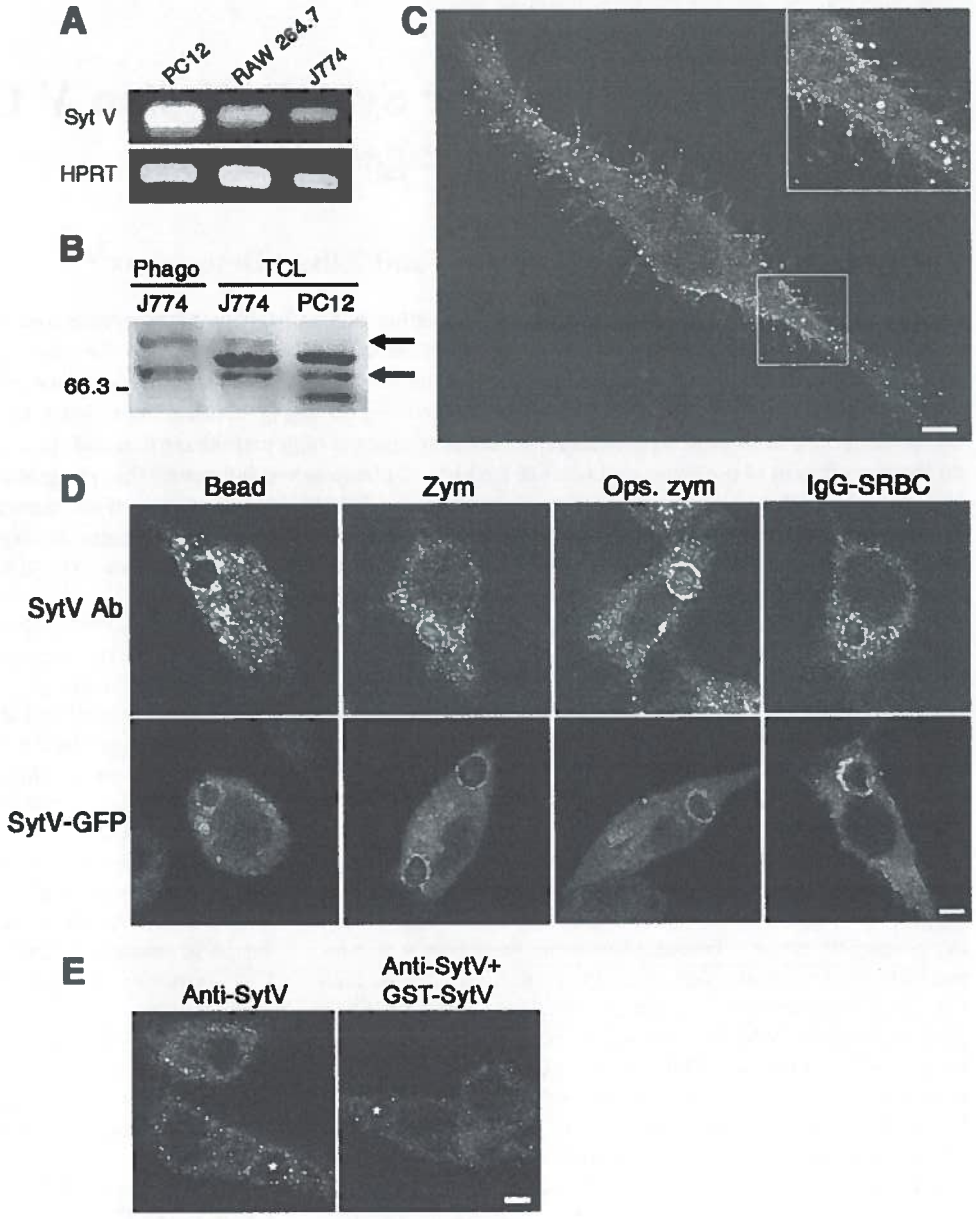

FIGURE 1. Syt V is expressed in macrophages and is recruited to phagosomes. *A*, Syt V is expressed in RAW 264.7 and J774 macrophages, as assessed by RT-PCR. PC12 cells were used as positive control. *B*, Syt V is present in total cell and phagosome lysates from J774 cells. Western blot analysis was performed on 30-μg 90-min-old phagosome lysates and 10 μg total cell lysates (TCL). PC12 cells were used as positive control. Arrows show the two Syt V forms present in macrophages. *C*, Syt V is localized on intracellular vesicles and on filopodia-like structures in RAW 264.7 cells, as determined by confocal microscopy. Bar, 5 μm. *D*, Syt V is recruited to phagosomes independently of the phagocytic receptor involved. RAW 264.7 cells or RAW 264.7 cells stably expressing the Syt V-GFP fusion protein were allowed to internalize either latex beads, zymozan, serum-opsonized zymozan, or IgG-SRBCs for 30 min. Syt V (*top panel*) and Syt V-GFP (*bottom panel*) were localized by confocal microscopy. Bar, 3 μm. *E*, Immunolocalization of Syt V in the presence of the GST-Syt V spacer domain fusion protein used to generate the anti-Syt V Ab eliminated most of the Syt V labeling both on intracellular vesicles and on zymozan-containing phagosomes (indicated by an *) in PEM. Bar, 3 μm. Results are representative of three independent experiments.

Syt V-GFP expression vector and stable transfection in RAW 264.7 cells

The SytV-GFP cDNA (26) was inserted into the *Not*I site of the bicistronic expression vector pCIN-4 (30). The resulting construct was electroporated into RAW 264.7 cells as described (31). Transfectants were selected in complete medium containing 500 μg/ml G418 (Life Technologies) and individual clones were harvested, expanded, and examined for Syt V-GFP expression.

RT-PCR

Total RNA was extracted with RNAzol B (Tel-Test), treated with DNaseI (BD Biosciences), and reverse transcribed with AMV reverse transcriptase (USB). cDNA was used for PCR using the following forward (F) and reverse (R) primers for Syt V: F: 5′-CCCTTTTTGGTGTCTCTCTTTTCG-3′ (AD-329) and R: 5′-AGTCCTTGGCAGGCAGATTGAC-3′ (AD-330). For hypoxanthine phosphoribosyltransferase, the primers were F: 5′-GTTGGATACAG GCCAGACTTTGTTG-3′ (AD-55) and R: 5′-GATTCAACTTGCGCT CATCTTAGGC-3′ (AD-56).

Phagosome preparation and isolation

Adherent macrophages (5×10^7 per 150 × 20 mm tissue culture dishes) were incubated with latex beads (0.75 μm diameter, 10% suspension, blue dyed; Sigma-Aldrich) diluted 1/25 in 10 ml complete medium at 37°C for 30, 60, 90, or 120 min. Cells were then washed three times in cold PBS at 4°C and scrapped with a rubber policeman in cold PBS. Phagosomes were isolated by flotation on a sucrose gradient as described (24).

Western blots

Cells and purified phagosomes were lysed in ice-cold lysis buffer (20 mM Tris-HCl (pH 7.5) and 1% Nonidet P-40) containing protease and phosphatase inhibitors. Phagosomal proteins (30 μg) and total cell lysates (10 μg) were separated on 8% SDS-PAGE, transferred onto Hybond-ECL membranes (Amersham Biosciences), and immunodetection was achieved by chemiluminescence (Amersham Biosciences).

Antibodies

The rabbit anti-Syt V spacer Ab was raised against the cytoplasmic region between the transmembrane and the C2 domain (aa 71–216) and was affinity-purified.The rat anti-Lamp1 developed by J. T. August (1D4B) was obtained through the Developmental Studies Hybridoma Bank at the University of Iowa, and the National Institute of Child Health and Human Development. The monoclonal anti-EEA1 Ab was from Dr. Michel Desjardins (Université de Montreal, Montreal, Canada). Monoclonal rat anti-mouse transferrin receptor TfR Ab was from Cedarlane Laboratories.

RNA interference (RNAi)

For the silencing of Syt V by RNAi, we used a small interfering RNA (siRNA) corresponding to nucleotides 94–112 of Syt V cDNA (28), whereas an siRNA specific to GFP (32) was used as a negative control. Adherent RAW 264.7 cells were transfected with siRNA duplexes at a final concentration of 240 nM using OligoFectamine (Invitrogen) as described (32). A BLAST search against the mouse genome sequence database was performed to ensure that the chosen siRNA sequences targeted only the mRNA of interest.

Phagocytosis assays

IgG-opsonized SRBC (IgG-SRBC) were prepared as described (19). Red fluorescent beads of different diameters (0.75 μm from Estapor microsphere and 3 μm from Polyscience) were opsonized with mouse IgG. Zymosan (Sigma-Aldrich), Zymosan-Alexa 488 and -Alexa 568 (Molecular Probes) and *L. donovani* promastigotes were opsonized with mouse serum (33). For synchronized phagocytosis assays, macrophages were incubated with particles at a particle-to-cell ratio of 15:1 (unless otherwise specified) for 20 min at 4°C. Excess particles were removed and phagocytosis was triggered by transferring the cells to 37°C for the indicated time points before processing for microscopy.

Microscopy and immunofluorescence

Macrophages were fixed, permeabilized using 0.1% Triton X-100, and nonspecific surface FcγR binding were blocked using 1% BSA, 2% goat serum, 6% milk, and 50% FBS. Particle internalization was quantified by immunofluorescence microscopy. Results are based on at least 100 cells chosen by blinded scoring in triplicate. For distribution and colocalization experiments, cells were labeled with the appropriate combinations of primary Abs (anti-Syt V, LAMP-1, transferrin receptor, EEA1, or PKC-α), and secondary Abs (anti-rabbit AlexaFluor 568 or AlexaFluor 488, anti-rat AlexaFluor 488, anti-mouse AlexaFluor 488, or anti-mouse AlexaFluor 568; Molecular Probes). All coverslips were mounted on slides with Fluoromount-G (Southern Biotechnology Associates). Detailed analysis of protein localization on the phagosome was performed essentially as described (29) using an oil immersion Nikon Plan Apo 100 (N.A. 1.4) objective mounted on a Nikon Eclipse E800 microscope equipped with a Bio-Rad Radiance 2000 confocal imaging system (Bio-Rad). Statistical analyses were performed using Student's two-tail two-sample unequal variance test.

Results

Syt V is expressed in macrophages

Using a proteomic approach, we sought to identify proteins in latex bead-phagosome lysates that coimmunoprecipitated with PKC-α (A.F.V. and A.D., unpublished observations), and we found several proteins including Syt V (NP_068689). Two Syt V sequences were reported at the same time, and the 491AA-Syt V identified by Li et al. (34) will be analyzed in this paper. Given the importance of Syts in the regulation of exocytosis and membrane fusion (13, 35), we further investigated the potential role of Syt V in phagocytosis. Syt V had not previously been shown to be expressed in macrophages and we confirmed by RT-PCR that it is expressed in the macrophage lines RAW 264.7 and J774 (Fig. 1*A*). The PC12 neuronal cell line was used as a positive control. Using an Ab against the Syt V spacer domain (26), we detected by Western blot the presence of Syt V in J774 and PC12 cell lysates as well as in 90 min-old latex bead-phagosome extracts (Fig. 1*B*). Confocal immunofluorescence microscopy revealed that Syt V is present on intracellular vesicles and on filopodia-like structures (Fig. 1*C*). After 30-min phagocytosis, we observed the recruitment of Syt V to phagosomes containing various particles (latex beads, zymozan, serum opsonized-zymozan, and IgG-SRBC) (Fig. 1*D*). Using RAW 264.7 cells stably expressing a Syt V-GFP fusion protein, we observed that similar to Syt V, Syt V-GFP was recruited to phagosomes containing either latex beads, zymozan, serum opsonized-zymozan, or IgG-SRBC (Fig. 1*D*). To assess the specificity of our anti-Syt V Ab, we performed immunofluorescence staining in the absence or the presence of the GST-Syt V spacer domain fusion protein used for immunization. As shown in Fig. 1*E*, presence of the GST-Syt V spacer domain strongly reduced Syt V staining on both intracellular vesicles and on zymozan-containing phagosomes in PEM. Taken together, these data indicate that Syt V is recruited to phagosomes, independently of the phagocytic receptors involved.

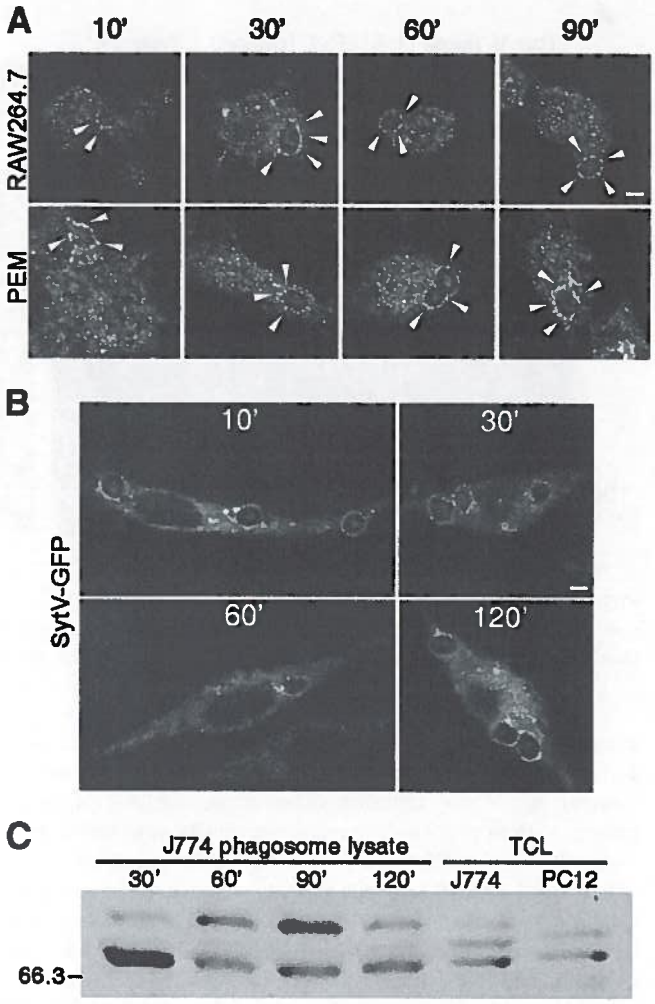

FIGURE 2. Syt V is recruited early to phagosomes and remains during the maturation process. *A*, Syt V was localized by confocal microscopy at various time points after the initiation of internalization of serum-opsonized zymozan by either RAW 264.7 cells (*upper row*) or PEM (*lower row*). Bar, 3 μm. *B*, Syt V-GFP was localized by confocal microscopy at various time points after the initiation of internalization of serum-opsonized zymozan by RAW 264.7 cells stably expressing Syt V-GFP. Bar, 3 μm. *C*, Two Syt V forms are present on latex bead-containing phagosomes isolated from J774 cells at various time points after the start of internalization. Western blot analysis was performed on 30-μg phagosomes lysates and 10 μg total cell lysates (TCL) from J774 and PC12 cells. Similar results were obtained in three independent experiments.

Syt V associates to phagosomes

To further characterize the recruitment of Syt V to phagosomes, we first determined its kinetics of phagosomal association during the phagocytosis of serum-opsonized zymozan. Confocal microscopy revealed that in both RAW 264.7 cells and PEM, Syt V was recruited early to phagosomes and remained throughout the maturation process (Fig. 2*A*). The recruitment of Syt V-GFP to phagosomes containing serum-opsonized zymozan followed a kinetics pattern similar to that of Syt V (Fig. 2*B*). Similarly, Western blot on J774 latex bead phagosomes lysates prepared at various time points after the start of phagocytosis showed that the relative

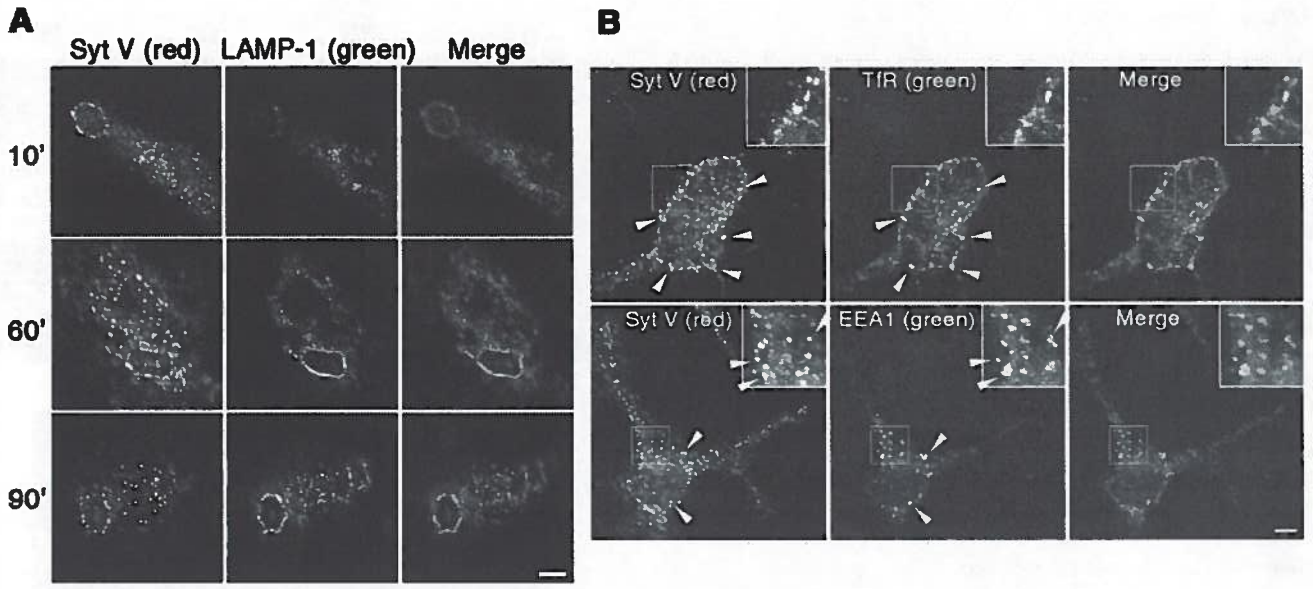

FIGURE 3. Intracellular localization of Syt V in PEM. *A*, Syt V and LAMP1 do not colocalize and associate to serum-opsonized zymozan-phagosomes with distinct kinetics. Bar, 3 μm. *B*, Syt V colocalizes with the recycling endosome marker transferin receptor (shown by arrowheads, *upper row*), whereas little colocalization was observed with the early endosome marker EEA1 (shown by arrowheads, *lower row*). Bar, 3 μm.

abundance of the two phagosome-associated Syt V forms varies during the phagosome maturation process (Fig. 2*C*). These two forms of Syt V may represent different posttranslational modifications, such as phosphorylation, as previously observed with Syt IV and Syt IX (36, 37). We next compared the recruitment kinetics of Syt V and LAMP1 to phagosomes containing serum opsonized-zymozan by confocal microscopy. Consistent with its lysosomal localization, we detected LAMP1 on phagosomes at later time points (60 and 90 min), whereas Syt V was present from early time points (Fig. 3*A*). The observation that Syt V and LAMP1 were recruited to phagosomes with distinct kinetics is consistent with the lack of colocalization of both proteins (Fig. 3*A*) and indicated that Syt V is not associated with late endosomal or lysosomal compartments. Furthermore, Syt V showed occasional colocalization with the early endosome marker EEA1, whereas it frequently colocalized with the recycling and early endosome marker transferrin receptor (Fig. 3*B*). These results indicate that Syt V associates with the recycling endosomal compartment.

Syt V is required for phagocytosis but not phagosome maturation

To study the potential role of Syt V in phagocytosis, we used RNAi to inhibit its expression. Transfection of RAW 264.7 cells with a siRNA to Syt V (28), significantly decreased Syt V levels

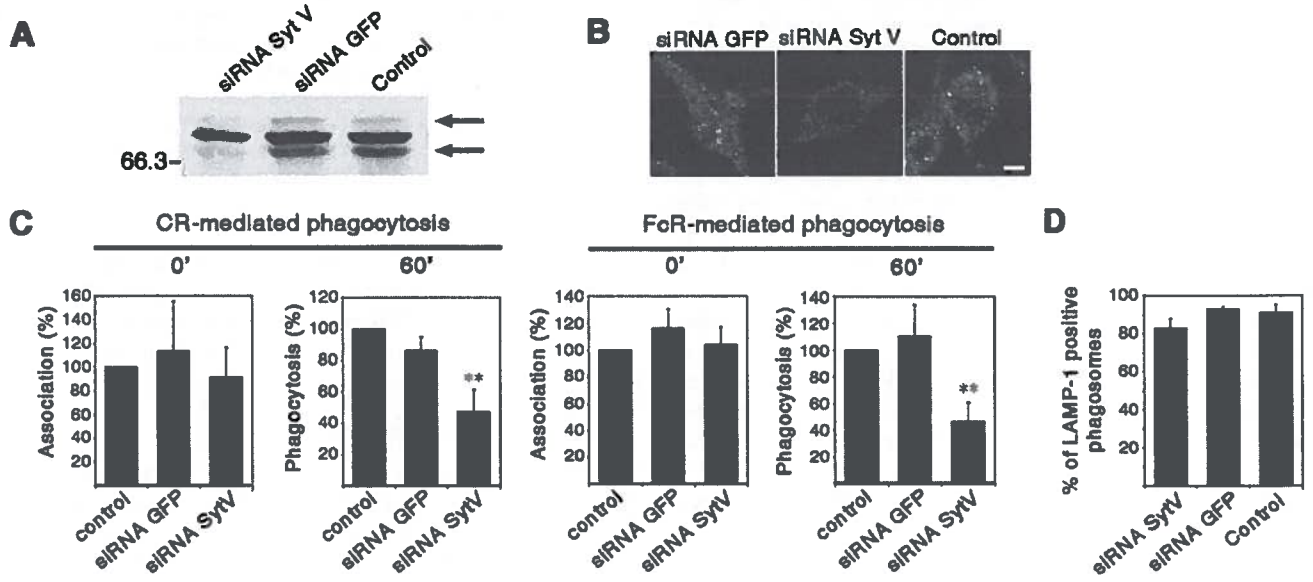

FIGURE 4. Silencing of Syt V impairs phagocytosis. RAW 264.7 cells were transfected with either a siRNA to Syt V or a siRNA to GFP, or only mock transfected (control), and incubated for 24 h. siRNA to Syt V efficiently reduced Syt V levels as shown by Western blot (*A*) and confocal immunofluorescence microscopy (*B*). Bar, 3 μm. In *A*, arrows show the two Syt V forms present in macrophages. The *middle band* is nonspecific. *C*, siRNA Syt V inhibited CR- and FcγR-mediated phagocytosis (60 min) but not particle binding (0 min). Particle association and phagocytosis were calculated on at least 100 cells, in triplicate. (**, $p \leq 0.0005$ vs siRNA GFP). *D*, LAMP1 is recruited to zymozan-phagosomes in siRNA Syt V-treated macrophages, as determined 90 min after the start of phagocytosis.

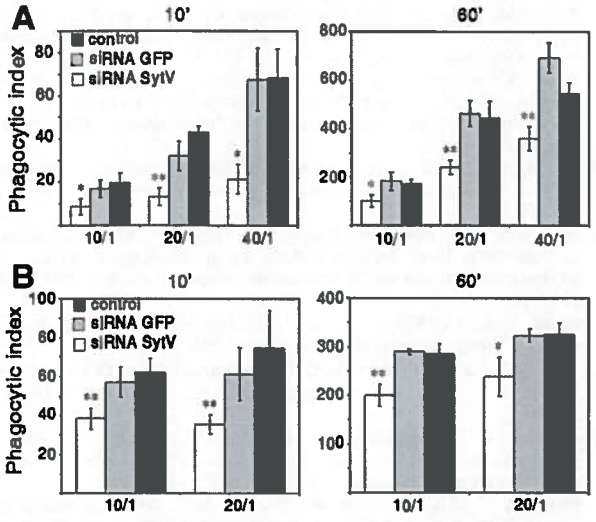

FIGURE 5. Inhibition of phagocytosis in siRNA Syt V-treated cells increases with particle load. The phagocytosis defect of cells treated with siRNA Syt V increases with particle load. Macrophages were incubated with increasing ratios of serum-opsonized zymozan (*A*) or *L. donovani* promastigotes (*B*) and particle internalization was determined after 10 min and 60 min. The phagocytic index was calculated on at least 100 cells in triplicate (*A* and *B*) (*, $p \leq 0.005$; **, $p \leq 0.0005$ vs RNAi GFP).

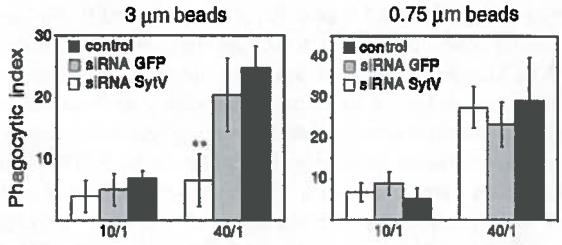

FIGURE 6. Inhibition of phagocytosis in siRNA Syt V-treated cells increases with particle size. The phagocytosis defect of cells treated with siRNA Syt V increases with particle size. Macrophages were fed with either 3- or 0.75-μm IgG-opsonised beads at ratios of 10:1 and 40:1 and particle internalization was determined after 10 min. The phagocytic index was calculated on at least 100 cells in triplicate (**, $p \leq 0.0005$ vs RNAi GFP).

after 24 h (Fig. 4*A*). In contrast, intensity of the two Syt V forms was similar in RAW 264.7 macrophages transfected with a siRNA to GFP and in control mock-transfected RAW 264.7 cells. Confocal immunofluorescence analysis indicated that Syt V was efficiently silenced by the siRNA Syt V treatment with most cells showing reduced fluorescence intensity (Fig. 4*B*). We next determined the impact of Syt V silencing on the phagocytosis of serum opsonized-zymozan and IgG-SRBC. Both CR- and FcγR-mediated phagocytosis were inhibited by over 50% in the absence of Syt V, revealing its role in phagocytosis (Fig. 4*C*). Importantly, this inhibition was not the consequence of a defective particle binding, as Syt V depletion had no effect on the association of serum opsonized-zymozan and IgG-SRBC to macrophages (Fig. 4*C*). Given that Syt V remains associated to phagosomes after particle internalization, we investigated its possible role in phagosome maturation. Silencing of Syt V had no effect on the recruitment of the lysosomal marker LAMP1 to zymosan-containing phagosomes (Fig. 4*D*), suggesting that Syt V does not a play a significant role in regulating interactions between phagosomes and lysosomes.

Phagocytosis of large particles and high particle loads is impaired in the absence of Syt V

To address the possibility that Syt V regulates membrane delivery at the phagocytic cup, we determined its requirement for phagocytosis under conditions of high particle loads and for the internalization of large particles. RAW 264.7 cells treated with siRNA Syt V were exposed to serum opsonized-zymozan at various particle-to-cell ratios (Fig. 5*A*). At 10 min after the initiation of phagocytosis, we observed a 50% inhibition of internalization for the 10:1 ratio and over 70% inhibition of internalization for the 40:1 particle-to-cell ratio in siRNA Syt V-treated cells (Fig. 5*B*) with respect to control cells. After 60 min, the impact of higher particle-to-cell ratio was less important than at 10 min. Similar results were obtained for the phagocytosis of the promastigote form of *Leishmania donovani*, a protozoan parasite that replicates inside macrophages (Fig. 5*B*).

We next compared the ability of siRNA Syt V-treated cells and control cells to internalize 0.75 μm and 3 μm IgG-opsonized latex beads at particle-to-cell ratios of 10:1 and 40:1. Silencing of Syt V strongly inhibited the internalization of 3 μm IgG-beads, whereas phagocytosis of 0.75 μm IgG-beads by siRNA Syt V-treated cells was similar to that observed in controls cells (Fig. 6). This suggests that Syt V is involved in the regulation of membrane supply under phagocytic conditions where important quantities of membrane are required.

Discussion

Syts play a key role in the regulation of Ca^{2+}-triggered exocytosis and membrane fusion, two important events associated to the phagocytic process. In this study, we identified the Ca^{2+}-dependent exocytosis regulator Syt V as a recycling endosome-associated protein that is recruited to the nascent phagosome in macrophages, independently of the phagocytic receptor involved. Silencing of Syt V by RNAi revealed a critical role for this protein in phagocytosis, particularly in the presence of large particles or a large particle load. Thus, given its role as a regulator of exocytosis (28), Syt V may control the mobilization of recycling endosomes as a source of endomembrane during phagocytosis.

Despite their role as regulators of membrane fusion events, few studies have addressed the potential involvement of Syts in the phagocytic process. The best-characterized Syt in phagocytosis is the ubiquitous Syt VII, which regulates Ca^{2+}-dependent exocytosis of lysosomes (14). In the absence of Syt VII, phagocytosis is impaired particularly under conditions of high membrane demand (17). In neutrophils, Syt II is present on granules and is recruited to the phagosome, but its role remains to be determined (18). Current knowledge on the distribution and function of Syt V is very limited. Previous studies showed that it is a dense-core vesicle-specific Syt that regulates Ca^{2+}-dependent exocytosis in brain and endocrine tissues. Hence, in neuronal PC12 cells and in the brain, Syt V is found on dense-core vesicles that undergo Ca^{2+}-dependent exocytosis and, in contrast to other Syts, is absent from synaptic-like microvesicles (26). Consistent with a direct role in Ca^{2+}-dependent stimulation of exocytosis, silencing of Syt V by RNAi strongly inhibited hormone exocytosis by pancreatic β cells (28). In macrophages, we found that Syt V is mainly associated to recycling endosomes and is also present on filopodia-like structures. Recycling endosomes are key players in phagocytosis as this subcompartment of the endocytic pathway is one of the prominent sources of endomembrane recruited to the phagocytic cup (11, 38). Hence, several recycling endosome-associated molecules involved in the regulation of membrane fusion

such as VAMP3, Rab11, and Arf6 are recruited to the nascent phagosomes and contribute to the internalization process (5–7, 39, 40). The recruitment of Syt V to the nascent phagosome is consistent with its localization on recycling endosomes and is functionally important, as phagocytosis of various types of particles was inhibited following its depletion by RNAi. This inhibition was particularly severe when macrophages depleted in Syt V were fed with large particles or with a large particle load. Given that Syt V is a regulator of exocytosis (26, 28), these observations are consistent with a role for Syt V in regulating focal exocytosis of recycling endosomes during phagocytosis. The possibility that Syt V acts in concert with known SNAREs and recycling endosome-associated regulators of phagosome formation (VAMP3, Rab11, and Arf6) remains to be determined. Recruitment of Syt V to the phagosome independently of the phagocytic receptor engaged and its requirement for CR- and FcγR-mediated phagocytosis indicate that Syt V is part of the general phagocytic machinery.

The association of Syt V with the phagosome throughout the maturation process raised the possibility that it regulates interactions with the endocytic system. However, acquisition of the lysosomal marker LAMP1 was normal in the absence of Syt V, indicating that Syt V is not involved in phagosome maturation. One possible role for phagosome-associated Syt V could be the regulation of phagosome maintenance and/or expansion (41, 42). Indeed, as intravacuolar microorganisms proliferate within their host cell, the area of phagosome membrane must increase to accommodate the replicating pathogens. This may involve interactions with host cell organelles and vesicular compartments, but the underlying mechanisms remain poorly understood.

Syt V was not only present on at the phagocytic cup and on phagosomes but also on plasma membrane, notably on filopodia-like structures. This finding is consistent with the possibility that Syt V-containing recycling endosomes fuse with the plasma membrane to release their content and suggests a more general role for Syt V. Delivery of membrane from recycling endosomes to the phagocytic cup allows rapid release of TNF-α and expands the membrane for phagocytosis (43). Upon macrophage activation, there is an increased vesicular and recycling endosomes trafficking to accommodate cytokine secretion and this is related to the up-regulation of the expression of relevant SNAREs (43–45). Current studies are addressing the possible role of Syt V in proinflammatory cytokine secretion during phagosome formation.

Acknowledgments

We thank Marcel Desrosiers for assistance with confocal microscopy and Dr. Eric Prina for comments and suggestions.

Disclosures

The authors have no financial conflict of interest.

References

1. Aderem, A., and D. M. Underhill. 1999. Mechanisms of phagocytosis in macrophages. *Annu. Rev. Immunol.* 17: 593–623.
2. Stuart, L. M., and R. A. Ezekowitz. 2005. Phagocytosis: elegant complexity. *Immunity* 22: 539–550.
3. Silverstein, S. C. 1977. Endocytic uptake of particles by mononuclear phagocytes and the penetration of obligate intracellular parasites. *Am. J. Trop. Med. Hyg.* 26: 161–169.
4. Hackam, D. J., O. D. Rotstein, C. Sjolin, A. D. Schreiber, W. S. Trimble, and S. Grinstein. 1998. v-SNARE-dependent secretion is required for phagocytosis. *Proc. Natl. Acad. Sci. USA* 95: 11691–11696.
5. Bajno, L., X. R. Peng, A. D. Schreiber, H. P. Moore, W. S. Trimble, and S. Grinstein. 2000. Focal exocytosis of VAMP3-containing vesicles at sites of phagosome formation. *J. Cell Biol.* 149: 697–706.
6. Cox, D., D. J. Lee, B. M. Dale, J. Calafat, and S. Greenberg. 2000. A Rab11-containing rapidly recycling compartment in macrophages that promotes phagocytosis. *Proc. Natl. Acad. Sci. USA* 97: 680–685.
7. Niedergang, F., E. Colucci-Guyon, T. Dubois, G. Raposo, and P. Chavrier. 2003. ADP ribosylation factor 6 is activated and controls membrane delivery during phagocytosis in macrophages. *J. Cell Biol.* 161: 1143–1150.
8. Braun, V., V. Fraisier, G. Raposo, I. Hurbain, J. B. Sibarita, P. Chavrier, T. Galli, and F. Niedergang. 2004. TI-VAMP/VAMP7 is required for optimal phagocytosis of opsonised particles in macrophages. *EMBO J.* 23: 4166–4176.
9. Becker, T., A. Volchuk, and J. E. Rothman. 2005. Differential use of endoplasmic reticulum membrane for phagocytosis in J774 macrophages. *Proc. Natl. Acad. Sci. USA* 102: 4022–4026.
10. Hatsuzawa, K., T. Tamura, H. Hashimoto, S. Yokoya, M. Miura, H. Nagaya, and I. Wada. 2006. Involvement of syntaxin 18, an endoplasmic reticulum (ER)-localized SNARE protein, in ER-mediated phagocytosis. *Mol. Biol. Cell* 17: 3964–3977.
11. Huynh, K. K., J. G. Kay, J. L. Stow, and S. Grinstein. 2007. Fusion, fission, and secretion during phagocytosis. *Physiology* 22: 366–372.
12. Jahn, R., T. Lang, and T. C. Sudhof. 2003. Membrane fusion. *Cell* 112: 519–533.
13. Sudhof, T. C. 2004. The synaptic vesicle cycle. *Annu. Rev. Neurosci.* 27: 509–547.
14. Martinez, I., S. Chakrabarti, T. Hellevik, J. Morehead, K. Fowler, and N. W. Andrews. 2000. Synaptotagmin VII regulates $Ca^{(2+)}$-dependent exocytosis of lysosomes in fibroblasts. *J. Cell Biol.* 148: 1141–1149.
15. Reddy, A., E. V. Caler, and N. W. Andrews. 2001. Plasma membrane repair is mediated by $Ca^{(2+)}$-regulated exocytosis of lysosomes. *Cell* 106: 157–169.
16. Roy, D., D. R. Liston, V. J. Idone, A. Di, D. J. Nelson, C. Pujol, J. B. Bliska, S. Chakrabarti, and N. W. Andrews. 2004. A process for controlling intracellular bacterial infections induced by membrane injury. *Science* 304: 1515–1518.
17. Czibener, C., N. M. Sherer, S. M. Becker, M. Pypaert, E. Hui, E. R. Chapman, W. Mothes, and N. W. Andrews. 2006. Ca^{2+} and synaptotagmin VII-dependent delivery of lysosomal membrane to nascent phagosomes. *J. Cell Biol.* 174: 997–1007.
18. Lindmark, I. M., A. Karlsson, L. Serrander, P. Francois, D. Lew, B. Rasmusson, O. Stendahl, and O. Nusse. 2002. Synaptotagmin II could confer Ca^{2+} sensitivity to phagocytosis in human neutrophils. *Biochim. Biophys. Acta* 1590: 159–166.
19. Breton, A., and A. Descoteaux. 2000. Protein kinase C-α participates in FcγR-mediated phagocytosis in macrophages. *Biochem. Biophys. Res. Commun.* 276: 472–476.
20. Brumell, J. H., J. C. Howard, K. Craig, S. Grinstein, A. D. Schreiber, and M. Tyers. 1999. Expression of the protein kinase C substrate pleckstrin in macrophages: association with phagosomal membranes. *J. Immunol.* 163: 3388–3395.
21. Larsen, E. C., J. A. DiGennaro, N. Saito, S. Mehta, D. J. Loegering, J. E. Mazurkiewicz, and M. R. Lennartz. 2000. Differential requirement for classic and novel PKC isoforms in respiratory burst and phagocytosis in RAW 264.7 cells. *J. Immunol.* 165: 2809–2817.
22. Zheng, L., T. P. Zomerdijk, C. Aarnoudse, R. van Furth, and P. H. Nibbering. 1995. Role of protein kinase C isozymes in Fcγ receptor-mediated intracellular killing of *Staphylococcus aureus* by human monocytes. *J. Immunol.* 155: 776–784.
23. Zheleznyak, A., and E. J. Brown. 1992. Immunoglobulin-mediated phagocytosis by human monocytes requires protein kinase C activation: evidence for protein kinase C translocation to phagosomes. *J. Biol. Chem.* 267: 12042–12048.
24. Ng Yan Hing, J. D., M. Desjardins, and A. Descoteaux. 2004. Proteomic analysis reveals a role for protein kinase C-α in phagosome maturation. *Biochem. Biophys. Res. Commun.* 319: 810–816.
25. Fukuda, M., and R. Sagi-Eisenberg. 2008. Confusion in the nomenclature of synaptotagmins V and IX: which is which? *Calc. Bind. Prot.* 3: 1–3.
26. Saegusa, C., M. Fukuda, and K. Mikoshiba. 2002. Synaptotagmin V is targeted to dense-core vesicles that undergo calcium-dependent exocytosis in PC12 Cells. *J. Biol. Chem.* 277: 24499–24505.
27. Gut, A., C. Kiraly, M. Fukuda, K. Mikoshiba, C. Wollheim, and J. Lang. 2001. Expression and localisation of synaptotagmin isoforms in endocrine (β)-cells: their function in insulin exocytosis. *J. Cell Sci.* 114: 1709–1716.
28. Iezzi, M., G. Kouri, M. Fukuda, and C. B. Wollheim. 2004. Synaptotagmin V and IX isoforms control Ca^{2+}-dependent insulin exocytosis. *J. Cell Sci.* 117: 3119–3127.
29. Lodge, R., and A. Descoteaux. 2005. *Leishmania donovani* promastigotes induce periphagosomal F-actin accumulation through retention of the GTPase Cdc42. *Cell. Microbiol.* 7: 1647–1658.
30. Rees, S., J. Coote, J. Stables, S. Goodson, S. Harris, and M. G. Lee. 1996. Bicistronic vector for the creation of stable mammalian cell lines that predisposes all antibiotic-resistant cells to express recombinant protein. *BioTechniques* 20: 102–104, 106, 108–110.
31. Stacey, K. J., I. L. Ross, and D. A. Hume. 1993. Electroporation and DNA-dependent cell death in murine macrophages. *Immunol. Cell Biol.* 71: 75–85.
32. Flandin, J. F., F. Chano, and A. Descoteaux. 2006. RNA interference reveals a role for TLR2 and TLR3 in the recognition of *Leishmania donovani* promastigotes by interferon-γ-primed macrophages. *Eur. J. Immunol.* 36: 411–420.
33. Lodge, R., T. O. Diallo, and A. Descoteaux. 2006. *Leishmania donovani* lipophosphoglycan blocks NADPH oxidase assembly at the phagosome membrane. *Cell. Microbiol.* 8: 1922–1931.

34. Li, C., B. Ullrich, J. Z. Zhang, R. G. W. Anderson, N. Brose, and T. C. Sudhof. 1995. Ca^{2+}-dependent and -independent activities of neural and non-neural synaptotagmins. *Nature* 375: 594–599.
35. Bai, J., and E. R. Chapman. 2004. The C2 domains of synaptotagmin: partners in exocytosis. *Trends Biochem. Sci.* 29: 143–151.
36. Mori, Y., M. Higuchi, Y. Hirabayashi, M. Fukuda, and Y. Gotoh. 2008. JNK phosphorylates synaptotagmin-4 and enhances Ca^{2+}-evoked release. *EMBO J.* 27: 76–87.
37. Haberman, Y., I. Ziv, Y. Gorzalczany, M. Fukuda, and R. Sagi-Eisenberg. 2005. Classical protein kinase C(s) regulates targeting of synaptotagmin IX to the endocytic recycling compartment. *J. Cell Sci.* 118: 1641–1649.
38. Braun, V., and F. Niedergang. 2006. Linking exocytosis and endocytosis during phagocytosis. *Biol. Cell* 98: 195–201.
39. Zhang, Q., D. Cox, C.-C. Tseng, J. G. Donaldson, and S. Greenberg. 1998. A requirement for ARF6 in Fcγ receptor-mediated phagocytosis in macrophages. *J. Biol. Chem.* 273: 19977–19981.
40. Allen, L. A., C. Yang, and J. E. Pessin. 2002. Rate and extent of phagocytosis in macrophages lacking vamp3. *J. Leukocyte Biol.* 72: 217–221.
41. Xu, S., A. Cooper, S. Sturgill-Koszycki, T. van Heyningen, D. Chatterjee, I. Orme, P. Allen, and D. Russell. 1994. Intracellular trafficking in *Mycobacterium tuberculosis* and *Mycobacterium avium*-infected macrophages. *J. Immunol.* 153: 2568–2578.
42. Ramsden, A. E., D. W. Holden, and L. J. Mota. 2007. Membrane dynamics and spatial distribution of *Salmonella*-containing vacuoles. *Trends Microbiol.* 15: 516–524.
43. Murray, R. Z., J. G. Kay, D. G. Sangermani, and J. L. Stow. 2005. A role for the phagosome in cytokine secretion. *Science* 310: 1492–1495.
44. Pagan, J. K., F. G. Wylie, S. Joseph, C. Widberg, N. J. Bryant, D. E. James, and J. L. Stow. 2003. The t-SNARE syntaxin 4 is regulated during macrophage activation to function in membrane traffic and cytokine secretion. *Curr. Biol.* 13: 156–160.
45. Stow, J. L., A. P. Manderson, and R. Z. Murray. 2006. SNAREing immunity: the role of SNAREs in the immune system. *Nat. Rev. Immunol.* 6: 919–929.

ANNEXE 3

Leishmania donovani lipophosphoglycan inhibits phagosomal maturation via action on membrane rafts

Martin E. Winberg, Åsa Holm, Eva Särndahl, Adrien F. Vinet, Albert Descoteaux, Karl-Eric Magnusson, Birgitta Rasmusson and Maria Lerm

Microbes and Infections, 11: 215-22

ELSEVIER

INSTITUT PASTEUR

Microbes and Infection 11 (2009) 215–222

www.elsevier.com/locate/micinf

Original article

Leishmania donovani lipophosphoglycan inhibits phagosomal maturation via action on membrane rafts

Martin E. Winberg [a,1], Åsa Holm [a,1,2], Eva Särndahl [a,3], Adrien F. Vinet [b], Albert Descoteaux [b], Karl-Eric Magnusson [a], Birgitta Rasmusson [a], Maria Lerm [a,*]

[a] *Div. of Med. Microbiology, Dept. of Clinical and Experimental Medicine, Faculty of Health Sciences, Linköping University, SE-581 85 Linköping, Sweden*
[b] *INRS-Institut Armand-Frappier, Laval, QC, Canada*

Received 8 September 2008; accepted 17 November 2008
Available online 3 December 2008

Abstract

Lipophosphoglycan (LPG), the major surface glycoconjugate on *Leishmania donovani* promastigotes, is crucial for the establishment of infection inside macrophages. LPG comprises a polymer of repeating Galβ1,4Manα-PO_4 attached to a lysophosphatidylinositol membrane anchor. LPG is transferred from the parasite to the host macrophage membrane during phagocytosis and induces periphagosomal F-actin accumulation correlating with an inhibition of phagosomal maturation. The biophysical properties of LPG suggest that it may be intercalated into membrane rafts of the host-cell membrane. The aim of this study was to investigate if the effects of LPG on phagosomal maturation are mediated via action on membrane rafts. We show that LPG accumulates in rafts during phagocytosis of *L. donovani* and that disruption of membrane rafts abolished the effects of LPG on periphagosomal F-actin and phagosomal maturation, indicating that LPG requires intact membrane rafts to manipulate host-cell functions. We conclude that LPG associates with membrane rafts in the host cell and exert its actions on host-cell actin and phagosomal maturation through subversion of raft function.

Keywords: *Leishmania*; Lipophosphoglycan; Membrane rafts; Phagosomal maturation; Actin

1. Introduction

The protozoan parasite *Leishmania donovani* causes visceral leishmaniasis (Kala Azar), and is transmitted to humans by infected *Phlebotomus* sand flies [1]. Its life cycle includes a flagellated, infective promastigote form primarily expressed in the gut of the sand fly, and an amastigote form, which is induced inside the macrophage phagosome in the mammalian host.

The ability of *L. donovani* to survive inside macrophages is crucial for establishment of infection [2], and depends on the action of several molecules including lipophosphoglycan (LPG) [3]. LPG is a polymer of the repeating Galβ1,4Manα-PO_4 unit linked to the membrane of the promastigote via a unique lipid anchor; 1-*O*-alkyl-2-*lyso*-phosphatidyl(*myo*)inositol with an unusually long saturated fatty acid chain of 24–26 C [4].

LPG has several effects on macrophage functions [5], including inhibition of phagosomal maturation [6–8]. This is illustrated by the finding that wild type (WT) promastigotes block phago-lysosomal formation, whereas mutants lacking phosphoglycans, including LPG, are found in a phago-lysosomal compartment [6–8]. LPG causes accumulation of F-actin around phagosomes carrying WT *L. donovani* [8]. The periphagosomal F-actin, which could act as a physical barrier to prevent phago-lysosomal fusion, is formed through impaired dissociation of the actin regulators Cdc42 and Rac1 from the phagosomal membrane [9–11]. Upon parasite attachment, LPG is transferred from the promastigote surface to the host-cell

* Corresponding author. Tel.: +46 13 22 47 79; fax: +46 13 22 47 89.
E-mail address: maria.lerm@liu.se (M. Lerm).
[1] These authors contributed equally.
[2] Present address: Department of Microbiology, Tumor and Cell Biology, Karolinska Institutet, Sweden.
[3] Present address: Department of Biomedicine, School of Health and Medical Sciences, Örebro University, Sweden.

1286-4579/$ - see front matter © 2008 Elsevier Masson SAS. All rights reserved.
doi:10.1016/j.micinf.2008.11.007

plasma membrane [12]. The lipid anchor of LPG is characterized by an extended, saturated fatty acid residue [13], suggesting that it may be intercalated into host-cell detergent-resistant membranes, DRM. We have recently shown that lipoarabinomannan (LAM) from *Mycobacterium tuberculosis*, whose molecular structure is reminiscent of LPG, is inserted into the membrane rafts of the host cell [14]. From this platform, LAM is able to delay phagosomal maturation, thereby being beneficial for *M. tuberculosis* virulence. The aim of the present study was to investigate whether LPG from *L. donovani* acts in a similar manner.

2. Methods

2.1. Cells

Human monocyte-derived macrophages were isolated from heparinised donor blood as previously described [14]. The cells were differentiated in Macrophage SFM supplemented with 100 U/ml penicillin, 100 mg/ml streptomycin, and 4 mM L-glutamine (Life Technologies). The cells were used after ten days of differentiation. Bone marrow-derived macrophages (BMM) were obtained by growing marrow cells from female BALB/c mice at 37 °C in 5% CO_2 in complete medium [Dulbecco's Modified Eagle Medium with glutamine (Life Technologies Inc., ON, Canada), containing 10% heat-inactivated FBS (Hyclone, Logan, UT), 10 mM HEPES pH 7.4, and antibiotics] in the presence of 15% (v/v) L929 cell-conditioned medium for seven days. BMM were made quiescent by culturing them in the absence of CSF-1 for 18 h prior to being used.

2.2. Cholesterol depletion

To deplete cholesterol, the medium was exchanged for fresh Macrophage SFM containing 10 mM β-cyclodextrin (βCD, Sigma Chemical Co) followed by incubation at 37 °C for 60 min. After three washes in 37 °C KRG with 2% bovine serum albumin (BSA, Boehringer-Mannheim GmBH) (KB), fresh Macrophage SFM was added. Using Amplex Red Cholesterol Assay Kit (Molecular Probes) we found that βCD extracted 60% of the cholesterol in the cells (not shown). Incubation in βCD made the cells round up, but viability was not significantly affected (not shown). Incubating the cholesterol-depleted cells in 10% AB serum over-night restored morphology and function (not shown).

2.3. Phagocytic prey and phagocytosis

Wild type *L. donovani* 1S promastigotes (WT) and the isogenic Galβ1,4Manα-PO_4-defective mutant *lpg2*$^-$KO, both expressing green fluorescent protein (GFP), were prepared as previously described [8]. The promastigotes were cultured at 26 °C in modified M199 medium with 500 μg/ml G418 (all from Gibco BRL/Life Technologies) [3]. Expression of GFP was assessed by fluorescence microscopy. The promastigotes were spun down and resuspended in the same volume of fresh growth medium 12–14 h before the experiment. Before addition to the macrophages, the promastigotes were again spun down and resuspended in fresh Macrophage SFM at 37 °C. Promastigotes in stationary phase of growth were added to the cells at a parasite-to-cell ratio of 10:1. After 20 min at 37 °C and 5% CO_2 (pulse), excess and unbound parasites were removed by three washes. Preparations for analysis of the distribution of LPG in the plasma membrane were fixed for 15 min at 4 °C in 2.0 % (w/v) paraformaldehyde (PFA, Sigma Chemical Co.) in KRG, and washed in PBS. For analysis of phagocytic capacity, periphagosomal F-actin and phagosomal maturation, incubation was continued at 37 °C for 30 min (chase), followed by fixation, as described above.

2.4. Fluorescent labelling

GM-1: cells were pre-fixed in 0.1% PFA in PBS, stained with Alexa Fluor 488-conjugated cholera toxin subunit B (CtxB) (Molecular Probes, Inc.) in PBS, washed and post-fixed for 15 min. LAMP-1 or LPG: fixed cells were incubated with PBS pH 7.6 with 2% BSA, 10% normal goat serum (Dakopatts AB) and 0.1% saponin (Sigma Chemical Co.), followed by washing and incubation with rat monoclonal antibodies against LAMP-1 (kindly provided by Dr. Sven Carlsson, Umeå University) or mouse monoclonal antibodies against LPG (CA7AE, Cedarlane Laboratories), washed and incubated with Alexa594 Fluor-conjugated goat anti-rat or anti-mouse antibodies (Molecular Probes, Inc.). Controls for unspecific labelling were made by substituting the primary antibody with purified rat or mouse IgG (not shown). F-actin: fixed cells were treated with PBS pH 7.6 with 2% BSA and 100 μg/ml lysophosphatidylcholine (Sigma Chemical Co.) and incubated with Alexa Fluor 594-conjugated phallacidin (Molecular Probes, Inc.). All cells were washed and mounted in an anti-fading medium with 20% Airvol 203 (Air Products and Chemicals, Utrecht, The Netherlands) and 4% Citifluor/Glycerol (Citifluor Ltd.) in 20 mM Tris buffer (pH 8.5) and left to set at 4 °C overnight.

2.5. Confocal microscopy

Confocal imaging was performed in a Sarastro 2000 microscope (Molecular Dynamics) equipped for dual activation and detection through a Nikon microscope with an ×60, NA 1.4 oil immersion objective. The 488 nm and 514 nm lines of the Argon laser were used for parallel excitation of FITC/GFP and Alexa594 Fluor. "535 nm" and "595 nm" beam splitters were employed for separation of the excitation and emission light, respectively. A 540DF30 band pass filter was employed for detection of the green signal (FITC/GFP) and an EFLP 600 long pass emission filter for the red signal (Alexa594 Fluor). This filter set-up ensured negligible red fluorescence in the green channel or vice versa.

2.6. Analysis of translocation of LAMP-1

Translocation of LAMP-1 to individual phagosomes was investigated in randomly selected confocal images of

cholesterol-depleted or control cells after phagocytosis of WT *L. donovani* promastigotes for 20 + 30 min or 1 μg/ml purified LPG for 50 min instead of the parasites. The translocation of LAMP-1 to individual phagosomes containing GFP-expressing promastigotes was classified as either (+) or (−). Typically, 50–100 cells, from preparations done in duplicate on two or three independent occasions were analyzed under each condition.

2.7. Quantification of phagocytosis and periphagosomal F-actin

Phagocytic capacity was assessed after a 30-min chase to allow maximal internalization of the promastigotes. The number of GFP-expressing promastigotes per cell was counted in randomly scanned confocal images of samples labelled with Alexa594-phallacidin. All data were normalized against controls phagocytosing *lpg2*$^{-}$KO promastigotes. The results were compiled from results from three independent experiments.

Periphagosomal F-actin was measured in randomly scanned confocal images of Alexa594-phallacidin-labelled samples containing GFP-expressing promastigotes as described in Ref. [8]. In short, the F-actin rim around each phagosome, *i.e.* periphagosomal F-actin, was manually traced in the red channel of the confocal image, the fluorescence intensity profile along the trace recorded, and the median intensity of the profile calculated. To avoid potential overlaps with cortical F-actin, only the part of the phagosome facing the cytosol was studied. The results were compiled from data obtained from samples prepared on at least three independent occasions. To compensate for possible variations in instrument performance between experimental days, all results were normalized against data from phagosomes in control cells incubated for 20 + 30 min with WT promastigotes and measured in parallel. The cells were focused in white light to avoid destruction of the fluorophores by bleaching and biased selection of certain sections of the preparations. Image analysis was performed on a Silicon Graphics OS2 workstation equipped with ImageSpace v3.2 (Molecular Dynamics).

2.8. Fractionation of cell membranes and detection of membrane components

Detergent-resistant membranes were isolated as described in Refs. [14,15] with some modifications. Briefly, adherent cells were incubated in 4 °C lysis buffer, containing 1% Triton X-100 (Merck–Schuchard), 2 μg/ml Aprotinin, 2 μg/ml Pepstatin, 2 μg/ml Leupeptin and 1 mM Pefa-block (all from Roche Diagnostics Corporation) for 30 min. Nuclei and whole cells were spun down at 500 *g* for 10 min. The supernatant was mixed with an equal volume of 85% sucrose (w/v in lysis buffer) and transferred to an ultracentrifugation tube. A step gradient was constructed by overlaying the sucrose-sample mixture with 5 ml 30% sucrose followed by a layer of 3 ml 5% sucrose. The gradient was centrifuged for 17–19 h at 200 000 *g* in an ultracentrifuge with a Beckman SW 41 rotor. After centrifugation, 10 fractions of 1 ml each were collected from top to bottom of the tube. The fractions were labelled 10 (top) to 1 (bottom, containing Triton X-100-soluble material). The fractions were transferred to nitrocellulose membranes by dot-blot, and blocked in 5% non-fat milk in Tris-buffered saline (TBS) with 0.05% Tween overnight at 4 °C. GM-1 was detected using horse radish peroxidase (HRP)-conjugated CtxB (1:2500, Sigma Chemical Co.). Mouse monoclonal antibodies (all diluted 1:1000) were used to detect the repeating Galβ1,4Manα-PO_4 units present on LPG (CA7AE, Cedarlane Laboratories), CD44 and CD45, followed by HRP-conjugated goat anti-mouse antibodies (1:5000) (all from DAKO). The blots were analyzed with a commercial enhanced chemiluminescence (ECL) detection kit (Amersham Bioscience). Labelling was quantified from digital images of the blots using ImageJ v1.32j.

2.9. Colocalization of LPG and lipid rafts

Late stationary phase *L. donovani* promastigotes were opsonized with mouse serum [10]. Zymosan particles (Sigma-Aldrich) were washed, and coated with purified LPG, kind gift from Dr. S. Turco, University of Kentucky, Lexington, KY, USA) as described [8]. For synchronized phagocytosis assays, macrophages were incubated at a particle-to-cell ratio of 10:1 for 15 min at 4 °C. Excess particles were removed and phagocytosis was triggered by transferring the cells at 37 °C for the indicated time points. Macrophages were next fixed, permeabilized, and blocked as previously described [16]. Cells were incubated with the anti-LPG mouse monoclonal antibody (CA7AE) and labelled with Alexa488 Fluor-conjugated goat anti-mouse antibody (Molecular Probes, Inc.) and Alexa Fluor 594-conjugated cholera toxin subunit B (Molecular Probes, Inc.). All coverslips were mounted on slides with Fluoromount-G (Southern Biotechnology Associates). Detailed analysis of protein localization on the phagosome was performed essentially as described [10] using an oil immersion Nikon Plan Apo 100 (N.A. 1.4) objective mounted on a Nikon Eclipse E800 microscope equipped with a Bio-Rad Radiance 2000 confocal imaging system (Bio-Rad).

2.10. Statistical analysis

Statistical analysis was performed using Student's *t*-test. Error bars are SEM.

3. Results

3.1. LPG localizes to membrane rafts in L. donovani-infected macrophages

The cholera toxin subunit B (CtxB) binds to glycosphingolipids with a strong affinity for GM-1 and a lower affinity for other gangliosides [17], and can therefore be used as a marker for membrane rafts [18]. Fluorescent labelling of MDM with CtxB revealed that a substantial part of the plasma membrane contained GM-1 (Fig. 2) Membrane extraction with cold Triton X-100 followed by density centrifugation,

fractionation and dot-blot [14] showed that GM-1 was present in fractions 7 and 8 (Fig. 1A), indicative of the membrane raft fraction [19]. Another raft marker, CD44 [20], was also enriched in fractions 7 and 8 (Fig. 1A), whereas CD45, a molecule which is excluded from rafts [21], was found only in fraction 1 corresponding to the Triton X-100 soluble fraction (Fig. 1A). Membrane rafts are enriched in cholesterol [22,23], and cholesterol depletion by agents such as β-cyclodextrin (βCD) disrupts their structure and function [24]. The cholesterol content of MDM was reduced by approximately 60% after incubation in 10 mM βCD for 60 min at 37 °C (not shown). Cholesterol-depleted macrophages remained adherent, but displayed a more rounded morphology compared to controls (not shown). Membrane fractionation showed a pronounced reduction of CD44 in rafts following incubation in βCD as well as a 50% loss of GM-1 reactivity (Fig. 1A). When MDM were infected with WT *L. donovani* promastigotes, dot-blot analysis of the membrane fractions revealed an enrichment of LPG in fractions 7 and 8 (corresponding to membrane rafts; Fig. 1B). However, the promastigote membrane itself also contains rafts rich in LPG [25], and the detergent-resistant membrane in fractions 7 and 8 could thus represent a mixture of macrophage and promastigote rafts. To assess whether the detected raft fractions originated from the macrophages and/or the parasites, we subjected the equal number of parasites as used for infections to Triton X-100 extraction followed by density gradient centrifugation and dot-blot. When comparing this sample with a preparation of macrophages plus promastigotes, we found that LPG originating from promastigote rafts represented approximately 50% of the total amount of LPG detected in fractions 7 and 8 (not shown).

To further demonstrate the localization of LPG in membrane rafts, we infected macrophages with either WT promastigotes or LPG-coated zymozan. As shown in Fig. 2A, at 10 min (left panel) and 30 min (right panel) after the initiation of phagocytosis, LPG was present in the phagosome

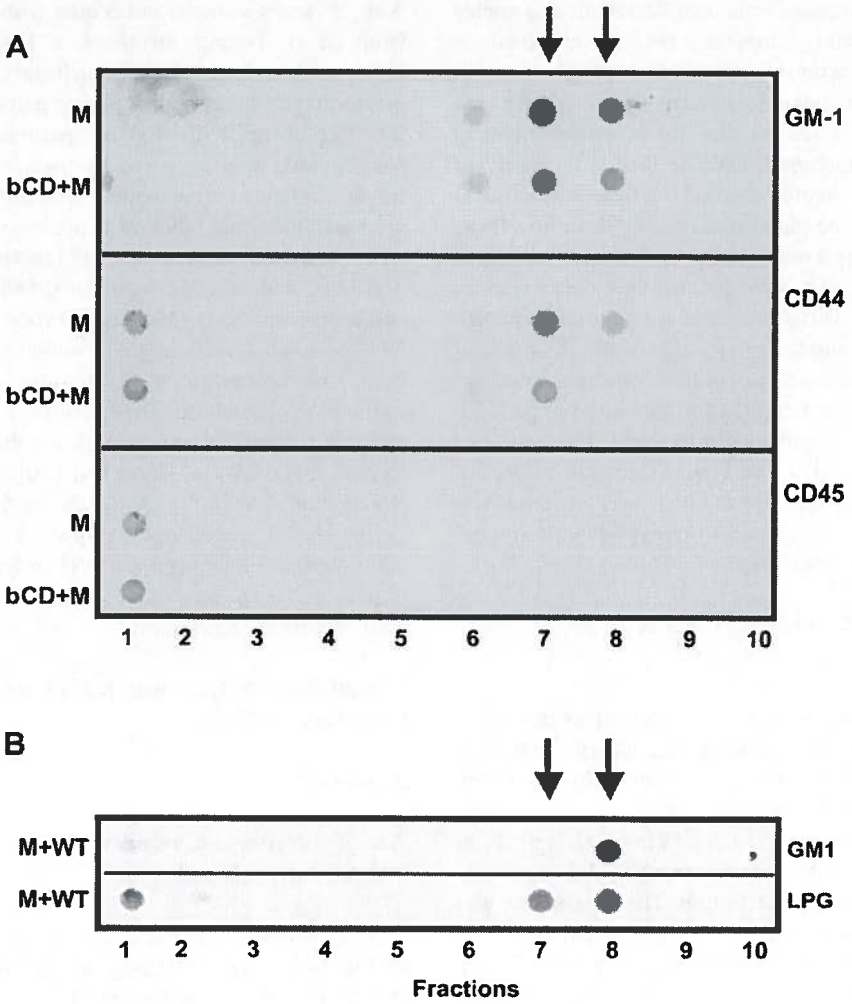

Fig. 1. Dot-blot analysis of membrane fractions from human monocyte-derived macrophages (MDMs). Lysates of MDMs were applied on a sucrose gradient and fractionated by centrifugation. Ten fractions were collected and analyzed using dot-blot. To disrupt membrane rafts the MDMs were preincubated in β-cyclodextrin (βCD) before lysis. GM1 was detected with the β-subunit of cholera toxin, CD44 and CD45 were detected with mouse monoclonal antibodies. Blots from representative experiments are shown ($n = 3–5$) in A. Arrows indicate fractions containing membrane rafts (fraction 7 and 8), characterized by the presence of GM1 and CD44 and the absence of CD45. B: Analysis of GM1 and LPG after membrane fractionation of MDMs infected with WT *L. donovani* promastigotes.

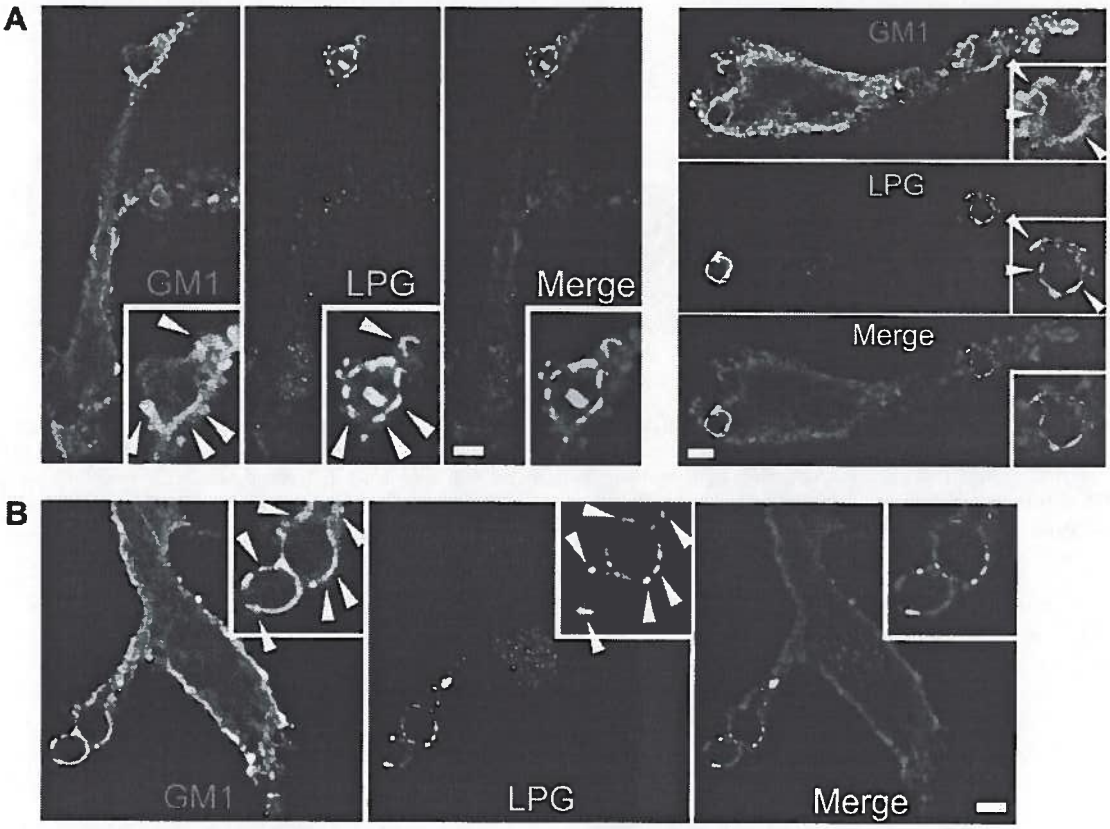

Fig. 2. Insertion of LPG into GM1-positive lipid rafts on phagosomal membranes. A. BMM were infected with WT promastigotes for 10 min (left panel) or 30 min (right panel), fixed, and labelled for LPG (green) and GM1 (red). Colocalization analysis showed that LPG is delivered early to GM1-enriched domain on newly forming phagocytic cup (left panel). Insertion of LPG into lipid microdomains is accompanied by a loss of the punctuated distribution of GM1 in the phagosomal membrane (right panel). B. BMM were allowed to internalize LPG-coated zymozan for 10 min, fixed, and labelled for LPG (green) and GM1 (red). LPG colocalizes with GM1-enriched domain. Bar, 3 μm.

membrane and colocalized with GM-1 (arrows). We also observed that at 30 min, the distribution of GM-1 labelling in the phagosomal membrane was more uniform than at 10 min, suggesting that LPG may influence raft integrity. Similar results were obtained following the internalization of LPG-coated zymozan, where colocalization of LPG and GM1 was observed at the phagosomal membrane (Fig. 2B).

3.2. *The effect of LPG on phagosomal maturation requires membrane rafts*

To further investigate the importance of membrane rafts in *Leishmania* pathogenesis, we studied the effect of cholesterol extraction on phagocytosis, periphagosomal F-actin and phagosomal maturation in *L. donovani*-infected cells. Macrophages ingested *lpg2*$^-$KO promastigotes slightly more effectively than WT promastigotes (Fig. 3). Cholesterol depletion reduced the capacity of macrophages to ingest *L. donovani* by 29% for *lpg2*$^-$KO promastigotes and by 36% ($p < 0.01$) for WT promastigotes compared to non-treated cells (Fig. 3). Quantification of periphagosomal F-actin around promastigote-containing phagosomes showed that its accumulation around phagosomes carrying WT promastigotes was reduced in cholesterol-depleted cells (1.0 ± 0.08 vs. 0.62 ± 0.06, $p < 0.001$; Fig. 4A). Cholesterol depletion itself caused a slight increase in periphagosomal F-actin (0.59 ± 0.04 vs. 0.46 ± 0.03, $p < 0.01$) around phagosomes containing the *lpg2*$^-$KO mutant (Fig. 4A). The decreased levels of F-actin around WT promastigote-containing phagosomes in cholesterol-depleted cells correlated with increased translocation of the late endosomal marker LAMP-1 to these phagosomes (Fig. 4B–E). Thus 62.5 (±5.9, SEM) % of WT promastigote-containing phagosomes were LAMP-1 positive in cholesterol-depleted macrophages, compared to 27.0 (±3.1, SEM) % in control cells ($p < 0.01$). We found no evidence of reduced transfer of LPG to the plasma membrane of cholesterol-depleted macrophages compared to controls (not shown).

4. Discussion

The aim of this study was to determine whether LPG affects the phago-lysosomal fusion machinery in human macrophages by disturbing membrane raft function. We found that LPG is transferred to membrane rafts of the host cells during infection in a way reminiscent of *M. tuberculosis* LAM [14]. Like LAM, LPG is known to retard the phagosomal maturation process in macrophages [8], and we show here that this ability of LPG is dependent on functional membrane rafts.

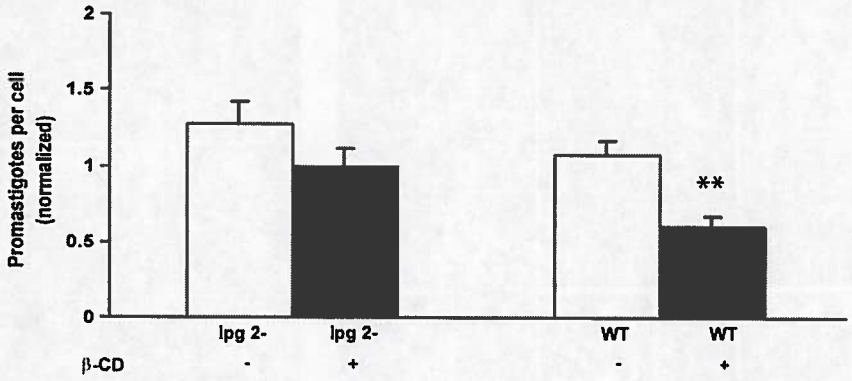

Fig. 3. Phagocytic capacity of monocyte-derived macrophages (MDMs) interacting with *L. donovani* promastigotes. Cholesterol was extracted from the plasma membrane of MDMs using β-cyclodextrin (βCD). The cells were then infected with GFP-expressing WT or *lpg2*$^-$KO promastigotes followed by fixation. The preparations were labelled with phallacidin and the average number of promastigotes per cell, in random confocal images, was assessed. Each group contains data from 124 to 308 cells from at least three independent experiments. Error bars indicate standard error of the mean (SEM). ** represents statistically significant differences $p < 0.01$.

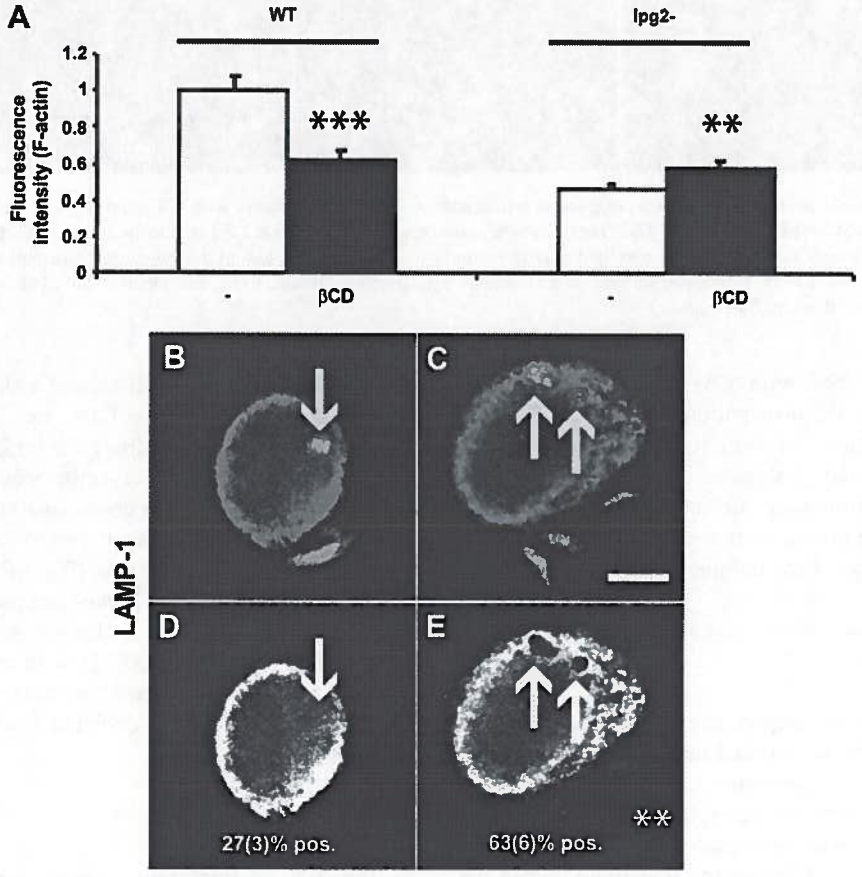

Fig. 4. Periphagosomal F-actin and translocation of LAMP-1 to *L. donovani* phagosomes. Monocyte-derived macrophages (MDMs; A open bars, B, D) or MDMs in which cholesterol has been extracted from the plasma membrane with β-cyclodextrin (βCD; A filled bars, C, E) were allowed to interact with GFP-expressing WT or *lpg2*$^-$KO promastigotes. (**A**) Fixed preparations were labelled with phallacidin, and examined by confocal microscopy. Periphagosomal F-actin was measured in randomly scanned confocal images. Each group contains data from 108 to 130 phagosomes from at least three independent experiments. Error bars indicate standard error of the mean (SEM). (**B–E**) Fixed cells were labelled with antibodies directed towards LAMP-1, and subjected to confocal microscopy. Images show the distribution of LAMP-1 (red channel; D–E) in MDMs containing WT promastigotes (green channel). Merged images are shown in B and C. The percentage of LAMP-1 positive phagosomes of more than 50 phagosomes for each condition and from three separate experiments was determined, and is shown in D (untreated, 27%) and E (βCD-treated, 63%). SEM is shown in brackets. Arrows indicate phagosomes. The scale bar is 10 μm. ** and ***, represent statistically significant differences, $p < 0.01$ and $p < 0.001$, respectively.

The consequences of LPG insertion into rafts, ultimately resulting in retarded phagosomal maturation, still remain obscure. We know from earlier studies that LPG causes an accumulation of periphagosomal F-actin [8] which is achieved by prevention of the release of active Cdc42 and Rac1, known regulators of F-actin, from the phagosomal membrane [9,10]. Although further investigation is required, the present data suggest that intact rafts are required for LPG to retain Cdc42 and Rac1 at the membrane, thereby preventing their inactivation. Similarly, functional membrane rafts are essential for recruitment and assembly of the NADPH oxidase complex [26]. Our data raise the possibility that association of LPG with these membrane microdomains contributes to the observed LPG-mediated inhibition of NADPH oxidase assembly at the phagosome membrane [27].

The reduced effect of LPG on periphagosomal F-actin and phagosomal maturation observed in cholesterol-depleted cells could equally well/alternatively be attributed to reduced transfer of LPG to membranes in these cells. However, this was ruled out by our control experiment showing that LPG translocated efficiently to membranes of cholesterol-depleted cells.

The observation that LPG localizes to the raft fraction of MDMs during infection with WT *L. donovani* promastigotes is not surprising since there is a striking biophysical resemblance between the LPG lipid anchor, with its unusually long, fully saturated fatty acid residue [13], and the highly saturated sphingolipids present in the target membrane [22].

Previous studies have shown that insertion of LPG into one leaflet of a lipid bilayer is sufficient to increase total membrane rigidity and inhibit membrane fusion [28,29]. Similarly, increased membrane rigidity due to integration of LAM has been shown to reduce phago-lysosomal fusion [30]. Thus, alteration of the biophysical properties of membranes carrying these microbial glycolipids may be an alternative explanation for the reduced ability of the host macrophages to accomplish phagosomal maturation upon infection.

Pucadyil et al. [31] found that cholesterol depletion resulted in reduced uptake of unopsonized WT *L. donovani* promastigotes while phagocytosis of opsonized promastigotes and *Escherichia coli* remained unaffected. This suggests that the receptor(s) responsible for internalization of unopsonized promastigotes are localized to membrane rafts, or depend on intact rafts for function. Our results showing reduced uptake of both WT and *lpg2*$^-$KO promastigotes after cholesterol-depletion point towards involvement of raft-associated receptors in the phagocytic process of *L. donovani*. However, since phagocytosis was not completely abolished in the absence of functional rafts additional uptake mechanisms may be involved.

We have previously shown that LPG prevents translocation of PKCα to the newly formed phagosomes, and that this correlates with accumulation of periphagosomal F-actin [8]. Macrophages depleted of cholesterol also fail to translocate PKCα to the membrane upon stimulation with phorbolmyristate acetate (unpublished data), but this only slightly increases the amount of F-actin around the phagosome (Fig. 4A, *lpg2*$^-$KO phagosomes). Therefore, we concluded that impaired translocation of PKCα only partially delivers an explanation for the accumulated F-actin at the *L. donovani* phagosome. A more profound effect of the interaction of LPG with rafts may be the retention of Cdc42 and Rac1 causing accumulation of F-actin [9,10] and an inhibition of the assembly of the NADPH oxidase at the phagosome membrane [27].

In conclusion, the present study shows that during phagocytosis of *L. donovani* promastigotes, LPG partitions to membrane rafts in the phagosomal membrane. Functional membrane rafts are required for the action of LPG on host cell actin and for inhibition of phagosomal maturation. Our results show that functional rafts of the host cell are required for LPG to exert its action and thus for *Leishmania* virulence. The transfer of glycolipids from pathogens to host-cell rafts, as observed with *M. tuberculosis* [14] and *L. donovani* (present study), may represent a general mechanism for manipulation of host-cell function.

Acknowledgements

We are grateful to Dr. Sam Turco, University of Kentucky, USA, for providing purified LPG and to Dr. Sven Carlsson, Umeå University, Sweden for providing the LAMP-1 antibody. The project was supported financially by the Swedish Medical Research Council (grants # 6251; K.E.M., # 13103; E.S.), the Swedish Research Council (grants # 621-2001-3570; 2007-3483; K.E.M., K.E.M., 529-2003-5994; M.L., 2005-7046; M.L. and 521-2002-6393; B.R.), the Swedish Society for Medical Research (B.R. and M.L.), the Swedish Medical Association (B.R., E.S.), Magn. Bergvalls Stiftelse (B.R.), Stiftelsen Lars Hiertas Minne (B.R., E.S.), Ekhaga Foundation (M.L.) and the Canadian Institutes of Health Research (grant # MOP-12933; A.D.). A.D. is the holder of a Canada Research Chair and was chercheur-boursier from the FRSQ. A.F.V. was partly supported by a studentship from the Foundation Armand-Frappier. The funders had no role in study design, data collection and analysis, decision to publish, or preparation of the manuscript.

References

[1] P.F.P. Pimenta, et al., Stage-specific adhesion of *Leishmania* promastigotes to the sandfly midgut, Science 256 (1992) 1812–1815.
[2] K.P. Chang, D.M. Dwyer, Multiplication of a human parasite (*Leishmania donovani*) in phagolysosomes of hamster macrophages in vitro, Science 193 (1976) 678–680.
[3] T.B. McNeely, S.J. Turco, Requirement of lipophosphoglycan for intracellular survival of *Leishmania donovani* within human monocytes, J. Immunol. 144 (1990) 2745–2750.
[4] S.J. Turco, A. Descoteaux, The lipophosphoglycan of *Leishmania* parasites, Annu. Rev. Microbiol. 46 (1992) 65–94.
[5] A. Descoteaux, S.J. Turco, Functional aspects of the *Leishmania donovani* lipophosphoglycan during macrophage infection, Microbes. Infect. 4 (9) (2002) 975–981.
[6] M. Desjardins, A. Descoteaux, Inhibition of phagolysosome biogenesis by the *Leishmania* lipophosphoglycan, J Exp Med 185 (1997) 2061–2068.
[7] S. Scianimanico, et al., Impaired recruitment of the small GTPase rab7 correlates with the inhibition of phagosome maturation by *Leishmania donovani* promastigotes, Cell. Microbiol. 1 (1999) 19–32.
[8] A. Holm, et al., *Leishmania donovani* lipophosphoglycan causes periphagosomal actin accumulation: correlation with impaired translocation of

PKCalpha and defective phagosome maturation, Cell. Microbiol. 3 (7) (2001) 439–447.
[9] M. Lerm, et al., *Leishmania donovani* requires functional Cdc42 and Rac1 to prevent phagosomal maturation, Infect. Immun. 74 (5) (2006) 2613–2618.
[10] R. Lodge, A. Descoteaux, *Leishmania donovani* promastigotes induce periphagosomal F-actin accumulation through retention of the GTPase Cdc42, Cell. Microbiol. 7 (11) (2005) 1647–1658.
[11] M. Lerm, et al., Inactivation of Cdc42 is necessary for depolymerization of phagosomal F-actin and subsequent phagosomal maturation, J. Immunol. 178 (11) (2007) 7357–7365.
[12] D.L. Tolson, S.J. Turco, T.W. Pearson, Expression of a repeating phosphorylated disaccharide lipophosphoglycan epitope on the surface of macrophages infected with *Leishmania donovani*, Infect. Immun. 58 (1990) 3500–3507.
[13] P.A. Orlandi, S.J. Turco, Structure of the lipid moiety of the *Leishmania donovani* lipophosphoglycan, J. Biol. Chem. 262 (1987) 10384–10391.
[14] A. Welin, et al., Incorporation of *Mycobacterium tuberculosis* lipoarabinomannan into macrophage membrane rafts is a prerequisite for the phagosomal maturation block, Infect. Immun. (2008).
[15] R. Xavier, et al., Membrane compartmentation is required for efficient T cell activation, Immunity 8 (6) (1998) 723–732.
[16] A.F. Vinet, M. Fukuda, A. Descoteaux, The exocytosis regulator synaptotagmin V controls phagocytosis in macrophages, J. Immunol. 181 (8) (2008) 5289–5295.
[17] R.G. Parton, Ultrastructural localization of gangliosides; GM1 is concentrated in caveolae, J. Histochem. Cytochem. 42 (2) (1994) 155–166.
[18] A.K. Kenworthy, N. Petranova, M. Edidin, High-resolution FRET microscopy of cholera toxin B-subunit and GPI-anchored proteins in cell plasma membranes, Mol. Biol. Cell. 11 (5) (2000) 1645–1655.
[19] C. Yuan, et al., The size of lipid rafts: an atomic force microscopy study of ganglioside GM1 domains in sphingomyelin/DOPC/cholesterol membranes, Biophys. J. 82 (5) (2002) 2526–2535.
[20] S. Ilangumaran, A. Briol, D.C. Hoessli, CD44 selectively associates with active Src family protein tyrosine kinases Lck and Fyn in glycosphingolipid-rich plasma membrane domains of human peripheral blood lymphocytes, Blood 91 (10) (1998) 3901–3908.
[21] P.W. Janes, S.C. Ley, A.I. Magee, Aggregation of lipid rafts accompanies signaling via the T cell antigen receptor, J. Cell. Biol. 147 (2) (1999) 447–461.
[22] D.A. Brown, E. London, Functions of lipid rafts in biological membranes, Annu. Rev. Cell. Dev. Biol. 14 (1998) 111–136.
[23] A.V. Samsonov, I. Mihalyov, F.S. Cohen, Characterization of cholesterol-sphingomyelin domains and their dynamics in bilayer membranes, Biophys. J. 81 (3) (2001) 1486–1500.
[24] S. Ilangumaran, D.C. Hoessli, Effects of cholesterol depletion by cyclodextrin on the sphingolipid microdomains of the plasma membrane, Biochem. J. 335 (Pt 2) (1998) 433–440.
[25] P.W. Denny, M.C. Field, D.F. Smith, GPI-anchored proteins and glycoconjugates segregate into lipid rafts in Kinetoplastida, FEBS Lett. 491 (1–2) (2001) 148–153.
[26] F. Vilhardt, B. van Deurs, The phagocyte NADPH oxidase depends on cholesterol-enriched membrane microdomains for assembly, EMBO J. 23 (4) (2004) 739–748.
[27] R. Lodge, T.O. Diallo, A. Descoteaux, *Leishmania donovani* lipophosphoglycan blocks NADPH oxidase assembly at the phagosome membrane, Cell. Microbiol. 8 (12) (2006) 1922–1931.
[28] I. Martin, et al., Lipophosphoglycan of *Leishmania donovani* inhibits lipid vesicle fusion induced by the N-terminal extremity of viral fusogenic Simian immunodeficiency protein, Eur. J. Biochem. 258 (1998) 150–156.
[29] B.J. Rasmusson, et al., Fusion of Sendai virus and individual host cells and inhibition of fusion by lipophosphoglycan measured with image correlation spectroscopy, Biochim. Biophys. Acta. 1404 (3) (1998) 338–352.
[30] E. Hayakawa, et al., A *Mycobacterium tuberculosis*-derived lipid inhibits membrane fusion by modulating lipid membrane domains, Biophys. J. 93 (11) (2007) 4018–4030.
[31] T.J. Pucadyil, et al., Cholesterol is required for *Leishmania donovani* infection: implications in leishmaniasis, Mol. Biochem. Parasitol. 133 (2) (2004) 145–152.

ANNEXE 4

The *Leishmania donovani* lipophosphoglycan excludes the vesicular proton-ATPase from phagosomes by impairing the recruitment of Synaptotagmin V

Adrien F. Vinet, Mitsunori Fukuda, Salvatore J. Turco, Albert Descoteaux

PLoS Pathogens, 5(10): e1000628. doi:10.1371/journal.ppat.1000628

The *Leishmania donovani* Lipophosphoglycan Excludes the Vesicular Proton-ATPase from Phagosomes by Impairing the Recruitment of Synaptotagmin V

Adrien F. Vinet[1], Mitsunori Fukuda[2], Salvatore J. Turco[3], Albert Descoteaux[1]*

1 INRS-Institut Armand-Frappier and Centre for Host-Parasite Interactions, Laval, Québec, Canada, 2 Department of Developmental Biology and Neurosciences, Tohoku University, Sendai, Miyagi, Japan, 3 Department of Biochemistry, University of Kentucky, Lexington, Kentucky, United States of America

Abstract

We recently showed that the exocytosis regulator Synaptotagmin (Syt) V is recruited to the nascent phagosome and remains associated throughout the maturation process. In this study, we investigated the possibility that Syt V plays a role in regulating interactions between the phagosome and the endocytic organelles. Silencing of Syt V by RNA interference revealed that Syt V contributes to phagolysosome biogenesis by regulating the acquisition of cathepsin D and the vesicular proton-ATPase. In contrast, recruitment of cathepsin B, the early endosomal marker EEA1 and the lysosomal marker LAMP1 to phagosomes was normal in the absence of Syt V. As *Leishmania donovani* promastigotes inhibit phagosome maturation, we investigated their potential impact on the phagosomal association of Syt V. This inhibition of phagolysosome biogenesis is mediated by the virulence glycolipid lipophosphoglycan, a polymer of the repeating Galβ1,4Manα1-PO_4 units attached to the promastigote surface via an unusual glycosylphosphatidylinositol anchor. Our results showed that insertion of lipophosphoglycan into ganglioside GM1-containing microdomains excluded or caused dissociation of Syt V from phagosome membranes. As a consequence, *L. donovani* promatigotes established infection in a phagosome from which the vesicular proton-ATPase was excluded and which failed to acidify. Collectively, these results reveal a novel function for Syt V in phagolysosome biogenesis and provide novel insight into the mechanism of vesicular proton-ATPase recruitment to maturing phagosomes. We also provide novel findings into the mechanism of *Leishmania* pathogenesis, whereby targeting of Syt V is part of the strategy used by *L. donovani* promastigotes to prevent phagosome acidification.

Citation: Vinet AF, Fukuda M, Turco SJ, Descoteaux A (2009) The *Leishmania donovani* Lipophosphoglycan Excludes the Vesicular Proton-ATPase from Phagosomes by Impairing the Recruitment of Synaptotagmin V. PLoS Pathog 5(10): e1000628. doi:10.1371/journal.ppat.1000628

Editor: Marilyn Parsons, Seattle Biomedical Research Institute, United States of America

Received May 5, 2009; **Accepted** September 23, 2009; **Published** October 16, 2009

Funding: This work was funded by grant MOP-12933 from the Canadian Institutes of Health Research and by an infrastructure grant from the FQRNT Regroupements Strategiques program. AD is the holder of a Canada Research Chair. AFV was partly supported by a studentship from the Fondation Armand-Frappier. The funders had no role in study design, data collection and analysis, decision to publish, or preparation of the manuscript.

Competing Interests: The authors have declared that no competing interests exist.

* E-mail: albert.descoteaux@iaf.inrs.ca

Introduction

Phagocytosis consists in the uptake and destruction of invading microorganisms, thereby playing an essential role in host defense against infection [1]. Following internalization, microbes end up in a vacuole, the phagosome, which engages in a maturation process involving highly regulated fusion and fission events with early and late endosomes, and with lysosomes [2,3]. This leads to the acidification of the phagosome and the acquisition of an array of hydrolases, culminating in the generation of a highly microbicidal environment [4]. Soluble N-ethylmaleimide-sensitive factor protein attachment protein receptor (SNARE)-mediated membrane fusion events regulate phagosome maturation by facilitating interactions with the endocytic compartments [5]. Hence, VAMP3 and syntaxin 13 are present transiently on the young phagosome to regulate early maturation steps, whereas VAMP7 and syntaxin 7 remain associated with the phagosome to regulate interactions with late endosomes/lysosomes [6–8]. The lysosome-associated Synaptotagmin (Syt) VII, which controls membrane delivery to nascent phagosomes [9], is also involved in phagolysosome fusion [9,10]. Other components and partners of these SNARE fusion machineries required during phagosome maturation remain to be identified.

Phagolysosome biogenesis is an important means of controling microbial growth. Yet, several pathogenic microorganisms have evolved mechanisms to subvert the phagosome maturation process, thus avoiding an encounter with the macrophage microbicidal machinery including exposition to reactive oxygen species and to acidification [4,11,12]. Protozoan parasites of the genus *Leishmania* cause a spectrum of diseases in humans, ranging from self-healing ulcers to potentially fatal visceral leishmaniasis, which affect millions of people worldwide. *Leishmania* is transmitted to mammals under its promastigote form during the bloodmeal of infected sand flies. Following phagocytosis by macrophages, promastigotes must avoid destruction to differentiate into amastigotes, the mammalian stage of the parasite that replicate inside acidic and hydrolase-rich parasitophorous vacuoles [13–15]. To avoid the microbicidal arsenal of macrophages, *L. donovani* and *L. major* promastigotes create an intracellular niche through the inhibition of phagolysosome biogenesis [16–19]. Genetic and biochemical approaches established that this inhibition is strictly dependent on the presence of lipophosphoglycan (LPG), an abundant surface glycolipid consisting of a polymer of Galβ1,4-Manα1-PO_4 units anchored into the promastigote membrane via an unusual glycosyl phosphatidylinositol [20,21]. Hence, phago-

Author Summary

Upon their internalization by macrophages, *Leishmania donovani* promastigotes inhibit phagolysosome biogenesis. This inhibition is mediated by the virulence glycolipid lipophosphoglycan (LPG), attached to the promastigote surface. We recently showed that the exocytosis regulator Synaptotagmin (Syt) V controls early steps of phagocytosis, and remains associated to the phagosome during the maturation process. Here, we show that Syt V contributes to phagolysosome biogenesis by regulating the acquisition of the hydrolase cathepsin D and the vesicular proton-ATPase. Insertion of LPG into lipid microdomains of the phagosome membrane excluded Syt V from phagosomes, enabling *L. donovani* promatigotes to inhibit the recruitment of the vesicular proton-ATPase to phagosomes, preventing their acidification. Collectively, our results provide novel insight into the mechanism of vesicular proton-ATPase recruitment to maturing phagosomes and reveal how the virulence glycolipid LPG contributes to the mechanism of *L. donovani* pathogenesis by preventing phagosome acidification.

somes harboring LPG-defective promastigotes quickly mature into functional phagolysosomes and coating of the Galβ1,4Manα1-PO_4-defective mutant *lpg2*-KO with purified LPG conferred the capacity to inhibit phagosome-lysosome fusion [16,17,19,22,23]. LPG-mediated phagosome remodeling is characterized by a periphagosomal accumulation of F-actin [22,23] and by the exclusion of cytosolic components of the NADPH oxidase from the phagosome membrane [24]. By creating an environment devoid of oxidants, *L. donovani* promastigotes evade a major microbicidal mechanism of macrophages and can initiate their differentiation into amastigotes. The ability of LPG to inhibit phagosome maturation is consistent with its role in the establishment of *L. donovani* and *L. major* promastigotes inside macrophages [24,25].

A possible mechanism by which LPG exerts its action on phagosome maturation involves the transfer of LPG from the parasite surface to lipid microdomains present in the phagosome membrane, causing a disorganization of these structures and preventing their formation after phagocytosis [26–29]. Phagosomal lipid microdomains are essential for the recruitment/assembly of the NADPH oxidase and the vacuolar proton-ATPase and are involved in the regulation of phagosome-endosome fusions [27,30,31]. Disruption of lipid microdomains by microbial virulence factors is likely to facilitate the establishment of infection through an effect on phagolysosomal biogenesis, as described for the cyclic β-1,2-glucans of *Brucella abortus* and the lipoarabinomannan of *Mycobacterium tuberculosis* [32,33]. How lipid microdomains regulate interactions between phagosomes and the endocytic system is unclear. The fact that proteins involved in membrane fusion such as SNAREs and Syts are located in lipid microdomains is consistent with these structures acting as fusion sites [34,35].

Recently, we identified the exocytosis regulator Syt V [36–39] as a recycling endosome-associated protein that is recruited to the forming phagosome independently of the phagocytic receptor engaged [40]. Silencing of Syt V by RNAi revealed a role for this protein during phagocytosis, particularly under conditions of high membrane demand, possibly through the mobilization of recycling endosomes as a source of endomembrane. The association of Syt V with the phagosome throughout the maturation process raised the possibility that Syt V regulates interactions with the endocytic system [40]. Here, we provide evidence for a novel function of Syt V in phagolysosome biogenesis, where it controls the acquisition of cathepsin D and the vesicular proton-ATPase. We also provide novel insight into the mechanism of *L. donovani* pathogenesis with the demonstration that insertion of LPG into GM1-containing microdomains impairs the association of Syt V to phagosome membranes, enabling *L. donovani* promatigotes to inhibit the recruitment of the vesicular proton-ATPase to phagosomes, thereby preventing their acidification.

Results

Silencing of Syt V impairs phagosomal recruitment of the vacuolar ATPase and cathepsin D

Syt V, a regulator of exocytosis, is recruited to the nascent phagosome and remains associated throughout the maturation process [40], suggesting that it may participate in the regulation of phagolysosome biogenesis. Maturing phagosomes sequentially interact with various endocytic organelles to acquire hydrolases such as cathepsins and the proton-vacuolar ATPase (V-ATPase), which is responsible for phagosome acidification [2,41,42]. To assess the potential role of Syt V in the acquisition of microbicidal features, we inhibited its expression by transfecting RAW 264.7 cells with a siRNA to Syt V [40] (Figure 1A) and we examined the localization of phagosomal markers following the internalization of Zymosan (Zym) or latex beads. Our results show that in the absence of Syt V, recruitment of both the early endosomal (EEA1) and the lysosomal (LAMP1) markers to Zym-containing phagosomes was normal (Figures 1B and S1A and B), whereas the acquisition of cathepsin D and the V-ATPase *c* subunit was inhibited (Figure 1B–E). Reduction in cathepsin D acquisition ranged from 25 to 35% for phagosomes containing beads and from 41 to 48% for phagosomes containing Zym, in five independent experiments. In the case of the V-ATPase *c* subunit, the reduction ranged from 30 to 50% for phagosomes containing beads and from 45 to 60% for phagosomes containing Zym in five independent experiments (Figure 1C–E). Interestingly, silencing of Syt V had no detectable effect on the acquisition of cathepsin B (Figure 1C). These results provide evidence that Syt V selectively regulates the phagosomal acquisition of cathepsin D and the V-ATPase *c* subunit.

L. donovani promastigotes impair the phagosomal association of Syt V

Given their ability to inhibit phagosome maturation [16,17,24], we explored the impact of *L. donovani* promastigotes and their LPG on the phagosomal association of Syt V. Accordingly, we infected the mouse macrophage cell line RAW 264.7 stably expressing a Syt V-GFP fusion protein (Syt V-GFP RAW 264.7 cells) with either wild-type (WT) *L. donovani* promastigotes, the LPG-defective *lpg1*-KO mutant, the Galβ1,4Manα1-PO_4-defective *lpg2*-KO mutant or the *lpg2*-KO add-back (*lpg2*-KO+*LPG2*). We used Zym as a positive control for the recruitment of Syt V to phagosomes [40]. Our results show that Syt V-GFP was present on over 80% of phagosomes containing either *lpg1*-KO promastigotes, *lpg2*-KO promastigotes, or Zym (Figure 2A and B). In contrast, we detected Syt V-GFP on 54 to 65% of phagosomes containing either WT or *lpg2*-KO+*LPG2* promastigotes in three independent experiments. Quantification analyses revealed a three-fold reduction in the levels of Syt V-GFP present on those positive phagosomes with respect to phagosomes containing either *lpg1*-KO or *lpg2*-KO promastigotes (Figure 2C). These observations suggested that LPG impairs the phagosomal recruitment of Syt V.

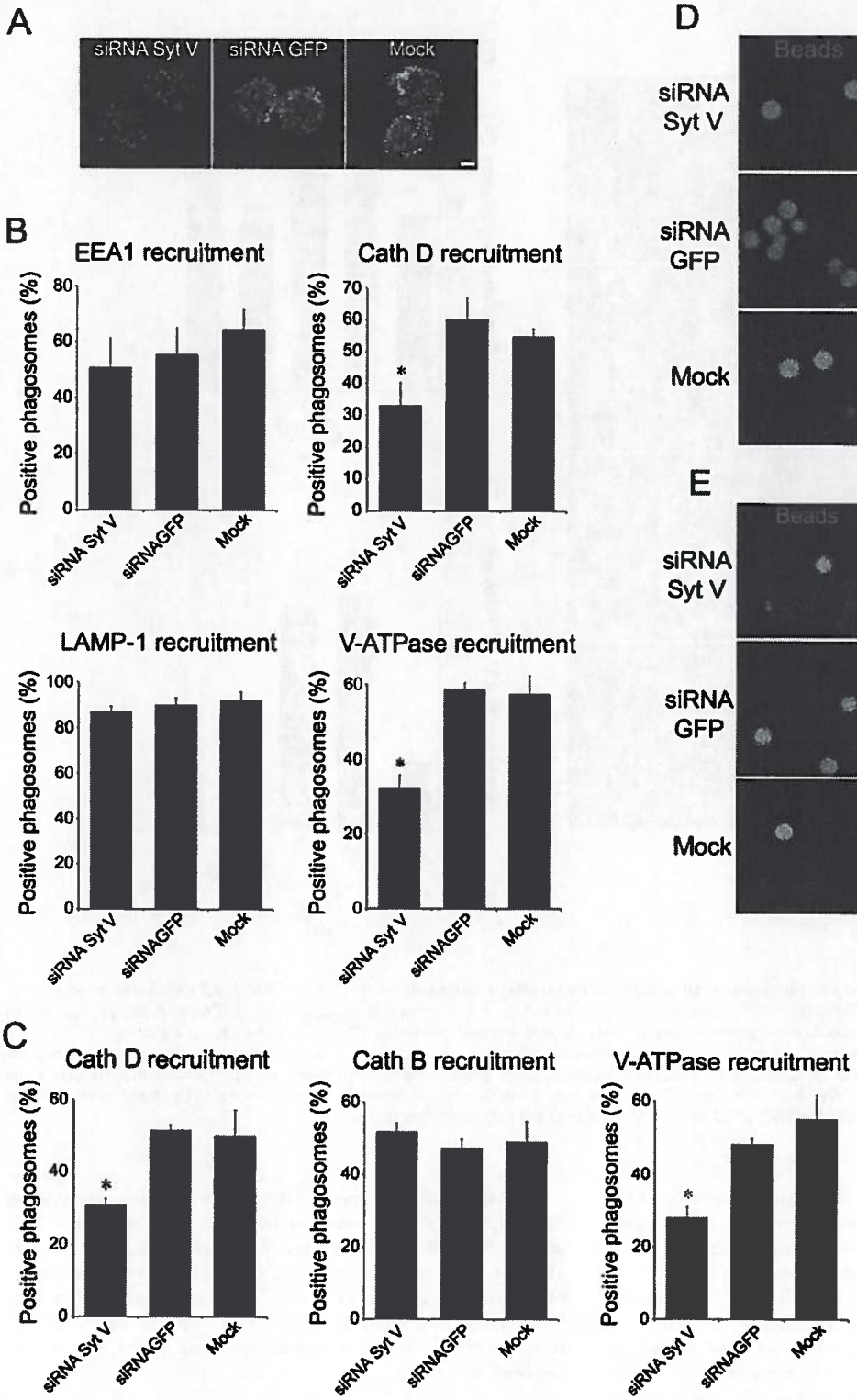

Figure 1. Silencing of Syt V impairs the recruitment of cathepsin D and the V-ATPase to phagosomes. RAW 264.7 cells were transfected with either a siRNA to Syt V, a siRNA to GFP, or only mock transfected, and incubated for 24 h. Efficiency of Syt V silencing was verified by confocal immunofluorescence microscopy (*A*). *B* and *C*, RAW 264.7 cells were allowed to internalize Zym (*B*) or latex beads (*C*) after siRNA transfection. Phagosomal recruitments were determined at 15 min for EEA1 and at 2 h for cathepsin D, cathepsin B, and LAMP1 on at least 100 phagosomes for each condition. Data are shown as the percentage of phagosomes showing recruitment. Five independent experiments were performed and the bars show the standard deviations of one representative triplicate (*, $p \leq 0.05$). *D* and *E*, representative confocal images illustrating the recruitment of cathepsin D (*D*) and of the V-ATPase (*E*) on phagosomes containing latex beads. Bar, 3 μm.
doi:10.1371/journal.ppat.1000628.g001

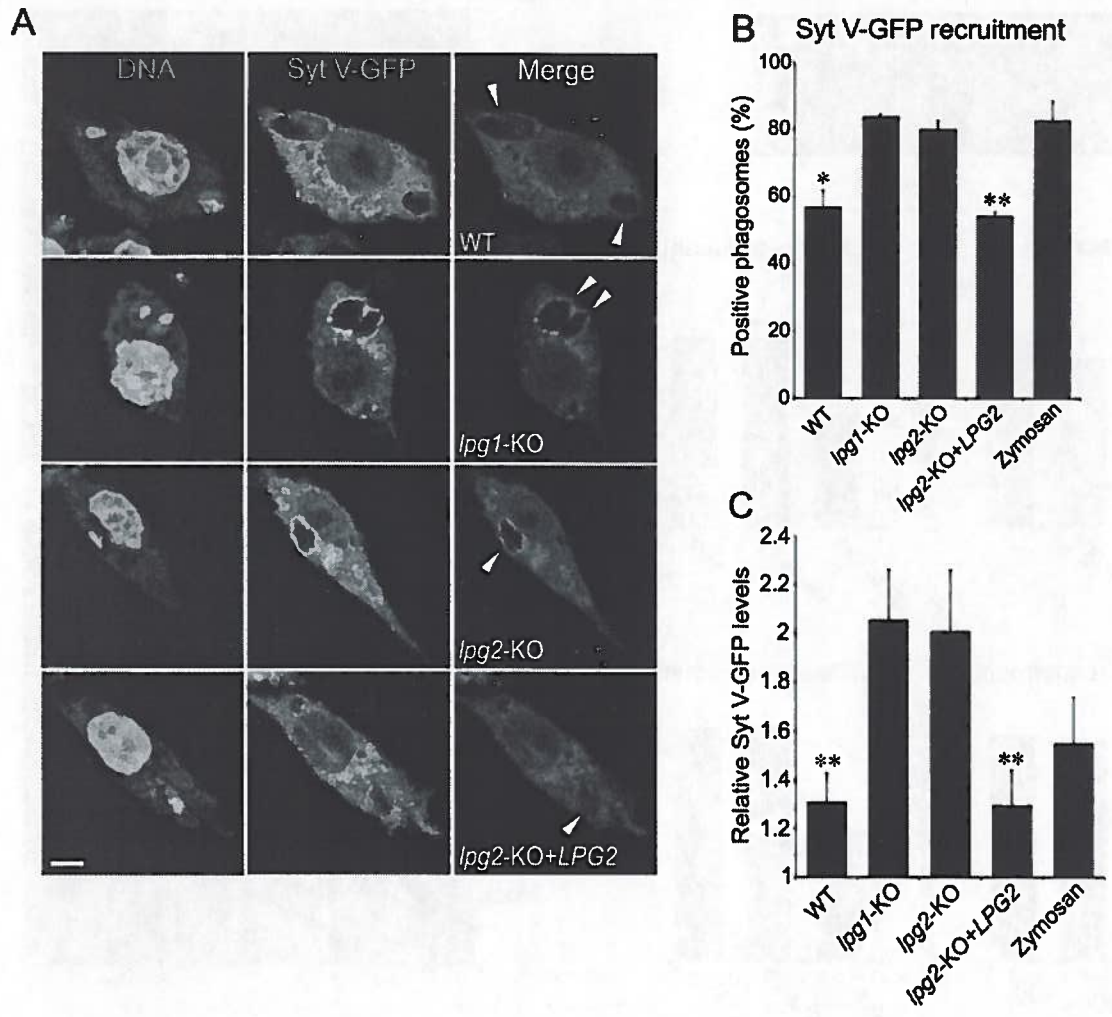

Figure 2. Syt V-GFP is excluded from *L. donovani* promastigote-containing phagosomes. Syt V-GFP RAW 264.7 cells were infected with either WT *lpg1*-KO, *lpg2*-KO, *lpg2*-KO+*LPG2 L. donovani* promastigotes or zymosan for 2 h, fixed and stained for DNA. *A*, Confocal images illustrating the presence of Syt V-GFP on parasite-containing phagosomes (shown by arrowheads). Presence (*B*) and relative levels (*C*) of Syt V-GFP were determined. Recruitment was determined on at least 100 phagosomes for each condition and expressed as a percentage of recruitment, and relative levels were determined by the P/C ratio as described in *Materials and Methods*. Three independent experiments were performed and the bars show the standard deviations of one representative triplicate (*, $p \leq 0.05$; **, $p \leq 0.005$; *B* and *C*, *p* values compare the presence and the accumulation of Syt V-GFP on phagosomes containing WT and *lpg2*-KO+*LPG2 vs lpg1*-KO and *lpg2*-KO parasites). Bar, 3 μm.
doi:10.1371/journal.ppat.1000628.g002

To directly address the impact of LPG on the recruitment of Syt V to phagosomes, we fed bone marrow-derived macrophages (BMM) with either Zym or Zym coated with purified LPG (LPG-Zym) [22]. Consistent with previous observations [17,22], we found a reduced acquisition of LAMP-1 on phagosomes containing LPG-Zym, whereas the recruitment of EEA1 to phagosomes containing Zym or LPG-Zym was similar (Figure 3A and B). In the case of Syt V, we detected its presence on 24 to 30% of phagosomes containing LPG-Zym compared to over 60% of phagosomes containing Zym at all time points tested in three independent experiments (Figure 3C and D). Quantification analyses showed that the levels of Syt V present on those positive phagosomes containing LPG-Zym was significantly lower than the Syt V levels on phagosomes containing Zym (Figure 3C and D). We obtained similar results with the Syt V-GFP RAW 264.7 cells (Figures 3E and S2). Furthermore, the signals for Syt V (green) and LPG (red) rarely superimposed on the phagosome membrane (Figure 4A), and fluorescence intensity line scans acquired along the periphery of phagosomes showed that the most intense LPG and Syt V signals never overlapped, at both 30 min and 120 min after the initiation of phagocytosis (Figure 4B). We made similar observations in Syt V-GFP RAW 264.7 cells (Figure 4C and D). Collectively, these results established that insertion of LPG into the phagosomal membrane caused the exclusion of Syt V in a very localized manner.

Recruitment of Syt V to GM1-containing microdomains of phagosome membranes is prevented by LPG

In rat brain synaptosomes, a fraction of Syt I and Syt II is present in lipid rafts [34]. To examine whether LPG-mediated exclusion of Syt V from phagosomes was related to the insertion of LPG into lipid microdomains [27,29] (Figure 5D), we first determined whether phagosome-associated Syt V was present in these microdomains. Our results clearly show that a fraction of Syt

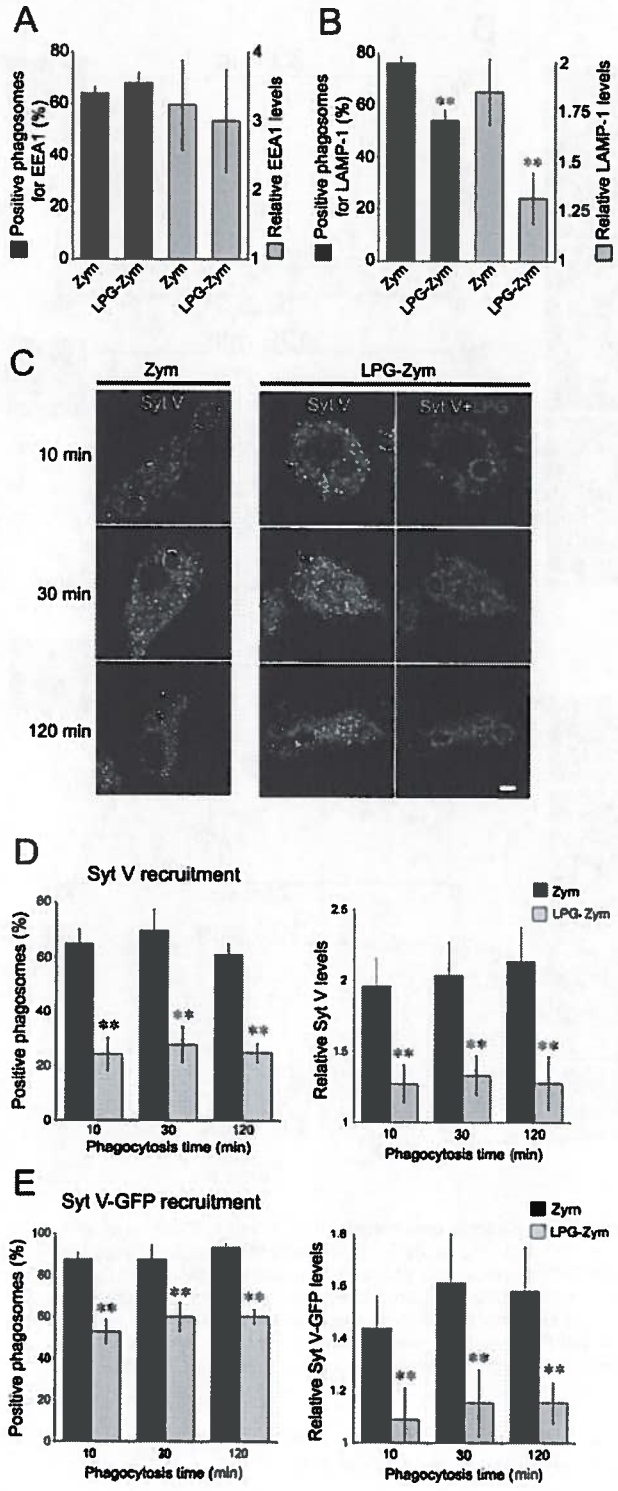

Figure 3. Recruitment of Syt V is impaired on phagosomes containing LPG-coated Zymosan. *A* and *B*, BMM were allowed to internalize Zym or LPG-Zym during 15 min (A) or 2 h (B), and prepared for confocal analysis. Presence (left y axis) and P/C ratio levels (right y axis) were determined for EEA1 (A) or LAMP-1 (B). *C* and *D*, BMM cells were allowed to internalize Zym or LPG-Zym for 10 min, 30 min or 2 h, fixed and stained for either endogenous Syt V (green) and LPG (red). The presence of Syt V and LPG on phagosomes is illustrated by confocal images (C). *D*. Quantification of Syt V recruitment (left panel) and relative Syt V levels (P/C ratio) on these phagosomes (right panel) were determined. *E*. Syt V-GFP cells were allowed to internalize Zym or LPG-Zym for 10 min, 30 min or 2 h, fixed and stained for LPG. Quantification of Syt V- recruitment (left panel) and relative Syt V levels on these phagosomes (right panel) were determined. The recruitment of EEA1, LAMP1 and Syt V was determined on at least 100 phagosomes for each condition, at least three independent experiments were performed and the bars show the standard deviations of one representative triplicate (*, $p \leq 0.05$; **, $p \leq 0.005$). Bar, 3 μm.
doi:10.1371/journal.ppat.1000628.g003

V colocalizes with GM1-microdomains on Zym-containing phagosomes (Figure 5A, arrowheads). Consistently, cholesterol depletion by methyl-β-cyclodextrin inhibited the recruitment of Syt V (Figure 5B and C). Having established that phagosomal Syt V associates with GM1-containing microdomains, we examined the localization of LPG, Syt V, and GM1 on phagosomes containing either Zym or LPG-Zym. For phagosomes containing Zym, the signals for Syt V (blue) and GM1 (red) superposed to a large extent and fluorescence intensity line scans acquired along the periphery of a representative phagosome showed that most of the Syt V and GM1 signals overlapped (Figure 5E and F, top panel). In contrast, on phagosomes containing LPG-Zym, the signals for LPG and GM1 colocalized, whereas most of the remaining Syt V signal was not associated with GM1 (representative phagosome, Figure 5E and F, bottom panel). These results established that association of LPG with GM1-containing microdomains resulted in the exclusion or dissociation of Syt V from the phagosome membrane.

L. donovani promastigotes exclude the V-ATPase from phagosomes via their LPG

The demonstration that Syt V regulates acquisition of the V-ATPase led us to verify the hypothesis that exclusion or dissociation of Syt V from phagosomes containing *L. donovani* promastigotes may impair the recruitment of the V-ATPase to these phagosomes. At 2 h after the initiation of phagocytosis, our results from three independent experiments showed a reduction in the recruitment of the V-ATPase *c* subunit on phagosomes containing WT promastigotes, ranging from 54 to 62% with respect to phagosomes containing either *lpg1*-KO or *lpg2*-KO promastigotes (Figure 6A and B). Co-localization of the V-ATPase *c* subunit with LAMP-1 on phagosomes containing *lpg1*-KO promastigotes showed that the V-ATPase *c* subunit was present on the phagosome membrane (Figure S3). As expected, phagosomes containing *lpg2*-KO+*LPG2* cells were similar to WT-phagosomes with respect to the presence of the V-ATPase. We next monitored the acidification of *L. donovani* promastigote-containing phagosomes using the lysosomotropic agent LysoTracker red as an indicator of phagosome pH. Our results showed a clear correlation between the presence of the V-ATPase *c* subunit and the association of LysoTracker red to phagosomes (Figure 6C). In Figure 1, we showed that silencing of Syt V inhibited recruitment of the V-ATPase *c* subunit to phagosomes containing Zym or latex beads. In Figure 6D, we show that silencing of Syt V abrogated recruitment of the V-ATPase *c* subunit to phagosomes containing *lpg1*-KO and *lpg2*-KO mutants. In the case of phagosomes containing either WT or *lpg2*-KO+*LPG2* promastigotes, Syt V silencing had the same effect as the presence of LPG on the recruitment of the V-ATPase *c* subunit (Figure 6D). Collectively, these results show that LPG enables *L. donovani* promatigotes to inhibit phagosomal recruitment of the V-ATPase by a Syt V-dependent mechanism and to prevent acidification. Remarkably, at 24 h after the initiation of phagocytosis, we detected the V-

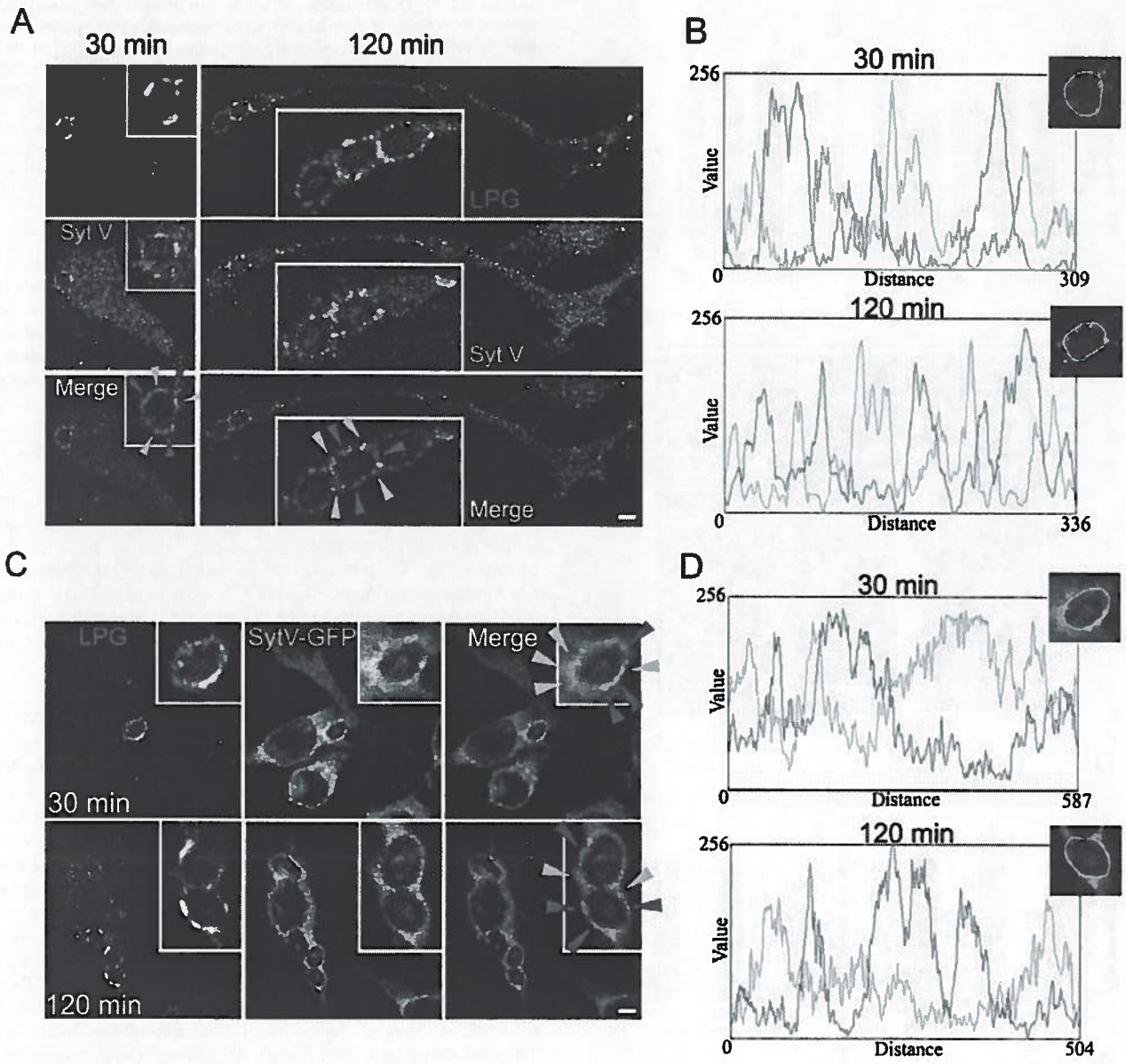

Figure 4. Exclusion of Syt V is restricted to the LPG insertion sites on the phagosome membrane. *A* and *B*, BMM were allowed to internalize Zym or Zym-LPG during 30 min or 2 h, and stained for Syt V (green) and LPG (red). Green arrowheads indicate a localized Syt V recruitment on phagosome membrane and red arrowheads indicate a localized LPG insertion into phagosome membrane (A). *C* and *D*, Syt V-GFP cells were allowed to internalize Zym or Zym-LPG for 30 min or 2 h, fixed and stained for LPG (red). Green arrowheads indicate a localized Syt V-GFP recruitment on phagosome membrane and red arrowheads indicate a localized LPG insertion into phagosome membrane (C). A rim around a representative phagosome formed in BMM (B) or in SytV-GFP cells (D) from *A* and *C* respectively, was manually traced with a one pixel width and fluorescence intensity profile of Syt V in green and LPG in red were represented in a graph for each phagocytosis time point. Bar, 3 μm.
doi:10.1371/journal.ppat.1000628.g004

ATPase *c* subunit on only 10 to 17% of phagosomes containing *L. donovani* promastigotes in three independent experiments, consistent with LPG still being present (Figure 7A and C). At this time point, we detected LysoTracker red on only 20% of phagosomes containing WT promastigotes (not shown), indicating that promastigotes remodel their intracellular niche to establish infection in a compartment that fails to acidify, at a time when differentiation into amastigotes takes place. In contrast, we detected the V-ATPase *c* subunit on 66 to 71% of phagosomes containing *L. donovani* amastigotes at both 2 h and 24 h after the initiation of phagocytosis (Figure 7B and C). This observation is consistent with the fact that amastigotes replicate in an acidic phagolysosomal compartment [14].

Discussion

The exocytosis regulator Syt V is recruited to the nascent phagosome and remains associated throughout the maturation process [40], leading us to investigate its potential role in modulating interactions between the phagosome and endocytic organelles. Our results revealed that whereas silencing of Syt V had no effect on the recruitment of EEA1, LAMP-1, and cathepsin

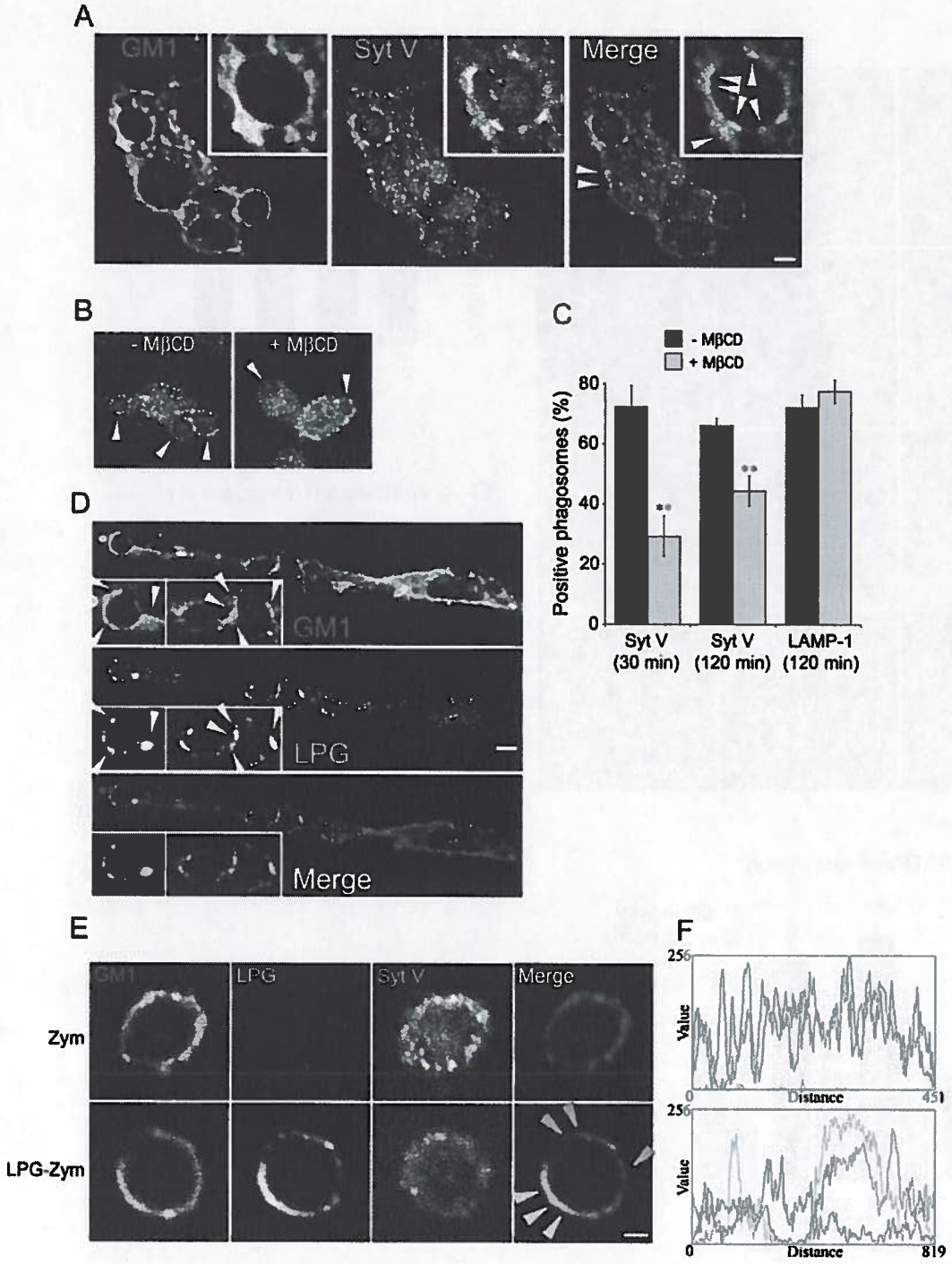

Figure 5. Recruitment of Syt V to GM1-containing microdomains of phagosome membranes is prevented by LPG. *A*, BMM were allowed to internalize Zym for 30 min, fixed and stained for endogenous Syt V (green) and GM1 (red). White arrowheads indicate examples of colocalization between Syt V and GM1-positive microdomains, indicating a Syt V enrichment on these microdomains. *B* and *C*, BMM were either left untreated or treated with 10 mmol/L MβCD for 1 h before the internalization of Zym for 30 and 120 min. Cells were then fixed and stained for Syt V and LAMP-1. Representative confocal images of Syt V recruitment on cells with or without MβCD treatment is presented (*B*), white arrowheads indicate phagosomes. Syt V acquisition is expressed as a percentage of phagosome recruitment for Syt V. At least 100 phagosomes for each condition were assessed. Three independent experiments were performed and the bars show the standard deviations of one representative triplicate (*C*) (**, $p \leq 0.005$). *D*, BMM were allowed to internalize Zym-LPG for 30 min, fixed and stained for LPG (green) and GM1 (red). White arrowheads indicate a colocalization between LPG and GM1-positive rafts. BMM were allowed to internalize Zym (*E*, upper panel) or LPG-Zym (*E*, lower panel) for 30 min, fixed and stained for Syt V (blue), LPG (green) and GM1 (red). Blue arrowheads indicate a local Syt V acquisition on phagosome membrane and yellow arrowheads indicate a local colocalization between GM1 microdomains and LPG. A rim around each phagosome was manually traced with a one pixel width and fluorescence intensity profile of Syt V in blue, LPG in green and GM1 in red were represented in a graph (*F*). Bars, 3 μm (*A*, *B* and *D*) or 1 μm (*E*).
doi:10.1371/journal.ppat.1000628.g005

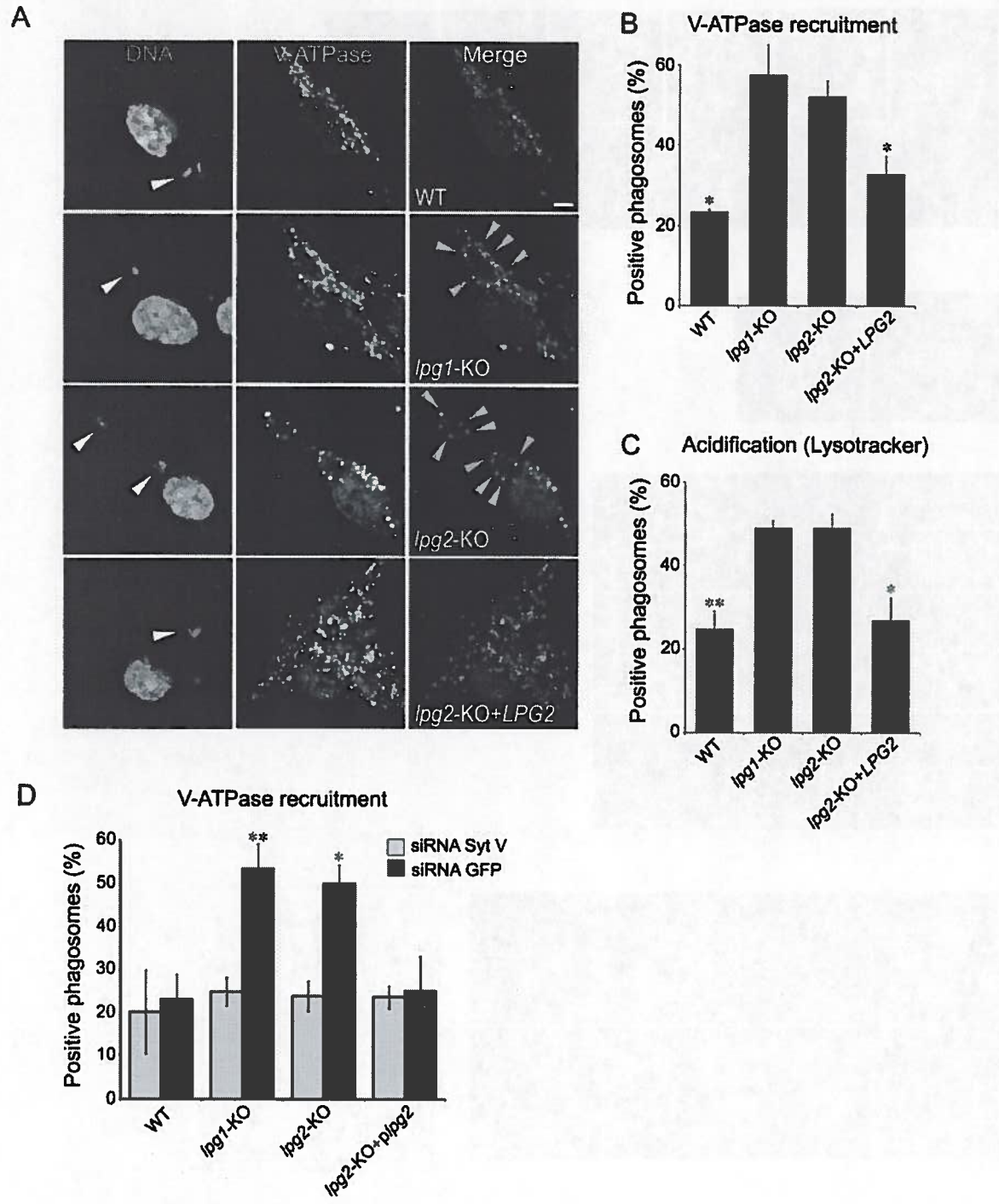

Figure 6. LPG prevents delivery to phagosomes of the V-ATPase and acidification through a Syt V-dependent mechanism. *A* and *B*, BMM cells were infected with either WT, *lpg1*-KO, *lpg2*-KO, *lpg2*-KO+*LPG2* promastigotes for 2 h, fixed and stained for V-ATPase (green) and DNA (blue). *A*, Confocal images illustrating V-ATPase acquisition (green arrowheads) on parasite-containing phagosomes (white arrowheads). *B*, V-ATPase acquisition was determined on at least 100 phagosomes for each condition. Three independent experiments were performed and the bars show the standard deviations of one representative triplicate (*, $p \leq 0.05$; *p* values compare the presence and the relative levels of V-ATPase on phagosomes containing WT and *lpg2*-KO+*LPG2* *vs* *lpg1*-KO and *lpg2*-KO parasites). *C*, BMM cells were incubated 2 h with Lysotracker red prior to infection with either WT, *lpg1*-KO, *lpg2*-KO, *lpg2*-KO+*LPG2* promastigotes for 2 h and then fixed. *D*, RAW 264.7 cells were transfected with either a siRNA to Syt V or a siRNA to GFP, incubated for 24 h and infected with either WT, *lpg1*-KO, *lpg2*-KO, *lpg2*-KO+*LPG2* promastigotes for 2 h. Macrophages were then fixed and stained for DNA and the V-ATPase. Phagosomal recruitments were determined on at least 60 phagosomes for each condition. Two independent experiments were performed and the bars show the standard deviations of one representative triplicate. Data are shown as the percentage of recruitment (*, $p \leq 0.05$; **, $p \leq 0.005$; *p* values compare the acquisition of V-ATPase on phagosomes containing WT and *lpg2*-KO+*LPG2* *vs* *lpg1*-KO and *lpg2*-KO parasites). Bar, 3 μm.
doi:10.1371/journal.ppat.1000628.g006

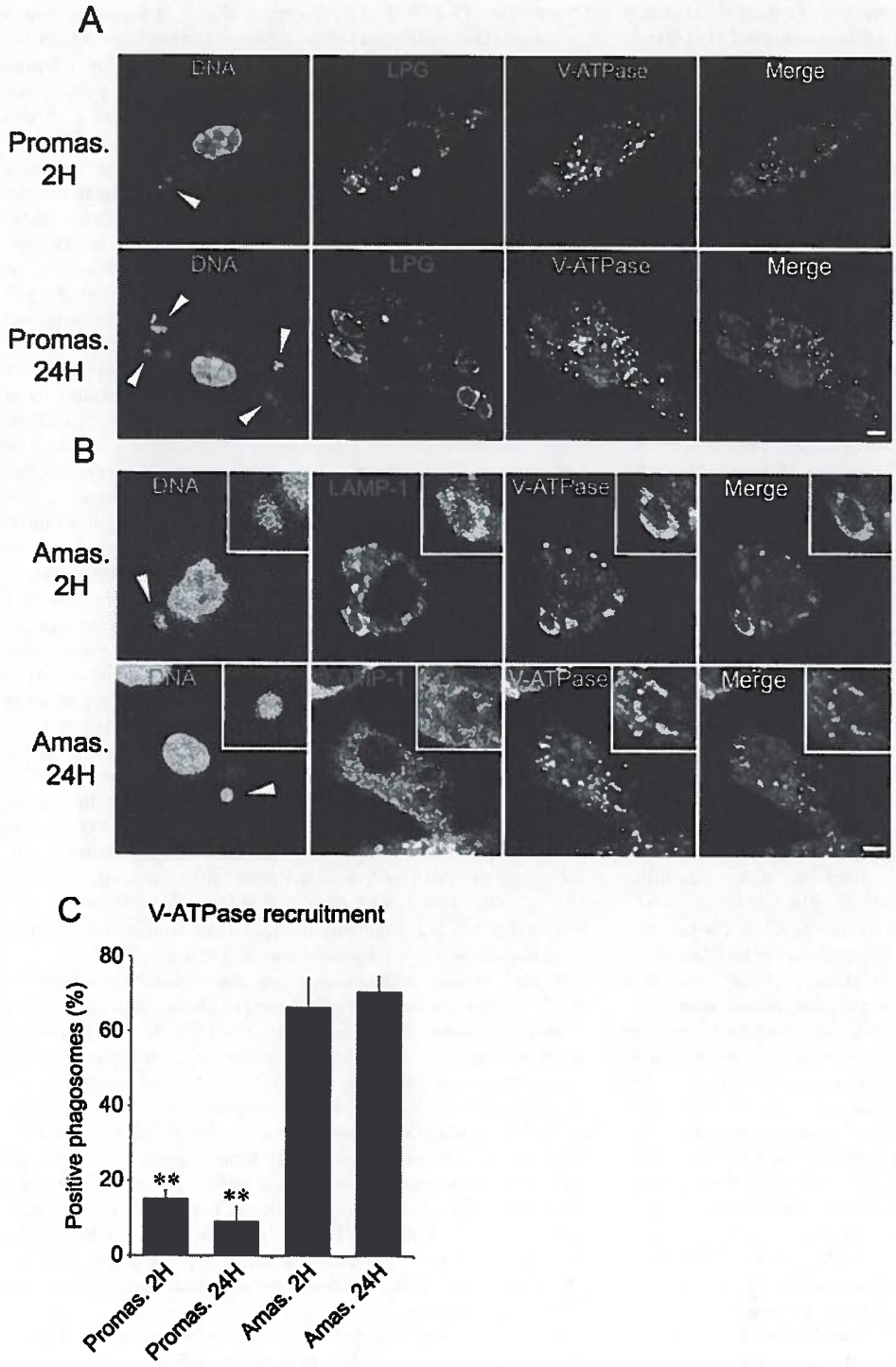

Figure 7. The inhibition of the V-ATPase acquisition on phagosomes is specific for the promastigote stage. *A–C*, BMM cells were infected with either WT promastigotes or amastigotes for 2 h and 24 h, fixed and stained for V-ATPase (green), LPG (red) and DNA (blue) (A) or V-ATPase (green), LAMP-1 (red) and DNA (blue) (B). *A* and *B*, Confocal images illustrating V-ATPase acquisition on parasite-containing phagosomes (white arrowheads). *C*, V-ATPase acquisition was determined on at least 100 phagosomes for each condition and expressed as a percentage of recruitment. Three independent experiments were performed and the bars show the standard deviations of one representative triplicate (**, $p \leq 0.005$; *p* values compare the acquisition of V-ATPase on phagosomes containing promastigotes *vs* amastigotes parasites). Bar, 3 μm.
doi:10.1371/journal.ppat.1000628.g007

B, it inhibited the phagosomal acquisition of cathepsin D and of the V-ATPase *c* subunit. These findings indicated that Syt V plays a role in phagolysosome biogenesis, possibly by regulating the interaction between phagosomes and a subset of late endosomes or lysosomes enriched in cathepsin D and in the V-ATPase *c* subunit. Alternatively, Syt V may be needed to reach the level of phagosome maturation necessary to acquire the machinery that regulates the recruitment of cathepsin D and the V-ATPase *c* subunit. Our finding that acquisition of cathepsin B and cathepsin D is mediated by distinct mechanisms supports the demonstration that various hydrolases appear sequentially, at various time points during phagosome maturation [42]. This view is also consistent with evidence that various subpopulations of early endosomes, late endosomes, and lysosomes co-exist and that these compartments contain significant heterogeneity [43]. Together with previous findings [27], our results show that phagosomal acquisition of the V-ATPase and LAMP-1 are mediated through distinct mechanisms. Hence, the observations that LAMP-1 is recruited to phagosomes independently of Syt V and that *L. donovani* promastigotes (and LPG) impair the recruitment of LAMP-1 point to the existence of other inhibitory mechanisms and illustrate the complexity of phagolysosome biogenesis. The role of Syt V in regulating interactions between the phagosome and the endosomal compartments thus seems specific and further studies will be necessary to understand its precise role during phagosome maturation. Recent studies by Andrews and colleagues revealed that the lysosome-associated Syt VII, which controls membrane delivery to nascent phagosomes [9], is involved in phagolysosome fusion [9,10]. It will be of interest to determine whether Syt V and Syt VII use similar mechanisms to regulate phagolysosome biogenesis.

To establish infection inside macrophages, *L. donovani* promastigotes, the form of the parasite transmitted to mammals by the sand fly vector, create an intracellular niche by inhibiting phagolysosome biogenesis [16]. Genetic and biochemical approaches revealed that this inhibition is mediated by the parasite surface glycolipid LPG [16,17,22]. Insight into the mechanism of this inhibition came from the observations that LPG transfers from the parasite surface to the nascent phagosome membrane [26], where it disrupts existing lipid microdomains and alters the formation of these structures after promastigote internalization [28,29]. Whereas the precise mechanism remains to be elucidated, the current model is that LPG inserts into lipid microdomains via its GPI anchor, thereby allowing the negatively charged Galβ1,4Man-PO_4 polymer of LPG to directly interfere with the clusterization of molecules into these microdomains. This model is consistent with the demonstration that alteration of membrane properties is dependent on the length of the Galβ1,4Man-PO_4 polymer [16,44]. Because of their role in clustering specific sets of proteins, membrane lipid microdomains are central to a wide variety of cellular processes, including regulated exocytosis [45,46]. Our findings that Syt V was present in GM1-enriched phagosome microdomains and that LPG inserts into or associates with these structures to interfere with the phagosomal association of Syt V thus provides new insight into the mechanism of LPG-mediated inhibition of phagolysosome biogenesis.

Acquisition of an array of hydrolases and acidification of the phagosome enable the generation of a highly microbicidal environment [4] and the creation of a compartment competent for antigen processing and presentation [47]. To circumvent killing following uptake by macrophages, several intracellular microorganisms interfere with phagosome acidification and maturation [4,12,48]. The discovery that *L. donovani* promastigotes establish infection inside a compartment from which the V-ATPase is excluded may thus be favorable for parasite survival. Incidentally, a recent study showed that phagosome acidification is defective in Stat1$^{-/-}$ macrophages and this correlated with an increased survival of *L. major* promastigotes, suggesting a role for acidic pH in the control of intracellular *Leishmania* growth early during infection [49]. Furthermore, the finding that phagosomes containing *L. donovani* promastigotes fail to acquire the V-ATPase and acidify even at 24 hours post-infection provides new insight on our undestanding of *Leishmania* biology. Indeed, in the absence of data on the pH of promastigote-containing phagosomes, it has been assumed that promastigotes initiate infection in an acidic environment and that differentiation of promastigotes into amastigotes is mainly triggered by a rapid exposure to an acidic environment and elevated temperature [50]. Exclusion of the V-ATPase raises the possibility that *L. donovani* promastigotes initiate the differentiation process in a non-acidified environment. Further studies will be required to fully address this point. An issue that remains unsolved pertains to the acquisition of phagolysosomal features and acidification of parasite-containing vacuoles upon completion of the differentiation of promastigotes into amastigotes. Indeed, previous work by Antoine and colleagues [14] established that *L. amazonensis* amastigotes reside within an acidic vacuole (pH 4.7–5.2), in agreement with the notion that *Leishmania* amastigotes are internalized within a vacuole that rapidly acquires lysosomal features and in which amastigotes proliferate [13,51]. Consistent with these previous reports, we showed the presence of LAMP-1 and the V-ATPase *c* subunit on phagosomes containing *L. donovani* amastigotes as early as 2 h after internalization. A possible explanation is that during the first few days post-infection, the presence of LPG in the phagosome membrane prevents acidification and maturation, allowing promastigote-to-amastigote differentiation to take place. The down-regulation of LPG biosynthesis below detectable levels in amastigotes [52] may enable phagosomes to gradually acquire lysosomal features and to acidify.

Little is known on the mechanisms that regulate recruitment of the V-ATPase to maturing phagosomes. The identification of Syt V as a regulator of this process and the fact that Syt V is present in microdomains of the phagosome membrane is consistent with the notion that these structures are important for the recruitment of the V-ATPase to the phagosome membrane [27]. Of interest, the V-ATPase *c* subunit has been previously identified in Triton X-100-resistant fractions from rat brain synaptic vesicles in association with synaptobrevin 2 and synaptophysin [53], leading the authors of that study to conclude that this interaction may play a role in recruiting the V-ATPase to synaptic vesicles. Whether Syt V is part of such a SNARE complex on phagosomes and the characterization of this complex are important issues that await further investigation.

In this study, we provided novel findings into the mechanism of *Leishmania* pathogenesis, whereby targeting of Syt V, which plays a role in the acquisition of phagosome microbicidal properties, is part of the strategy used by *L. donovani* promastigotes to create a niche propitious to the establishment of infection within mammalian hosts (see working model, Figure 8). Interestingly, phagocytosis of either zymosan or *lpg2*-KO promastigotes coated with the virulence glycolipid lipoarabinomannan from *Mycobacterium tuberculosis*, impaired the phagosomal association of Syt V (Figure S4). Whether other intracellular microorganisms use a similar mechanism to remodel their intracellular niche remains to be investigated.

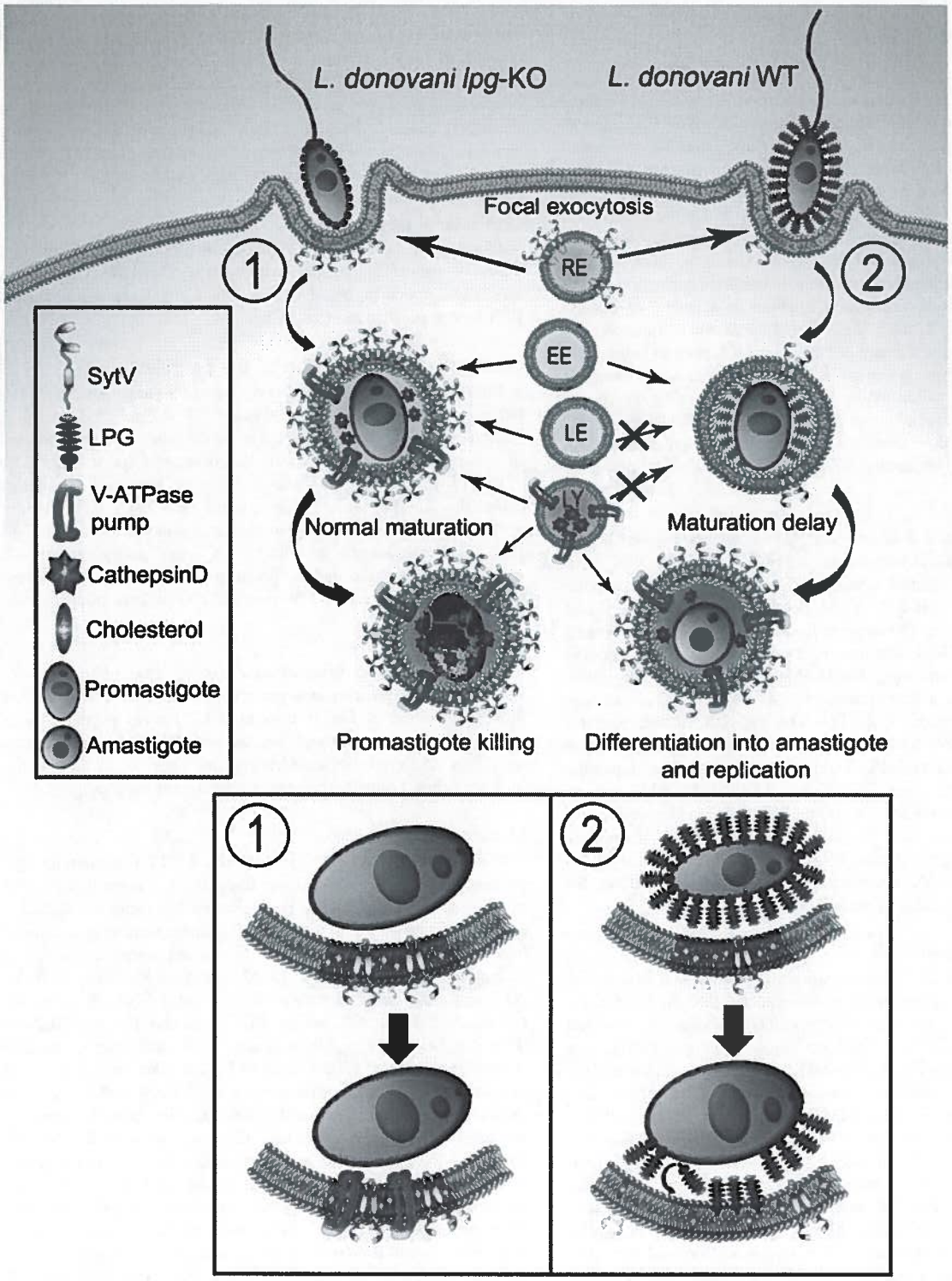

Figure 8. Working model for the exclusion of the V-ATPase from *L. donovani* promastigote-harboring phagosomes. Both WT and LPG-defective *L. donovani* promastigotes bind to macrophages, inducing the phagocytic process. During this step, membrane from internal vesicles such as recycling endosomes (RE) bearing Syt V participate to the membrane supply necessary for the formation of the nascent phagosome. LPG transfers to the phagosome membrane and inserts into lipid microdomains, excluding Syt V from the newly formed phagosome. Exclusion of Syt V impairs phagolysosome biogenesis, including acquisition of cathepsin D and V-ATPase (2) when compared to phagosomes harboring *L. donovani* promastigotes lacking LPG (1), which interact with the endosomal compartment (early endosomes, EE; late endosomes, LE; lysosomes, LY). This creates an intracellular niche that fails to acidify, at a time when promastigotes differentiate into amastigotes, which are resistant to the microbicidal properties of the phagolysosome. Mutants lacking LPG are degraded by the phagolysosomal environment.
doi:10.1371/journal.ppat.1000628.g008

Materials and Methods

Macrophages

All animals were handled in strict accordance with good animal practice as defined by the Canadian Council on Animal Care, and all animal work was approved by the Comité institutionel de protection des animaux of INRS- Institut Armand-Frappier (protocol 0811-08). BMM were obtained by growing bone marrow cells from female BALB/c mice at 37°C in 5% CO_2 for 7 days in Dulbecco Modified Eagle Medium with L-glutamine (Life Technologies) supplemented with 10% heat-inactivated FBS (Hyclone, Logan, UT), 10 mM Hepes (pH 7.4) and antibiotics (complete medium) in the presence of 15% (v/v) L929 cell-conditioned medium as a source of colony-stimulating factor (CSF)-1 [54]. BMM were made quiescent by culturing them in the absence of CSF-1 for 18 h prior to being used. The murine macrophage cell line RAW 264.7 was grown in complete medium in a 37°C incubator with 5% CO_2. Stably transfected RAW264.7 cells expressing Syt V-GFP (Syt V-GFP RAW 264.7 cells) were previously described [40]. Transfectants were cultured in complete medium containing 500 μg/ml G418 (Life Technologies).

Parasites

Leishmania donovani promastigotes (Sudanese strain 1S) were grown at 26°C in RPMI 1640 medium supplemented with 20% heat-inactivated FBS, 100 μM adenine, 20 mM 2-[N-morpholino]ethanesulphonic acid (pH 5.5), 5 μM hemin, 3 μM biopterin, 1 μM biotin and antibiotics. The isogenic *L. donovani* LPG-defective mutants *lpg1*-KO and *lpg2*-KO were described previously [55]. The *lpg1*-KO mutant secretes repeating Galβ1,4Manα1-PO_4-containing molecules, but lacks the ability to assemble a functional LPG glycan core [56], precluding synthesis of LPG. The *lpg2*-KO mutant expresses the truncated LPG Gal(α1,6)Gal>(α1,3)Gal(β1,3)[Glc(α1-P)]Man(α1,3)Man(α1,4)GN(α1,6)-PI, and does not synthesize repeating Galβ1,4Manα1-PO_4 units [57]. The *lpg2*-KO+*LPG2* add-back was grown in the presence of 50 μg/ml G418. For infections, promastigotes were used in late stationary phase of growth. *L. donovani* amastigotes (Strain LV9) were isolated from the spleen of infected female LVG Golden Syrian hamsters (Charles River, St-Constant, QC, Canada), as described [58].

Reagents and antibodies

The rabbit anti-Syt V spacer antiserum was raised against the cytoplasmic region between the transmembrane and the C2 domain (aa 71–216) [37] and was affinity-purified. The rat monoclonal antibody against LAMP-1 developed by J. T. August (1D4B) was obtained through the Developmental Studies Hybridoma Bank at the University of Iowa, and the National Institute of Child Health and Human Development. The rabbit antiserum against the 16 kDa proteolipid subunit (*c* subunit) of the V_0 sector of the V-ATPase was kindly provided by Dr. Mhairi Skinner (University of Guelph, ON, Canada) [59]. The mouse monoclonal antibody against EEA1 was from BD Transduction Laboratories. The rabbit antiserum against cathepsin B was from Millipore and the rabbit antiserum against cathepsin D was from Upstate. The mouse monoclonal anti-LPG (CA7AE) was prepared from hybridoma supernatant [60]. Methyl-β-cyclodextrin (MβCD) was from Sigma (St-Louis, MO, USA). LPG was isolated from the log phase cultures of *L. donovani* promastigotes as previously described [61,62]. Purified lipoarabinomannan (LAM) from H37Rv strain of *Mycobacterium tuberculosis* was from Colorado State University (Fort Collins, CO, USA).

RNA interference

Syt V silencing by RNAi was performed as previously described [40] using a small interfering RNA (siRNA) corresponding to nucleotides 94–112 of the Syt V cDNA [38], whereas a siRNA specific to GFP was used as a negative control [63]. Adherent RAW 264.7 cells were transfected with siRNA duplexes at a final concentration of 240 nM using OligoFectamine (Invitrogen) as described [63]. A BLAST search against the mouse genome sequence database was performed to ensure that the chosen siRNA sequences targeted only the mRNA of interest.

Cholesterol depletion

Cholesterol depletion was achieved by incubating macrophages with 10 mmol/L methyl-β-cyclodextrin (MβCD) (Sigma) in serum-free medium at 37°C for 1 h. Cells were washed with PBS before particle internalization.

Coating and opsonization of the particles

Purified LPG and LAM were sonicated and added to the particles at a final concentration of 25 μM in PBS, pH 7.3, incubated at 37°C for 1 h. Particles were washed and resuspended in complete medium prior to phagocytosis experiments. The efficiency of LPG coating was assessed by immunofluorescence using the anti-repeating unit antibody CA7AE. Complement opsonization of *L. donovani* promastigotes was done as described [23] and complement opsonisation of beads and zymosan was carried out by incubating the particles in DMEM supplemented with 10% mouse serum for 30 min at 37°C prior to phagocytosis.

Phagocytosis assay

For synchronized phagocytosis assays, macrophages were incubated with particles at a particle-to-cell ratio of 15:1 (unless otherwise specified) for 15 min at 4°C. Excess particles were removed by several thorough washes with DMEM and phagocytosis was triggered by transferring the cells to 37°C for the indicated time points before processing for microscopy.

Immunofluorescence

Macrophages were fixed for 10 min in PBS containing 2% paraformaldehyde, permeabilized using 0.1% Triton X-100, and nonspecific binding to surface FcγR was blocked using 1% BSA, 2% goat serum, 6% milk, and 50% FBS. For immunostaining, cells were labeled with the appropriate combinations of primary antibodies or antisera (anti-Syt V, LAMP-1, EEA1, cathepsin D, cathepsin B, V-ATPase, LPG), and secondary antibodies (anti-rabbit, anti-mouse or anti-rat AlexaFluor 488, 568 or 647; Molecular Probes). DRAQ5 (Biostatus, Leicestershire, UK) was used to visualize macrophage and parasite nuclei and CTX-B-568 or 647 (Molecular Probes) was used to visualize GM1-enriched rafts. Syt V-GFP RAW 264.7 cells were fixed and directly incubated with DRAQ5 before being mounted or subjected to immunofluorescence. Of note, we used Syt V-GFP RAW 264.7 cells to localize Syt V following infection with *L. donovani* promastigotes because our antiserum against Syt V cross-reacts with *Leishmania* epitopes. All coverslips were mounted on glass slides with Fluoromount-G (Southern Biotechnology Associates). Detailed analysis of protein presence and localization on the phagosome was performed using an oil immersion Nikon Plan Apo 100 (N.A. 1.4) objective mounted on a Nikon Eclipse E800 microscope equipped with a Bio-Rad Radiance 2000 confocal imaging system (Bio-Rad, Zeiss). Images were obtained using appropriate filters, through the sequential scanning mode of the LaserSharp software (Bio-Rad Laboratories, Zeiss) with a Kalman filter of at least 6.

Phagosome acidification

BMM were preloaded with the acidotropic dye LysoTracker Red (Molecular Probes, Eugene, OR) diluted in DMEM (1:1000) for 2 h at

37°C. Cells were washed and infected with promastigotes for 2 h at 37°C as described in *Phagocytosis assay*. Cells were then rinsed, fixed with 2% paraformaldehyde for 10 min, washed and directly incubated 20 min with DRAQ5 before being mounted for confocal analysis.

Quantification of phagocytosis and protein recruitment on phagosomes

To assess the recruitment of proteins of interest, we assessed the presence or absence of staining on the phagosome membrane for each protein, and at least 100 phagosomes were randomly scanned for each condition. To quantify the levels of Syt V and Syt V-GFP (Figures 2C, 3D and 3E), EEA1 (Figure 3A) or LAMP-1 (Figure 3B), we determined the relative staining intensity as follows. The 488 and 568 nm excitation channels (emission 515/30 and 600/40 respectively) were separated and the protein staining rim around each phagosome was manually traced with a one pixel width. The fluorescence intensity of individual pixels was determined using the software Image J and an average intensity was calculated for each fluorescence intensity profile. To normalize intensity values of all phagosomes, cytosol intensity was also evaluated in the proximity area of the phagosome under study but far enough from the phagosome membrane to avoid quantifying residual phagosome fluorescence. Final phagosome intensity was expressed as the ratio of phagosome intensity (P) on cytosol intensity (C), thus P/C. In all cases, we ensured that signal intensity was not at saturation and the 20 more intense staining for each condition were selected and the average compared for the intensity level of each protein.

Statistical analyses

Statistical analyses were performed using Student's two-tail two-sample unequal variance test.

Supporting Information

Figure S1 Kinetics of EEA1 and LAMP-1 phagosomal recruitment are normal in the absence of Syt V. *A*. Representative confocal images illustrating EEA1 recruitment at 10 min of phagocytosis and LAMP-1 recruitment at 120 min of phagocytosis. Bar, 3 μm. *B*. RAW 264.7 cells were transfected with siRNAs to either Syt V or GFP, and incubated for 24 h. Cells were allowed to internalize Zym and phagosomal recruitments were determined at 10, 30, 60 and 120 min for EEA1 and LAMP1 on at least 100 phagosomes for each condition. Two independent experiments were performed and the bars show the standard deviations of one representative triplicate.
Found at: doi:10.1371/journal.ppat.1000628.s001 (3.91 MB PDF)

Figure S2 Recruitment of Syt V-GFP is reduced on phagosomes containing LPG-coated zymosan. Syt V-GFP cells were allowed to internalize Zym or LPG-Zym for 10 min, 30 min or 2 h, fixed and stained for LPG (red). Recruitment and relative levels of Syt V-GFP on phagosomes are illustrated by confocal images. Bar, 3 μm.
Found at: doi:10.1371/journal.ppat.1000628.s002 (1.40 MB PDF)

Figure S3 V-ATPase recruitment on phagosome membrane containing *lpg*-deficient promastigotes. BMM cells were infected with *lpg1*-KO promastigotes for 2 h, fixed and stained for the V-ATPase c subunit (green), LAMP-1 (red) ,and DNA (blue). The V-ATPase *c* subunit is present on the phagosome membrane, which is also positive for LAMP-1.
Found at: doi:10.1371/journal.ppat.1000628.s003 (1.15 MB PDF)

Figure S4 Recruitment of Syt V is prevented on phagosomes containing particles coated with the *Mycobacterium tuberculosis* lipoarabinomannan. *A* and *B*, SytV-GFP cells were allowed to internalized Zym or LAM-Zym (A), *lpg2*-KO or LAM-*lpg2*-KO (B) for 30 min or 2 h. The presence (*A* and *B*, left graph) and relative levels (*A* and *B*, right graph) of Syt V-GFP were determined. Three independent experiments were performed and the bars show the standard deviations of one representative triplicate (*, $p \leq 0.05$; **, $p \leq 0.005$).
Found at: doi:10.1371/journal.ppat.1000628.s004 (0.66 MB PDF)

Acknowledgments

We are grateful to Dr. Mhairi Skinner (University of Guelph, Canada) for the rabbit antiserum against the 16 kDa proteolipid subunit of the V-ATPase and Marcel Desrosiers for expert assistance with confocal microscopy. Lipoarabinomannan was obtained as part of NIH, NIAID Contract No. HHSN266200400091C, entitled "Tuberculosis Vaccine Testing and Research Materials," which was awarded to Colorado State University. We thank Dr. Michel Desjardins, Guillermo Arango-Duque, and Christine Matte for critical comments on this manuscript.

Author Contributions

Conceived and designed the experiments: AFV AD. Performed the experiments: AFV. Analyzed the data: AFV AD. Contributed reagents/materials/analysis tools: MF SJT. Wrote the paper: AFV AD.

References

1. Aderem A, Underhill DM (1999) Mechanisms of phagocytosis in macrophages. Annu Rev Immunol 17: 593–623.
2. Vieira OV, Botelho RJ, Grinstein S (2002) Phagosome maturation: aging gracefully. Biochem J 366: 689–704.
3. Jutras I, Desjardins M (2005) Phagocytosis: at the crossroads of innate and adaptive immunity. Annu Rev Cell Dev Biol 21: 511–527.
4. Haas A (2007) The phagosome: compartment with a license to kill. Traffic 8: 311–330.
5. Stow JL, Manderson AP, Murray RZ (2006) SNAREing immunity: the role of SNAREs in the immune system. Nat Rev Immunol 6: 919–929.
6. Bajno L, Peng XR, Schreiber AD, Moore HP, Trimble WS, et al. (2000) Focal exocytosis of VAMP3-containing vesicles at sites of phagosome formation. J Cell Biol 149: 697–706.
7. Collins RF, Schreiber AD, Grinstein S, Trimble WS (2002) Syntaxins 13 and 7 function at distinct steps during phagocytosis. J Immunol 169: 3250–3256.
8. Braun V, Fraisier V, Raposo G, Hurbain I, Sibarita JB, et al. (2004) TI-VAMP/VAMP7 is required for optimal phagocytosis of opsonised particles in macrophages. Embo J 23: 4166–4176.
9. Czibener C, Sherer NM, Becker SM, Pypaert M, Hui E, et al. (2006) Ca^{2+} and synaptotagmin VII-dependent delivery of lysosomal membrane to nascent phagosomes. J Cell Biol 174: 997–1007.
10. Roy D, Liston DR, Idone VJ, Di A, Nelson DJ, et al. (2004) A process for controlling intracellular bacterial infections induced by membrane injury. Science 304: 1515–1518.
11. Meresse S, Steele-Mortimer O, Moreno E, Desjardins M, Finlay B, et al. (1999) Controlling the maturation of pathogen-containing vacuoles: a matter of life and death. Nat Cell Biol 1: E183–188.
12. Gruenberg J, van der Goot FG (2006) Mechanisms of pathogen entry through the endosomal compartments. Nat Rev Mol Cell Biol 7: 495–504.
13. Chang KP, Dwyer DM (1976) Multiplication of a human parasite (*Leishmania donovani*) in phagolysosomes of hamster macrophages in vitro. Science 193: 678–680.
14. Antoine JC, Prina E, Jouanne C, Bongrand P (1990) Parasitophorous vacuoles of *Leishmania amazonensis*-infected macrophages maintain an acidic pH. Infect Immun 58: 779–787.
15. Antoine JC, Prina E, Lang T, Courret N (1998) The biogenesis and properties of the parasitophorous vacuoles that harbour *Leishmania* in murine macrophages. Trends Microbiol 6: 392–401.
16. Desjardins M, Descoteaux A (1997) Inhibition of phagolysosomal biogenesis by the *Leishmania* lipophosphoglycan. J Exp Med 185: 2061–2068.
17. Scianimanico S, Desrosiers M, Dermine JF, Meresse S, Descoteaux A, et al. (1999) Impaired recruitment of the small GTPase rab7 correlates with the inhibition of phagosome maturation by *Leishmania donovani* promastigotes. Cell Microbiol 1: 19–32.
18. Dermine JF, Scianimanico S, Prive C, Descoteaux A, Desjardins M (2000) *Leishmania* promastigotes require lipophosphoglycan to actively modulate the fusion properties of phagosomes at an early step of phagocytosis. Cell Microbiol 2: 115–126.

19. Späth GF, Garraway LA, Turco SJ, Beverley SM (2003) The role(s) of lipophosphoglycan (LPG) in the establishment of *Leishmania major* infections in mammalian hosts. Proc Natl Acad Sci U S A 100: 9536–9541.
20. Turco SJ, Descoteaux A (1992) The lipophosphoglycan of *Leishmania* parasites. Annu Rev Microbiol 46: 65–94.
21. Descoteaux A, Turco SJ (1999) Glycoconjugates in *Leishmania* infectivity. Biochim Biophys Acta 1455: 341–352.
22. Holm A, Tejle K, Magnusson KE, Descoteaux A, Rasmusson B (2001) *Leishmania donovani* lipophosphoglycan causes periphagosomal actin accumulation: correlation with impaired translocation of PKCα and defective phagosome maturation. Cell Microbiol 3: 439–447.
23. Lodge R, Descoteaux A (2005) *Leishmania donovani* promastigotes induce periphagosomal F-actin accumulation through retention of the GTPase Cdc42. Cell Microbiol 7: 1647–1658.
24. Lodge R, Diallo TO, Descoteaux A (2006) *Leishmania donovani* lipophosphoglycan blocks NADPH oxidase assembly at the phagosome membrane. Cell Microbiol 8: 1922–1931.
25. Späth GF, Epstein L, Leader B, Singer SM, Avila HA, et al. (2000) Lipophosphoglycan is a virulence factor distinct from related glycoconjugates in the protozoan parasite *Leishmania major*. Proc Natl Acad Sci U S A 97: 9258–9263.
26. Tolson DL, Turco SJ, Pearson TW (1990) Expression of a repeating phosphorylated disaccharide lipophosphoglycan epitope on the surface of macrophages infected with *Leishmania donovani*. Infect Immun 58: 3500–3507.
27. Dermine JF, Duclos S, Garin J, St-Louis F, Rea S, et al. (2001) Flotillin-1-enriched lipid raft domains accumulate on maturing phagosomes. J Biol Chem 276: 18507–18512.
28. Dermine JF, Goyette G, Houde M, Turco SJ, Desjardins M (2005) *Leishmania donovani* lipophosphoglycan disrupts phagosome microdomains in J774 macrophages. Cell Microbiol 7: 1263–1270.
29. Winberg ME, Holm A, Sarndahl E, Vinet AF, Descoteaux A, et al. (2009) *Leishmania donovani* lipophosphoglycan inhibits phagosomal maturation via action on membrane rafts. Microbes Infect 11: 215–222.
30. Shao D, Segal AW, Dekker LV (2003) Lipid rafts determine efficiency of NADPH oxidase activation in neutrophils. FEBS Lett 550: 101–106.
31. Vilhardt F, van Deurs B (2004) The phagocyte NADPH oxidase depends on cholesterol-enriched membrane microdomains for assembly. Embo J 23: 739–748.
32. Arellano-Reynoso B, Lapaque N, Salcedo S, Briones G, Ciocchini AE, et al. (2005) Cyclic β-1,2-glucan is a *Brucella* virulence factor required for intracellular survival. Nat Immunol 6: 618–625.
33. Welin A, Winberg ME, Abdalla H, Sarndahl E, Rasmusson B, et al. (2008) Incorporation of *Mycobacterium tuberculosis* lipoarabinomannan into macrophage membrane rafts is a prerequisite for the phagosomal maturation block. Infect Immun 76: 2882–2887.
34. Gil C, Soler-Jover A, Blasi J, Aguilera J (2005) Synaptic proteins and SNARE complexes are localized in lipid rafts from rat brain synaptosomes. Biochem Biophys Res Commun 329: 117–124.
35. Kay JG, Murray RZ, Pagan JK, Stow JL (2006) Cytokine secretion via cholesterol-rich lipid raft-associated SNAREs at the phagocytic cup. J Biol Chem 281: 11949–11954.
36. Li C, Ullrich B, Zhang JZ, Anderson RG, Brose N, et al. (1995) Ca^{2+}-dependent and -independent activities of neural and non-neural synaptotagmins. Nature 375: 594–599.
37. Saegusa C, Fukuda M, Mikoshiba K (2002) Synaptotagmin V is targeted to dense-core vesicles that undergo calcium-dependent exocytosis in PC12 cells. J Biol Chem 277: 24499–24505.
38. Iezzi M, Kouri G, Fukuda M, Wollheim CB (2004) Synaptotagmin V and IX isoforms control Ca^{2+}-dependent insulin exocytosis. J Cell Sci 117: 3119–3127.
39. Fukuda M, Sagi-Eisenberg R (2008) Confusion in the nomenclature of synaptotagmins V and IX: which is which? Calcium Binding Proteins 3: 1–4.
40. Vinet AF, Fukuda M, Descoteaux A (2008) The exocytosis regulator synaptotagmin V controls phagocytosis in macrophages. J Immunol 181: 5289–5295.
41. Desjardins M, Huber LA, Parton RG, Griffiths G (1994) Biogenesis of phagolysosomes proceeds through a sequential series of interactions with the endocytic apparatus. J Cell Biol 124: 677–688.
42. Garin J, Diez R, Kieffer S, Dermine JF, Duclos S, et al. (2001) The phagosome proteome: insight into phagosome functions. J Cell Biol 152: 165–180.
43. Rogers LD, Foster LJ (2007) The dynamic phagosomal proteome and the contribution of the endoplasmic reticulum. Proc Natl Acad Sci U S A 104: 18520–18525.
44. Miao L, Stafford A, Nir S, Turco SJ, Flanagan TD, et al. (1995) Potent inhibition of viral fusion by the lipophosphoglycan of *Leishmania donovani*. Biochemistry 34: 4676–4683.
45. Lang T (2007) SNARE proteins and 'membrane rafts'. J Physiol 585: 693–698.
46. Salaun C, James DJ, Chamberlain LH (2004) Lipid rafts and the regulation of exocytosis. Traffic 5: 255–264.
47. Ramachandra L, Song R, Harding CV (1999) Phagosomes are fully competent antigen-processing organelles that mediate the formation of peptide:class II MHC complexes. J Immunol 162: 3263–3272.
48. Huynh KK, Grinstein S (2007) Regulation of vacuolar pH and its modulation by some microbial species. Microbiol Mol Biol Rev 71: 452–462.
49. Späth GF, Schlesinger P, Schreiber R, Beverley SM (2009) A novel role for Stat1 in phagosome acidification and natural host resistance to intracellular infection by *Leishmania major*. PLoS Pathog 5: e1000381. doi:10.1371/journal.ppat.1000381.
50. Zilberstein D, Shapira M (1994) The role of pH and temperature in the development of *Leishmania* parasites. Annu Rev Microbiol 48: 449–470.
51. Berman JD, Dwyer DM, Wyler DJ (1979) Multiplication of *Leishmania* in human macrophages in vitro. Infect Immun 26: 375–379.
52. McConville MJ, Blackwell JM (1991) Developmental changes in the glycosylated phosphatidylinositols of *Leishmania donovani*. Characterization of the promastigote and amastigote glycolipids. J Biol Chem 266: 15170–15179.
53. Galli T, McPherson PS, De Camilli P (1996) The V0 sector of the V-ATPase, synaptobrevin, and synaptophysin are associated on synaptic vesicles in a Triton X-100-resistant, freeze-thawing sensitive, complex. J Biol Chem 271: 2193–2198.
54. Descoteaux A, Matlashewski G (1989) c-fos and tumor necrosis factor gene expression in *Leishmania donovani*-infected macrophages. Mol Cell Biol 9: 5223–5227.
55. Privé C, Descoteaux A (2000) *Leishmania donovani* promastigotes evade the activation of mitogen-activated protein kinases p38, c-Jun N-terminal kinase, and extracellular signal-regulated kinase-1/2 during infection of naive macrophages. Eur J Immunol 30: 2235–2244.
56. Huang C, Turco SJ (1993) Defective galactofuranose addition in lipophosphoglycan biosynthesis in a mutant of *Leishmania donovani*. J Biol Chem 268: 24060–24066.
57. Descoteaux A, Luo Y, Turco SJ, Beverley SM (1995) A specialized pathway affecting virulence glycoconjugates of *Leishmania*. Science 269: 1869–1872.
58. Reiner NE (1982) Host-parasite relationship in murine leishmaniasis: pathophysiological and immunological changes. Infect Immun 38(3): 1223–1230.
59. Skinner MA, MacLaren LA, Wildeman AG (1999) Stage-dependent redistribution of the V-ATPase during bovine implantation. J Histochem Cytochem 47: 1247–1254.
60. Tolson DL, Turco SJ, Beecroft RP, Pearson TW (1989) The immunochemical structure and surface arrangement of *Leishmania donovani* lipophosphoglycan determined using monoclonal antibodies. Mol Biochem Parasitol 35: 109–118.
61. Orlandi PA, Jr., Turco SJ (1987) Structure of the lipid moiety of the *Leishmania donovani* lipophosphoglycan. J Biol Chem 262: 10384–10391.
62. Russo DM, Turco SJ, Burns JM, Jr., Reed SG (1992) Stimulation of human T lymphocytes by *Leishmania* lipophosphoglycan-associated proteins. J Immunol 148: 202–207.
63. Flandin JF, Chano F, Descoteaux A (2006) RNA interference reveals a role for TLR2 and TLR3 in the recognition of *Leishmania donovani* promastigotes by interferon-γ-primed macrophages. Eur J Immunol 36: 411–420.